

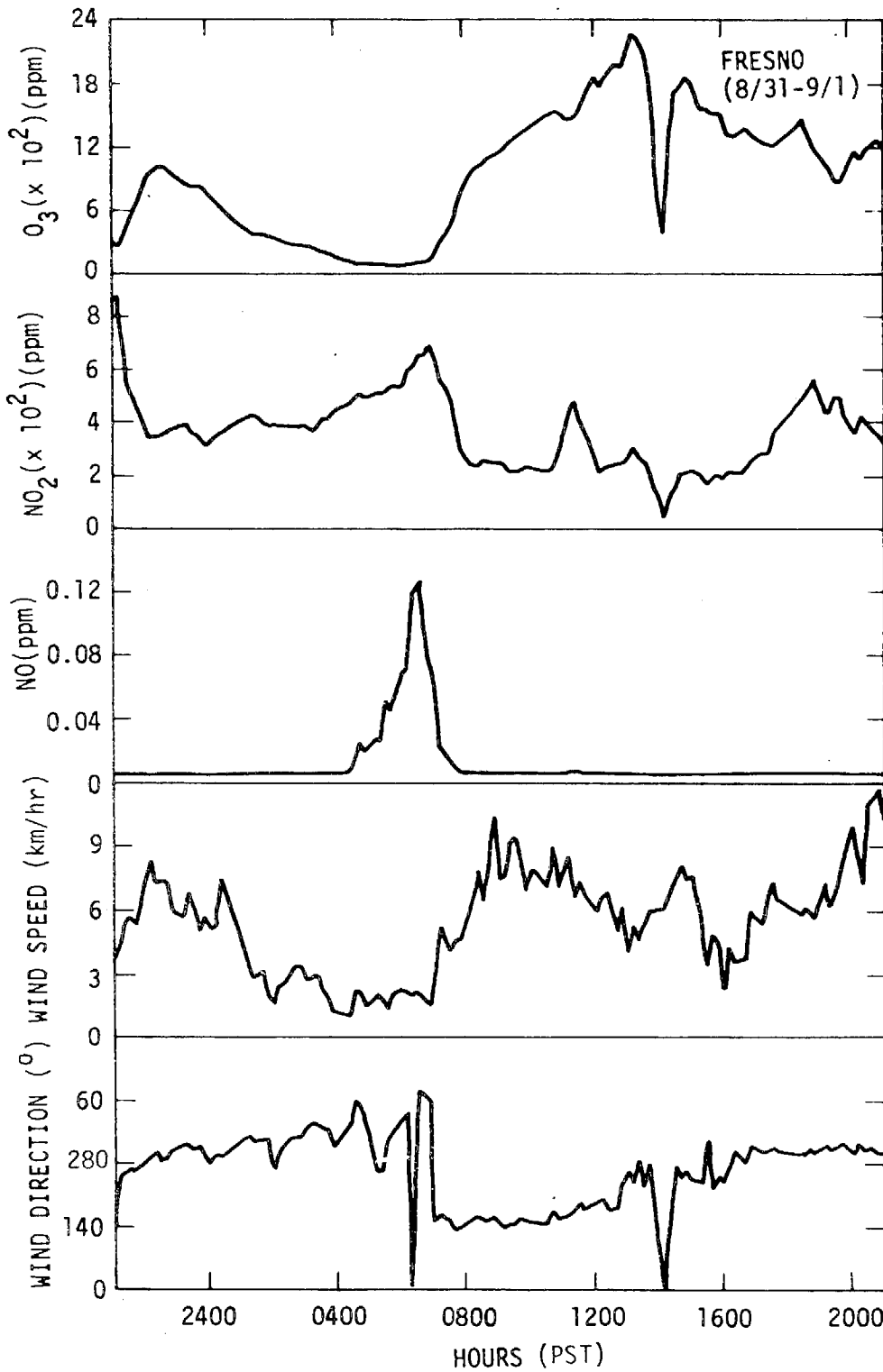
SC524.25FR

5. FRESNO - AUGUST 31 AND SEPTEMBER 1, 1972

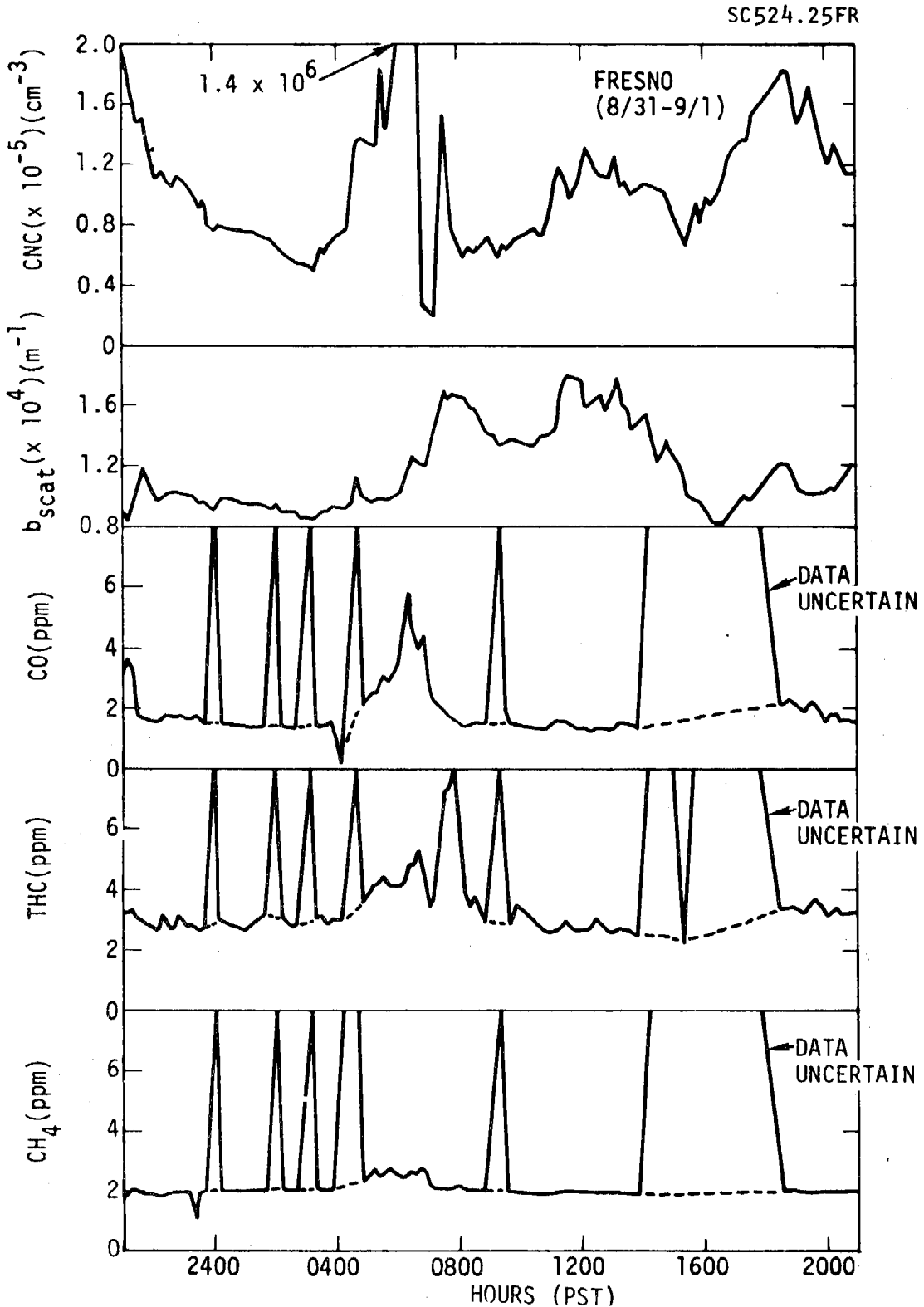
Of all the intensive episodes that were investigated with the mobile laboratory during the 1972 season, the results taken at the Fresno County Fairgrounds approached most closely the simple picture of photochemical smog development, where the development of the ozone peak was accompanied by a maximum in the integral scattering coefficient, and in a maximum of the large particle fraction of the aerosol. The data in Fresno are of considerable interest in that the oxidant level achieved on August 31-September 1 approached that obtained in Pomona in 1972, indicating light to moderate photochemical smog in the San Joaquin Valley. The presence of smog is well established from previous aerometric data in this region. Diurnal patterns for pollutant gases for Fresno during this period are shown in Figure 4-11. The NO and CO early morning peaks are seen, with the increase in motor vehicle traffic and anthropogenic activity. Total hydrocarbon data show anomalous behavior, coming later in the morning than the CO and NO peaks. NO₂ is observed to be generally quite low, with midmorning maximum just after 1100. The ozone maximum was at 1300 on this day, and the ozone level exceeded 0.2 ppm. The diurnal patterns for the aerosol parameters are shown in Figure 4-11b. Here, it is seen that b_{scat} shows a weak maximum during the midday. However, it is interesting to note the b_{scat} is certainly not considered to be at all high, compared to conditions often observed in the South Coast Basin with photochemical smog. Coinciding with the maximum b_{scat} were maxima in total volume concentration and surface concentration of aerosol. In contrast, the Aitken nuclei were seen to show a maximum with the early morning increase in anthropogenic activity, while the remainder of the day the condensation nuclei count was considerably lower, with a slight secondary maximum about 1900 PST.

The heavy element patterns for Fresno on August 31-September 1 are shown in Figure 4-12. The lead and bromine in this case are not exceptionally well correlated in their changes; however, one can see the early morning peak developing in the iron, lead and zinc. There is an interesting feature in this data in that the iron and calcium concentrations are quite high at Fresno. This may be related to contributions from stationary sources in the San Joaquin Valley.

SC524.25FR

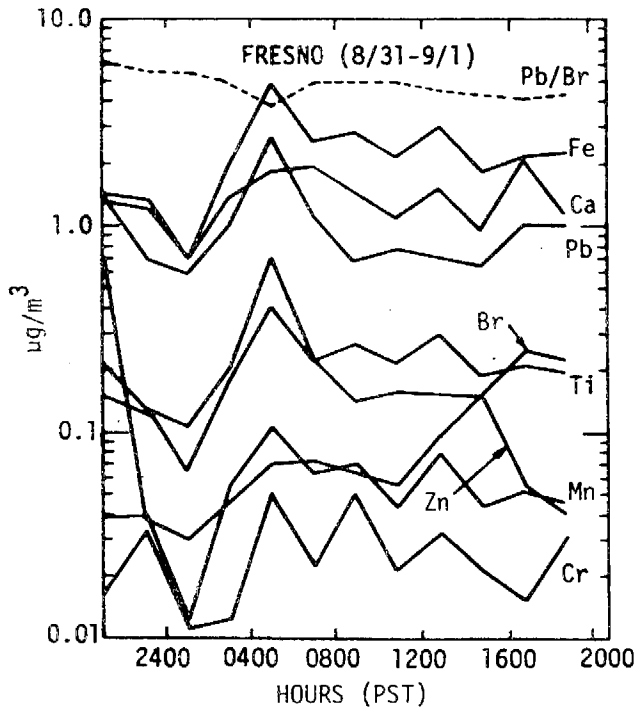


a. Ozone, Nitrogen Dioxide, Nitric Oxide, Wind Speed, and Wind Direction
 Figure 4-11. Diurnal Patterns for Fresno
 on August 30-31, 1972 (Sheet 1 of 2)



b. Condensation Nuclei Concentration, Extinction Coefficient, Carbon Monoxide, Total Hydrocarbons and Methane
Figure 4-11. Diurnal Patterns for Fresno on August 30-31, 1972 (Sheet 2 of 2)

SC524.25FR



a. Total Filters

b. After Filters

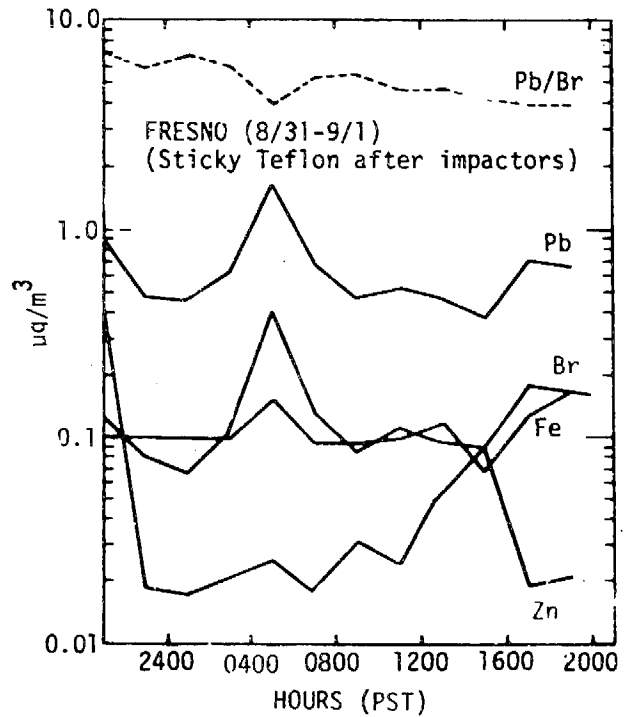


Figure 4-12. Diurnal Patterns of Heavy Elements for Fresno August 31 - September 1, 1972

SC524.25FR

The after filter data accompanying the results in Figure 4-12a are shown in Figure 4-12b. Here, the diurnal pattern of lead and bromine are similar to those observed for the total filter case; yet, as would be expected, the lead and bromine are somewhat lower in concentration. In this case, the iron concentration is considerably lower than on the total filter, indicating that the source of iron particles in Fresno was in the large particle range.

B. SELECTED EPISODES FROM THE 1973 PROGRAM

The 1973 observational study provided a broad range of information on conditions ranging from light to heavy smog in the South Coast Basin. Conditions were experienced at different locations that represented very intense photochemical activity. Examination of the results generally revealed diurnal changes that were qualitatively similar to those observed in 1972 at equivalent locations. Study of the data taken in 1973 was concentrated on the secondary aerosol processes contributing to smog so that the discussion below excludes further review of the heavy element results.

1. WEST COVINA - JULY 23-26, 1973

One of the most striking series of data was obtained at West Covina during two days that experienced oxidant levels exceeding 0.4 ppm. The July 23-26 period is of particular interest in that it was the first attempt by the Environmental Protection Agency to advise curtailment of activities in the South Coast Basin based on forecasted oxidant behavior.

The episodes began the night of July 23, and observations were continued intermittently through July 26, the day that the inversion broke up and created conditions for a significant reduction in smog intensity.

The changes experienced on the first day are shown in Figure 4-13. The observations indicate the classical gas phase patterns of smog evolution with the peak oxidant occurring in the middle afternoon, and the NO_x concentration peaking in the morning. Accompanying the ozone maximum is the SO_2 maximum and the relative humidity minimum. The ozone level on this day exceeded 0.5 ppm.

The winds were light with variable direction at night followed by the common southwesterly flow of the sea breeze during the midday.

The aerosol behavior showed a sharp morning maximum in b_{scat} and the

SC524.25FR

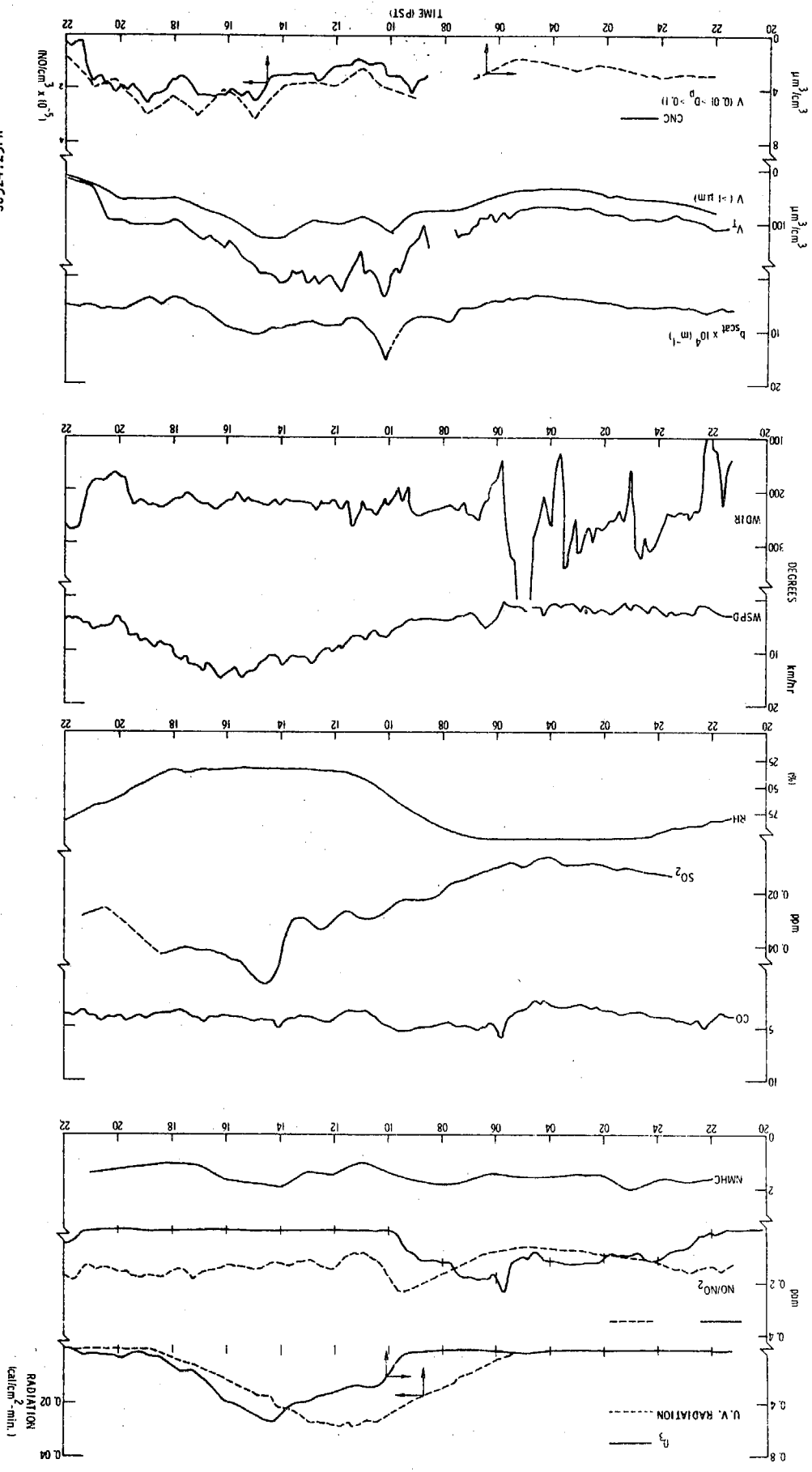


Figure 4-13. Diurnal Changes at West Covina - July 23-24, First Day of Intense Pollution Episode

SC524.25FR

particle volume followed by a general increase in the light scattering range through midday. The CNC were quite variable and in the range of 10^5 particles/cm³.

Figure 4-14 shows the conditions experienced during the following day, July 24. The general pattern of behavior of the aerometric parameters was similar to the previous day. The oxidant peak reached only 0.4 ppm, but lasted substantially longer.

The data on July 25 were intermittent because of a breakdown of the data acquisition system. However, there are sufficient results to give a picture of the changes through the day.

The sequence between July 24 and July 25 fails to show any strong differences in gas pollutants despite the fact that the second day represents a mixture of smog residue remaining overnight combined with fresh emissions resulting from the low inversion conditions during this period.

The patterns measured during the third day shown in Figure 4-15 again are similar, but the oxidant levels were significantly lower. By early morning of July 26, the inversion had broken, and fresher air penetrated inland. Even so, the ground, wind speed and direction were similar to previous days.

In contrast to the previous days, the light scattering peaked in the morning and not with the ozone maximum. On this day, the particle volume is less well correlated with b_{scat} than in other cases.

Again, the examination of the data on July 26, the third day in the series, fails to indicate major diurnal differences in the pollutant gas behavior.

Changes in Aerosol Chemistry

The data obtained for daily variations in $\text{SO}_4^{=}$, NO_3^- , and non-carbonate carbon at West Covina for the period July 23-24, 1973 through July 25-26, 1973 are shown in Figure 4-16. Beginning the night of July 23, 1974, the changes in particulate sulfur indicate a maximum during the midafternoon of the first day that corresponds well with the ozone maximum and the maximum in non-carbonate carbon concentration. In contrast, the nitrate has a maximum concentration that relates well with the NO_x maximum in the morning.

There are distinctions between the size distributions of the three major

SC524 .25FR

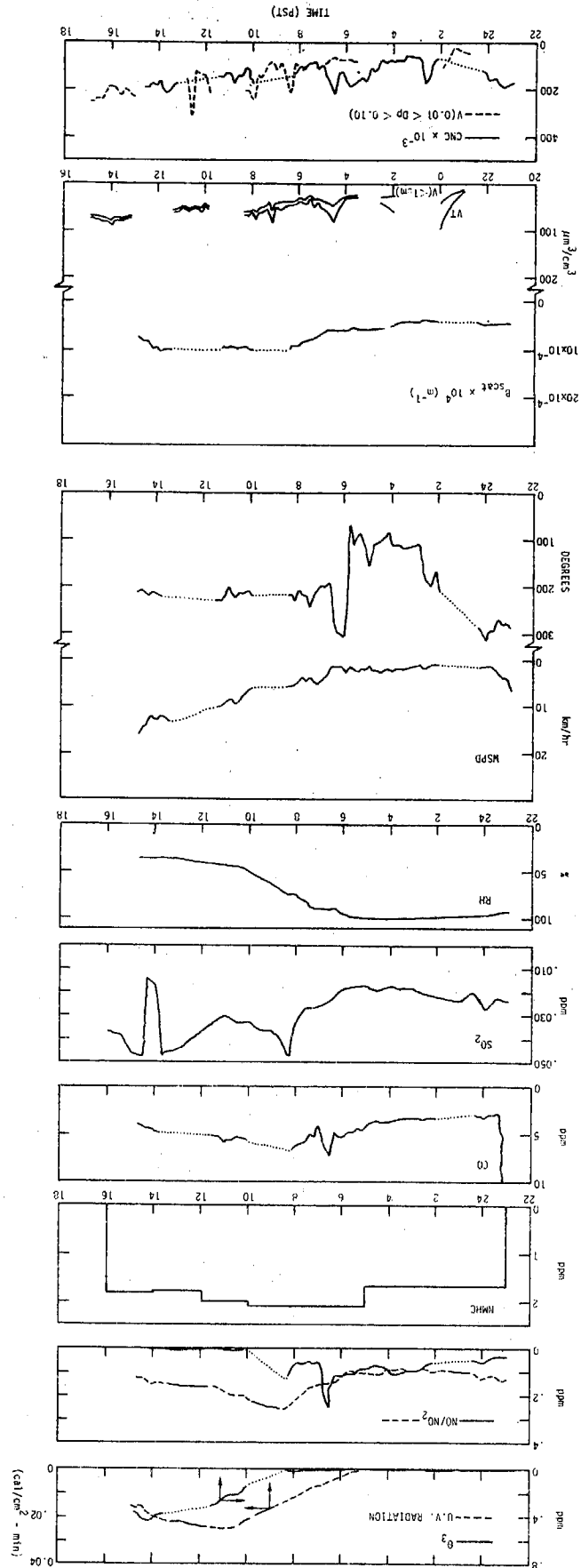


Figure 4-14. Diurnal Changes at West Covina - July 24-25, 1973
Second Day of Intense Pollution Episode

SC524.25FR

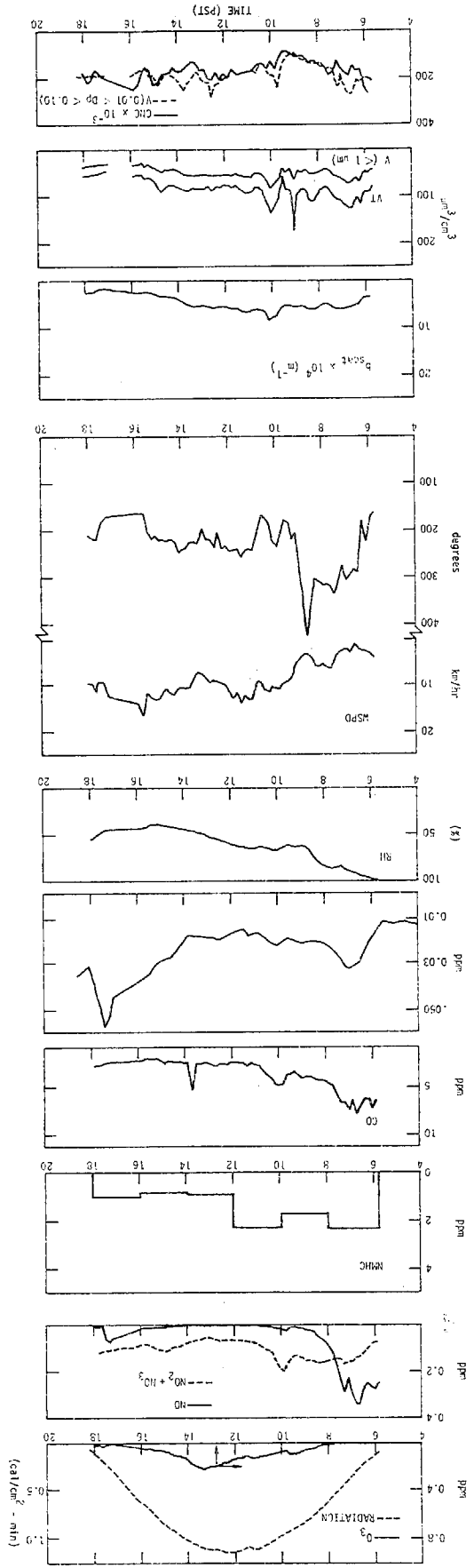


Figure 4-15. Diurnal Changes at West Covina - July 26, 1973
Third Day of Intense Pollution Episode

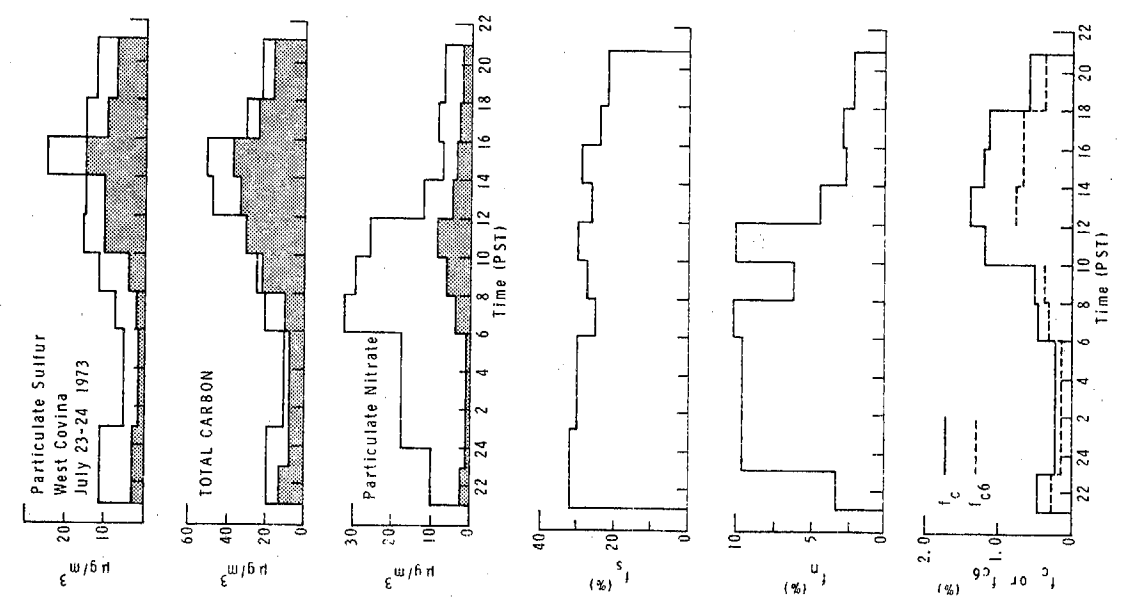
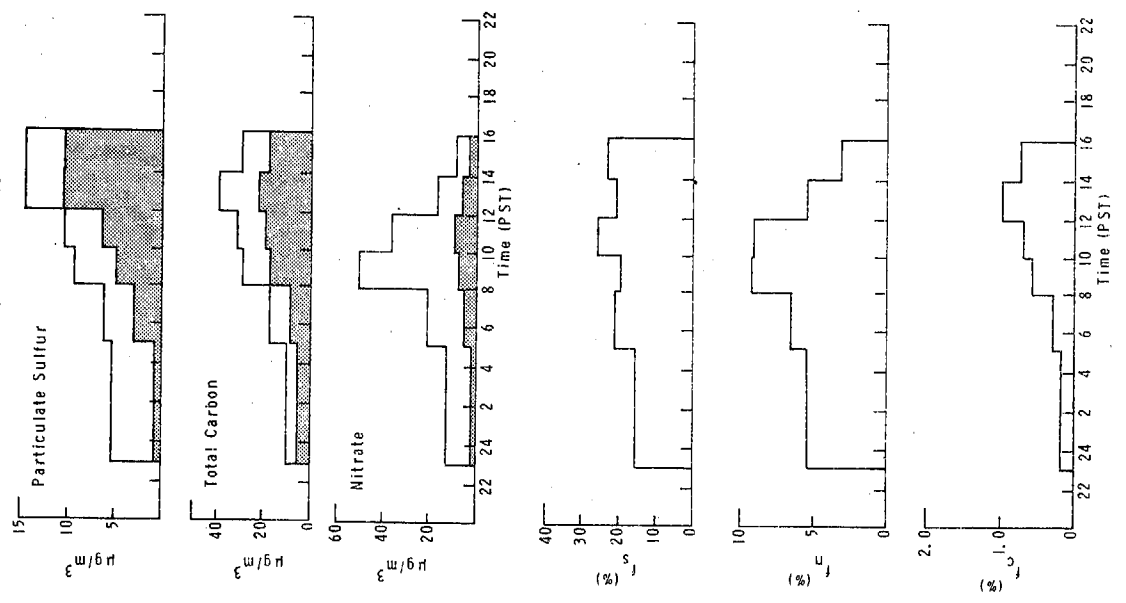
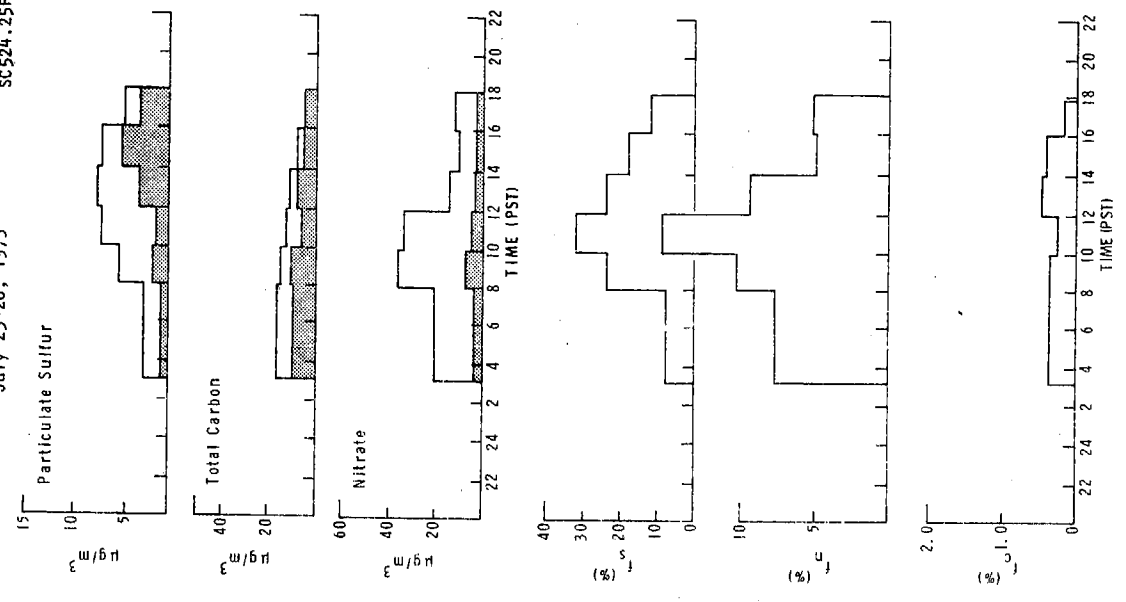


Figure 4-16. Diurnal Changes at West Covina
July 23-26, 1973 4-53

Constituent in particles
<math><0.5\mu\text{m}</math> diameter

SC524.25FR

aerosol components. The sulfur ranges from being concentrated in the larger particles at night to being identified more with the small particles ($< 0.5 \mu\text{m}$) during the day. In contrast, the carbon is found primarily with the particles less than $0.5 \mu\text{m}$, except during the morning heavy traffic period between 0600 and 0800 AM. The nitrate was found to link heavily with particles larger than $0.5 \mu\text{m}$ diameter except for the midafternoon period.

A useful index of the conversion of material into aerosol particles, as for example $\text{SO}_2 \rightarrow \text{SO}_4^{=}$, can be defined by normalizing the concentration of the material in the particulate phase by the total amount of material present. These conversion ratios based on mass per unit volume, are defined as follows:

1) Sulfur

$$f_S = \frac{\text{particulate sulfur based on sulfate}}{(\text{particulate sulfur from sulfate} + \text{gaseous sulfur from } \text{SO}_2)} \quad (4.1)$$

2) Nitrogen oxide*

$$f_N = \frac{\text{particulate nitrogen based on } \text{NO}_3^-}{(\text{particulate nitrogen from } \text{NO}_3^- + \text{gaseous nitrogen from } \text{NO}_2)} \quad (4.2)$$

3) Non-carbonate secondary carbon

$$f_C = \frac{(\text{particulate carbon} - \text{primary particulate carbon})}{[(\text{particulate carbon} - \text{primary carbon}) + \text{non-methane hydrocarbon vapor}] \quad (4.3)$$

For purposes of estimation of f_C , the primary carbon has been assumed to be equal to

$$\alpha \times \text{lead concentration, where } \alpha = 1.0.^+$$

The f_N ratio also could be defined in terms of the total NO_x . However, for purposes of this study NO_2 has been used because of the identification of NO_3^- with aqueous media. NO is insoluble in water, while NO_2 is soluble; NO_2 reacts with water to provide essentially a very high equivalent solubility (see also Section V).

+This underestimates the primary carbon contribution because of the contributions from non-automobile sources (see also Chapter X).

SC524.25FR

In Equation 4.3, the non-methane hydrocarbon mass concentration has been calculated by assuming a conversion from parts per million vapor (as CH_4) by a vapor density of $2 \times 10^{-3} \text{ gm/cm}^3$, which is equivalent to a C_3 hydrocarbon vapor such as propane. C_3 is presumed to be a useful average carbon number for non-methane hydrocarbons.

The conversion ratios for the West Covina data are shown in Figure 4-16 with the other diurnal changes. The variations in these ratios make more clear the impact of the secondary conversion processes. On the first two days in this series, the sulfur ratio, f_s , remained nearly constant, varying from 0.2 - 0.3. On the third day, July 26, a stronger variation in f_s was observed, with a maximum in midmorning. In contrast to the sulfur behavior, the nitrogen ratio is more variable, has a morning maximum on all three days, and an average level of 0.05 to 0.10. The carbon ratio, as defined above, remained below 0.01, except during midday of July 24. Generally, a midafternoon maximum is shown that follows closely the behavior of ozone.

2. POMONA - AUGUST 16-17, 1973

The Los Angeles County fairgrounds was visited again in 1973 to provide additional data in this area complementing the 1972 sampling program. Unfortunately, the fairgrounds was undergoing painting and clean up during our stay in 1973, which may have provided a local source for nuclei and hydrocarbons. Such an influence was not readily detectable in the data, however.

An example of the 1973 Pomona results is shown in Figure 4-17 for the episode covering August 16-17, 1973. The gas pollutant behavior displays the familiar changes, with ozone peaking in midafternoon. The non-methane hydrocarbons remain nearly constant at approximately 1 ppm concentration, yet a systematic decrease is seen after early morning. The SO_2 concentrations follow the ozone behavior, as in West Covina. CO shows a maximum during the morning traffic period.

During this episode the familiar sea breeze pattern developed with westerly, brisk winds from midmorning through the afternoon.

In this case, the light scattering and particle volume displays a midday maximum over approximately the same period as the ozone buildup,

SC524-25FR

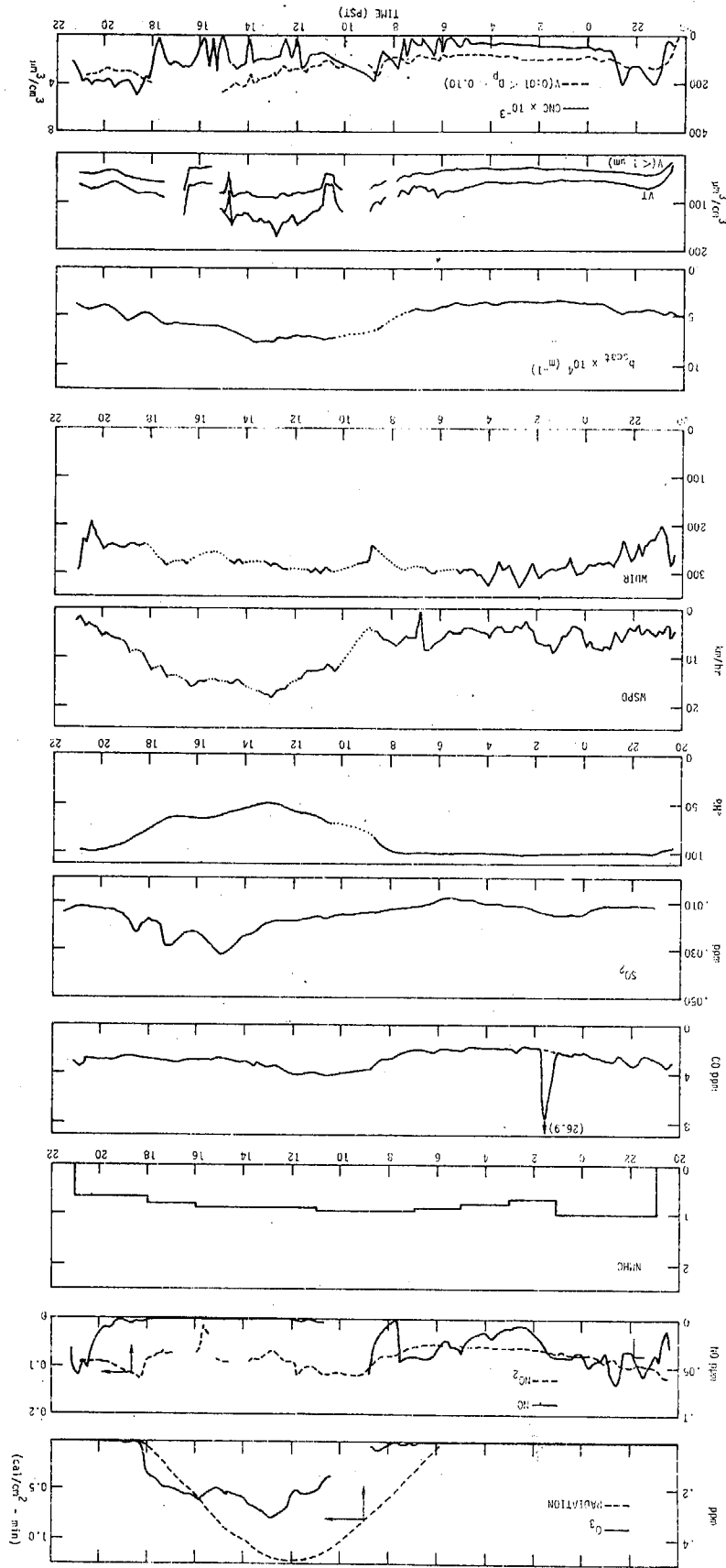


Figure 4-17. Diurnal Changes at Pomona
August 16-17, 1973

SC524.25FR

while the Aitken nuclei were maximum at night or during the 0800-1000 AM heavy traffic period.

Changes in Aerosol Chemistry

The behavior of the major aerosol constituents is shown in Figure 4-18. In this episode, the particulate sulfur reaches a maximum late in the afternoon with the SO_2 maximum. The total carbon displays a maximum from 1200-1400 PST closely corresponding to the ozone maximum. Again the nitrate develops a strong transient maximum with the morning NO_x maximum, but builds up again at lower levels during the night with high humidity.

The distinction in particle size between species again appears in these data. The particulate sulfur shifts from concentration in larger particles at night more to the submicron range during the day. Yet the conversion ratio for sulfur remains roughly constant between 0.25 - 0.35, but showing a weak maximum at midafternoon.

The total carbon was found principally in the submicron particles below $0.5 \mu\text{m}$ diameter, and a maximum concentration developed by midafternoon. The carbon conversion ratio peaked with ozone in the early afternoon, with values exceeding 1%.

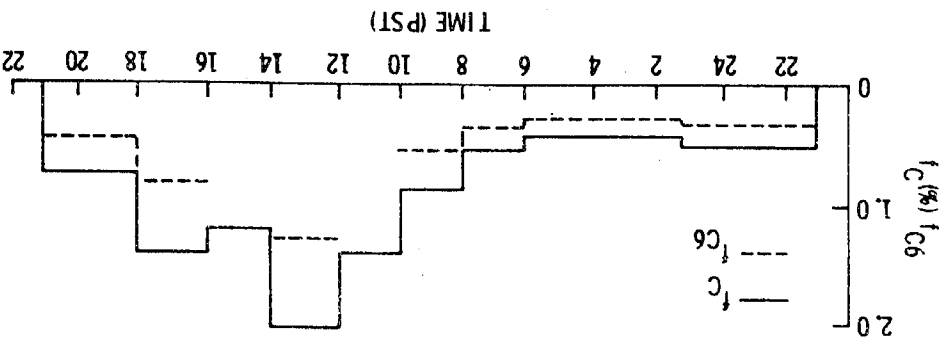
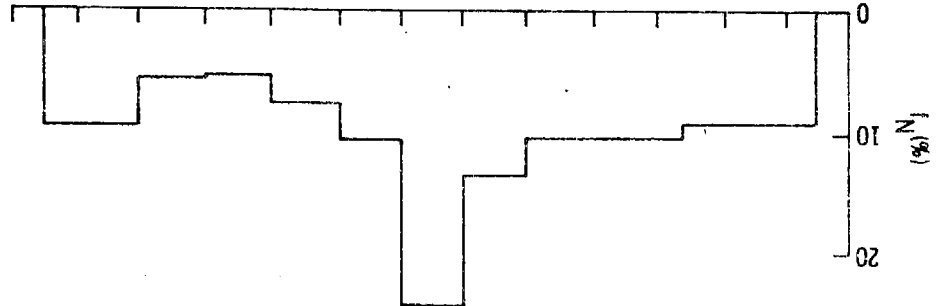
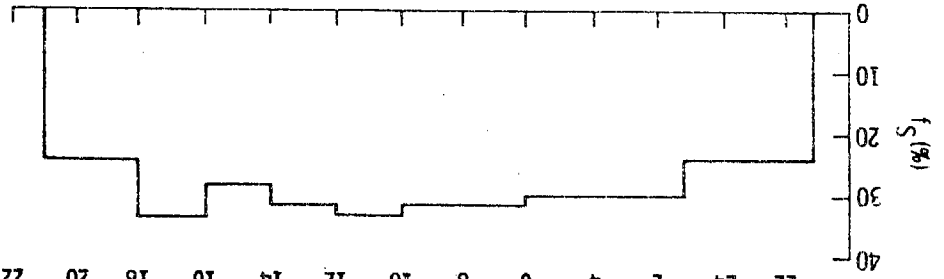
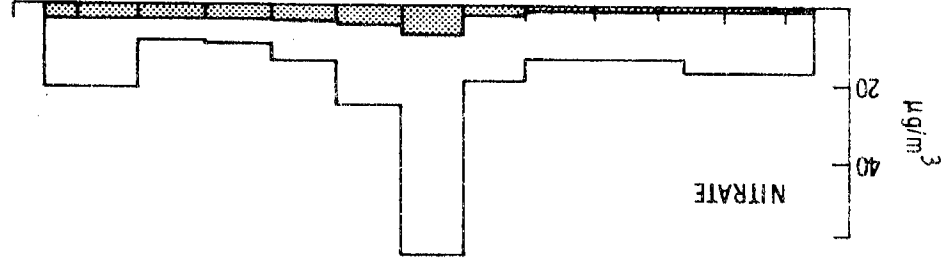
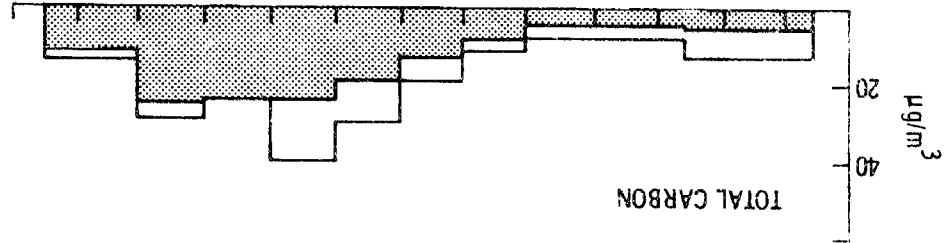
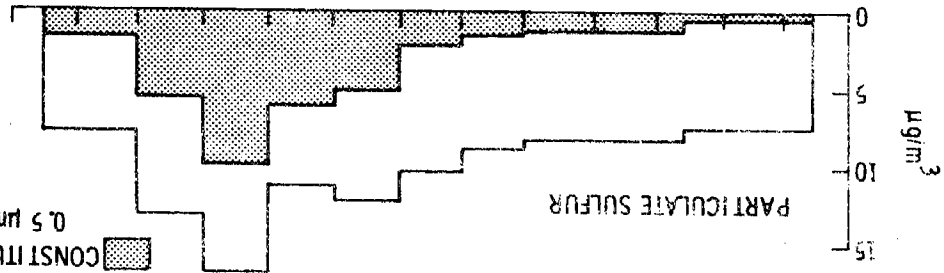
The nitrate again was concentrated in the larger particles at Pomona. The nitrogen conversion ratio displayed a strong maximum from 0800-1000 AM with a minimum in the midafternoon.

3. RUBIDOUX EPISODES

a. Case 1 - September 5-6, 1973

Two episodes at the Rubidoux site have been selected to show the nature of smog behavior in the eastern portion of the air basin. The first case is the period September 5-6, 1973, which is shown in Figures 4-19 and 4-20A. This case corresponds to the day of the blimp flight. The data show once again the expected qualitative changes in the photochemical pollutant gases. In the Riverside area, however, there is a strong influence of air transport on such patterns, as indicated, for example, by the appearance of the ozone maximum later in the afternoon compared with sites farther westward. Unfortunately, on this day the Varian sulfur chromatograph was inoperative so that

CONSTITUENT IN PARTICLES
0.5 μm diameter



SC524.25FR

VOLUME IV



Figure 4-18. Diurnal Patterns for Aerosol Constituents for Pomona August 17, 1973

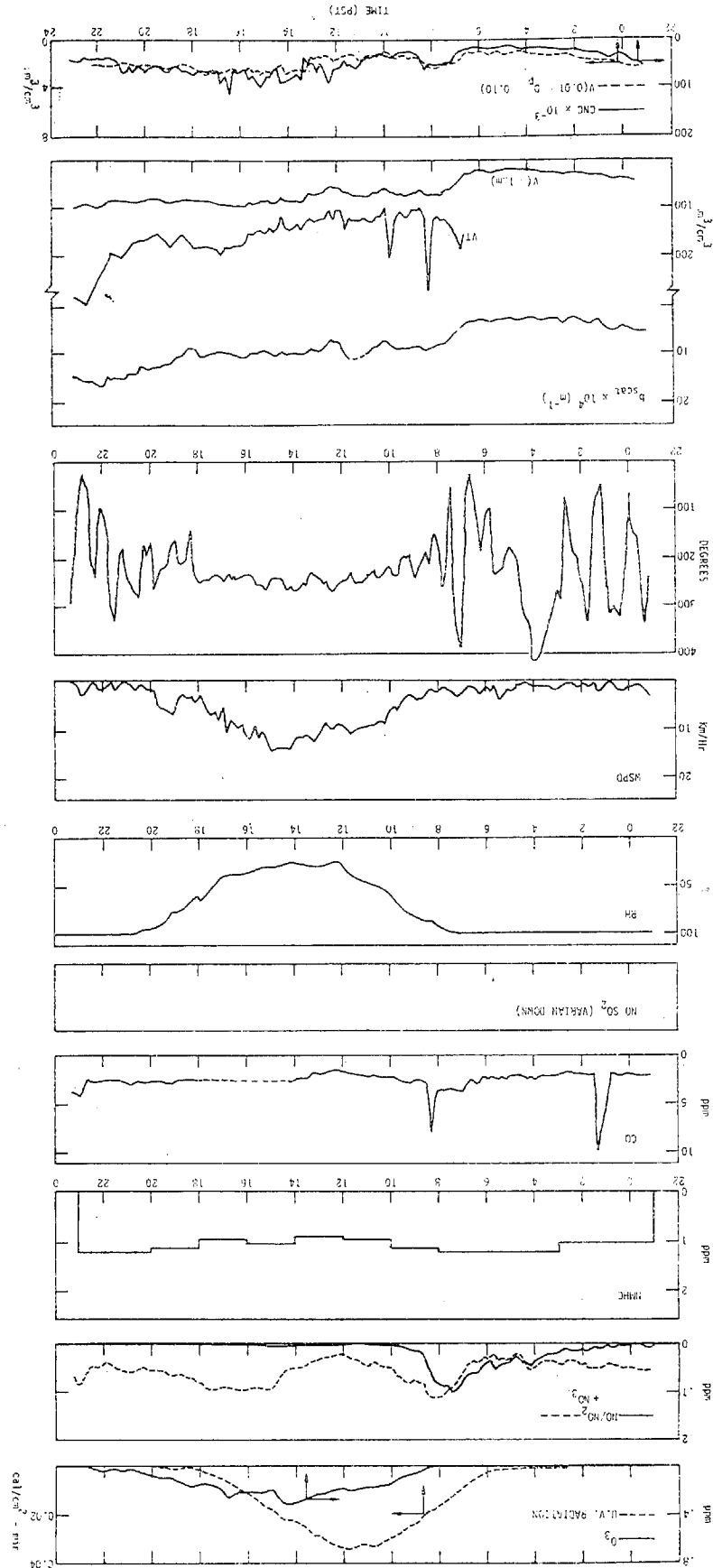
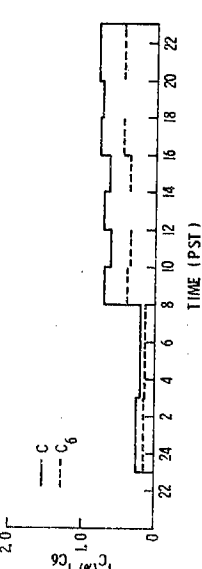
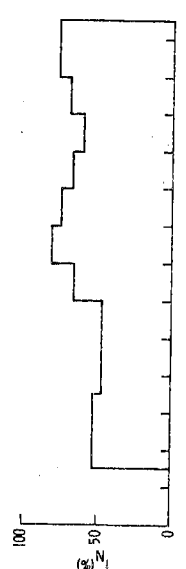
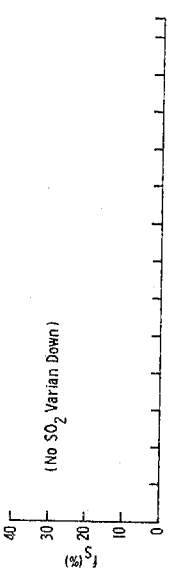
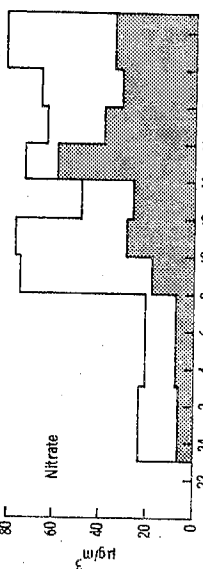
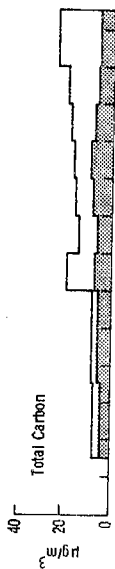
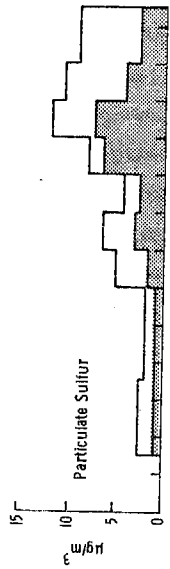


Figure 4-19. Diurnal Changes at Rubidoux
September 5-6, 1973

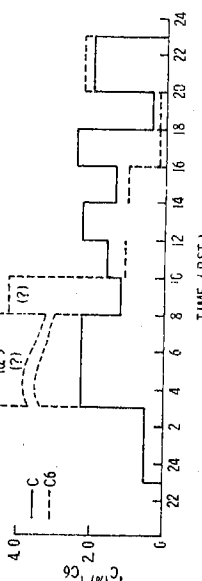
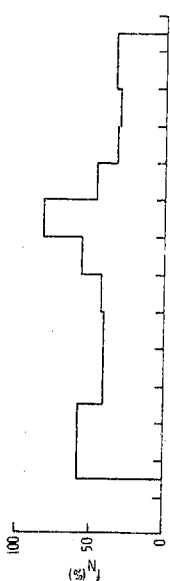
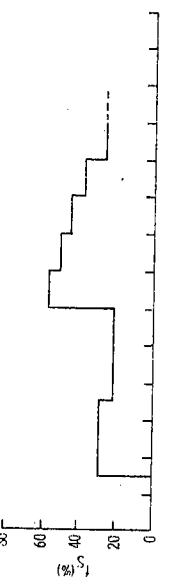
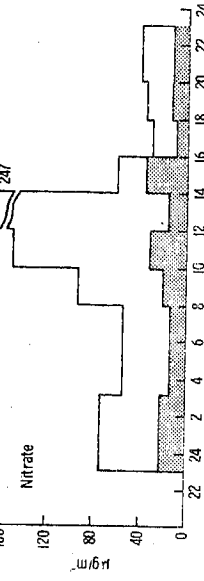
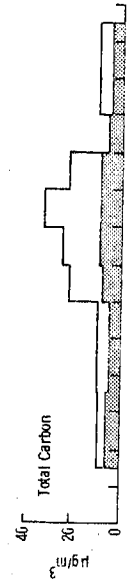
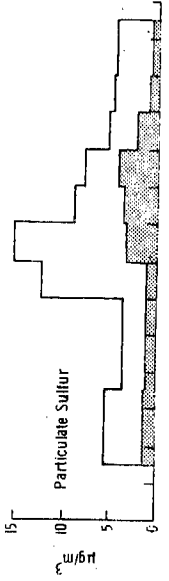
VOLUME IV

September 5-6, 1973



Constituent in particles <0.5µm in diameter

September 19-20, 1973



September 27-28, 1973

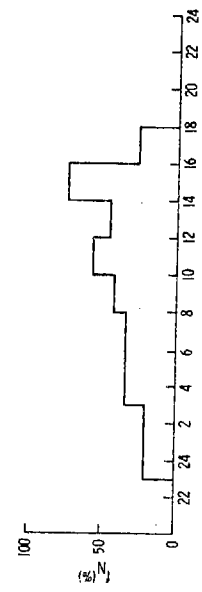
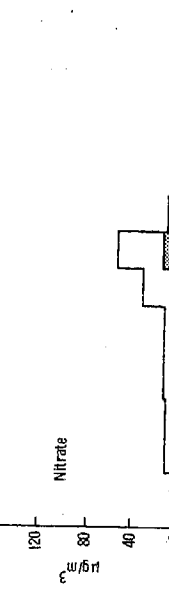
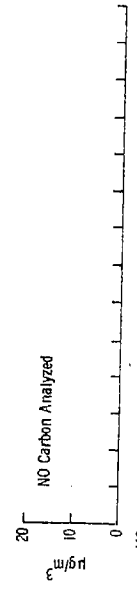
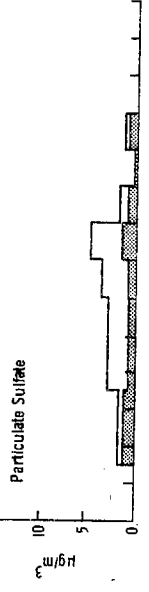


Figure 4-20. Diurnal Patterns for Aerosol Constituents for Rubidou.

September 1973

SC524.25FR

the sulfur gas results were unavailable.

The winds show the typical sea breeze configuration with light west winds in midday. However, there is evidence of stagnation in this area during the night, which is a common phenomenon in the eastern part of this air basin.

The aerosol behavior here is of interest. The value of b_{scat} is significantly larger much of the day compared to other sites to the west. During the day, b_{scat} was $10 \times 10^{-4} \text{ m}^{-1}$ or greater even though the oxidant concentrations only reached a maximum of about 0.3 ppm. In contrast with the high concentration of material in the range $> 0.1 \mu\text{m}$ diameter, the Aitken nuclei concentration was significantly lower at this site than found farther west.

Changes in Aerosol Chemistry

The diurnal behavior of the key aerosol components is shown in Figure 4-20. For September 6, 1973, the particulate sulfur experienced a peak in late afternoon accompanying the maximum ozone concentration. The particulate carbon increased during the day and continued to rise throughout the episode. The nitrate showed a morning maximum as observed at the western sites, but increased again in late afternoon and at night on September 6. Very high levels of nitrate were detected compared with sites to the west whereas the sulfate and carbon concentrations were about the same as other locations.

A distribution of constituents with respect to particle size was found where the sulfate shifted during the day from larger particles to smaller ones. The nitrate generally was found more in the larger particles, except during the afternoon. In contrast to other sites, however, the carbon was in larger particles during this episode than observed further west, particularly during the day.

The nitrate ratio at Rubidoux is much larger than observed elsewhere. It is uncertain whether this reflects a loss of NO_x to the surface during eastward transport, or the strong conversion of NO_x species to nitrate by chemical processes at the east side of the Basin.

b. Case II - September 19-20, 1973

The second episode studied at Rubidoux is shown in Figure 4-21. In this

SC524.25FR

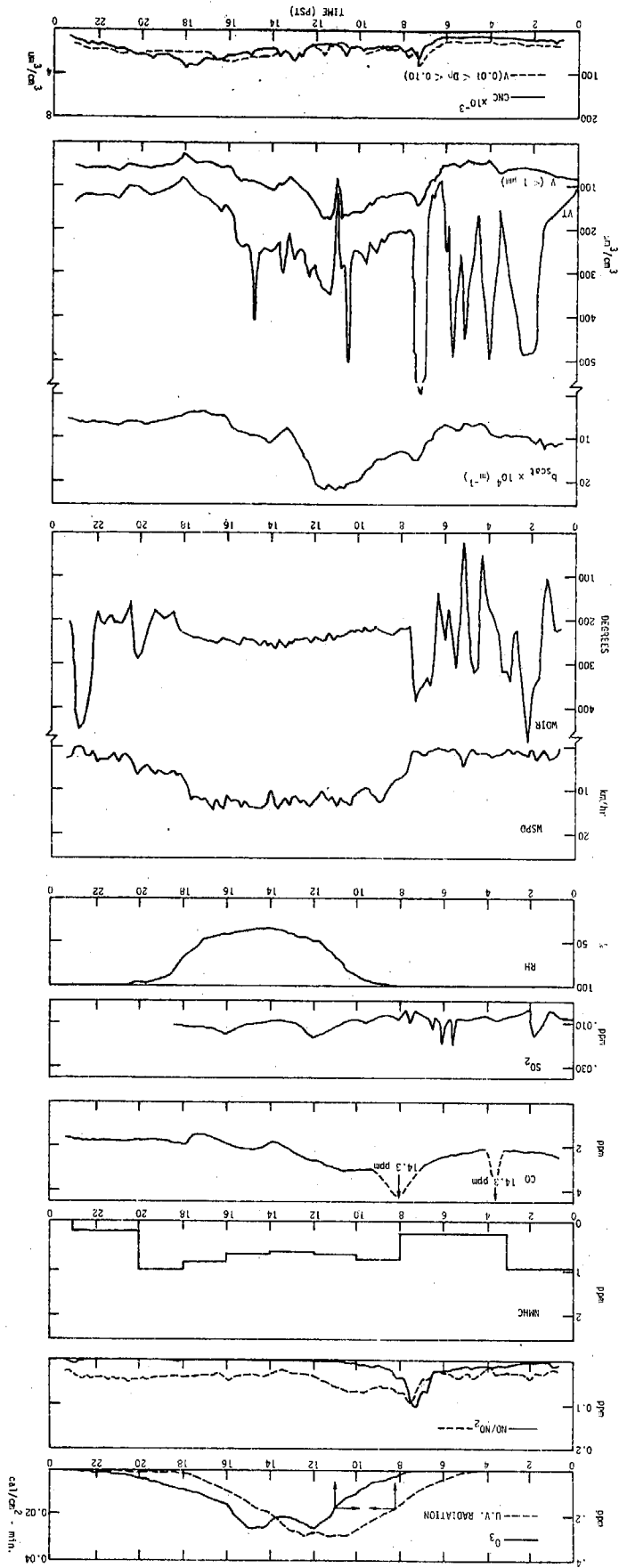


Figure 4-21. Diurnal Change at Rubidoux
September 20, 1973

SC524.25FR

case the apparent transport effect is revealed in the dual ozone maxima, one at noon and the other late in the day. Interestingly enough, the SO_2 pattern shows a similar double peak. The behavior of other pollutant gases is similar to other sites.

The wind pattern again shows the typical sea breeze regime, with very light winds at night.

On this day, b_{scat} was observed to be very high in the morning but decreased in the afternoon to levels well below 10^{-3}m^{-1} . There were large oscillations in the particle volume during the night and early morning, whose origins are uncertain. However, the volume in the fraction $< 1 \mu\text{m}$ shows a remarkable similarity to the b_{scat} data. Again in this episode the Aitken nuclei concentrations are significantly lower than at other sites in 1973, particularly at night.

Changes in Aerosol Chemistry

The September 19-20 period, in contrast to the September 6 episode (see Figure 4-20), the particulate sulfur showed a maximum at morning and midday with the first SO_2 maximum. The total carbon displayed a maximum somewhat later. The nitrate behavior in this case showed a very intense maximum of $247 \mu\text{g}/\text{m}^3$ in the early afternoon, which evidently overshadowed the morning maximum observed on other occasions. Again, the nitrate levels are much higher than elsewhere in the Basin.

The sulfur conversion ratio was variable, with a maximum value of ~ 0.60 in the late morning while the nitrate conversion ratio peaked in the early afternoon, approaching unity. The carbon ratio was variable, ranging from 1-2% much of the day, but showing an unsystematic behavior which differs from the midday maximum observed on other occasions.

The size distribution of constituents differed from other cases on September 20, 1973. More of the particulate sulfur was found in the larger particles, particularly during the midday, which appears to be similar to the nitrate distribution. Similarly, more carbon was found in larger particles during the midday, as compared with other cases.

Because of the interest in the behavior of the aerosol species at Rubidoux, data for nitrate and sulfate for the episode on September 28, 1973

SC524.25FR

were added to Figure 4-20. This case was a day in which a build-up of pollutants took place in the morning, but an east wind condition developed by mid-day preventing the further evolution of smog in the Rubidoux/Riverside area.

As expected, the concentrations of nitrate and sulfate are significantly lower in this case than days with heavier pollution. Again the size distribution of nitrate and sulfate in this case shows a concentration of both species in the larger particles during the day, but in contrast the sulfate appears to be identified with the smaller particles at night. It is interesting that the humidity was quite low (< 40%) during the afternoon on September 28, 1973.

The conversion ratios for sulfur and nitrate are indicated in Figure 4-20 for the September 28 episode. A greater sulfur conversion ratio was found in the morning when the pollution levels and the humidity were higher than in the afternoon. However, the nitrate conversion ratio showed an apparent maximum in later afternoon, which is quite different from other cases examined.

4. DOMINGUEZ HILLS

The last site the mobile laboratory visited in 1973 was Dominguez Hills on the southwest side of the Los Angeles area. This location was chosen to look for the influences of pollutant behavior just downwind from several major stationary sources. To the south are the Stauffer Chemical Works that produce sulfuric acid, as well as refineries and large power plants. To the west are several refineries and chemical plants.

The diurnal changes for two different episodes at Dominguez Hills are given in Figures 4-22 and 4-23. The first case, on October 4-5, 1973, was a day of high relative humidity strongly influenced by winds from the south. However, the second case displayed a wider variation in humidity and a dominance of a westerly wind.

At this location, concentrations of NO_x and hydrocarbons were similar to

SC524.25FR

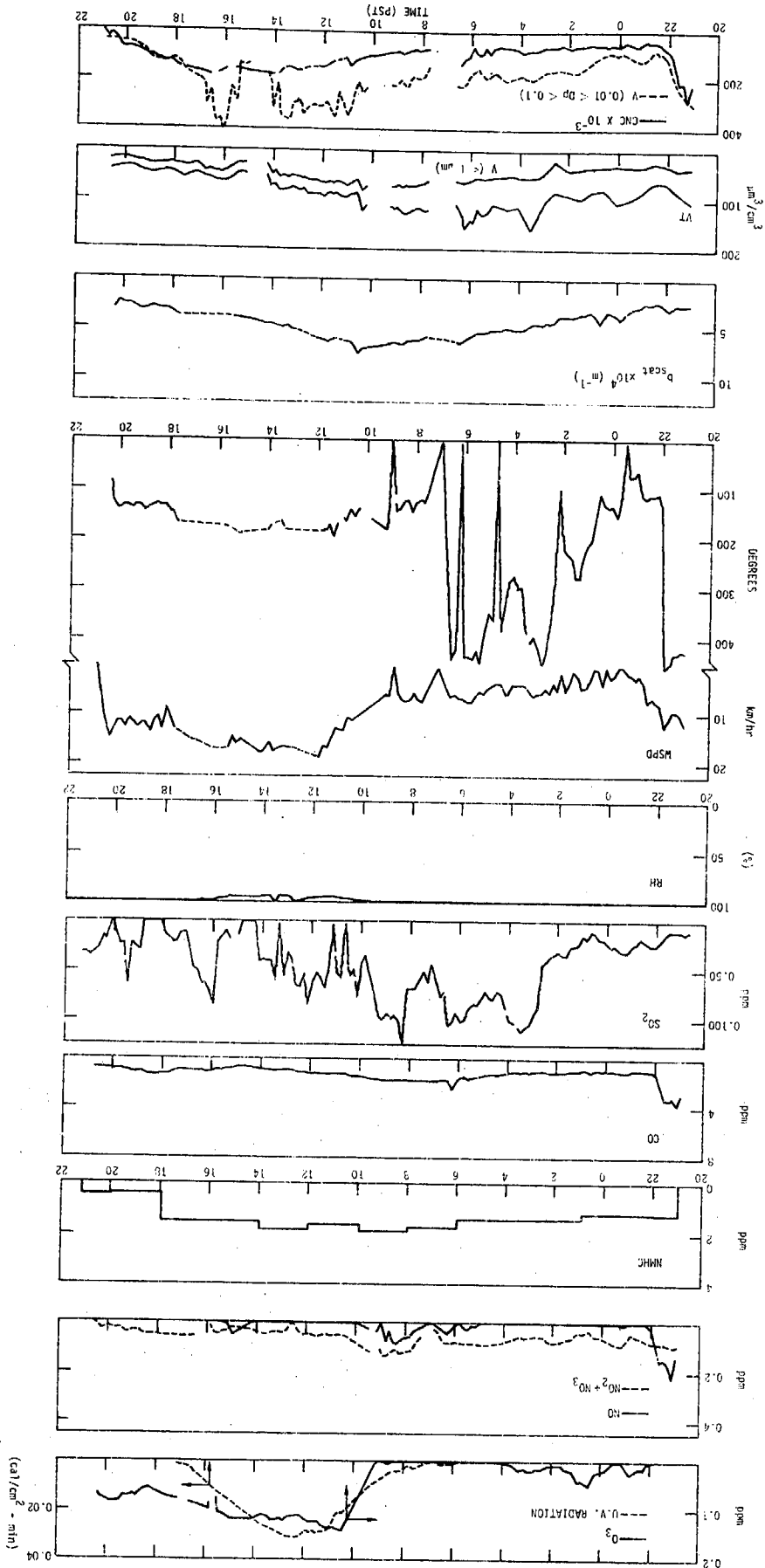


Figure 4-22. Diurnal Changes at Dominguez Hills
October 4-5, 1973

SC524-25FR

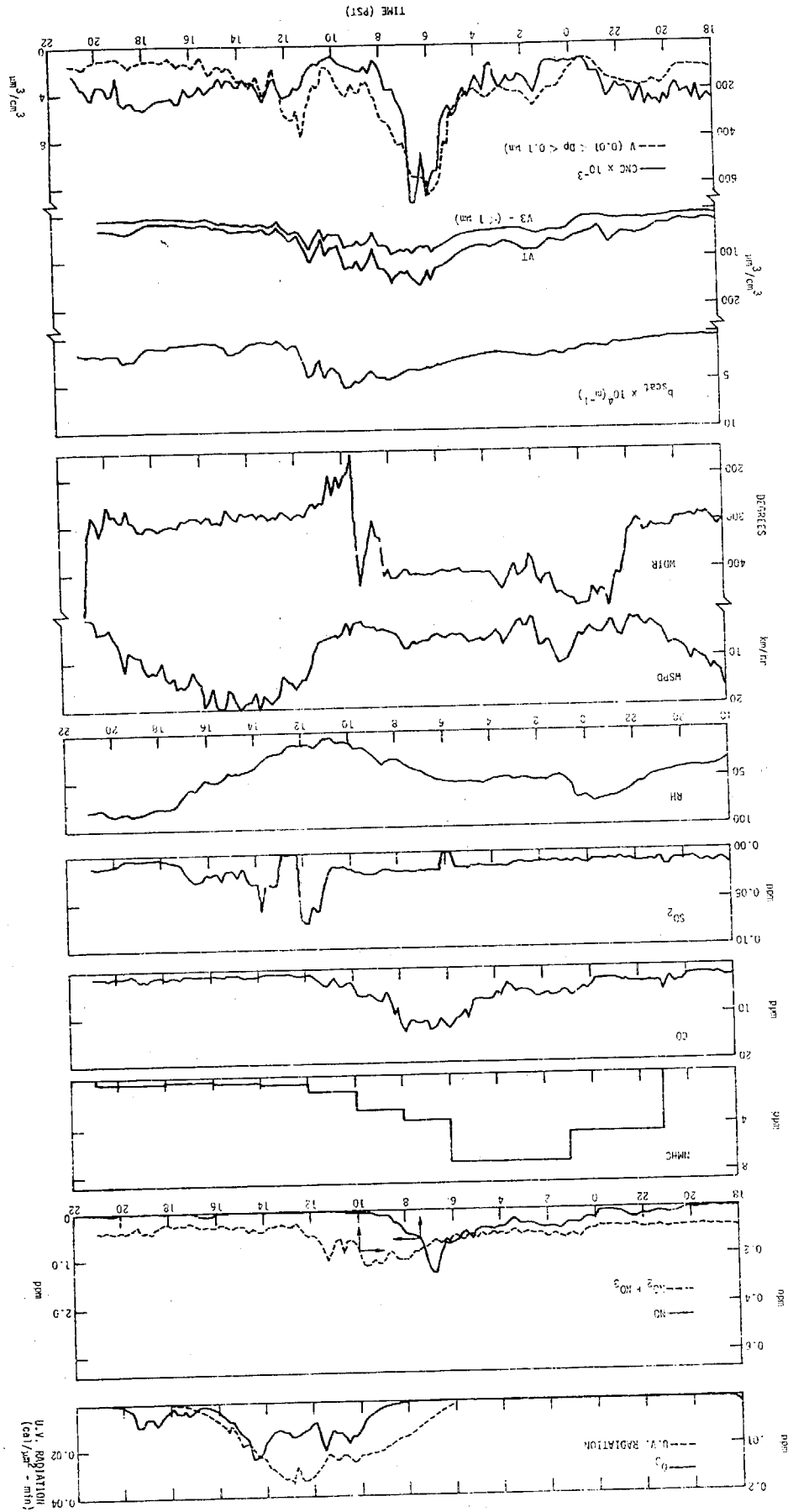


Figure 4-23. Diurnal Changes at Dominguez Hills
October 10-11, 1973

SC524.25FR

other places. If anything, the non-methane hydrocarbon concentrations were somewhat higher than elsewhere. This is not surprising because the site is surrounded by oil wells and refineries. The levels of oxidant found at Dominguez were lower than elsewhere but were not insignificant. October 10-11 possibly showed more variation in ozone buildup than seen elsewhere. Large amounts of CO were observed in the morning of October 11. Presumably, this associated with heavy local traffic.

The SO₂ levels at Dominguez Hills on October 5 were higher than observed elsewhere but were lower on October 11, 1973.

The light scattering from aerosols did not exceed $7 \times 10^{-4} \text{ m}^{-1}$ during either episode. A midday maximum in b_{scat} was observed with maxima in submicron particle volume concentration. High levels of Aitken nuclei concentration were experienced in the early morning of October 5. The Aitken nuclei concentrations on October 11 were significantly lower than observed on October 5.

Changes in Aerosol Chemistry

The changes in key aerosol chemistry accompanying the patterns in Figures 4-22 and 4-23 are shown respectively in Figures 4-24a and b. On October 5 the particulate sulfur reached a maximum of $15 \mu\text{g}/\text{m}^3$ at midday with the highest SO₂ concentrations of the day. The total carbon peaked somewhat later at 1200-1400 PST, but the nitrate was maximum at night.

On October 11, 1973 a similar result for sulfate was found, but the nitrate displayed a strong maximum in the morning; the concentrations of nitrate were higher on October 11, 1973 than the previous episode, but the sulfate concentrations were substantially lower.

The size distribution of sulfate differed substantially between the two cases. On October 5 most of the sulfate was found in particles larger than $0.5 \mu\text{m}$, while the reverse was true on October 11. On both days, the nitrate was found in the larger particles in the morning. However, on October 5 the nitrate shifted to the submicron particles in the afternoon.

The conversion ratios for sulfur differed substantially over the two episodes. On the earlier day, f_s was between 10% and 20%, but on October 11 the ratio dropped below 10%. The nitrate conversion ratio was variable, but generally remained at about 5%. On October 5, the observed carbon conversion

SC524-25FR

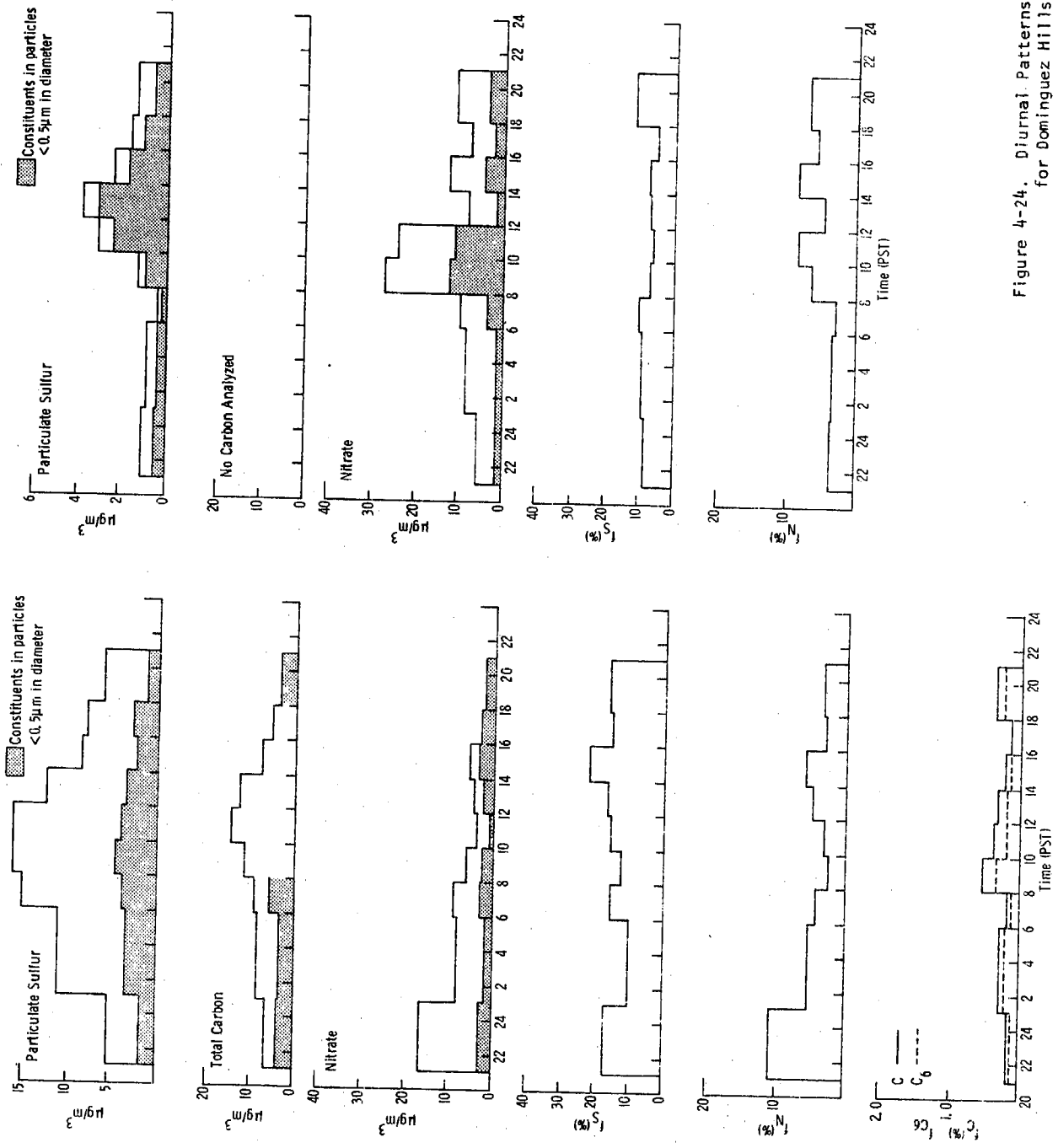


Figure 4-24. Diurnal Patterns of Aerosol Constituents for Dominguez Hills A(WK), B(WL)

SC524.25FR

ratio showed low values, generally less than 0.5%, with two weak maxima occurring at peak traffic hours.

C. CONCLUDING REMARKS

Examination of the diurnal changes in pollutant gases and aerosols indicate that they are closely related phenomenologically in most cases. These coupled changes are linked to the combined influences of atmospheric chemistry and meteorological effects, including advection of pollutants emitted from similar sources. Evidence of photochemical processes emerges from data taken even at very remote sites in California.

The behavior of the volume concentration of particles in the range below 1 μm diameter corresponds well to the changes in light scattering coefficient, as expected. In comparison, the total number concentration of aerosols, as measured by the Aitken or condensation nuclei concentration, varies somewhat independently of b_{scat} . Maxima in total number concentration are frequently observed during periods of peak traffic in the urban areas.

Review of the results indicates that sulfate and non-carbonate carbon concentrations vary in a pattern similar to one another in most cases, with a maximum at the same time as the maximum in the ozone and sulfur dioxide concentrations. On the other hand, the nitrate was found to differ in daily change from the other key aerosol constituents. Nitrate displayed a sharp maximum in the morning along with the maximum in NO_x . It also showed a significantly larger 24-hr average concentration in the eastern parts of the Basin. Sulfate was found to be more uniformly distributed spatially than nitrate.

The marked changes in nitrate concentration as compared with sulfate can be illustrated considering data taken August 17, 1973. Figure 4-25 illustrates the variation of sulfate and nitrate concentrations in time and space on this day in one section of the Basin. At Anaheim, the peak in both nitrate and sulfate concentrations occurred at approximately 0700*. The wind pattern, which persisted throughout the day, carried the material directly toward Riverside along the western slope of the Puente Hills, a trajectory relatively free of additional pollutant sources. Based on the reported wind speed, the morning peak from Anaheim arrived in Riverside at about 10-11 am. This

*Midpoint for 2-hr samples

SC524.25FR

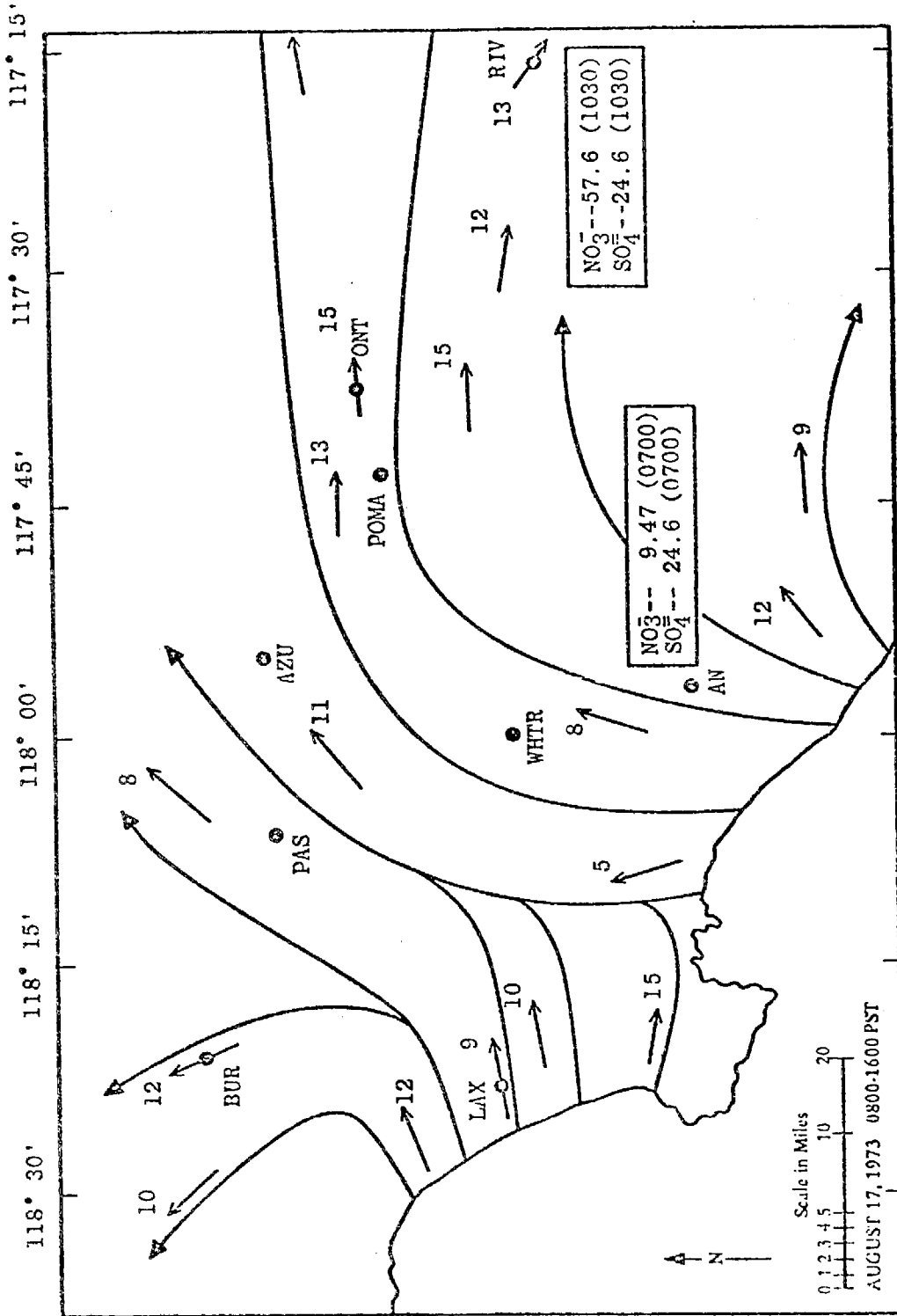


Figure 4-25. The Variation of Nitrate and Sulfate Levels in Time and Space

SC524.25FR

coincides with a maximum observed in Riverside at 1030* for both nitrate and sulfate. The figure demonstrates that nitrate increased substantially while the sulfate concentration remained unchanged.

Values of the conversion ratios are shown in summary in Table 4-1. Averages are given for night periods from 1800-0600 PST, and for day from 0600 to 1800 PST. There are noticeable differences at all stations between night and day. At receptor locations in the central and eastern parts of the South Coast Basin, there is an increase in sulfate and secondary carbon conversion. In most locations a nitrate conversion increase also is found. The marked increase in nitrate conversion on the eastern side of the Basin is well illustrated. At the source dominated area of Dominguez Hills, the night and day pattern differs from other locations. In particular, there actually is a decrease in day time nitrate and carbon conversion ratio here compared with the increase observed elsewhere.

The size distributions of the key constituents differ somewhat. The non-carbonate carbon was present mainly in the particles less than 0.5 μm diameter. Sulfate displayed a variable distribution. During the night and early morning, sulfate was largely contained in particles greater than 0.5 μm diameter, but through the midday and afternoon much of the sulfate was found to be in the smaller particles. Generally, nitrate existed principally in the particles larger than 0.5 μm diameter. On the eastern side of the South Coast Basin, however, more nitrate was observed in the submicron particle fraction. In samples taken at Rubidoux, for example, size distributions of sulfate and nitrate based on 22-hr averaged data showed essentially identical results.

A further comparison of the nature of the sulfate and nitrate distribution is made with the five stage Lundgren impactor data shown in Figures 4-26, 4-27, and 4-28. Particle size is plotted against $\Delta \text{mass}/\Delta \log$ (particle-diameter) so that the area beneath the curve is proportional to the mass of the chemical species in that size interval. In Figure 4-26 the sulfate size distributions are notable for their similarity; all show maximum sulfate contents on stage 4 (geometric mean particle size 0.87 μm).

*Midpoint for 2-hr samples

SC524.25FR

TABLE 4-1

SOME AVERAGE VALUES OF THE CONVERSION RATIO FOR SECONDARY
AEROSOL CONSTITUENTS IN THE SOUTH COAST AIR BASIN

(N = 1800-0600 PST; D = 0600-1800 PST)

LOCATION	SULFUR (%)		NITROGEN (%)		CARBON (%)	
	f_s		f_N^+		f_C	
	N	D	N	D	N	D
A. Western/Coastal						
1. Dominguez	11.9	11.9	5.3	4.65	0.42	0.21
B. Central						
1. Pasadena*	-	29	-	5.8	-	-
2. West Covina	18	24	5.8	7.4	0.26	0.627
C. Eastern						
1. Pomona	27	31	9.4	11.1	0.52	1.23
2. Riverside/ Rubidoux	22.5	29.3	51.1	51.6	0.28	0.39

* From Grosjean and Friedlander (1974)

+ Based on NO₂

SC524.25FR

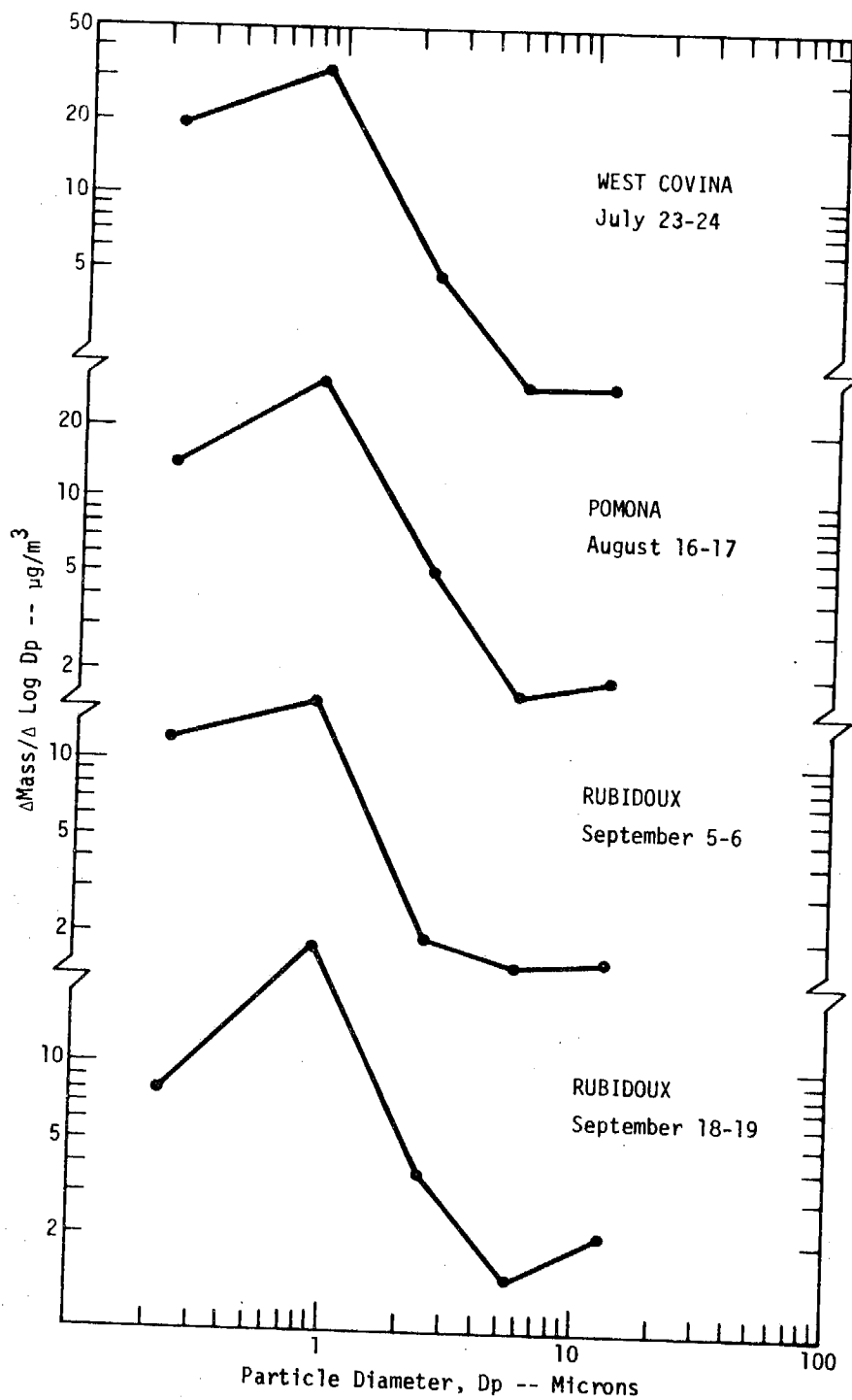


Figure 4-26. 24-Hour Average Size Distributions for Sulfate at Receptor Sites, 1973

SC524.25FR

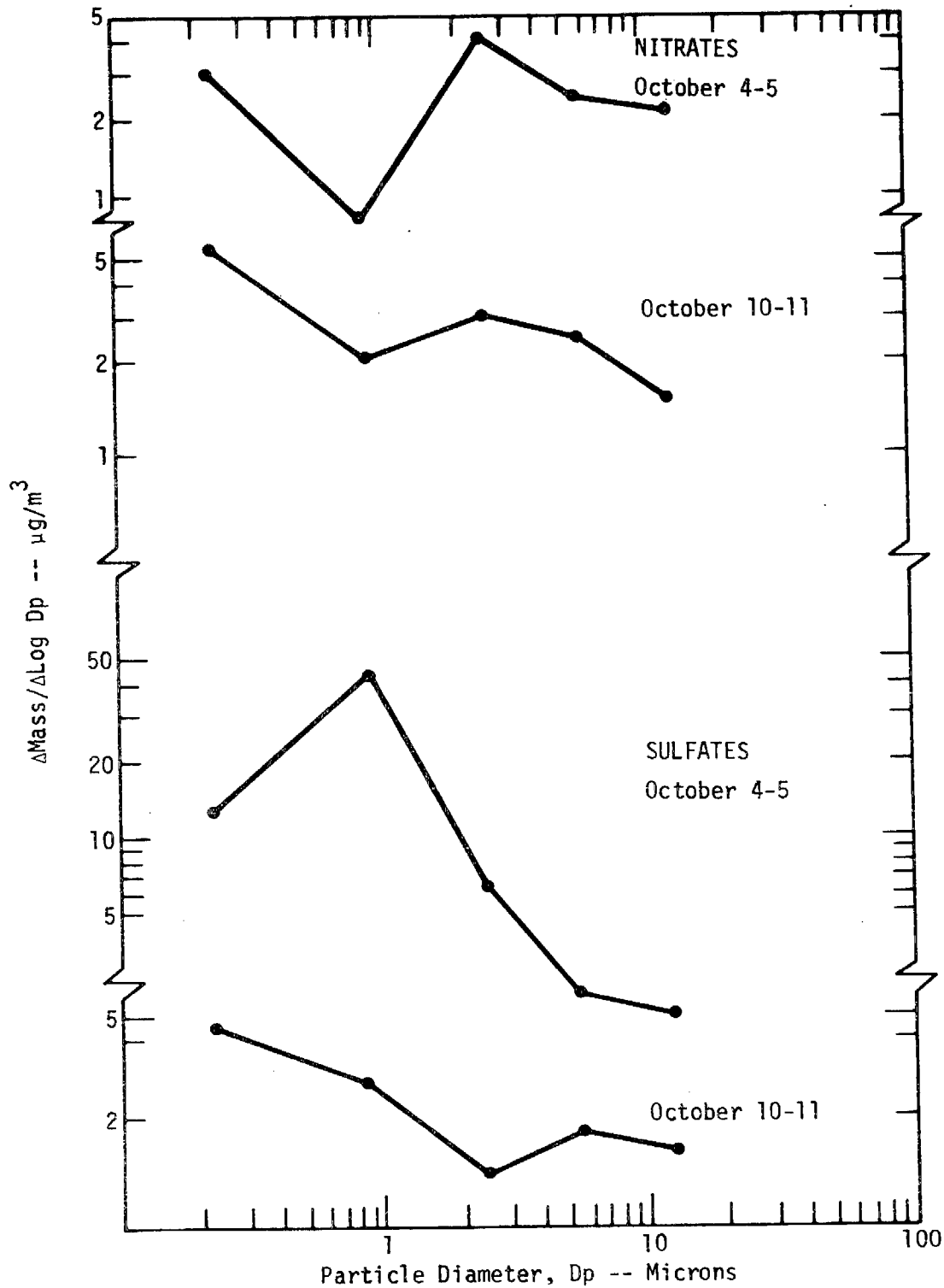


Figure 4-27. 24-Hour Average Size Distributions for Sulfate and Nitrate at Dominguez Hills, 1973

SC524.25FR

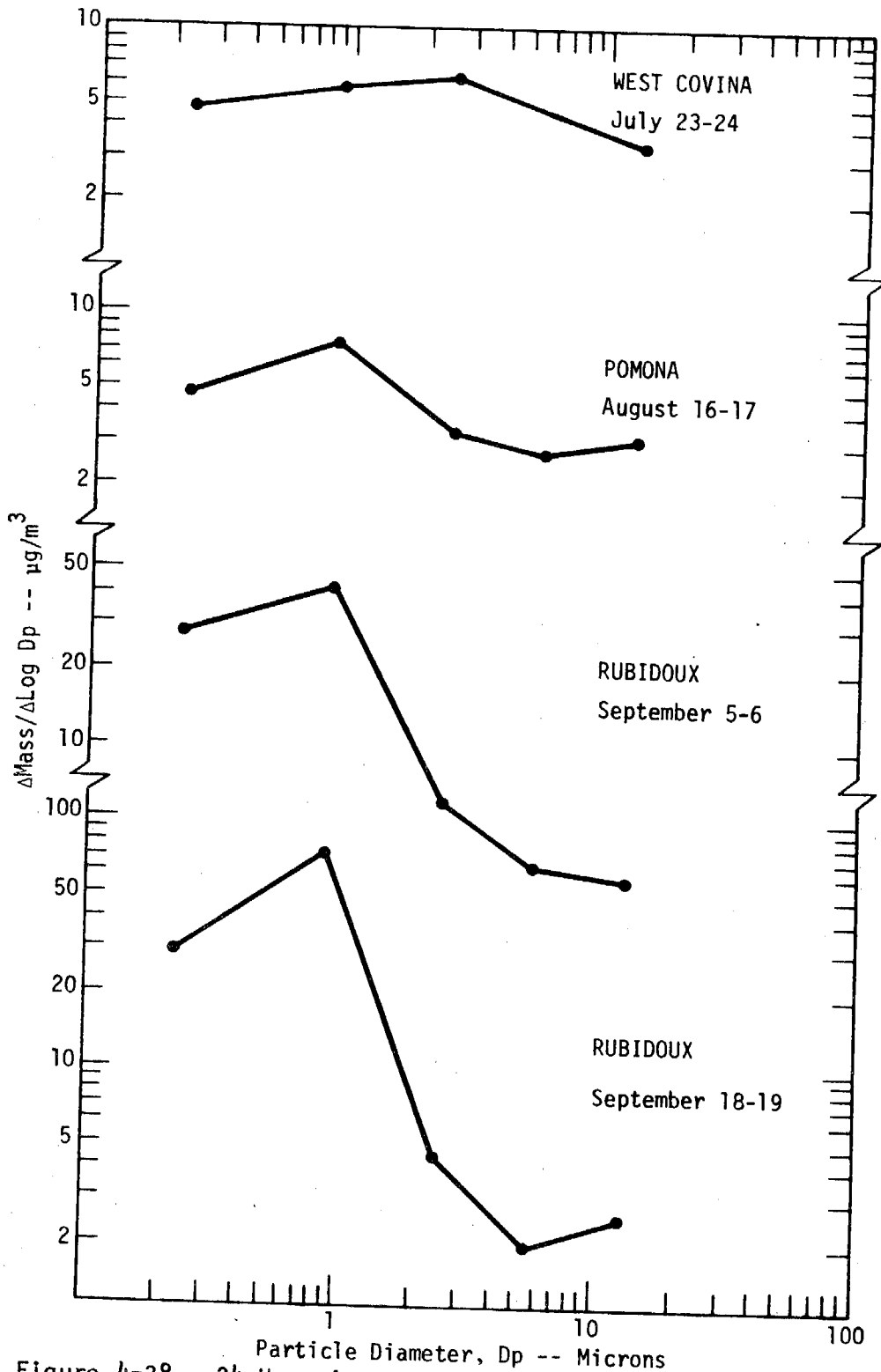


Figure 4-28. 24-Hour Average Size Distributions for Nitrate at Receptor Sites, 1973

SC524.25FR

Figure 4-27 shows the size distributions for both sulfate and nitrate at a source enriched site, Dominguez Hills. On October 4-5, the sulfate distribution strongly resembles that for the receptor sites. On October 10-11, the sulfate level was relatively low and the distribution shifted somewhat toward smaller particle size. However, as shown below, the mass median diameter is not appreciably altered.

The 24-hr average particle size distributions for nitrate (Figure 4-28) display a remarkable change from a nearly flat distribution at West Covina to a sulfate-like size distribution at Rubidoux. The observed size distribution must, of course, reflect the relative importance of small and large particle nitrate formation mechanisms and, since nitrates are quite hygroscopic, possibly the ambient humidity at the time of maximum nitrate concentration.

The size distributions obtained here for sulfate are in excellent agreement with previously reported values obtained in the South Coast Basin and in the San Francisco Bay Area with a Goetz aerosol spectrometer sampling for 8-hr daylight periods.⁽¹⁹⁾ The mass median diameters (mmd), reported by Ludwig et al of the Stanford Research Institute, ranged from 0.24 to 0.55 μm for Vernon, South Pasadena and Menlo Park. Lundgren reported an average mass median diameter for sulfate of 0.3 μm sampling in Riverside with values ranging from 0.1-0.6 μm .⁽²⁰⁾ These results compare to values of 0.4 and 0.3 μm obtained for Cincinnati and Chicago, respectively, by Nader and co-workers employing an Anderson sampler.⁽²¹⁾

Available data for nitrate size distributions are quite limited; Lundgren reported for Riverside an average mmd of 0.8 μm , with values ranging from 0.6 to 1.2 μm .⁽²⁰⁾ These values are in the range found in the present study for the entire Basin but somewhat greater than the ACHEX values for Rubidoux.

Finally, the conversion ratio is useful as one measure of the secondary conversion processes in the air that generate aerosol. These ratios have been calculated for several cases of ACHEX data and their changes reveal substantial differences in behavior of sulfate, nitrate, and secondary carbon. Away from source dominated areas, the sulfur conversion f_s , is generally relatively constant, in the range of 0.2 - 0.3. The nitrate conversion ratio is much more variable, often displaying a morning maximum with maximum NO_x .

SC524.25FR

On the average, the f_N ratio is $\sim 5\%$ except in Rubidoux, where this ratio was found to be an order of magnitude higher. The secondary carbon ratio, f_C , usually was 1% or less. This parameter normally had a daily maximum at mid-day, accompanying the maximum in ozone concentration.

SC524.25FR

V. SULFUR AND NITROGEN AEROSOL CHEMISTRY

This section follows the development in Section IV and explores in more detail several important aspects of the behavior of sulfur and nitrogen in the aerosols, as well as in gas-particle interactions. The section begins with further discussion of the diurnal changes in sulfur chemistry, particularly as they relate to motor vehicle emissions. In subsequent material, the known mechanisms of sulfur oxide and nitrogen oxide oxidation are reviewed as they relate to interpretation of the ACHEX results.

A. OXIDIZED AND REDUCED SULFUR SPECIES

Analysis of aerosol samples taken in the ACHEX by photoelectron spectroscopy (ESCA) indicated that the particulate sulfur species are far more complicated than sulfate alone. Examples of ESCA spectra of aerosol samples are shown in Figure 5-1. Here several oxidized states of sulfur appear as well as species that are reduced relative to free sulfur. (22)

It is important to recognize that the particulate sulfur chemistry involves much more than the sulfate. For purposes of the ACHEX, virtually all of the analysis has been confined to the more "classical" chemistry of water soluble sulfate and total sulfur. Yet, the 1972 data using ESCA are useful in providing a glimpse of future analyses, in that some information was obtained on two classes of sulfur. Oxidized species have been categorized as S^+ , while free sulfur and species reduced to valence states more negative are considered S^- . In this abbreviated notation, S is used to indicate SO_2 .

To illustrate the features of conversion of sulfur gases to aerosol, samples of 1972 data for SO_2 and particulate S^+ and S^- are shown in Figures 5-2a, 5-2b, and 5-2c. Here, the cases of the Harbor Freeway, Pasadena, and Pomona have been selected. Data from Georgii (23) are also included. Comparison between the gaseous oxidized sulfur and particulate oxidized sulfur at the Harbor Freeway in Figure 5-2a suggests that there is a correspondence between the two at this location through midday. Furthermore, the ratio S^+/S^- is approximately unity during much of the day, which is quite distinct from the Pomona case, shown in Figure 5-2c. The reduced sulfur S^- was seen

SC524.25FR

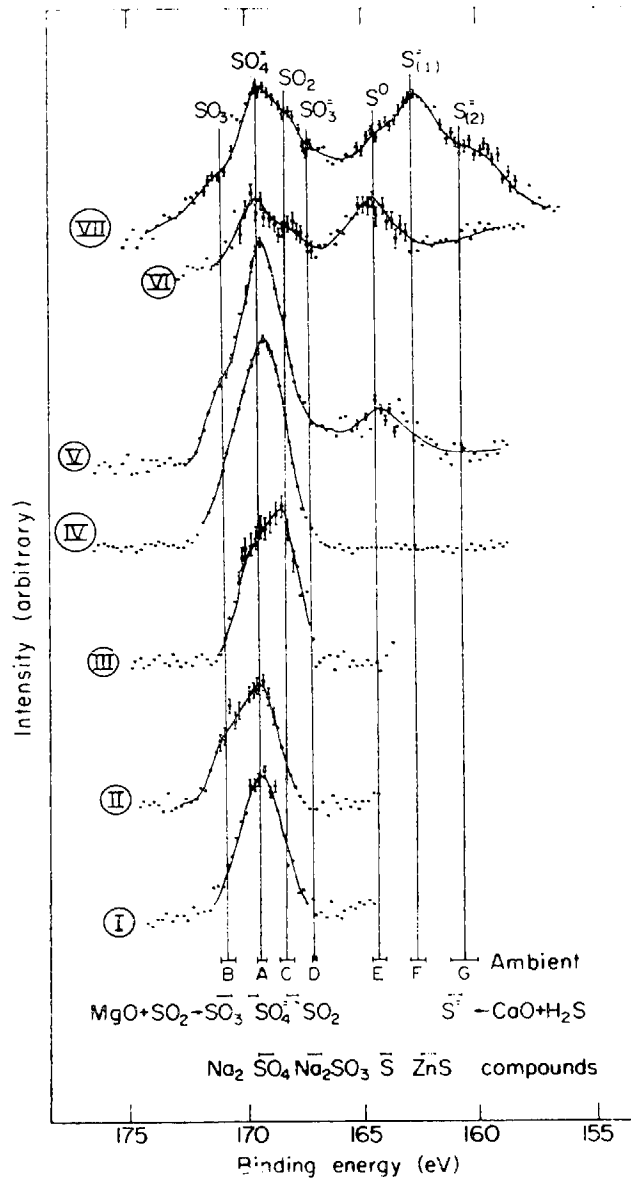
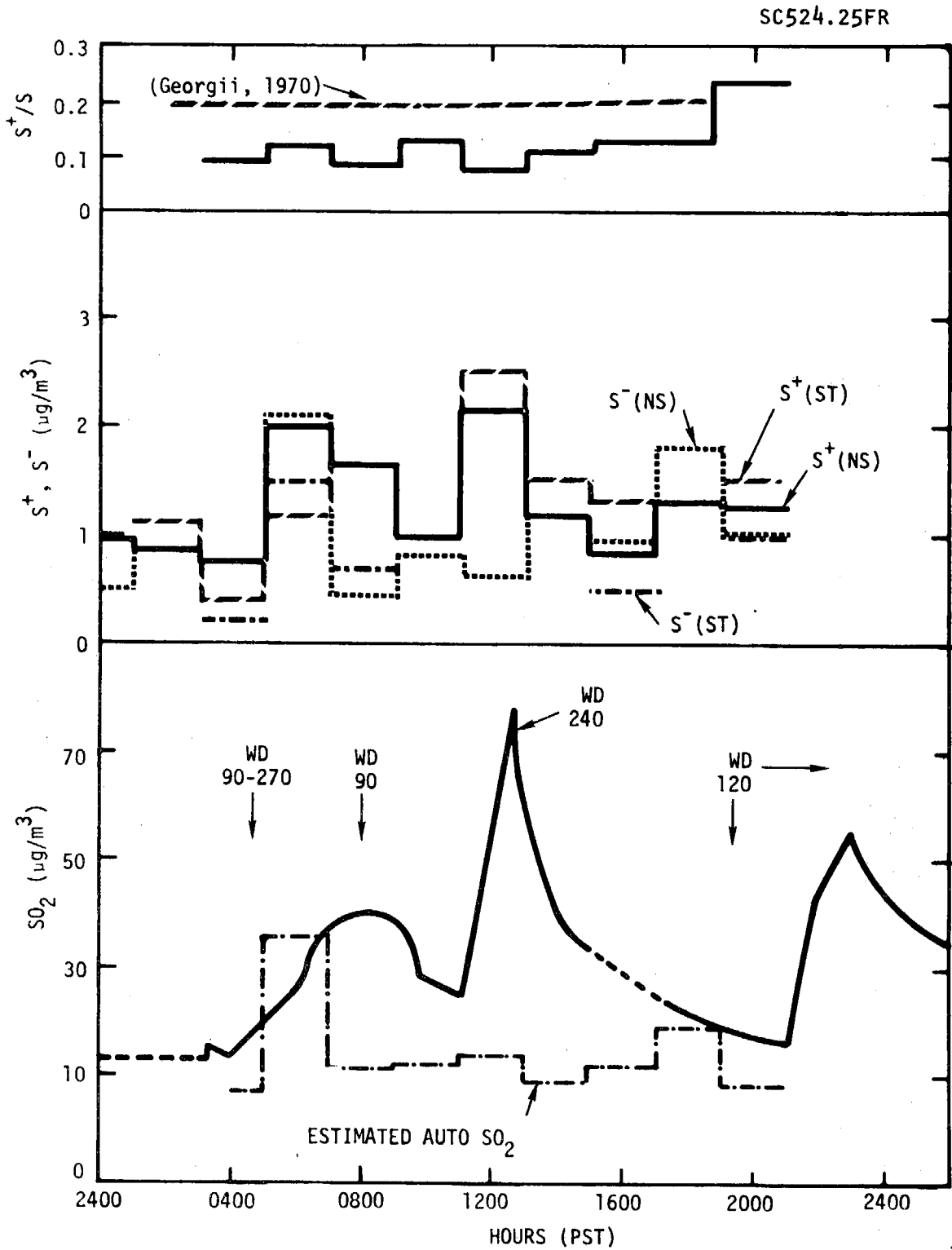


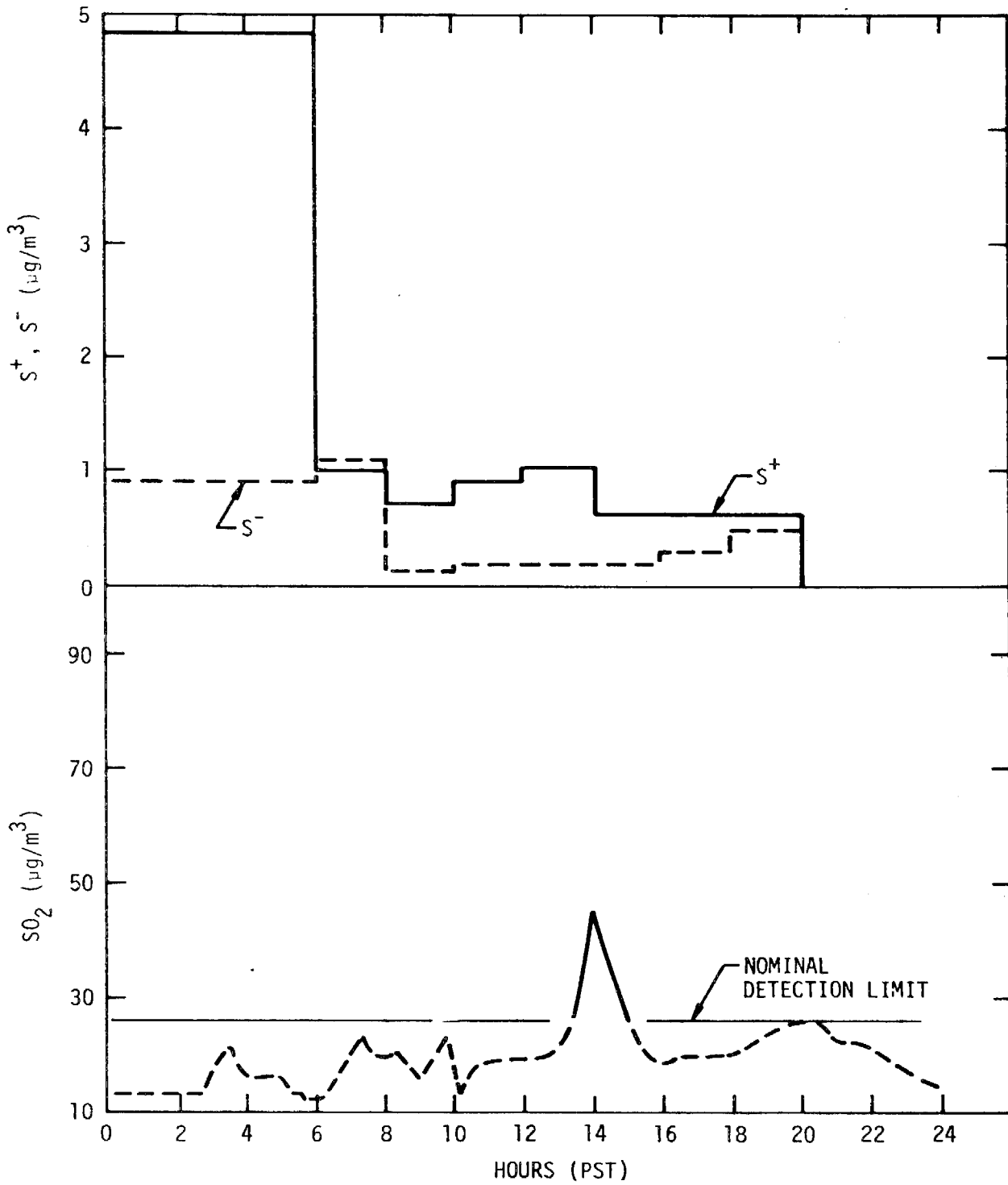
Figure 5-1. Sulfur 2p Photoelectron Spectra of Ambient Pollution-Aerosol Samples Collected in ACHEX and Analyzed by Craig *et al.* (22) The Spectra are Arranged in Order of Increasing Complexity. Sulfur 2p Binding Energies Derived From Ambient Spectra are Indicated Together With Sulfur 2p Binding Energies of Some Simple Compounds and Sulfur Species Produced by Absorption of SO₂ on MgO and H₂S on CaO. The Binding Energies of Ambient Samples are Assigned to SO₃, SO₄, SO₂, SO₃, S⁰ and Two Kinds of S⁻ Ions.



a. Harbor Freeway - September 20, 1972

Figure 5-2. SO_2 and Particulate S^+ and S^- Collected Using Sticky (ST) and Nonsticky (NS) Substrates. The Wind Direction (WD) is Indicated. (Sheet 1 of 3)

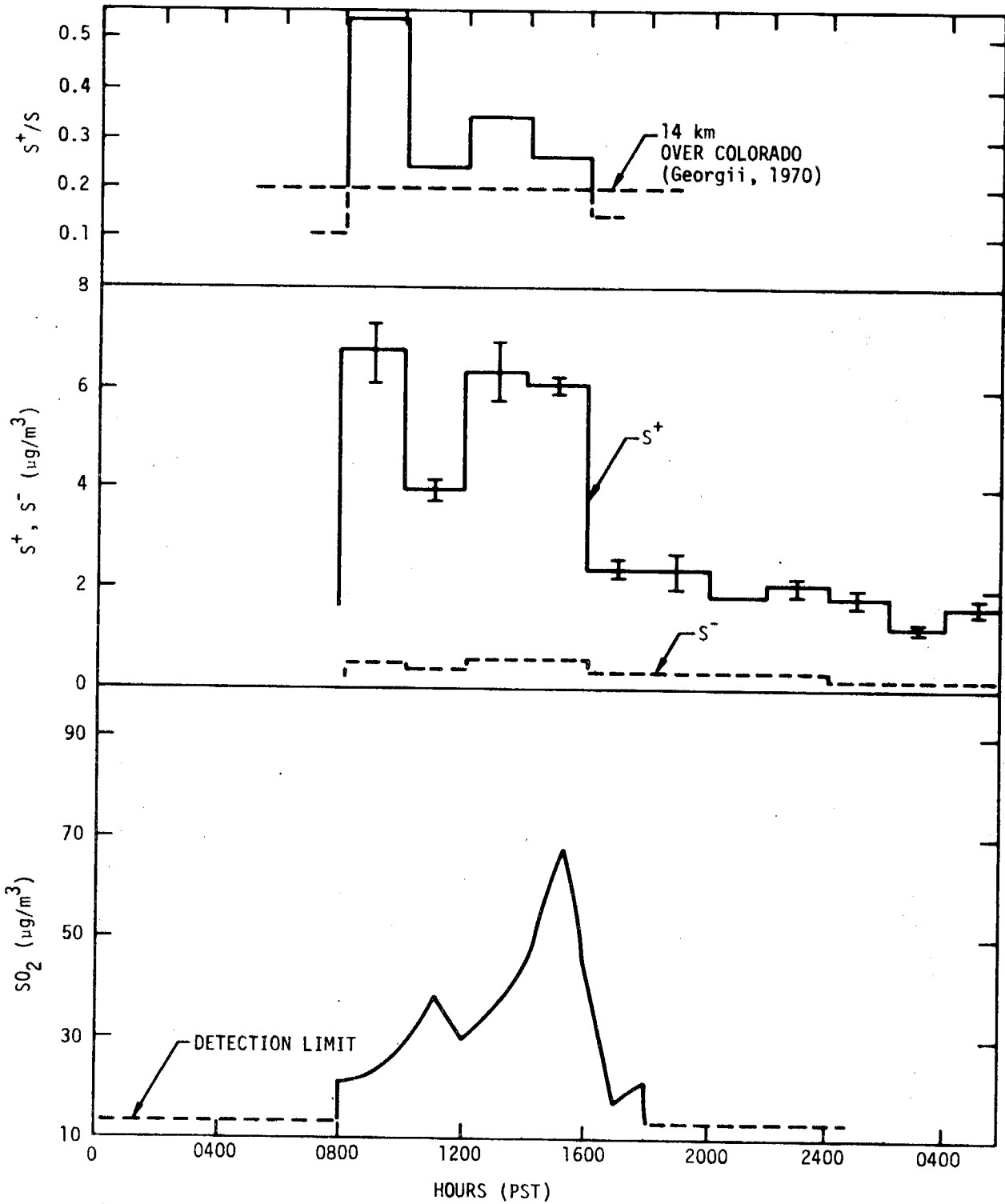
SC524.25FR



b. Pasadena - September 20, 1972

Figure 5-2. SO_2 and Particulate S^+ and S^- (Sheet 2 of 3)

SC524.25FR



c. Pomona - October 24, 1972

Figure 5-2. SO_2 and Particulate S^+ and S^- (Sheet 3 of 3)

SC524.25FR

in Figure 4-5 to follow the pattern of lead closely. This correspondence in particulate S suggests that automobile exhaust contains a significant fraction of sulfur as condensed material.

Comparison between the after filter and total filter lead pattern (Figure 4-5a) and the SO_2 diurnal pattern (Figure 5-2a) indicates that the two peaks in the SO_2 concentration do not coincide with the lead peak. Furthermore, the 0800 SO_2 peak comes from a period when the wind direction was $\sim 90^\circ$, and the midday SO_2 peak is identified with winds from $\sim 240^\circ$. Thus, it is tentatively concluded that the SO_2 variation at the Harbor Freeway was only partly related to the automobile traffic.

The SO_2 emissions in Los Angeles⁽²⁴⁾ are largely attributed to stationary sources identified with the power plants and the petroleum and chemical industries. These are located principally south and west of the Harbor Freeway site. Assuming that the SO_2 in the air measured at the Harbor Freeway constitutes a partially reacted condition, compared with locations farther east, then the S^+/S ratio* should be relatively low at this location.

To estimate the S^+/S ratio at the Freeway, a correction should be made for the maximum S expected from auto exhaust. On the average, the S/Pb in gasoline from Southern California is ≈ 0.9 . Assuming that all the S is converted to SO_2 except for S^- , and normalizing to lead on the total filter, the SO_2 from autos is estimated and is shown in the dotted curve in Figure 5-2a. Qualitatively, this calculation confirms the conclusion that the midday SO_2 must come from sources other than the Harbor Freeway. However, there is an uncertainty in this approach, in that more auto SO_2 is estimated than was observed in the early morning. The values of the S^+/S ratio, as corrected for auto SO_2 , are indicated in Figure 5-2a and are generally $\lesssim 0.1$ after correcting for the spurious influence of S from the automobile. Thus, qualitatively, air passing over downtown Los Angeles from the west or southwest reflected conversion of SO_2 to sulfate corresponding to $\text{S}^+/\text{S} \lesssim 0.1$ on

* S^+/S = particulate oxidized sulfur/gaseous sulfur from SO_2 . This ratio is related to f_s as $(\text{S}/\text{S}^+ + 1)^{-1}$.

SC524.25FR

this day. Late in the day, however, an apparently higher value of 0.25 was detected, suggesting more aged air, as speculated by Georgii⁽²³⁾.

The results of the sulfur analysis at Pasadena represent a useful comparison with the Harbor Freeway data on the same day. A comparison between SO_2 and S^+ and S^- is shown in Figure 5-2b. This day was quite dry in Pasadena, with relative humidity $\leq 40\%$ and visibility exceeding 17 miles most of the day. Except for the early morning hours, the oxidized particulate sulfur (S^+) content was $\sim 1 \mu\text{g}/\text{m}^3$. During the 0600 to 0800 morning and 1800-2000 evening traffic peaks, the ratio of S^-/S^+ approached unity; while during midday, this ratio dropped to ~ 0.2 . On this day, the total sulfur in the air remained below the detection limit of 10 ppb, except for the midafternoon peak. The Pasadena S peak lagged the Harbor Freeway midday peak by ~ 1 hr. Using the ratio of S^+/S as an index of converted sulfur, it is seen that this ratio was the order of 0.2 minimum during the night, while it decreased to ~ 0.05 by midday on September 20.

This evidence qualitatively indicates that the SO_2 oxidation process on September 20 over the Basin was rather weak, and comparable to the conversion seen at the Harbor Freeway.

The results taken at Pomona on October 24 are in marked contrast to the results of September 20 in Pasadena. The Pomona results are shown in Figure 5-2c. As previously noted, this was the day when the highest light scattering coefficient was observed in the period of 0800 to 1000. The air was more moist with morning relative humidity exceeding 70%, but decreasing to $\sim 50\%$ during the midday.

During the midday, the SO_2 concentration at Pasadena increased to levels approaching those observed at the Harbor Freeway. The maximum in SO_2 level occurred at about 1500. Although there was a strong increase in particulate oxidized sulfur during daylight hours, the diurnal patterns do not correspond well. The first apparent maximum in S^+ occurs in the morning, when the relative humidity was high, while the SO_2 is beginning to increase. Indeed, the highest S^+/S ratio was found at 0900. However, the S^+/S ratios throughout the day in Pomona generally exceeded 0.2, as contrasted to Pasadena. The lack

SC524.25FR

of correspondence between S^+ and SO_2 may be related to an accidental SO_3 spill that apparently took place in the Southwest part of Los Angeles October 23rd. Only a weak increase in S^- was observed. The ratio of S^-/S^+ in Pomona is the order of 0.1 most of the day in contrast to the Harbor Freeway.

Data from the humidified nephelometer indicate that aerosols can absorb significant quantities of water when the relative humidity exceeds 65 to 70%. Furthermore, the waterometer data show that substantial quantities of unbound water are present in the Los Angeles aerosol. With the amount of NH_3 present in the Los Angeles air, corresponding to tens of $\mu g/m^3$, and high relative humidity, it is reasonable to expect that the quasi-aqueous oxidation mechanism, involving SO_2 absorption to form SO_3^- , of Scott and Hobbs⁽²⁵⁾ would play a dominant role in SO_4^- formation. The data on sulfur chemistry examined at the end of ACHEX-1 were consistent with the idea that the rate of SO_2 oxidation to SO_4^- is substantially increased in Los Angeles air with high relative humidity, reflecting increased aerosol liquid water content. It was felt that this oxidation process could take place in the absence of photochemical processes, and indeed, it might take place equally effectively during the night. More recent findings are discussed immediately after the following analysis of motor vehicle emissions, and again in Section C-2-a.

1. SULFUR AND MOTOR VEHICLE EMISSIONS

One of the surprises that has come from the initial analysis of the data is the relation between particulate sulfur and motor vehicle emissions. Unexpectedly, the work of Cahill⁽²⁶⁾ on the x-ray fluorescence analysis of samples taken upstream and downstream of a freeway showed high concentrations of particulate sulfur, presumably coming from automobile exhausts. Our results qualitatively bear out this conclusion.

The emission of particulate sulfur from automobiles is deduced from a correlation between reduced sulfur (S^-) and lead. Figure 5-3 shows the proposed correlation for data selected on the basis of downwind conditions at the Harbor Freeway. The data in the diagram suggest that the correlation is fair. The correlation appears satisfactory for after filter (AF) data for

SC524.25FR

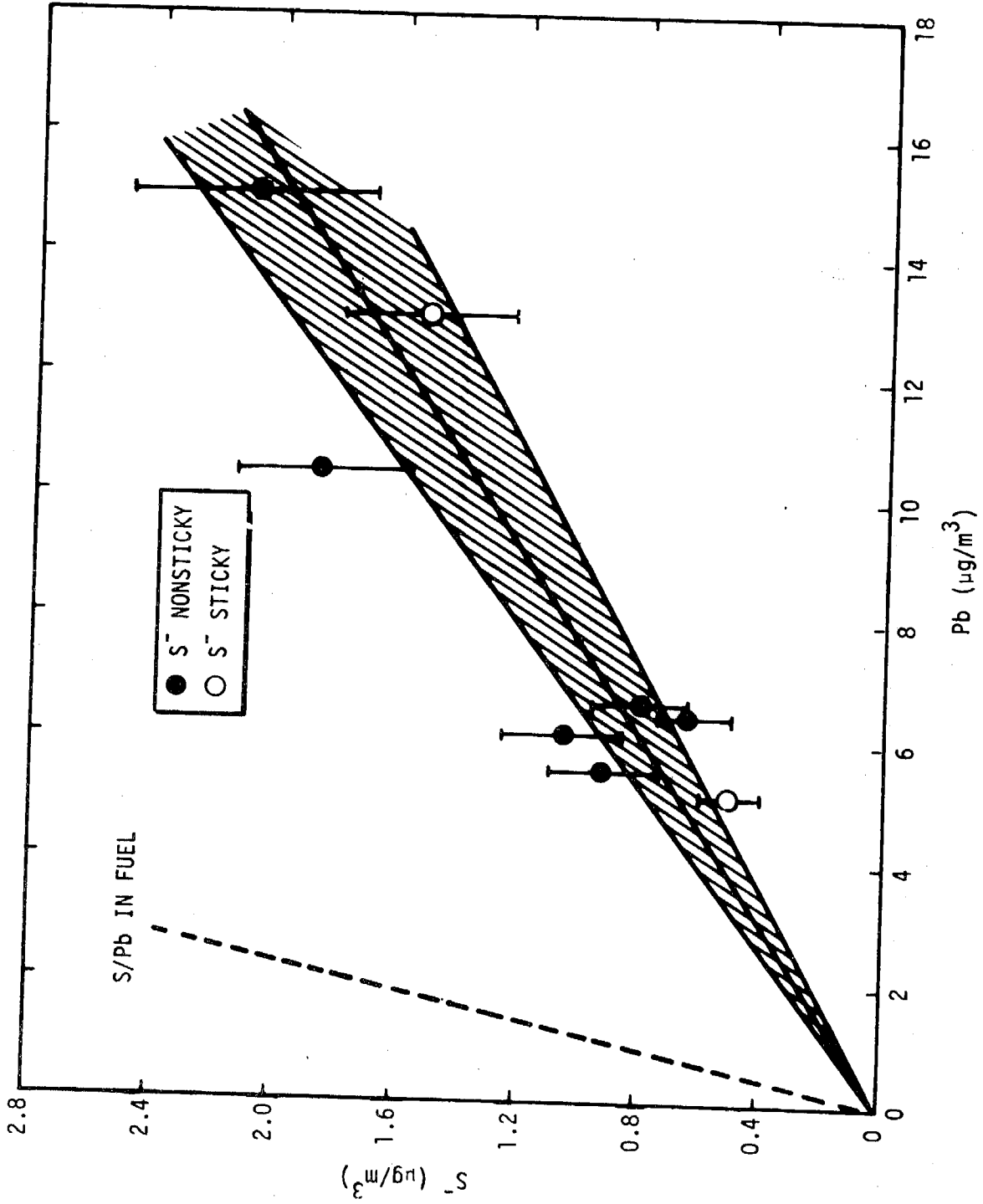


Figure 5-3. Correlation Between Reduced Sulfur and Lead on the After Filter - Harbor Freeway (Downwind Conditions)

SC524.25FR

both sticky (ST) and the nonsticky (NS) substrates. The data are limited, but a bounce-off effect may be present and may influence the S^-/Pb ratio observed.

The ESCA sulfur measurements on the silver membrane (TG) total filter, indicated no correlation of S^+ and Pb. Interestingly enough, the S^-/Pb on the total filter was systematically lower than the values shown in Figure 5-3. This loss of S^- may be related to the electrochemical coupling between Ag_2O and S^- . That is, Ag_2O can oxidize S^- to SO_3^- and generate Ag on the filter, if oxidation potentials are considered.

For comparison, the S/Pb ratio common to gasoline is shown. Here S is given on the average as 2.5 g/gal. while Pb is 2.75 g/gal. on the average. Thus, the particulate reduced sulfur represents ~ 20% of the sulfur content in fuel. The remainder of sulfur in the fuel is released as SO_2 or S^+ in the vehicle exhaust with a possible contribution of particulate.

The Harbor Freeway sulfur data can be used to interpret data taken elsewhere in the Basin, as they are influenced by the automobile. A test of S to Pb correlation for Pasadena, Pomona, and Riverside is shown in Figure 5-4. The data at Pasadena for September 20 suggest essentially no correlation of S^+ with Pb. The offset of S^+ suggests that as $Pb \rightarrow 0$, there may be a background level of S^+ of $\sim 0.6 \mu g/m^3$, which is reasonable, but somewhat lower than the value estimated in Section 3-1. The Riverside data for September 20 show a wide scatter, but generally have a larger S^+/Pb ratio than in the line for Pasadena. This would suggest S^+ from stationary sources on this day. Pomona data for October 24 show a similar scatter indicating that stationary sources are a major factor in particulate S^+ .

An interesting contrast to the September 20 episode in Pasadena is the case of August 24. Both days showed a low oxidant level, but August 24 was a very moist overcast day, with morning drizzle, as compared with the dryness of September 20. In the August 24 data, there is a significantly stronger relation of S^+ with Pb than on September 20, which may be related to the conversion rate. It is noted that Pb, of course, should reflect not only auto emissions, but also the general level of pollution in an air mass traveling into Pasadena from downtown Los Angeles. In the case of Pasadena on

SC524.25FR

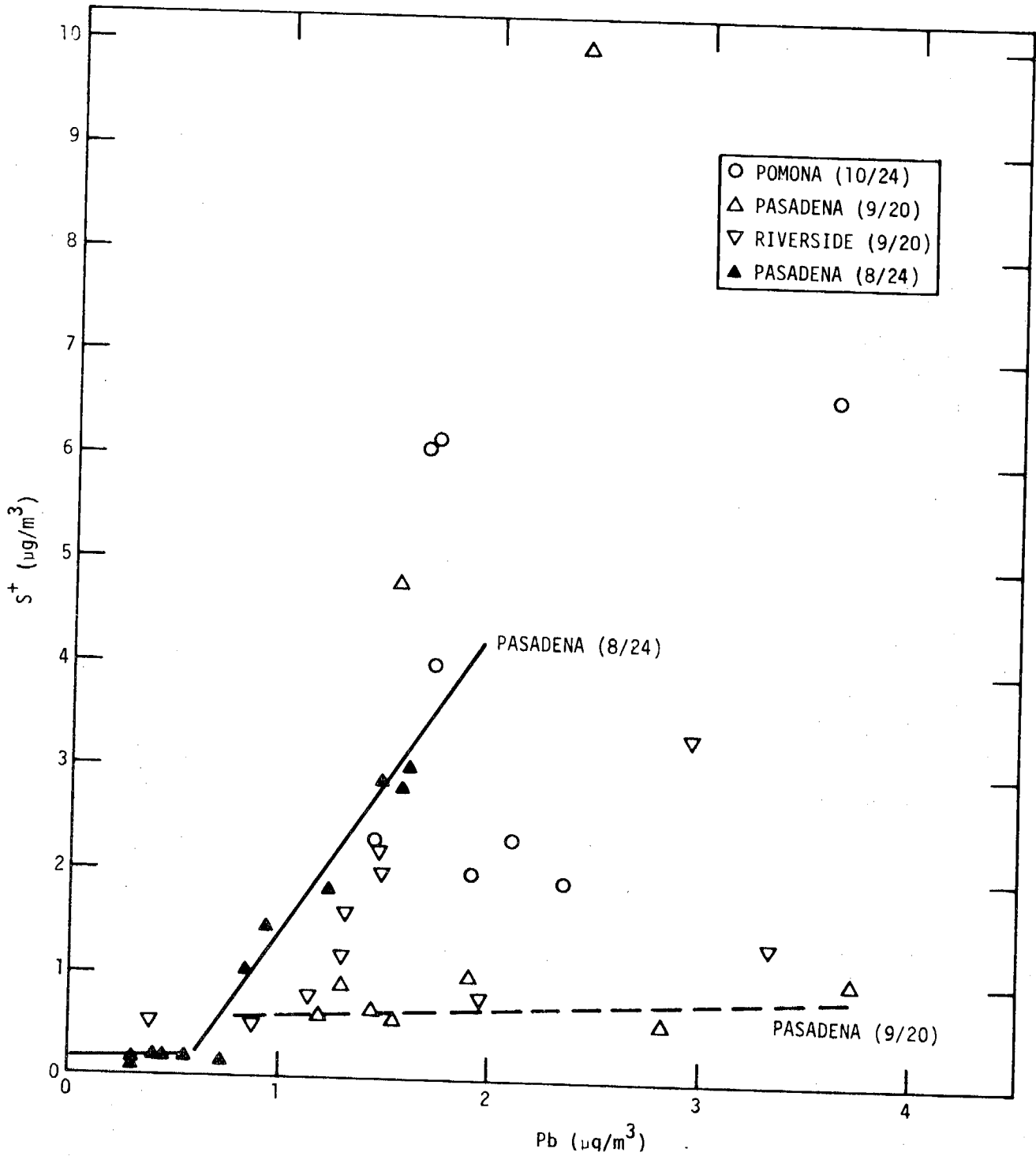


Figure 5-4. Correlation Between Oxidized Sulfur (S^+) and Lead - Pasadena, Pomona, and Riverside

SC524.25FR

August 24, the data show a constant S^+ as $Pb \rightarrow 0$. Again, this is identified with the background S^+ , which is $\sim 0.2\mu\text{g}/\text{m}^3$ for this day.

A corresponding set of data for the ratio of S^- to Pb is shown in Figure 5-5. The dotted line is the correlation for the freeway data. Here, most of the S^- data is scattered above the motor vehicle line. However, a few points lie below the correlation line. These may be indicative of an oxidation of S^- to S^+ during aging of aerosols in the Los Angeles atmosphere.

The sulfur data for S^+ and S^- vs Pb for San Jose are shown in Figure 5-6. The correlation line from the Harbor Freeway is also shown for S^- . In this case, S^+ at San Jose is scattered; several points are significantly above the correlation line, indicating a dominance of stationary sources. Interestingly enough, the S^- data generally show an independence of Pb and lie well below the freeway correlation line. This difference again may be associated with aerosol aging, or there maybe a systematic difference in sulfur in fuels used in the Bay Area.

In any case, the differences point to the potential usefulness of this approach for investigation of the sources of particulate sulfur.

2. EVIDENCE OF SULFATE PHOTOCHEMISTRY

Comparison of the variation in conversion ratios with key changes in trace gases provides additional insight into the mechanisms of aerosol formation in the atmosphere. For example, analysis of the ACHEX data taken in 1973 shows that the conversion ratio f_S is not significantly dependent on relative humidity. There was a small difference, however, between the f_S based on total sulfate concentration and f_S based on the submicron particles. As indicated in Figure 5-7a, the f_S for all particles displayed considerable scatter, but increased slightly with relative humidity. In contrast, the results in Figure 5-7b for the submicron ratio show a small decrease with relative humidity. A strong apparent influence of photochemistry is demonstrated for submicron sulfate formation by the systematic increase in f_S ($< 0.5 \mu\text{m}$) with ozone concentration. Here ozone is considered an indicator for intensity of smog. The consistency of this trend is shown in Figure 5-8. These results, combined with the day-night differences shown in Table 4-1, provide, for the first

SC524.25FR

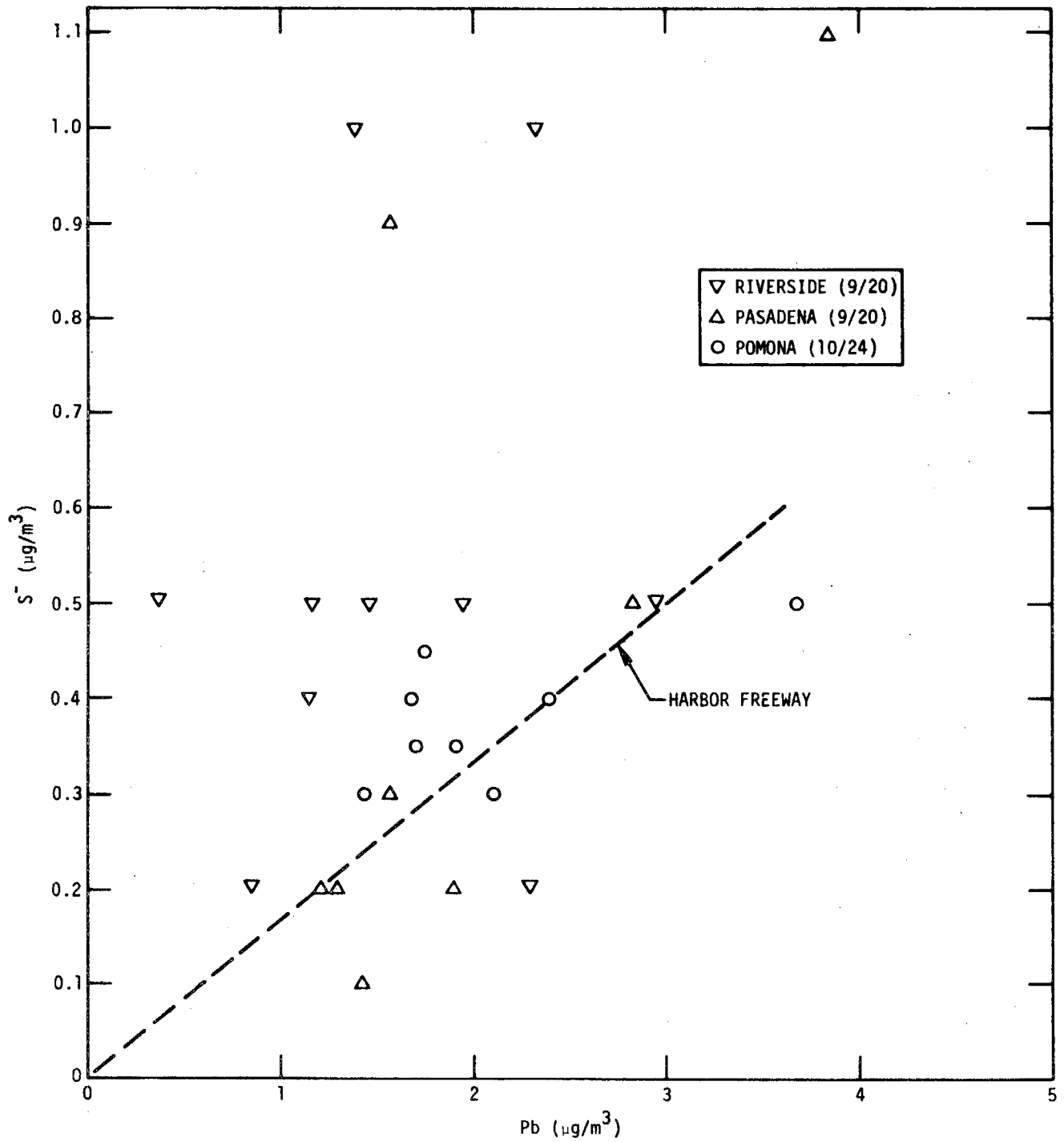


Figure 5-5. Correlation Between Reduced Sulfur (S^{2-}) and Lead - Pasadena, Pomona, and Riverside

SC524.25FR

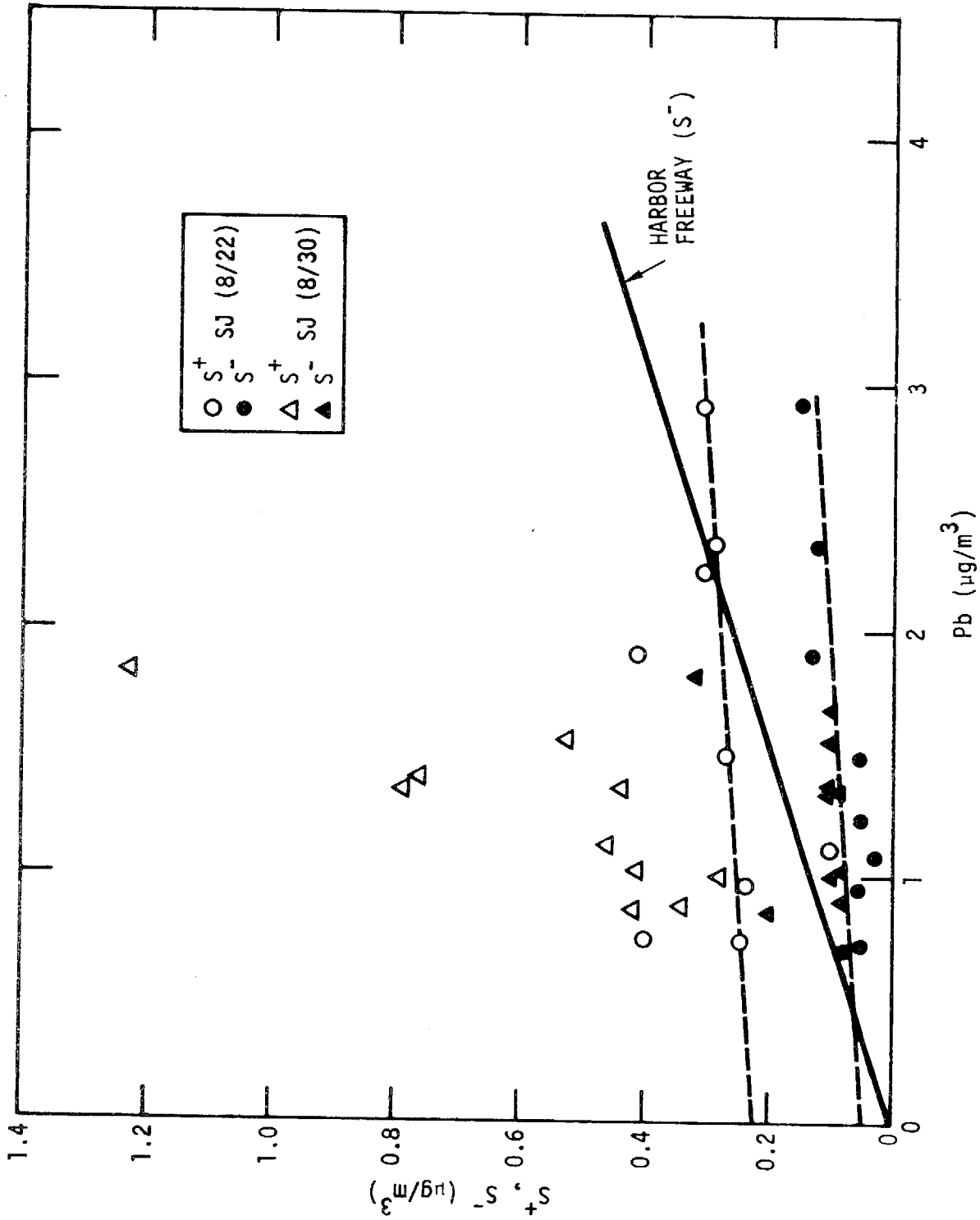


Figure 5-6. Correlation Between Sulfur and Lead - San Jose

SC524.25FR

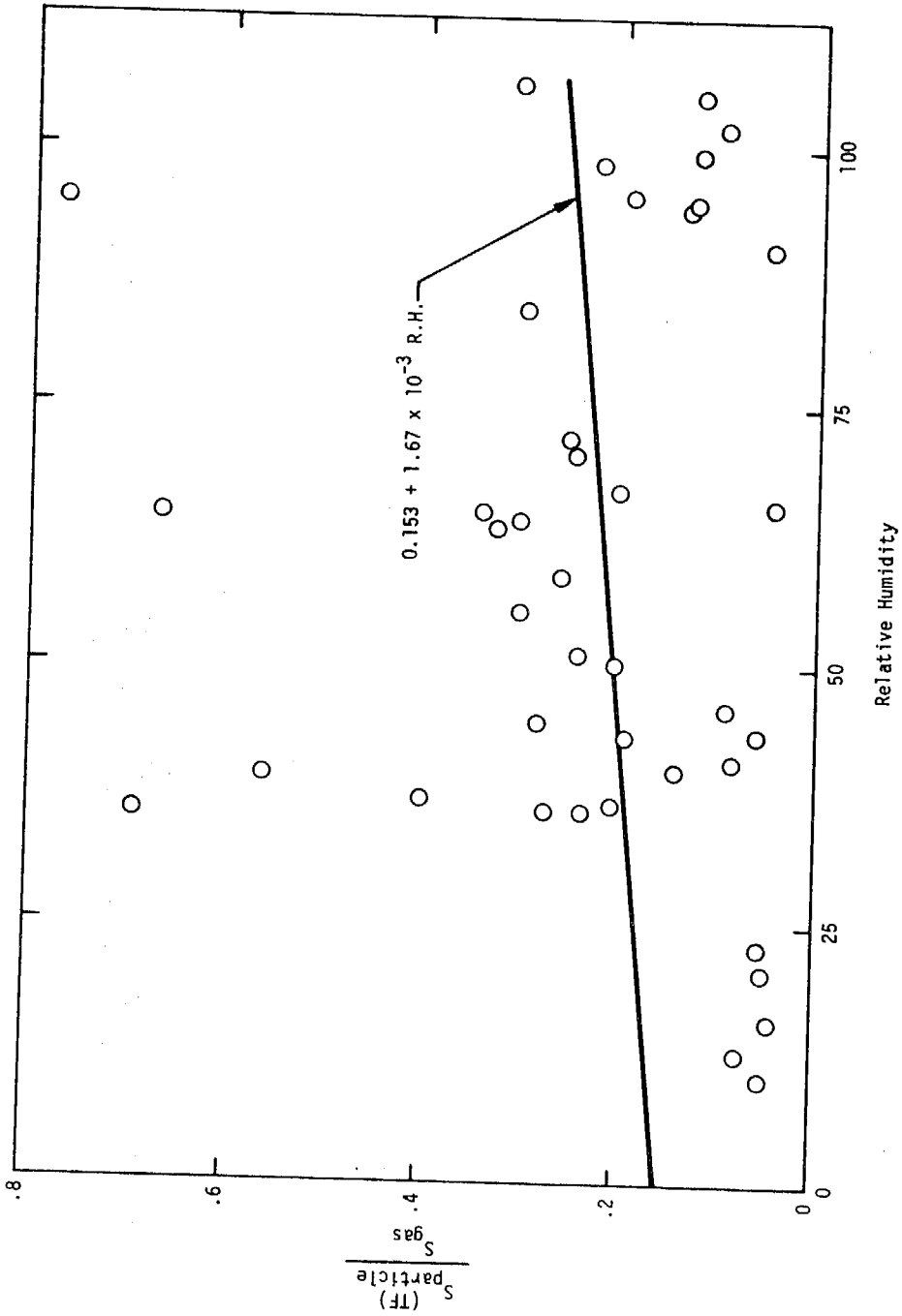


Figure 5-7a. Scatter Diagram of the Ratio of Particulate Sulfate on Total Filter as Sulfur to Sulfur Dioxide Reduced to Sulfur vs. Relative Humidity. Correlation Coefficient = 0.188, $\sigma = 0.247$.

SC524.25FR

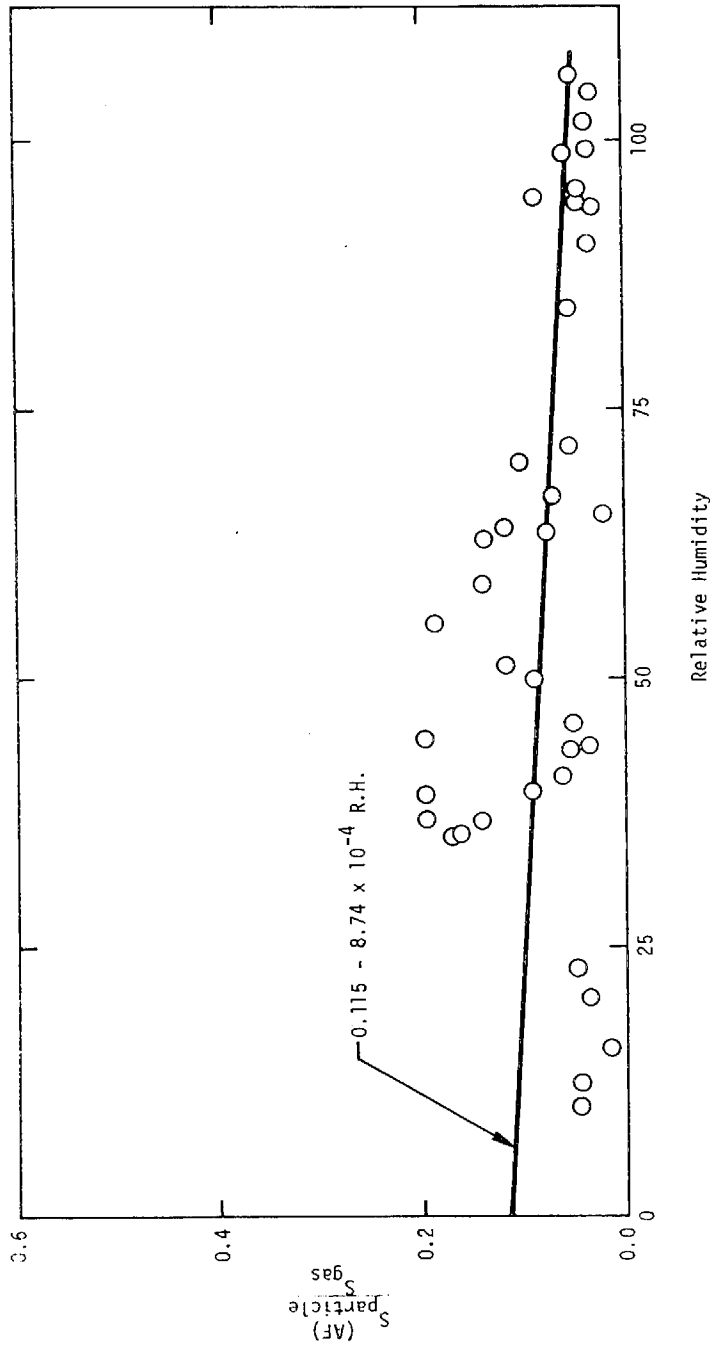


Figure 5-7b. Scatter Diagram of the Ratio of Particulate Sulfate on After Filter as Sulfur to Sulfur Dioxide Reduced to Sulfur vs. Relative Humidity. Correlation Coefficient = -0.294 , $\sigma = 8.06 \times 10^{-2}$.

SC524.25FR

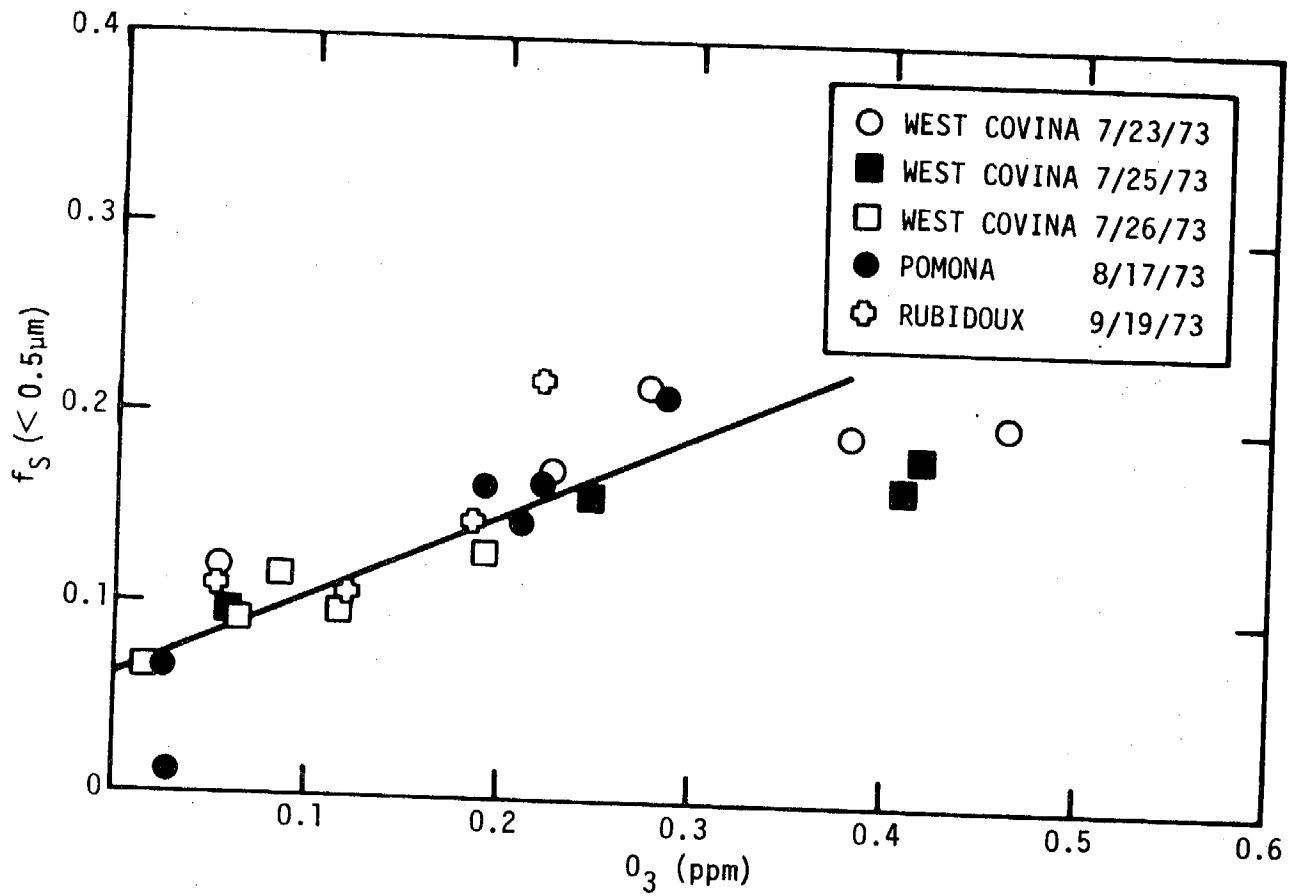


Figure 5-8. Scatter Diagram of the Conversion Ratio f_s Based on Particles Less Than $0.5 \mu\text{m}$ vs. 2 Hour Averaged Ozone Concentration

SC524.25FR

time, satisfactory circumstantial evidence for photochemical oxidation of SO_2 in smog.

Further clues to the sulfate formation mechanism come from comparison of sulfate conversion and the behavior of particulate non-carbonate carbon. The conversion ratio f_s ($< 0.5 \mu\text{m}$) is correlated with changes in particulate carbon, as indicated in Figure 5-9. Thus the formation of aerosols involving sulfate and organic carbon is closely coupled in Los Angeles smog.

3. ESTIMATED RATES OF CONVERSION

Very limited information is presently available on the rates of conversion of aerosol precursor gases in the atmosphere. There are reports in the literature that tropospheric residence times of SO_2 and NO_x are the order of a few days, while reactive hydrocarbon vapors of high molecular weight evidently will not survive more than a day.

Some estimates of the quasi-first order rates of SO_2 oxidation have been reported that range from 0.1% to $> 10\% \text{ hour}^{-1}$ depending on many factors, including relative humidity (e.g. Calvert⁽²⁷⁾). Recent work, for example, of Husar et al.⁽²⁸⁾ near St. Louis suggests an oxidation rate of less than 1% in the absence of photochemical reactions. However, in the presence of photochemical activity SO_2 oxidation rates varying from 2 to $13\% \text{ hour}^{-1}$ have been estimated from Los Angeles data by Roberts and Friedlander.⁽²⁹⁾ These workers based their analysis on a quasi-first order oxidation model by assuming that the initial value of f_s from the major stationary sources was 5% and using the surface wind trajectories across the Los Angeles Basin that entered Pasadena on days when $\text{SO}_2 + \text{SO}_4^{=}$ data were available from Roberts' experiments. A similar model can be applied to the ACHEX results for West Covina and Pomona. It is assumed that (a) on the average, f_s is 11% from the southwest region of Los Angeles, and (b) the SO_2 emissions from these major sources are the only ones of interest as air is transported across the Basin. Using the surface air trajectories on the days in late July and mid August derived from surface wind data, one finds that application of the Roberts and Friedlander approach yields a conversion rate for sulfate between 3% and 10% per hour.

SC524.25FR

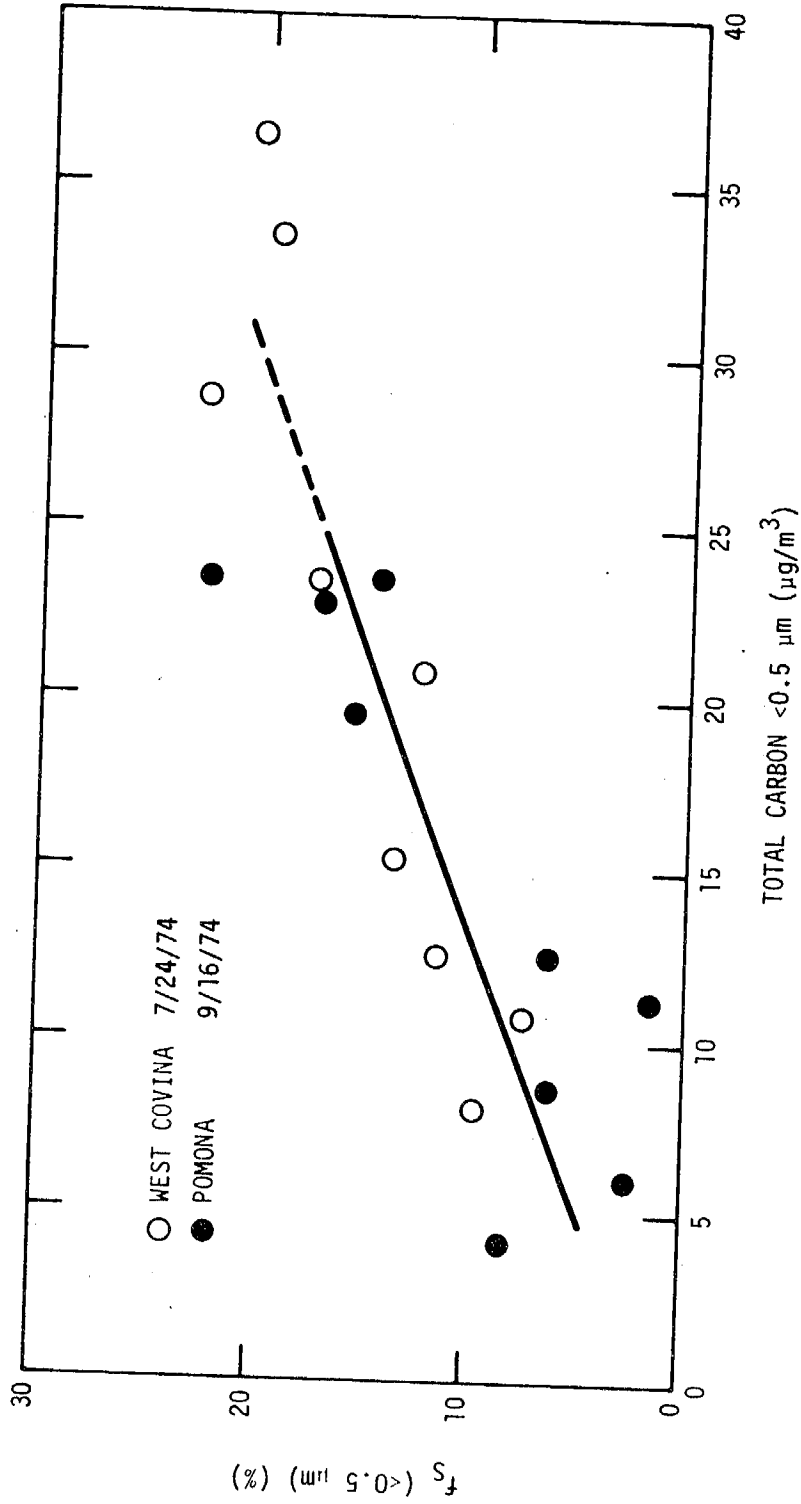


Figure 5-9. Scatter Diagram of the Conversion Ratio f_s Based on Particles Less Than $0.5 \mu\text{m}$ vs Total Carbon Less Than $0.5 \mu\text{m}$ Diameter. (Based on 2 Hour Averaged Filter Data.)

SC524.25FR

B. NITRATE AEROSOLS

Organic nitrate has been found to constitute only a small fraction of the nitrate in the Los Angeles aerosol (e.g., O'Brien et al., Reference 30). Therefore, the inorganic salts are of greatest interest in this study. The evidence previously cited suggests that ammonium nitrate is the principal constituent of the aerosol. The behavior of nitrate is split into two categories, the first is the transient, rapid production observed in the morning, and the second is the systematic but "slow" increase which leads to the high concentrations of NO_3^- in the eastern part of the Basin.

As in the case of sulfate, the conversion ratio f_N provides clues to the nature of the chemical reactions involved in nitrate formation. The ACHEX nitrate data were examined for correlation with ozone, NO , NO_2 , relative humidity, $\text{SO}_4^{=}$, and non-carbonate carbon. These correlations indicate that no systematic, useful relation could be established between NO_3^- and precursors or smog indicators, nor with other smog variables.

It is puzzling, for example, that f_N for either the total particle mass concentration or that confined to $< 0.5 \mu\text{m}$ is poorly correlated with humidity differences as well as with NO_2 , NO_x , and ozone concentrations. The apparent independence of f_N and NO_2 is illustrated by the scatter diagram shown in Figure 5-10. Another example of poor correlation for NO_3^- is shown in Figure 5-11. Here the ratio of particulate nitrogen from nitrate to gaseous nitrogen from total NO_x is plotted against ozone concentration. Such results suggest that the high nitrate content of the aerosol cannot be the result of a spurious absorption of gaseous NO_2 at the moist filter medium. If this were the case, one would expect a proportionality between f_N and NO_2 concentration. By the same argument, NO_3^- does not appear to form by a gas diffusion limited absorption of NO_2 in wet particles. On the other hand, the data suggest that conversion to nitrate may be dominated by other nitrogen oxide intermediates such as NO_3 , N_2O_5 , or HNO_2 which build up in the morning with photochemical activity. However, these intermediates are more likely to be in high concentration at midday rather than midmorning in smog. The rapid transient increase in nitrate in the midmorning does not seem to be related closely to the systematic increase in nitrate eastward across the Los Angeles Basin.

SC524.25FR

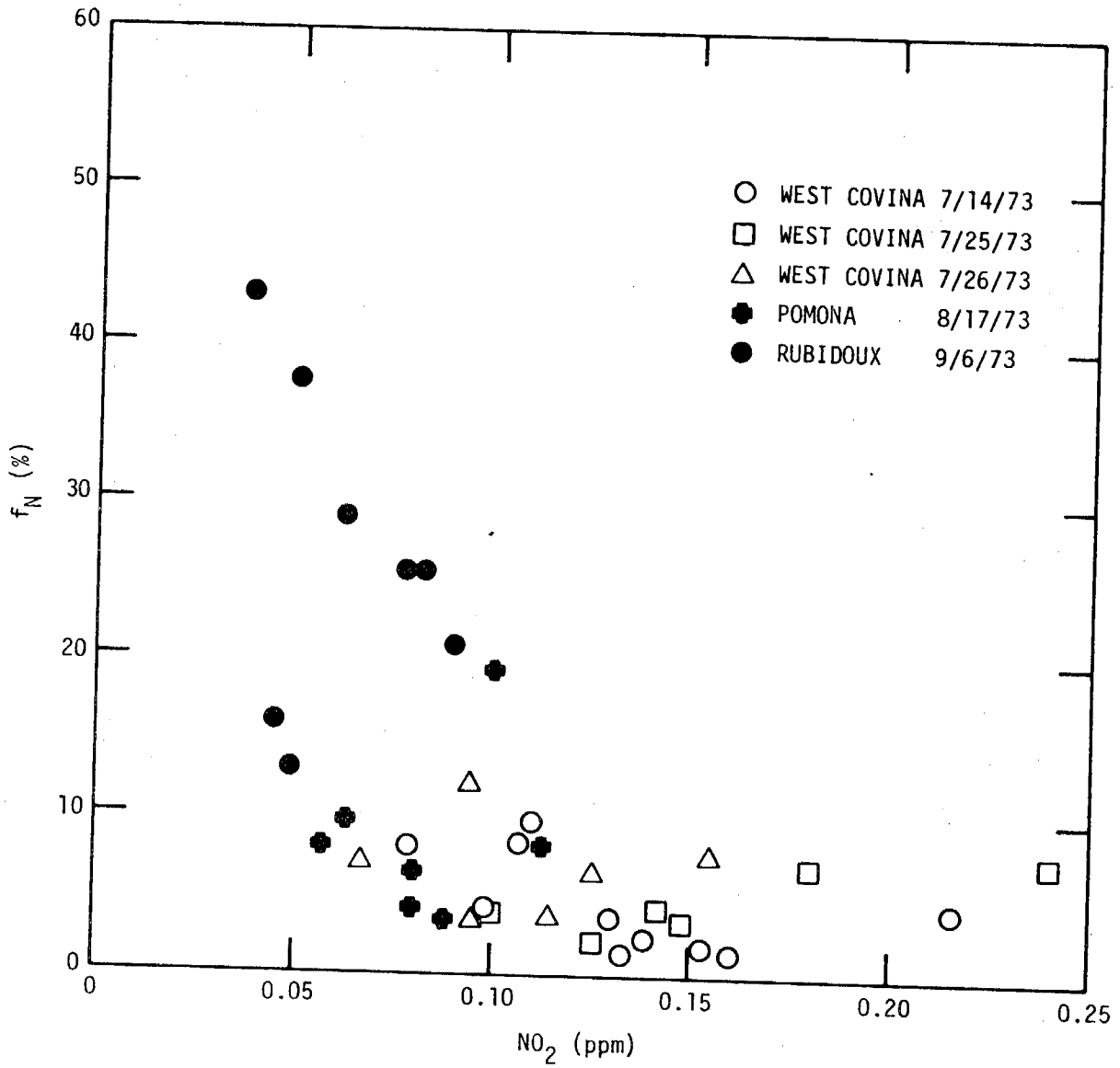


Figure 5-10. Scatter Diagram of the Nitrogen Oxide Conversion Ratio f_N vs. Two Hour Averaged NO_2 Concentration

SC524.25FR

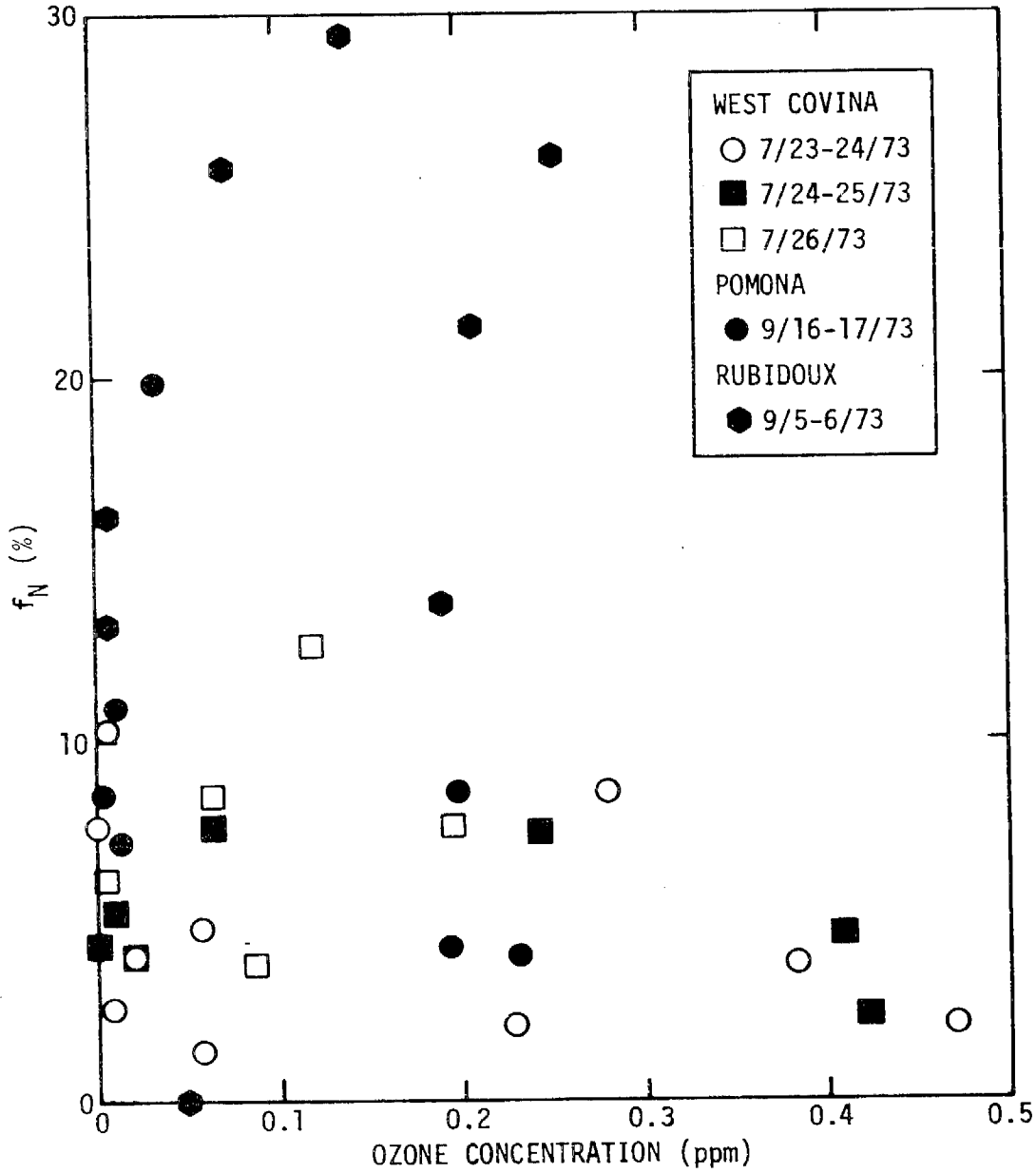


Figure 5-11. Scatter Diagram of the Particle to Gas Phase Nitrogen Ratio Against Ozone

SC524.25FR

There is virtually no quantitative information available on the rates of conversion of NO_x to nitrate. However, the Los Angeles experience previously discussed suggests that two extremes may be present. A rapid transient conversion may exist as a part of the morning photochemical nitrogen oxide cycle, giving a formation at high humidity of some nitrate at a local production rate exceeding SO_2 oxidation.

The second nitrate formation process, which gives rise to high levels on the east side of the Basin, is slower than the morning transient. The rate of nitrate formation in this second case can be estimated by analogy to sulfate. Assume that (a) the nitrate formation is a quasi-first order process, (b) the bulk of the NO_x responsible for nitrate is injected into the Los Angeles area on the western and west central side of the Basin in the morning, and (c) the initial f_N in the unreacted air masses is $< 5\%$. Then considering the rate of air transport as in the case of the sulfate estimation and the data in Table 4-1, calculation suggests that the conversion rate for nitrate must be similar to that for sulfate, despite the apparent greater homogeneity of sulfate distribution than the nitrate distribution. This follows from the data and the fact that a significant amount of the NO_x is injected farther inland than SO_2 as a result of morning traffic.

Further investigation of the nitrate data in connection with the distribution of NO_x sources, the air transport and NO_x removal phenomena in the South Coast Basin is necessary to obtain a more quantitative picture of the behavior of the nitrogen oxides. Pollution in the vertical structure of the surface layers of the atmosphere may also have to be accounted for, since advection and mixing of high concentrations of partially reacted materials near the inversion base may play a significant role in high nitrate levels on the eastern side of the Basin.

C. MECHANISMS OF AEROSOL FORMATION

It is appropriate to include here a summary of the current knowledge of aerosol formation mechanisms as a framework for any further interpretation of the ACHEX data in the light of chemical processes in the atmosphere. The air chemistry proposed, of course, must be consistent with the observations of ACHEX and other studies.

SC524.25FR

The chemical and physical processes that lead to aerosol formation in the atmosphere are probably very complex, with no single mechanism dominating the phenomenon. Unlike the chemical laboratory, the atmosphere is very "dirty" in that it contains substantial amounts of airborne particles which are continuously interacting with trace gases. Water as vapor and in the condensed phase likely plays a critical role in aerosol evolution, both in growth and removal from the atmosphere. Thus, in elucidating atmospheric aerosol behavior, one must account for both homogeneous processes of precursor formation and heterogeneous interactions.

1. PHYSICAL CONSTRAINTS

Regardless of the chemistry, certain physical constraints exist on aerosol-gas interactions. These restrictions relate mainly to (a) the thermodynamic stability of condensed particles of small diameter, (b) particle nucleation and condensation processes, and (c) gas phase diffusion limited rates combined with absorption or adsorption on particles.

Particles must be close to or at equilibrium with respect to the surrounding vapor to exist in air for any length of time. Thus, the partial pressure of condensed species on particles must be less than or equal to the saturation vapor pressure at atmospheric temperature for stability. This presents no great problem for most inorganic salts or for sulfuric acid, even at parts per billion concentration in the gas phase. However, it places a severe constraint on the ability of HNO_3 to exist as a pure compound or as an acid diluted in water. The vapor pressure data reviewed by Toon and Pollack⁽³¹⁾, for example, indicate that HNO_3 has a partial pressure over aqueous solutions more than 100 times higher than concentrated H_2SO_4 , making nitric acid aerosol far less stable in the atmosphere than sulfuric acid.

Accumulation of condensed material as aerosols in the atmosphere may take place by two basic processes: first by condensation of super-saturated vapor or by chemical reaction leading to spontaneous formation of new particles; second, by condensation, absorption or reaction on existing particles. In the latter case, the chemical reactions actually may take place on the surface of, or within, existing particles.

SC524.25FR

For condensable precursors, particle formation may occur by homogeneous nucleation or by heterogeneous nucleation. It is generally accepted, but not proven, that heterogeneous processes are most likely in the atmosphere because of the large number of existing nuclei. One can readily see, however, that growth by condensation is limited by the rate of diffusion of vapor to the surfaces of nuclei. If conditions exist in which aerosol precursors evolve chemically at a rate exceeding the diffusional transfer, then supersaturation could build up to high enough levels to permit heteromolecular (homogeneous) nucleation of new particles. It can be shown that H_2SO_4 can undergo heteromolecular nucleation at atmospheric concentrations in the absence of nuclei, but it is unlikely that HNO_3 could nucleate because of its relatively high vapor pressure. So little is known about the products of aerosol forming organic reactions and their relevant physical properties that nothing can be said about the importance of homogeneous nucleation in this case.

The fact that few new particles are observed in cities away from combustion sources or in rural areas, particularly in highly reactive atmospheres like Los Angeles, makes it unlikely that heteromolecular nucleation is a widely important formation process in the troposphere. The general decrease in nuclei concentration with altitude with more nearly constant large particle concentration suggests that new particle formation normally plays a small role at high altitude, too. Yet, this conclusion is by no means well established in the case of sulfuric acid behavior above 10 km altitude.

Growth of particles by accumulation on existing particles can be classed as two broad processes. If the precursor is supersaturated, growth will occur at a vapor diffusion limited rate, which depends on the supersaturation, the temperature, the particle size, and the accommodation coefficient at the surface. The dependence of the growth rate on particle size changes with the ratio of particle diameter and mean free path of the suspending gas. At one extreme, the growth depends on volume to the 2/3 power; at the other, growth is proportional to volume to the 1/3 power. When the precursor is unsaturated, growth still may take place by irreversible absorption, or by chemical reactions in the particle. In this case, the rate law should be proportional

SC524.25FR

to the particle volume if the reaction is uniform throughout the particle. If the formation of material is limited by reactions in the particle, then the conversion ratio should not be dependent on the gaseous precursor concentration.

There is insufficient data available to determine the rate law or physical mechanism most likely to predominate in atmospheric aerosol growth. However, there are clues to differences in the processes from the Los Angeles data. The shape of the curve representing the particle volume number distribution of tropospheric aerosol is such that the $1/3$ (diameter) and $2/3$ (surface) moments are concentrated in the submicron fraction, while the first moment (volume) is weighted toward larger particles. Thus the observed accumulation of sulfate and organic carbon on the small particles in smog suggests a surface or vapor diffusion controlled process. In contrast, the collection of NO_3^- in larger particles at a rate independent of the NO_2 concentration may indicate a volume controlled reaction in the particles. The shift in NO_3^- to smaller particles between the east central and the eastern parts of the Los Angeles Basin is of interest in this case and remains unexplained.

It is of interest that the influence of thermodynamic equilibrium must enter the growth process of particles. If the radius of the particles is very small, the partial pressure of condensable species can increase significantly with decreasing radius of curvature. From Kelvin's relation, examination of values of surface tension for a range of materials suggests that this effect will constrain growth to particles greater than 0.05 to 0.1 μm diameter. This appears to be consistent with available observations of atmospheric growth and the distribution of secondary chemical components.

2. CHEMICAL REACTIONS FOR PRECURSORS

Physical processes of phase change, absorption and stabilization restrict the maximum rate of formation and the classes of materials expected in aerosols generated in the atmosphere. Yet in many instances, the rate controlling process in the production mechanism may be the precursor formation. In the case of any of the secondary constituents, there are a variety of possible chemical mechanisms that may occur in the atmosphere. It is likely, in fact, that different mechanisms take place in parallel, or complement one another so that no one process is dominant.

SC524.25FR

a. Sulfate Reactions

The oxidation reactions of SO_2 have been reviewed by several investigators including Bufalini⁽³²⁾ and Calvert.⁽²⁷⁾ There are more than a dozen sulfate forming reactions that may be relevant to atmospheric processes. These can be grouped in terms of homogeneous gas phase reactions and heterogeneous reactions involving suspended particles. A summary of the two groups is listed in Tables 5-1 and 5-2. The homogeneous reactions are broken down into sub-categories whose end products are SO_3 or RO_2SO_2 , and ROSO_2 . Although the rates of reaction of these species with water or other species have not been reported, it is assumed that the reactions with water are fast to form H_2SO_4 and not the rate determining step in $\text{SO}_4^{=}$ production.

Table 5-1 lists three classes of homogeneous reactions. The first consists of inorganic oxidation mechanisms to form SO_3 , while the second involves organic radical oxidation agents generating SO_3 or RO_2SO_2 . The third group of reactions forms ROSO_2 species. All of the reactions listed are exothermic and are favored thermodynamically. However, the first five reactions have been considered severely rate-limited on the basis of available rate data (e.g. Calvert⁽²⁷⁾). The remaining reactions listed appear to have rates that are sufficiently rapid to be of importance in the atmosphere, at least for polluted air with active photochemical processes. For comparison, estimates of the fractional conversion rate of SO_2 to $\text{SO}_4^{=}$ is given in the Table. These results are based on Calvert's computer simulations. These were based on an estimation of reactive intermediates after a 30-minute period of sunlight irradiation at zenith angle of 40° , with initial concentrations in ppm of $\text{NO}_2 = 0.025$, $\text{NO} = 0.075$, $\text{C}_4\text{H}_8 = 0.10$, $\text{CH}_2\text{O} = 0.10$, $\text{CH}_3\text{CHO} = 0.06$, $\text{CO} = 10$, $\text{CH}_4 = 1.5$, $\text{SO}_2 = 0.05-0.1$, and R.H. = 50% at 25°C .

The reactions (7) and (8) correspond to the interpretation of Cox and Penkett's⁽³³⁾ observations that SO_2 is oxidized at appreciable rates in the dark in ozone-olefin-air mixtures. The higher rate of $3\% \text{ hour}^{-1}$ was found for cis-2-pentene, while the lower rate of $0.4\% \text{ hour}^{-1}$ was found for propylene. Cox and Penkett suggested that either of two intermediates were involved in the SO_2 oxidation reaction. These are the ozonide reaction (7) or the

SC524.25FR

TABLE 5-1

 ESTIMATED RATES OF THEORETICALLY POSSIBLE HOMOGENEOUS REMOVAL PATHS
FOR SO₂ IN A SIMULATED POLLUTED ATMOSPHERE (FROM CALVERT(27))

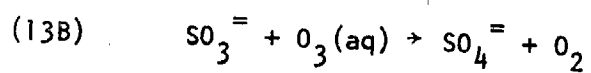
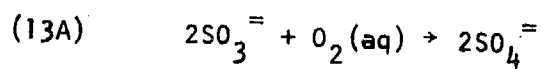
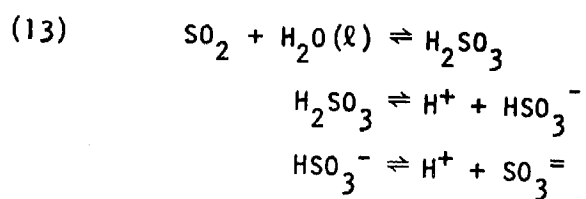
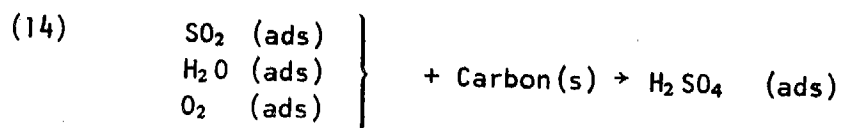
	ΔH_{298} , kcal/mole	Approx. Rate, % per hr.
A. Inorganic Reactions Forming SO ₃		
(1) SO ₂ + 1/2 O ₂ + Sunlight → SO ₃	-24	< 0.021
(2) O(³ P) + SO ₂ + <u>M</u> → SO ₃ + <u>M</u>	-83	0.014
(3) O ₃ + SO ₂ → SO ₃ + O ₂	-58	0.00
(4) NO ₂ + SO ₂ → SO ₃ + NO	-10	0.00
(5) NO ₃ + SO ₂ → SO ₃ + NO ₂	-33	0.00
(6) NO ₂ O ₅ + SO ₂ → SO ₃ + N ₂ O ₄	-24	0.00
B. Organic Reactions Forming SO ₃		
(7) $\begin{array}{c} \text{O}_3 \\ \diagdown \quad \diagup \\ \text{CH}_2 - \text{CH}_2 \end{array} + \text{SO}_2 \rightarrow \text{SO}_3 + 2\text{CH}_2\text{O}$	-81	< 0.4-3.0
(8) •CH ₂ OO• + SO ₂ → SO ₃ + CH ₂ O	~ -117	< 0.4-3.0
CH ₂ =O - O + SO ₂ → SO ₃ + CH ₂ O	~ -85	
(9) HO ₂ + SO ₂ → HO + SO ₃ (a)	-19	0.85
→ HO ₂ SO ₂ (b)	-25	?
(10) CH ₃ O ₂ + SO ₂ → CH ₃ O + SO ₃ (a)	-30	0.16
→ CH ₃ O ₂ SO ₂ (b)	< -25	?
C. Reactions Forming HOSO ₂ or ROSO ₂ Radical		
(11) HO + SO ₂ → HOSO ₂ •	~ -82	~ 0.23-1.4
(12) CH ₃ O + SO ₂ → CH ₃ OSO ₂ •	~ -73	~ 0.48

 TOTAL POTENTIAL RATE OF CONVERSION OF SO₂ TO SO₃ (OR
SULFATES) IN MODERATE SMOG ≈ 1.7 - 5.5% PER HOUR

SC524.25FR

TABLE 5-2

HETEROGENEOUS REACTIONS TO FORM SULFATE

A. AqueousB. Non-Aqueous

SC524.25FR

zwitterion intermediates from the O_3 -olefin reaction. The zwitterion has a diradical character and may be illustrated as reaction (8). Calvert's calculation of olefin- O_3 intermediates such as those in reactions (7) and (8) do not favor their importance as oxidizing agents. However, other radical species from the ozonide or zwitterion intermediates may be of interest, including those summarized by Reactions (9 - 12). These classes of reactions may well account for SO_2 oxidation in the ozone-olefin mixtures.

Recently, the potential importance of radical addition reactions in the third class listed in Table 5-1 for SO_2 oxidation has become more fully appreciated. Such reactions are exemplified in the series (9) to (12).

The rate of the HO_2 reaction has been measured by Davis *et al.*⁽³⁴⁾ With such data, the fractional rate of SO_2 disappearance may reach $\sim 1\%$ in a moderate photochemical smog. Assuming that the rate of the CH_3O_2 - SO_2 reaction is the same as HO_2 - SO_2 reaction, Calvert has estimated that the former will contribute a fractional oxidation rate of $0.2\% \text{ hour}^{-1}$ in moderate smog.

The OH radical- SO_2 reaction (11) appears to be of particular importance in the lower stratosphere where OH concentrations are estimated to be high. (35,36) Calvert⁽²⁷⁾ has estimated the typical reaction rates for OH or CH_3 radical SO_2 reactions on the basis of analogies to reaction rates of CH_3 , C_2H_5 , and CFH_2CH_2 . These rates are listed as $0.23\% \text{ hour}^{-1}$ and $0.5\% \text{ hour}^{-1}$ respectively at the lower range.

Measurements of the rate constant for the $OH + SO_2 + M \rightarrow HOSO_2 + M$ reaction are emerging from recent fundamental studies. Hamilton⁽³⁷⁾ has summarized the preliminary values of the rate constant for this reaction. At $\sim 300^\circ K$ the rate constant for this reaction ranges from Wayne's value of $\sim 7 \times 10^9 \text{ l. mole}^{-1} \text{ sec}^{-1}$ for 1 atm Ar to Payne *et al.*'s⁽³⁸⁾ value of $1.1 \times 10^8 \text{ l. mole}^{-1} \text{ sec}^{-1}$ for 18 torr N_2 and 20 torr H_2O . Calvert⁽²⁷⁾ has used $1.1 \times 10^9 \text{ l. mole}^{-1} \text{ sec}^{-1}$ to estimate the upper limit of $1.4\% \text{ hour}^{-1}$ listed in Table 5-1.

The radical addition products, such as $HOSO_2$, should react rapidly with other species to generate sulfuric acid, peroxy-sulfuric acid, alkylsulfates and mixed intermediates such as $HOSO_2ONO_2$. Any of these ultimately should lead to sulfate in the presence of water.

SC524.25FR

Summing all of the known homogeneous reactions for SO_2 oxidation, it is possible to rationalize a theoretical rate of sulfate production in the range $1.7\text{--}5.5\%$ hour^{-1} for moderate photochemical smog conditions. However, such rates are clearly highly dependent on the presence of unstable intermediates at relatively high concentrations. This is by no means a universal condition in non-urban air or in cities with minimal photochemical activity, as measured for, example, by ozone levels.

For conditions where photochemically induced homogeneous reactions cannot be important, the heterogeneous processes must be considered. The known reactions are listed in Table 5-2. These have been categorized as aqueous and non-aqueous reactions. The class of reactions that have been used most frequently to explain high SO_2 rates in the presence of liquid water containing aerosols is the system involving SO_2 absorption in water followed by oxidation by dissolved O_2 to form sulfate. Catalysis of the oxidation by heavy metal salts such as Mn ion can cause rates of oxidation in excess of 1% hour^{-1} in clean water solutions (e.g., Johnstone and Coughanowr⁽³⁹⁾, Matteson *et al*⁽⁴⁰⁾). The absorption of SO_2 can be promoted by the buffering effect of simultaneous absorption of ammonia. Scott and Hobbs⁽²⁵⁾ have shown that the aqueous SO_2 oxidation process can be enhanced significantly by ammonium ion. Indeed the estimates and experiments of Miller and dePena⁽⁴¹⁾ and Corn and Cheng⁽⁴²⁾ suggest that rates of SO_2 oxidation in fog can approach 10% hour^{-1} .

It is well known that ozone is quite soluble in water. Therefore, one expects that absorption of both ozone and SO_2 would contribute to significant oxidation of SO_2 . Experiments of Penkett⁽⁴³⁾ have shown that oxidation of SO_2 at 7 ppb in the presence of water droplets and ozone at 5 ppm can be as large as 13% hour^{-1} . Thus, foggy or cloudy air mixed with photochemical smog, such as sometimes found along the Pacific Coast, could well give rise to an important $\text{SO}_4^{=}$ forming mechanism. Furthermore, such an aqueous mechanism could be significant at middle altitudes over continents even at background ozone levels.

SC524.25FR

The reported rates of SO_2 oxidation in clean water droplets must be considered an upper limit. It is questionable whether they can ever be achieved in the atmosphere since such aqueous reactions have been shown to be suppressed significantly by organic contaminants. The work of Fuller and Christ⁽⁴⁴⁾ and later of Schroeter⁽⁴⁵⁾ has shown that the aqueous absorption of SO_2 and its subsequent oxidation is reduced as much as an order of magnitude by dissolved organic acids or alcohols. This type of material is known to be present in the atmospheric aerosol sampled at the ground, so one can expect that the aqueous oxidation will probably be most efficient in relatively clean conditions of clouds well away from the earth's surface.

The heterogeneous mechanisms of SO_2 oxidation in the absence of liquid water are poorly understood. However, the recent work of Novakov et al.⁽⁴⁶⁾ has shown that $\text{SO}_4^{=}$ can be produced rapidly on the surface of carbon particles suspended in water vapor and air. These workers have observed that significant amounts of $\text{SO}_4^{=}$ can be found on carbon particles generated by combustion of hydrocarbons in air enriched with ppm levels of SO_2 .

It is difficult to assess the significance of carbon or organic particles in the oxidation of SO_2 in the free atmosphere. There is little doubt that adsorption of SO_2 on carbon particles freshly generated by combustion can provide a surface catalyzed oxidation medium. Indeed experiments such as those of Yamamoto et al.⁽⁴⁷⁾ have shown that SO_2 oxidation can be as high as $30\% \text{ hour}^{-1}$ on activated charcoal particles $< 5 \mu\text{m}$ in diameter. Their work also indicates that this rate is strongly reduced by sulfuric acid collection in the micropores of the charcoal. The work of Yamamoto et al. further emphasizes that such a heterogeneous oxidation mechanism depends on a variety of factors, ranging from grain size of the carbon, temperature, concentration of SO_2 , H_2O vapor, and oxygen, as well as the micropore structure of the particle surface. It would seem that oil, gummy, wet particles collected from the atmosphere would be poorly suited for non-aqueous reactions to form sulfate since their micropore structure would be minimal. Yet such a mechanism cannot be ruled out from consideration at this time.

SC524.25FR

b. Nitrate Forming Reactions

Like the production of sulfates, nitrates in atmospheric aerosols can be formed by a wide variety of homogeneous reactions as well as heterogeneous reactions. The pathways of nitrate generation are less well understood than those leading to sulfate, but it is likely that they are interrelated at least in some circumstances.

Since both nitrous acid and nitric acid are much more volatile than sulfuric acid, it does not appear possible that particulate nitrogen oxide species will exist in the atmosphere in pure form. Thus the production of nitrate must involve formation of a condensable species such as NH_4NO_3 in the gas phase, or the absorption of a nitrogen oxide constituent on particles followed by stabilization through chemical reaction. Such heterogeneous processes can, of course, take place in an aqueous or non-aqueous medium.

The precursors for particulate nitrate formation are summarized in Table 5-3. These are classified in terms of (a) important nitrogen oxides, (b) volatile acids HONO , and HONO_2 , and (c) gaseous nitrates.

Because nitric oxide is relatively insoluble and nonreactive with water, the important nitrate forming atmospheric oxides of nitrogen are believed to be NO_2 , NO_3 , and N_2O_5 . These species are formed mainly in the atmosphere by the well known "smog" reactions (16-20) and are not emitted primarily from material or anthropogenic sources.

With the nitrogen oxides coexisting with water vapor and sulfuric acid, the volatile nitrous and nitric acids can be formed via the reactions (21 - 24). The mixed intermediates involving sulfuric acid are of interest as they link the NO_x and SO_x chemistry. Once the volatile acids are formed, they may react with ammonia in the gas phase to form, for example, NH_4NO_3 (reaction 25). The nitrogen oxides also react with radicals such as RO_2 to form organic nitrates and nitrites including peroxy acetylnitrate (PAN). Reaction (25) has been hypothesized by Calvert⁽²⁷⁾ on the basis of an analogy to the $\text{NH}_3\text{-HCl}$ reaction. For concentrations of NH_3 and HONO_2 at ~ 1 pphm, Calvert's⁽²⁷⁾ work suggests that the ammonia reaction may represent a significant removal path of HONO_2 to form aerosols.

SC524.25FR

TABLE 5-3

REACTIONS POTENTIALLY INVOLVED IN NITRATE FORMATION

<u>Species</u>	<u>Rate Constants</u> ($\text{ppm}^{-1} \text{min}^{-1}$)
A. Nitrogen Oxides	
(15) $\text{O}_3 + \text{NO} \rightarrow \text{NO}_2 + \text{O}_2$	21.8
(16) $\text{O} + \text{M} + \text{NO} \rightarrow \text{NO}_2 + \text{M}$	
(17) $\text{RO}_2^* + \text{NO} \rightarrow \text{NO}_2 + \text{R}'\text{OH}$	
(18) $\text{O}_3 + \text{NO}_2 \rightarrow \text{NO}_3 + \text{O}_2$	
(19) $\text{NO}_3 + \text{NO}_2 \rightleftharpoons \text{N}_2\text{O}_5$	
B. Volatile Acids	
(20) $\text{N}_2\text{O}_5 + \text{H}_2\text{O} \rightarrow 2 \text{HONO}_2$	2×10^{-5}
(21) $\text{HO} + \text{NO}_2 + \text{M} \rightarrow \text{HONO}_2 + \text{M}$	1×10^4 (M = 1 atm N_2)
(22) $\text{NO} + \text{NO}_2 + \text{H}_2\text{O} \rightarrow 2 \text{HONO}$	
(23) $\text{HOSO}_2\text{O} + \text{NO} \rightarrow \text{HOSO}_2 \text{ONO}$ $\quad \quad \quad + \text{H}_2\text{O} \rightarrow \text{H}_2\text{SO}_4 + \text{HONO}$	
(24) $\text{HOSO}_2\text{O} + \text{NO}_2 \rightarrow \text{HOSO}_2 \text{ONO}_2$ $\quad \quad \quad + \text{H}_2\text{O} \rightarrow \text{H}_2\text{SO}_4 + \text{HONO}_2$	
C. Gaseous Nitrate	
(25) $\text{NH}_3 + \text{HONO}_2 \rightarrow \text{NH}_4\text{NO}_3$	$\sim 10^{-6}$
(26) $\text{RO}_2^* + \begin{matrix} (\text{N}_2\text{O}_5 \\ (\text{NO}_2) \end{matrix} \rightarrow \begin{matrix} \text{R}^1\text{C}=\text{O} \\ \quad \quad \quad \backslash \\ \quad \quad \quad \text{ONO}_2 \end{matrix}$ $\quad \quad \quad +$ $\quad \quad \quad \begin{matrix} \text{R}^1\text{C}=\text{O} \\ \quad \quad \quad \backslash \\ \quad \quad \quad \text{ONO} + \dots \end{matrix}$	10

SC524.25FR

It is possible that condensable organic nitrates are formed via reaction (25) in the gas phase. Certainly the observation of such materials from smog chamber experiments (O'Brien et al. (48)) would provide some evidence for such cases. However, it is known that volatile organic nitrates such as PAN readily hydrolyze in an aqueous medium to form nitrite ion (Reaction 31, Table 5-4). Thus the presence of such compounds resulting from gas phase reactions could lead to particulate nitrate after stabilization with ammonium ion or another cation.

Of the gas phase reactions involved to form nitric acid vapor, (20) and (21) are believed to be most important. Using currently accepted rate constraints for these reactions, Calvert has estimated that

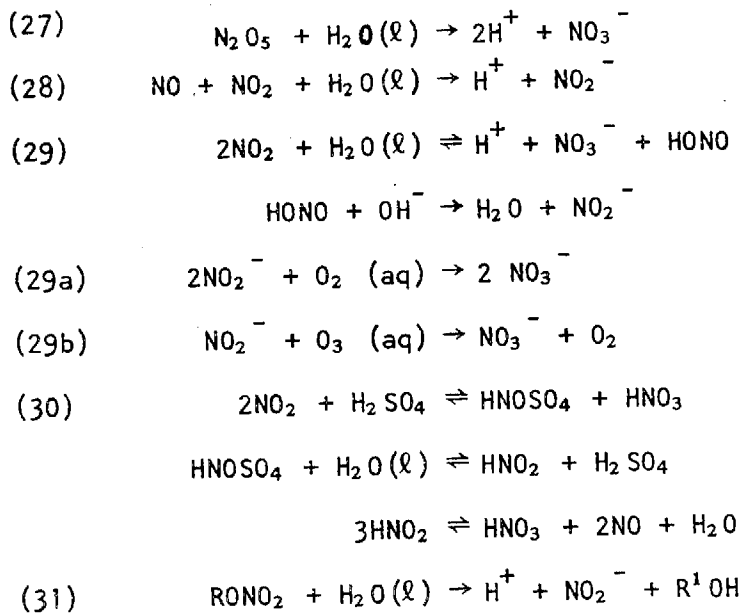
$$R_{20} \approx 0.5-2 \times 10^{-5} \text{ ppm min}^{-1}$$

$$R_{21} \approx 2-6 \times 10^{-5} \text{ ppm min}^{-1}$$

in moderate photochemical smog. Thus, it would appear that reaction (21) is of principal importance for HONO_2 formation in smog. The rate of conversion of NO_2 to HONO_2 by this reaction should be in the range of 2-8% hour⁻¹ for the conditions used in the calculations in Table 5-1. (27) With absorption in wet aerosols and neutralization with ammonium ion, this is not unreasonable for the upper limit of estimated nitrate formation rate in Los Angeles smog in the morning "peak" condition. Once the nitrogen oxides are present or the acids begin to form, the interaction of these species with moist aerosols can take place. Some potentially important reactions are given in Table 5-4. Here the complexities of the aqueous reactions of NO_x become apparent. All of the nitrogen oxides contained in the atmosphere will react with liquid water to form traces of nitrate and nitrite. These reactions are generally reversible, however, so that the anions must be stabilized by a base such as NH_4^+ . In the presence of dissolved oxygen or ozone, nitrite ion can be oxidized to nitrate in analogy to the aqueous sulfate formation reactions.

SC524.25FR

TABLE 5-4
 AQUEOUS REACTIONS OF NITROGEN OXIDES



SC524.25FR

None of the nitrate reactions has been studied with atmospheric application in mind. However, there is a variety of information in the chemical literature dealing with NO_x absorption in water. There is ample evidence, for example, from studies reported by Nash⁽⁴⁹⁾ and Borok⁽⁵⁰⁾ that NO_2 at trace levels in air is readily absorbed in aqueous solutions. The efficiency of absorption varies widely, however, depending on the acid-base content of the solution.

If significant quantities of concentrated sulfuric acid are formed in atmospheric aerosols, nitrate formation via absorption of NO_2 to form nitrosylsulfuric acid, HNOSO_4 , may be of interest. The rate of absorption of NO_2 in sulfuric acid is fast, but the efficiency appears to be relatively low, according to Baranov *et al.*⁽⁵¹⁾. Again it appears that ammonia absorption or another base has to be involved to drive the equilibria to nitrate production. Thus, in all of these aqueous reactions, nitrate formation may be limited by the concentration of ammonia rather than by any of the nitrogen oxide species.

D. APPLICATION OF MECHANISMS TO THE ATMOSPHERE

1. SULFATE FORMATION

In the case of photochemical smog in Los Angeles, comparison of the observations with expectations of chemistry suggests qualitatively that several mechanisms probably play a role in sulfate and nitrate formation. The evidence is compelling that submicron sulfate particles are produced photochemically as a part of the smog mechanism. Such formation is coupled closely with the changes in organic aerosol during the day and is well correlated with the delay required to produce the high levels of oxidant.

The reactions that appear to be most significant for submicron sulfate are homogeneous in nature, either involving a dark reaction of ozone and olefins, or the groups of free radical reactions such as OH attack on SO_2 . The accumulation of sulfate on the submicron particle fraction during the day is consistent with a vapor diffusion limited process with a condensable or reactive precursor such as H_2SO_4 or HSO_3 radical.

The ACHEX data can be used to crudely test the relevance of the dark reaction of ozone and olefins to the formation of sulfate in smog. Cox and

SC524.25FR

Penkett found that the rate of SO_2 oxidation was proportional to the product of the ozone and the olefin concentration. If it is assumed that the total olefin concentration is proportional to the non-methane hydrocarbon (NMHC) concentration measured at the same time as sulfate and ozone, then the conversion ratio f_S based on sulfate in the submicron fraction (previously identified as the photochemically related sulfate) should correlate with the ozone concentration $[\text{O}_3]$ times the NMHC concentration. Such a test is shown in Figure 5-12. There is an apparent systematic increase of f_S ($< 0.5 \mu\text{m}$) with low values of the product $[\text{O}_3] \times [\text{NMHC}]$. At values of this product above 0.2, however, f_S evidently becomes independent of the product. The data presented in this way are less well correlated than the simpler relationship with ozone alone.

The relationship plotted in Figure 5-12 fails to take account of air transport so that simplistic conclusions about the relevance of the dark reaction between ozone and olefins cannot be made at this time. The absence of a clear relationship between sulfate and either ozone or non-methane hydrocarbons should not be interpreted as indicating that photochemically induced intermediates are unimportant in the production of sulfate.

Because of the strong correlation between f_S ($< 0.5 \mu\text{m}$) and particulate carbon in Figure 5-9, an alternate mechanism of catalytic SO_2 oxidation on carbonaceous particles cannot be ruled out. However, this appears to be a less likely mechanism in the ambient atmosphere than photochemically related processes.

The accumulation of sulfate in the larger particles at night and early morning suggests alternate mechanisms involving aqueous particle reactions also are important part of the time.

The behavior of sulfate in the larger particles shows a poorer correlation with ozone and carbon in Los Angeles air, but the correlation with relative humidity change is also weak. It is likely that aqueous sulfate formation mechanisms play some role in total sulfate behavior in Los Angeles, particularly at night or in conditions of fog or haze with high liquid water content. The inhibiting influence of organics in aqueous urban aerosols is uncertain, but may be a factor in the apparent variability of sulfate generation from day to day in Los Angeles.

SC524.25FR

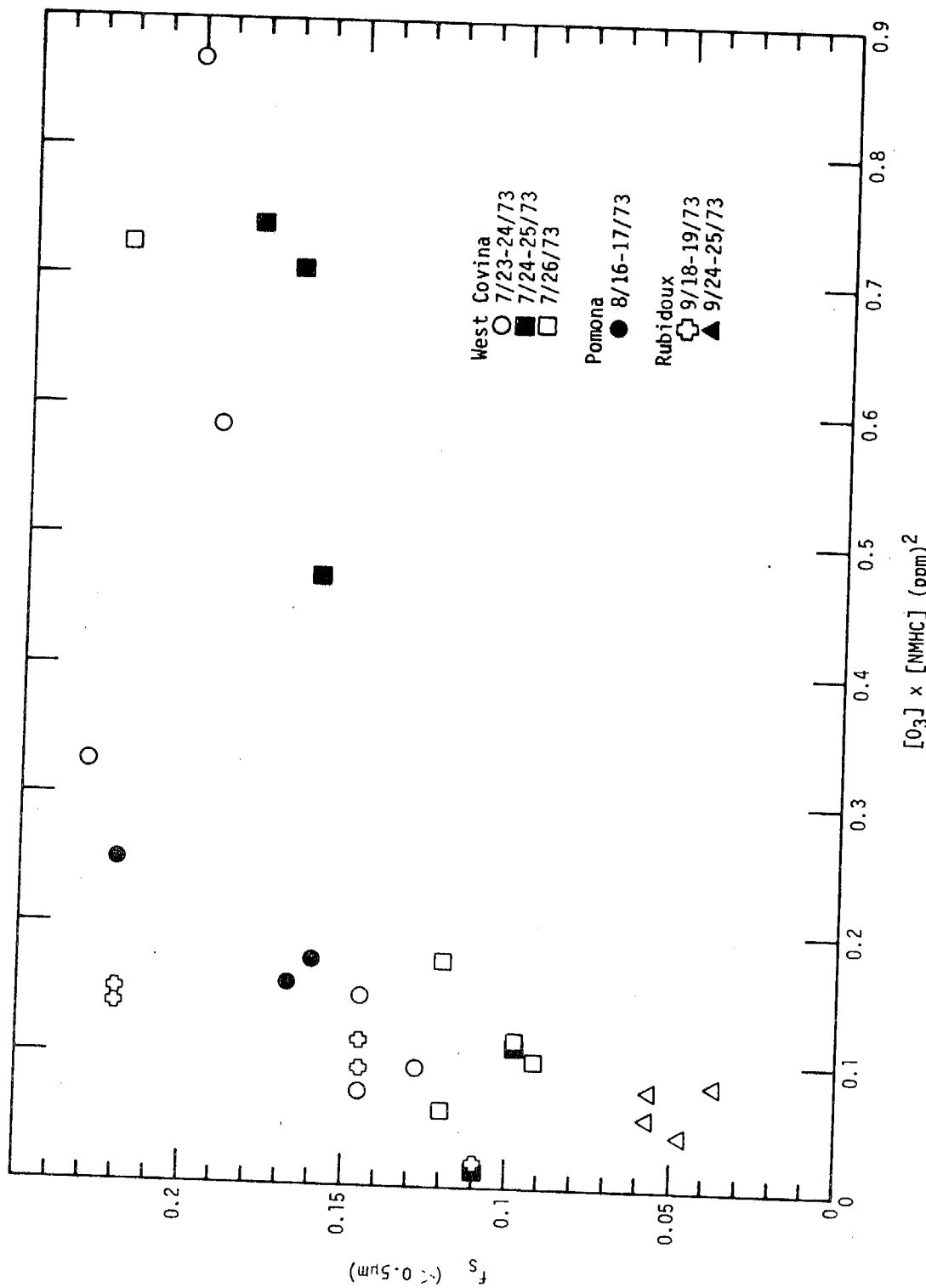


Figure 5-12. The Dependence of the Sulfate Conversion Ratio on the Product of the Ozone and Non-Methane Hydrocarbon Concentrations

SC524.25FR

Extrapolation of the experience in Los Angeles to other situations in the troposphere is difficult because of a lack of suitable observational data. However, it is likely that the photochemical formation of sulfate will begin to be important whenever ozone exceeds 0.1 - 0.2 ppm in air and reactive hydrocarbons are present. At the ground, the reactions in aqueous media are likely to be important in both urban and non-urban air if photochemically induced processes are absent. Away from the ground in the middle and upper troposphere, reactive hydrocarbon and free radical concentrations should be rather low under most circumstances. The presence of organics in aerosols at cloud level and above should be minimal so that the aqueous oxidation processes globally should play a dominant role between 2 km and 10 km altitude.

2. NITRATE FORMATION

The knowledge of nitrate forming processes applicable to the atmosphere provide a less convincing basis for explaining the behavior of this ion than is the case for sulfate. The key difference in mechanisms evidently is centered around the volatility of nitrous and nitric acid and their equilibria in aqueous solution. The Los Angeles experience emphasizes the distinct difference in nitrate evolution as compared with sulfate. There appear to be two extremes of behavior, first a short term transient production accompanying the NO_x peak in the morning and second a much slower, but systematic production to give high concentrations of NO_3^- after two to three hours of air mass transport across the Los Angeles Basin. The overall NO_3^- production correlates poorly with ozone, NO_x , and NO_2 , but the transient peak in the morning takes place at high relative humidity.

The evidence suggests that nitrate could be generated via homogeneous gas phase reactions or by heterogeneous, aqueous processes. It seems that intermediate species other than NO_2 are involved at least during the morning transient period. The lack of dependence of the nitrate conversion ratio on NO_2 or NO_x may suggest a droplet rate controlled NO_3^- formation after absorption. The complicated equilibria involved in nitrogen oxide ion solutions underscores the potential importance of basic substances such as NH_4^+ necessary to neutralize acidic particles. It is likely that NH_3 plays a

SC524.25FR

critical role in stabilizing nitrate in aerosol particles. This conclusion can be drawn from the Los Angeles experience since there are relatively high ammonia concentrations in the air over the eastern parts of the Basin where the highest nitrate levels are observed.

Interpretation of nitrate formation in the troposphere is difficult at present because of the paucity of atmospheric aerosol data. However, it is likely that photochemical processes are important since the highest nitrates are generally observed in cities with high oxidant levels, particularly in Los Angeles. Again it would seem that NH_3 plays a crucial role in nitrate generation if acids are involved. Thus one would expect that less nitrate would be present at higher altitudes away from the principal sources of NH_3 .

SC524.25FR

VI. CARBON AEROSOL CHEMISTRY

The third major ingredient in California aerosols that results from atmospheric processes is the organic particles. As discussed later in Section VIII, primary sources of organics cannot account for a major portion of the non-carbonate carbon found in aerosols. Therefore, secondary processes must be responsible for much of this material.

A. CHARACTERIZATION OF ORGANIC FRACTION

Although considerable effort was devoted to characterizing organic aerosols in the ACHEX, several questions remain about their nature. In particular, the identification of specific compounds or classes of compounds remains limited quantitatively. Only by such information can a satisfactory understanding of the organic aerosol production process be achieved.

Characterization of the organic aerosol was pursued along two lines. The first was an attempt to develop a simple, inexpensive quantitative analysis for total organic (or non-carbonate) carbon that could be used to distinguish between primary emissions and secondary aerosols. The second approach was to use solvent extraction methods combined with detailed infrared analysis and high resolution mass spectroscopy to identify important chemical characteristics of the organic aerosol.

1. TOTAL CARBON ANALYSIS

The elemental carbon analysis adopted several years ago by AIHL⁽¹⁵⁾ has proved to be a very useful, simple measure of non-carbonate carbon, since very little carbonate is found in aerosols compared with organic carbon. In principle, this approach could be extended to characterize thermogravimetrically different fractions of the non-carbonate carbon. To test this approach, it was hypothesized that three classes of organic carbon exist in atmospheric aerosols that could be identified with different sources. A fraction volatilized at temperatures between 60°C and 310°C was assumed to be the secondary aerosol (CVL). A second fraction volatilized between 310°C and 485°C was identified with primary emissions of atomized lubricating oils or partially burned fuel (CPR). A pyrolyzable fraction of carbon residue removable at

SC524.25FR

temperatures greater than 450°C was considered elemental in nature, presumably as soot from combustion processes (CNV).

An attempt was made in the 1973 ACHEX to characterize aerosol organics thermogravimetrically into the three "source" classes.⁽⁵²⁾ Extensive application of this method was discontinued after early comparisons with the AIHL total carbon method. In general, the thermogravimetric technique yielded a total carbon content (CVL + CNV + CPR) less than the elemental method by 20-40%. This appears to be the result of inconsistencies in the calibration and response of the detectors in the two methods.

Additional investigation of the thermogravimetric method indicated, however, that there was some degradation of the volatile and non-volatile fractions during the heating of the samples. Therefore, this approach is believed to be of limited value despite its apparent simplicity. For purposes of the analysis in this study, the elemental carbon values have been used with the sum of the CVL, CNV, CPR fractions to characterize the non-carbonate carbon.* No attempt has been made to interpret the differences in behavior of individual thermogravimetric fractions of the carbon.

2. SOLVENT EXTRACTION

The initial approach of simple extraction by cyclohexane used in the 1972 ACHEX samples showed that only a small fraction of the total organics can be extracted by use of a non-polar solvent. Extraction by the sequential use of increasingly polar solvents proved to be more useful, as found by other investigators (e.g., References 30, 53).

The total extractables for the twelve 1973 episodes, in $\mu\text{g}/\text{m}^3$, are listed in Table 6-1 for the cyclohexane and successive benzene and $\text{CH}_3\text{OH}-\text{CHCl}_3$ extractions. Also listed are the percent of the total particulate mass extracted, the carbon extracted and the percentage carbon content of the extracts. The last column lists the sum of the soluble carbon obtained by the benzene and the methanol-chloroform solvent extractions.

On the average, benzene extracted approximately 76% more material than

*It is assumed that carbonate is a negligible fraction of the carbon in aerosol, as found several years ago by Mueller *et al.*

SC524.25FR

TABLE 6-1
SOLVENT EXTRACTION OF 24-HOUR FILTERS

	Cyclohexane Extractable		Benzene Extractable		CH ₃ OH-CHCl ₃ Extractable ⁸⁾			Ratio Benzene: Cyclohexane	Σ C _{ext} (μg/m ³)
	μg/m ³ 1)	% Total Mass 2)	μg/m ³ 3)	% Total Mass 2)	% Carbon 4)	% Total Mass 3)	% Carbon 4)		
TA0185RV	4.9	--	11.0	--	62.6	12.0	39.3	2.2	11.6
TB0196RV	7)	--	16.6	14.9	61.7	16.4	33.0	--	15.9
TC0205RV	8.8	8.4	18.1	17.0	65.8	23.8	43.7	2.1	22.3
TD0218RV	6.6	10.3	10.9	17.2	67.4	16.3	34.5	1.7	12.9
TE0277RV	7.4	17.8	7.6	18.2	65.2	10.0	32.3	1.0	8.2
UF0282RV	5.4	7.7	11.0	14.6	72.2	13.3	38.3	2.0	13.0
US0299RV	6.1	13.1	9.0	20.0	62.0	11.0	29.6	1.5	8.9
VHG221RV	7.9	7.1	13.7	12.3	61.5	60.0	9.3	1.7	14.0
V10260RV	5.3	4.0	10.5	8.1	60.2	52.2	6.6	2.0	9.7
VJ0232RV	3.8	6.0	5.3	8.3	59.8	15.8	17.0	1.4	5.9
WK0235RV	3.8	4.7	7.8	9.7	43.6	7.8	36.6	2.0	6.3
WL0253RV	9.0	15.7	11.5	20.2	60.5	9.0	18.2	1.3	8.6
Average	6.3±1.8	9.5±4.7	11.1±3.7	14.6±4.4	61.9±6.8	20.6±17.2	24.8±12.5	1.7±0.4	9.1±3.7

1. Relative error 23% for TA0185RV. Other values range from 4 to 11%.
2. Relative error 10% for TA0185RV. Other values range from 3 to 6%.
3. Relative error 9% for TA0185RV. Other values range from 1 to 4%.
4. Relative error 6%.
5. Relative error of 7 to 12%.
6. Relative error of 14 to 17%.
7. Sample lost during analysis.
8. Following initial extraction with benzene.

SC524.25FR

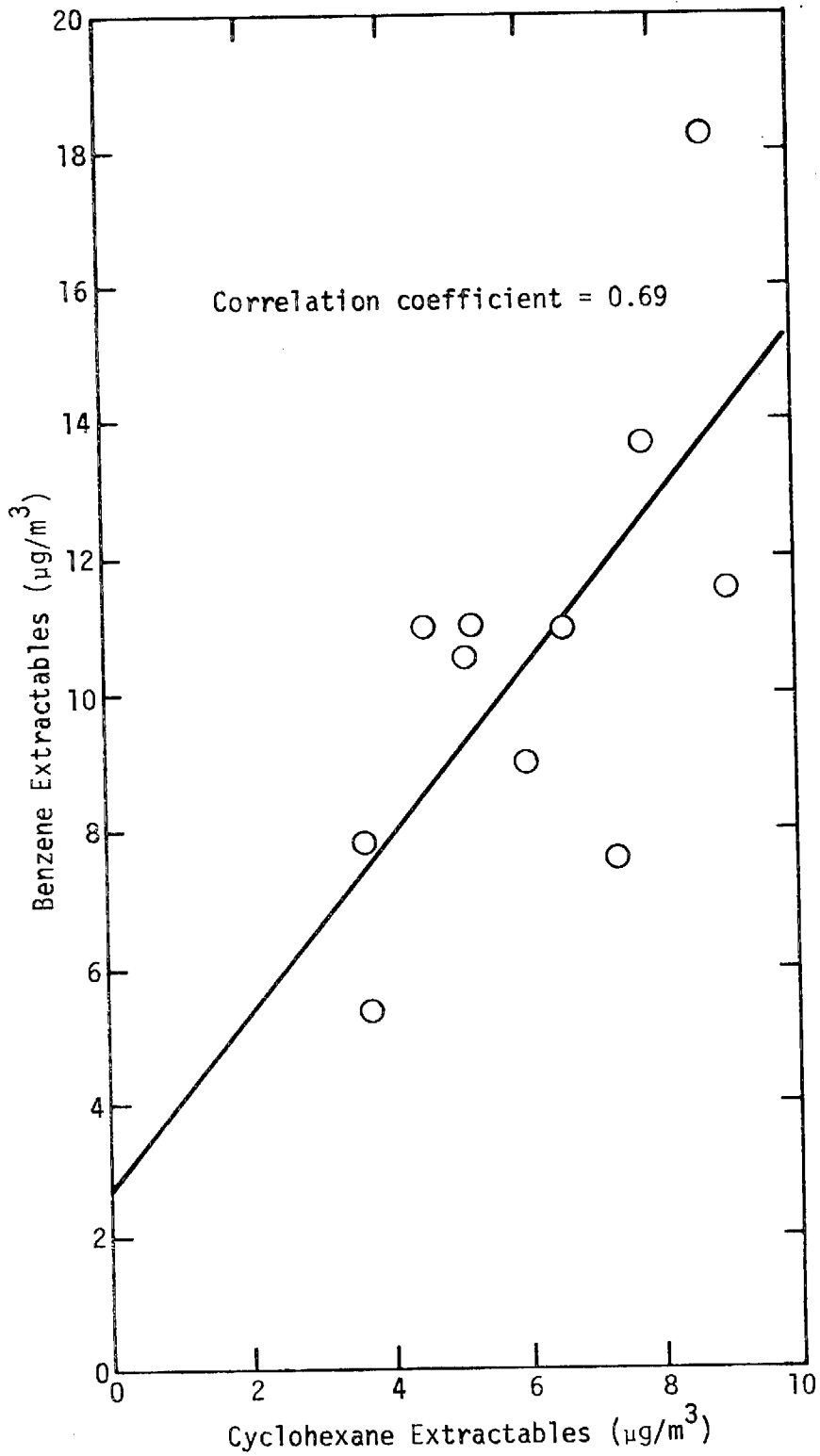


Figure 6-1. Benzene vs Cyclohexane Extractables

SC524.25FR

cyclohexane, varying from an equivalent amount for Episode TE to twice the amounts for Episodes TA, TC, UF, VI and WK; the mean ratio benzene/cyclohexane solubles was 1.7 ± 0.4 . In Figure 6-1 the benzene extractables are plotted against those for cyclohexane. The scatter about the regression line is considerable and the correlation coefficient is 0.69.

The methanol-chloroform solvent mixture extracted an additional amount nearly equal, on a mass basis, to the prior benzene extraction except for the Episodes VH, VI and VJ taken in the Riverside area where the final extraction yielded from three to five times the mass extracted in benzene. In all cases the cyclohexane and benzene extracts had the texture of a tacky gum while the $\text{CH}_3\text{OH-CHCl}_3$ solubles were brittle and, in the cases of the Riverside episodes, had a definite crystalline appearance. The inorganic, crystalline component of the Riverside extracts was identified by infrared spectroscopy and x-ray diffraction to be predominantly ammonium nitrate.

The carbon content of the cyclohexane and benzene extracts was approximately 60%, with some variation. In contrast to this, the methanol-chloroform extracts exhibited much lower carbon contents, especially for samples collected near Riverside; the overall mean percent carbon with the mixed solvent extract was $28 \pm 12\%$ with those from Riverside averaging $11 \pm 4\%$.

Table 6-2 compares the efficiency of cyclohexane, benzene and 1:2 v/v MeOH-HCCl_3 for extraction of carbon from the particulate samples expressed as percent of total carbon present (CEL). Clearly by use of the nonpolar solvents cyclohexane and benzene, most of the carbon remains unextracted. The question is, what proportion of this remainder is elemental carbon? By extraction with MeOH-CHCl_3 , about half of the C remaining after benzene extraction is solubilized and, therefore, not in elemental form. If the remainder after MeOH-CHCl_3 extraction is equated to elemental C, then on the average only 22% of the total carbon present exists in this form. Since some of this insoluble fraction may still not be elemental, this technique provides only an upper limit to the true level of elemental carbon present.

The preceding method for estimating elemental carbon may be compared with that previously employed, viz., equating carbon not volatilized at up to 485°C with elemental carbon using the DuPont Thermal Analyzer.⁽⁵²⁾ This comparison,

SC524.25FR

TABLE 6-2

COMPARISON OF EXTRACTION EFFICIENCY OF CYCLOHEXANE,
BENZENE AND BENZENE + MeOH-HCCl₃
(Basis carbon)¹

	Cyclohexane Extracted C CEL %	Benzene Extracted C CEL %	Benzene + MeOH-HCCl ₃ CEL %
TA0185RV	--	41	81
TB0196RV	--	43	65
TC0205RV	21	52	97
TD0218RV	31	57	100
TE0277RV	43	46	77
UF0288RV	22	48	79
UG0299RV	34	51	82
VA0221RV	31	56	93
VI0260RV	20	41	63
VJ0232RV	30	40	74
WK0239RV	18	32	59
WL0253RV	38	50	62
Mean	28.8 ± 8.3	46.4 ± 7.3	77.7 ± 13.9

¹CEL is total carbon on the initial filter sample by a combustion technique.²⁾

SC524.25FR

shown in Table 6-3, reveals that the CNV values are typically much greater (mean value $6.3 \pm 2.3 \mu\text{g}/\text{m}^3$) than the elemental carbon estimated by solvent extraction (mean value $3.2 \pm 2.4 \mu\text{g}/\text{m}^3$). Since the latter is here judged to be a reliable upper limit to the true elemental carbon, the validity of the CNV approach to estimating elemental carbon is seriously challenged.

In explaining the source of the error in the thermal analysis approach, the first hypothesis considered is the formation of refractory (i.e., non-volatile) carbon during the heating process. While studies with pure hydrocarbons (e.g., paraffin wax) indicated negligible formation of non-volatiles, such decomposition might be enhanced with the organics present in atmospheric particulates. To test this hypothesis, aliquots of the benzene and methanol-chloroform extracts from three episodes were heated to approximately 500°C under nitrogen in the DuPont apparatus and any residual carbon determined with the Total Carbon Analyzer. While organics unvolatized at this temperature might have been initially present, the presence of elemental carbon is excluded because of the use of the extract fractions.

As shown in Table 6-4, 7-10% of the carbon extractable in benzene was converted to refractory carbon (or was so initially). For the methanol-chloroform extracts this value increased to 32-42%. Thus, the initial presence or formation of substantial amounts of material classed as CNV from extracts initially free from elemental carbon confirms that CNV values are poor estimates of elemental carbon in the particulate sample.

The sum of the CNV values (in $\mu\text{g}/\text{m}^3$) for the extracts from benzene and MeOH-CHCl_3 can be subtracted from the CNV values for the original filter sample to obtain a better estimate of the elemental carbon present. This correction is also shown in Table 6-4 for the three episodes studied. For two of the three cases the "insoluble carbon" values ($\text{CEL-C}_{\text{ext}}$) are already within 20% of the CNV values. For Episode UF the insoluble carbon is less than half the CNV. The degree of agreement between the corrected values for CNV and the insoluble carbon values is shown in the last column. For the Episode UF the correction was clearly inadequate to obtain agreement between elemental carbon estimates by solvent extraction and thermal analysis. The other episodes are not considered a reliable test of the correction.

SC524.25FR

TABLE 6-3
COMPARISON OF SOLVENT EXTRACTION AND THERMAL ANALYSIS
FOR CHARACTERIZING CARBONACEOUS FRACTIONS¹⁾

Sample	CEL ²⁾	CEL-C _{ext} ³⁾	CEL-C _{ext} (%) CEL	CNV ⁴⁾	CNV/CEL (%)
TA0185RV	14.4	2.8	19	6.57	45.6
TB0196RV	24.1	8.4	35	9.21	38.2
TC0205RV	22.9	0.6	3	10.0	43.7
TD0218RV	12.8	-0.1	0	7.12	55.6
TE0277RV	10.7	2.5	23	4.11	38.4
UF0288RV	16.4	3.4	21	8.07	49.2
UG0299RV	10.9	2.0	18	3.62	33.2
VH0221RV	15.1	1.1	7.3	8.32	55.1
VI0260RV	15.3	5.6	37	6.46	42.2
VJ0232RV	8.0	2.1	26	3.21	40.2
WK0239RV	10.6	4.3	41	4.73	44.6
WL0253RV	13.9	5.3	38	4.35	32.4
Mean	14.6 ± 4.8	3.2 ± 2.4		6.3 ± 2.3	

1. Units are $\mu\text{g}/\text{m}^3$ except as noted.

2. Total carbon (by combustion).

3. Total carbon (by combustion) minus carbon solubilized by benzene + MeOH-HCCl₃ extractions. This represents an upper limit to the elemental carbon present.

4. Carbon remaining on filter after heating to about 500°C in the Du Pont Analyzer and used to approximate elemental carbon.

SC524.25FR

TABLE 6-4

 NON-VOLATILE CARBON FORMATION IN SOLVENT EXTRACTS
OF ATMOSPHERIC PARTICULATE SAMPLES

	CNV for Extracts ($\mu\text{g}/\text{m}^3$)		CNV for Extracts % of Total Carbon in Extract)		CNV- Σ CNV for Extracts ¹⁾ ($\mu\text{g}/\text{m}^3$)	CNV- Σ CNV for Extracts ²⁾ CEL-C _{ext}
	Benzene	MeOH-CHCl ₃	Benzene	MeOH-CHCl ₃		
TB0196RV	0.80	2.26	7.6	41.8	6.2	0.74
UF0288RV	0.53	1.64	6.7	32.1	5.9	1.7
VI0260RV	0.62	1.20	9.8	35.4	4.6	0.82

1. The CNV value for the original particulate sample less the sum of the CNV values for the two solvent extracts.
2. The CEL-C_{ext} is defined in Table 6.3, footnote 3.

SC524.25FR

It is, of course, possible that a conversion to non-volatile carbon occurs to a much greater extent when the heating process is done with the original glass filters. Many elements such as vanadium, titanium, iron and lead are present (but largely absent in the extracts) which are known to catalyze various dehydrogenation and degradation reaction which could substantially enhance the non volatile carbon formed.

The results of this work can be summarized as follows: benzene extracted about 75% more material from atmospheric samples than did cyclohexane. On sequentially extracting filters with a mixture of methanol-chloroform following extraction with benzene a brittle extract is obtained. For the Riverside episode this was identified as predominantly NH_4NO_3 . The benzene and cyclohexane extracts appeared to be tacky gums with carbon content of about 60% while the carbon content of the $\text{CH}_3\text{OH}-\text{CHCl}_3$ extracts averaged about 28% with the Riverside sample about 10%.

Comparing the fractions of carbon extractable by the three solvent systems, cyclohexane, benzene and benzene + $\text{MeOH}-\text{HCCl}_3$ extracted 28, 47 and 78%, on the average, of the carbon in the original sample.

Defining the solvent insoluble carbon as an upper limit to the elemental carbon present, the samples averaged 22% elemental carbon (basis total carbon). The use of CNV values for estimating elemental carbon was shown to be often in substantial error, and gave higher values than those obtained by solvent extraction. Non-volatile carbon formation during thermal analysis appears to be most likely an explanation of the error.

3. PHYSICAL METHODS

The development of new physical techniques for organic analysis over the past few years provides considerable promise for characterizing organic particles in the detail required for development of control procedures. Of the two methods tested in the ACHEX, high resolution mass spectroscopy (HRMS) shows perhaps the most interesting possibilities for analysis, particularly if it is coupled with chromatography.

Infrared analysis of impactor samples was undertaken in the ACHEX. These determinations were made by Stephens and Price, using the SAPRC technique⁽⁵⁴⁾ and by P. Cunningham of the Argonne National Laboratories. The

SC524.25FR

infrared spectra of impactor samples taken by the Riverside group showed little organic material. However, their impactor only sampled material $> 1 \mu\text{m}$ diameter, thus missing most of the organics that are present in the size below $1 \mu\text{m}$. Cunningham's analysis of Lundgren impactor samples showed the presence of organics by the observations of the C-H and C = O absorption bands.

Other exploratory spectra of filter samples of aerosol, including those taken by the Science Center staff, have indicated evidence of organics, with substantial oxygenated material, as shown by the presence of O-H, C = O, and C-O-C bands.

The application of HRMS to characterization of organic aerosols has evolved out of the work at the University of Washington.⁽⁵⁵⁾ As a result of this work, it has been possible to identify several important constituents or thermal degradation products of the smog aerosol that go beyond earlier work on polynuclear aromatics. In particular, the detection of significant quantities of carboxylic acids and dicarboxylic acids with other oxygenated materials has provided new insight into the organic fraction. Using such data, it is possible now to foresee the determination of specific organics, other than the polynuclear aromatics, that may be of interest for health hazards, instead of using solvent extracted organics as an index. This development, though in its early stages, must be considered an important milestone in aerosol chemistry.

Preliminary analysis of ACHEX samples taken in 1972 at Pomona indicated that diurnal changes in ratios of oxygenates to alkanes might reveal information on the mechanism of secondary aerosol formation.

A classification of organic material identified by HRMS for a series of samples taken at West Covina during the heaviest smog encountered in the ACHEX are listed in Table 6-5. The data indicate that the identified organic aerosol contains large quantities of saturated and unsaturated hydrocarbons in combination with carboxylic acids, dicarboxylic acids, substituted phenols and α -pinene. Other materials identified include aromatics, alcohols, aldehydes, nitriles, nitrates, and derivatives. Some of these organics may represent decomposition products of other compounds in the aerosol as a result of the analytical procedures used.

SC524.25FR

TABLE 6-5
HRMS ANALYSIS OF AEROSOL SAMPLES IN HEAVY SMOG AT WEST COVINA, JULY 23-24, 1973
(Concentration in $\mu\text{g}/\text{m}^3$)

Sample	Time (PST)	Penta-methyl-benzene	Napthalene	Nitro-napthalene	HOC(CH ₂)s-COH	CHO-CH=CH-CH(CH ₂) ₂ -CHO	Pinonols Acid	Alkenes C12-C30	Alkenes C30-C50	Alkenes C50-POLY	Alkenes C12-C30	Alkenes C30-C50	Alkenes C50-POLY	Alkenes
T80197RV	2121-0120	.010	.0060	--	.022	.38	--	.21	.33	.23	.15	.42	.47	.47
T80195RV	0123-0621	.019	.015	.0018	.031	.28	.37	.30	.79	.46	.11	.84	.80	.80
T80198RV	0624-0820	.008	.016	.0085	.17	.31	.60	.33	1.6	.67	.17	1.2	1.5	1.5
T80199RV	0822-1020	.029	.013	--	.11	1.2	--	.51	1.0	.26	.28	1.0	.81	.81
T80200RV	1023-1220	.011	.0071	.0042	.062	1.0	.42	.43	.57	.27	.15	.61	.59	.59
T80201RV	1222-1420	.069	.0074	.0074	.81	1.6	1.1	.32	1.0	.61	.27	1.0	.95	.95
T80202RV	1422-1620	.080	.014	--	.86	2.7	--	.43	2.7	.84	.47	2.5	2.0	2.0
T80203RV	1623-1823	--	.027	--	.077	1.4	2.7	.29	1.6	.73	.27	1.4	1.6	1.6
T80204RV	1825-2122	--	.016	.0042	.49	.64	--	.15	1.0	.32	.14	1.0	.82	.82

Sample	Time (PST)	Total Alkanes	Total Alkenes	Alkyl Benzenes	Subst. Styrene	Total Alkyl Nitriles	Total Anides	Total Mon R-Sub. Phenols	Total Carboxylic Acid	Total Acids as Acetic Acid	HOO(CH ₂) ₄ -CH ₂ OHO ₂	Alpha-Pinene	Norpinonic Acid	Glutaric Acid
T80197RV	2121-0120	.88	1.2	.14	.15	.050	.25	1.3	1.4	1.0	.044	2.0	.64	.20
T80195RV	0123-0621	2.0	1.9	.22	.19	.088	.33	1.7	1.4	1.0	--	2.6	--	.12
T80198RV	0624-0820	3.1	3.0	.29	.33	.075	.39	3.6	2.1	1.7	.031	5.2	--	.14
T80199RV	0822-1020	2.1	2.8	.30	.36	.097	.60	2.1	3.6	2.1	.080	3.8	.39	.51
T80200RV	1023-1220	1.6	1.5	.23	.37	.079	.56	3.2	2.2	1.9	--	3.1	1.9	.20
T80201RV	1222-1420	2.3	3.0	.37	.52	.27	1.5	4.6	5.7	4.4	.18	5.9	.98	.20
T80202RV	1422-1620	4.4	5.4	.56	.64	.20	.80	5.8	6.7	5.4	.081	7.7	--	.63
T80203RV	1623-1823	3.0	3.7	.39	.83	.16	.51	2.8	4.5	3.7	.42	5.7	--	.64
T80204RV	1825-2122	1.7	2.2	.20	.29	.13	.45	1.4	2.6	2.3	--	3.4	.49	.57

SC524.25FR

Although the patterns are not fully consistent, it appears that there is an increase in oxygenated material just after the morning traffic peak hours from 0800-1000, and during midday. There is also an increase in alkanes and alkenes during these periods.

The changes in different fractions of the organic material relative to alkanes or other indicator parameters including total acids are shown in Table 6-6. There appears to be a significant enhancement of total organic acid relative to alkanes in the morning from 0800 to 1000 PST. The variations in oxygenated materials and hydrocarbons in many cases display a minimum in midday followed by a large increase by late afternoon. At this time these data are difficult to interpret in the light of smog chemistry because insufficient samples have been analyzed to establish consistencies in the patterns of behavior of the different fractions.

Further work of this kind combined with other new methods of analysis is strongly recommended as part of a broader program to improve the knowledge of the behavior of organic compounds in the polluted atmosphere.

B. MECHANISM OF ORGANIC PARTICLE FORMATION

Of the three major contributors to secondary aerosol production from pollutant gases, perhaps the least is known about the mechanism for the formation of organics. The fact the organic material tends to be concentrated in the particles with a diameter less than $0.5 \mu\text{m}$ strongly supports the hypothesis that organic precursors are generated in the gas phase, or at least in a vapor diffusion limited process involving the particles. Therefore, the equilibrium constraint of low vapor pressure is particularly important for stability of the organic aerosols. The bulk of the organic vapors that have been identified in the ambient air have carbon numbers less than four, as shown, for example, in Table 6-7. The reactions of such materials at parts per billion concentrations cannot generate easily condensable material without polymerization reactions. This can be seen readily by examining vapor pressure data of organic compounds.

Among compounds with the same carbon number the oxygenated materials, and particularly carboxylic acids, have the lowest vapor pressure. Table 6-8 gives examples of vapor pressures of oxygenated compounds with a carbon

SC524.25FR

TABLE 6-6
SOME CHARACTERISTIC RATIOS FOR THE ORGANIC COMPONENT AS DETERMINED BY HRMS,
BASED ON ANALYSIS OF SAMPLES TAKEN AT WEST COVINA, JULY 23-24, 1973

Sample	Time (PST)	Total Alkenes		Total Acid		Glutaric Acid		Dicarboxylic Acids		HOOC(CH ₂) ₄ CH ₂ ONO ₂		Alkyl Nitriles		Norpinonic Acid		
		Total Alkenes	Alkanes	Total Acid	Alkanes	Total Alkenes	Alkanes	Total Alkenes	Alkanes	Total Alkenes	Alkanes	Total Alkenes	Alkanes	Total Alkenes	Alkanes	Total Alkenes
T80197RV	2121-0120	1.31	1.08	.867	.227	.867	.227	.867	.227	.0498	.0561	.0561	.324			
T80195RV	0123-0621	.782	.733	.500	.0887	.500	.0887	.500	.0887	--	.0646	.0646	--			
T80198RV	0624-0820	.976	.550	.464	.0456	.464	.0456	.464	.0456	.0100	.0244	.0244	--			
T80199RV	0822-1020	1.02	1.71	.624	.244	.624	.244	.624	.244	.0381	.0453	.0453	.105			
T80200RV	1023-1220	.317	.636	.723	.0679	.723	.0679	.723	.0679	--	.0260	.0260	.615			
T80201RV	1222-1420	.838	1.23	.651	.0546	.651	.0546	.651	.0546	.0499	.0744	.0744	.164			
T80202RV	1422-1620	1.21	1.21	.628	.141	.628	.141	.628	.141	.0182	.0441	.0441	--			
T80203RV	1623-1823	1.23	1.23	.794	.212	.794	.212	.794	.212	.137	.0541	.0541	--			
T80204RV	1825-2122	1.33	1.41	.657	.343	.657	.343	.657	.343	--	.0805	.0805	.145			

Sample	Time (PST)	Alkenes C12-C30		Alkenes C30-C50		Alkenes C50-POLY		Alkenes C12-C30		Alkenes C30-C50		Alkenes C50-POLY		Subst. Styrene		Pinonic Acid		Nitro-naphthalene		Pentamethyl Benzene		
		Total	Alkanes	Total	Alkanes	Total	Alkanes	Total	Alkanes	Total	Alkanes	Total	Alkanes	Total	Alkanes	Total	Alkanes	Total	Alkanes	Total	Alkanes	Total
T80197RV	2121-0120	.241	.375	.257	.131	.360	.405	.165	.140	.119	.123	.0115										
T80195RV	0123-0621	.216	.582	6.73	.104	.787	23.5	.140	.140	.119	.123	.0115										
T80198RV	0624-0820	.108	.527	.218	.0563	.402	.485	.106	.106	.117	.545	.00255										
T80199RV	0822-1020	.246	.485	5.90	.129	.478	3.34	.170	.170	.117	.545	.0140										
T80200RV	1023-1220	.149	.195	4.29	.159	.664	19.7	.126	.126	.136	.601	.00362										
T80201RV	1222-1420	.0878	.287	4.56	.0895	.348	2.85	.146	.146	.181	.517	.0181										
T80202RV	1422-1620	.0959	.595	.190	.0880	.473	.378	.145	.145	--	--	--										
T80203RV	1623-1823	.0974	.519	.243	.0710	.381	.438	.276	.276	.474	.474	--										
T80204RV	1825-2122	.0902	.621	.194	.0621	.466	.376	.170	.170	--	--	--										

SC524.25FR

TABLE 6-7

SOME HYDROCARBON VAPORS IN SOUTHERN CALIFORNIA
(After Stephens & Burleson, 1969)

<u>Species</u>	<u>(ppb)</u>
Methane	2355
Ethane	63.6
Acetylene	77.0
Ethylene	65.6
Propene	19.2
1,3 Butadiene	3.6
1 Butene	2.6
Isobutene	5.2
Cyclopentene	4.4
Trans-2-Butene	1.4
Trans-2-Pentene	2.4
2-Methyl Butene 2	2.6

SC524.25FR

TABLE 6-8

 SOME BOILING POINTS AND VAPOR PRESSURES
OF OXYGENATED ORGANIC COMPOUNDS

<u>Species</u>	<u>Carbon Number</u>	<u>B.P. (°C)</u>	<u>Vapor Pressure (mm Hg)</u>
Propionic Acid	3	141.1	1 (4.6°C)
butyl ester	-	145.4	
Propionaldehyde	3	48.8	10 mm (19.4°C)
1-Propanol	3	165	40 (23.8°C)
Butyraldehyde	4	75.7	-
Butyric Acid	4	163.5	1 (25.5°C)
propyl ester	-	143	-
Caproic Acid	6	205	1 (71.4°C)
Caprylic Acid	8	237.5	-
Caprylaldehyde	8	163.4	1 (73.4°C)
Lauric Acid	12	225 (100 mm)	1 (121°C)
			~ .005 (20°C)

SC524.25FR

number of three and larger. Even in the case of Lauric Acid (C_{12}) the vapor pressure is about equivalent to 1 ppm vapor in air, which is much larger than the 1 ppb concentration range required for condensation to form aerosol in the atmosphere. Thus, the vapor pressure of organic compounds provides a very severe constraint on secondary production of organic aerosols. Even so, the evidence is overwhelming from atmospheric data and laboratory experiments that organic aerosols can be generated by atmospheric reactions.

At this time, there is virtually no information on the composition of olefins greater than C_6 in the ambient atmosphere so that the organic aerosol precursors have not been identified in urban air. However, taking a difference between the non-methane hydrocarbon (NMHC) concentration and the $< C_6$ hydrocarbon fraction identified by chromatography suggests that the $> C_6$ fraction may be about half of the NMHC concentration. This can be shown readily by combining the data from the chromatographic analysis and from the Beckman 6800.

The chromatograph results from the samples returned from the field in bottles for laboratory analysis have been summed to obtain a number for (identified) non-methane hydrocarbons with a carbon number less than 6. The difference between these values and the NMHC measured by the Beckman 6800 gas chromatograph in the mobile laboratory should provide a measure of the $> C_6$ fraction. These results for the 1973 ACHEX data are shown in Table 6-9. The results are shown in summary for a given episode.

The data in Table 6-9 suggest that (a) there is poor identification of the low molecular weight hydrocarbon fraction, (b) the Beckman analyzer is giving too large a reading of NMHC, or (c) there is a large fraction of hydrocarbon vapors of molecular weight equivalent to material larger than C_6 . In the first case, this appears unlikely because essentially all significant peaks from chromatographic analysis of the light vapors have been identified. The second does not appear likely either since the Beckman 6800 readings are similar to observations of CH_4 and NMHC by other techniques. However, studies should be made to confirm this conclusion. This leaves the last conclusion open, suggesting that it is reasonable to expect that significant quantities of high molecular weight olefins are present at ppb concentrations in urban

SC524.25FR

TABLE 6-9

 SUMMARY OF ESTIMATION OF NON-METHANE HYDROCARBON
 FRACTION WITH CARBON NUMBER LARGER THAN SIX

(Concentrations in ppm)

<u>Episode</u>	<u>NMHC*</u>	<u>NMHC ($\leq C_6$)⁺</u>	<u>NMHC ($> C_6$)</u>
West Covina (TB)	1.58	0.22	1.36
Pomona (UF)	0.67	0.15	0.52
Rubidoux (VH)	1.11	0.16	0.95
Rubidoux (VI)	0.25	0.20	0.05
Dominguez Hills (WK)	1.09	0.22	0.87

* Beckman 6800 data

+ Bottle sample data

SC524.25FR

air, at least for limited periods of time. These compounds will be quite reactive in the smog chain and may well prove to be the aerosol precursors.

If the olefins of carbon number six and larger are more appropriate for defining a conversion ratio than NMHC, f_c can be rewritten as

$$f_{C_6} = \frac{[\text{non-carbonate carbon} - \text{primary non-carbonate carbon}]}{[\text{carbon-primary carbon}] + \text{NMHC} (> C_6)} \quad (4.3A)$$

This relation is used instead of f_c from Equation 4.3 with the ACHEX data assuming the bottle samples for hydrocarbon approximate a 2-hr average sample over the period of the filter sample. Here, NMHC (> C_6) is converted into $\mu\text{g}/\text{m}^3$ arbitrarily by using a vapor density of 4×10^{-3} gm/liter for an "average" high molecular weight hydrocarbon vapor. Diurnal patterns of f_{C_6} are compared with f_c for several cases in Figures 4-6, 4-18, 4-20 and 4-24. The behavior of f_{C_6} with time is similar to that found for f_c , with similar values for the two parameters. Thus, in a qualitative sense the use of f_c defined by NMHC appears to be an adequate measure of hydrocarbon conversion in the absence of better knowledge of the > C_6 vapor fraction.

Polymerized organic material can be produced by reactions of olefins or other hydrocarbons with a strong oxidant such as sulfuric acid or ozone. Significant olefin polymerization in sulfuric acid requires very concentrated acid. The aqueous H_2SO_4 at equilibrium with humidity encountered in surface air will be approximately 40% acid. This is unlikely to be strong enough to promote extensive organic aerosol formation. On the other hand, the chemistry of hydrocarbon reactions in smog strongly points to the importance of the ozone-olefin reaction.

The attack of ozone on the olefinic bond remains a subject of controversy. One approach that can serve to illustrate the broad features of the reaction as related to aerosol formation is Story's model as shown in Figure 6-2.

The ozone adds to the olefinic band forming a zwitterion, which can result in an epoxide or a molozonide. The latter can follow one of three added paths to generate peroxides or polymeric material. Addition of water in the system can provide added paths for decomposition of the peroxides to form acids or aldehydes.

SC524.25FR

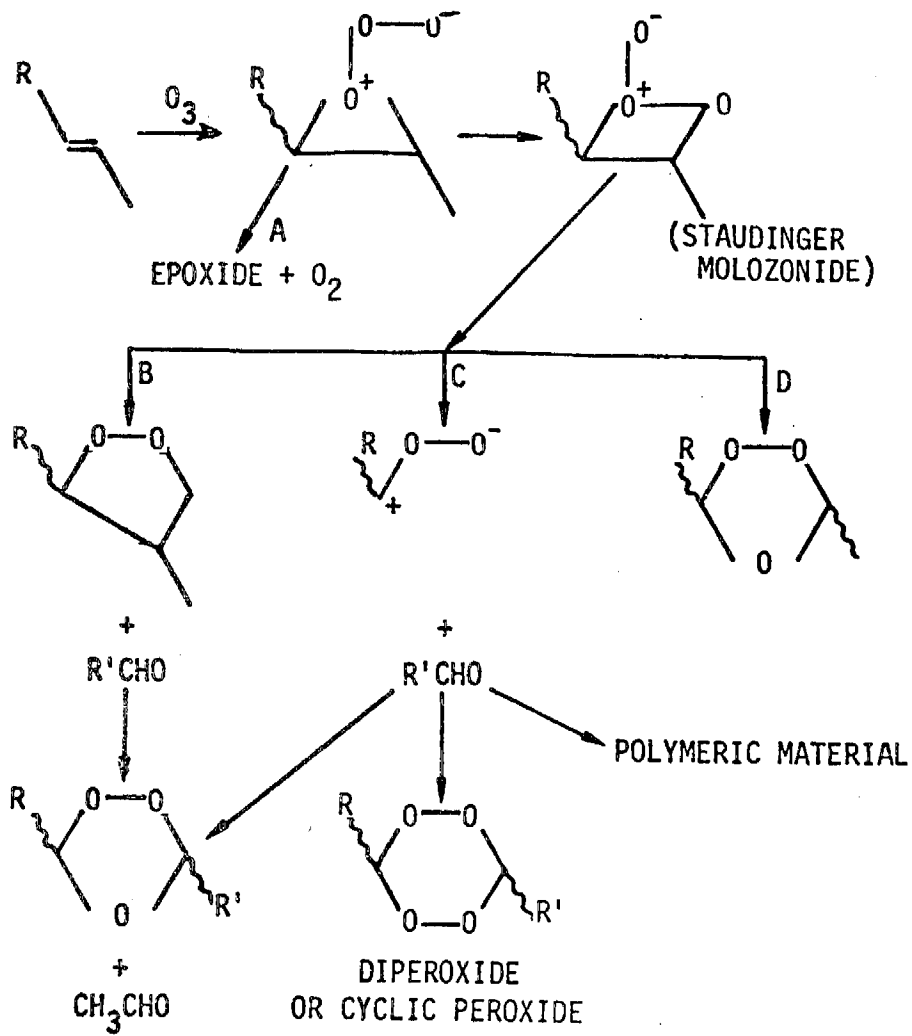


Figure 6-2. Story's Model of Organic Aerosol Formation

SC524.25FR

The recent experiments of Burton et al⁽⁵⁶⁾ have shown that the ozone (terminal) olefin mechanism for aerosol production is initially first order in ozone and olefin. The constant relating the rate of mass concentration change increases with carbon number of the olefin. The significance of this effect is illustrated in the data shown in Figure 6-3. Here the experimental variation in generation of condensable material from the reaction between ozone and several terminal olefins is shown for an ozone concentration of ~ 12 ppm. Significant production of aerosol is observed over a reaction time of 10 seconds mainly for the larger molecular weight species.

C. APPLICATION TO THE ATMOSPHERE

Organic material is universally present in tropospheric aerosol samples. The presence of organics in aerosols can be attributed to primary, natural and anthropogenic sources, as well as to secondary processes in that atmosphere. The details of the secondary reactions are essentially unknown, but an important candidate based on laboratory studies is the ozone reaction with cyclic or linear olefins of carbon number larger than approximately six. The principal limitation in producing organic aerosols in the atmosphere appears to be the vapor pressure of condensable species.

The data taken in Los Angeles indicate that most of the non-carbonate carbon found is made up of a substantial amount of oxygenated material with some organic nitrate present. The organic reactions yield mainly sub-micron particles; production seems to correlate well with changes in ozone as well as with sulfate.

The concentration of organics in the sub-micron particle fraction provides circumstantial evidence for a gas phase formation reaction followed by vapor diffusion controlled growth on existing particles. The presence of significant quantities of oxygenated material and the correlation with ozone buildup are consistent with the expectation that the ozone-olefin reaction is important.

Extrapolation of these data to olefins at the ppb level and ozone of 10 pphm suggests an organic material production rate of tenth's $\mu\text{g}/\text{m}^3$ per hour, which is somewhat lower than deduced from atmospheric observations.

SC524.25FR

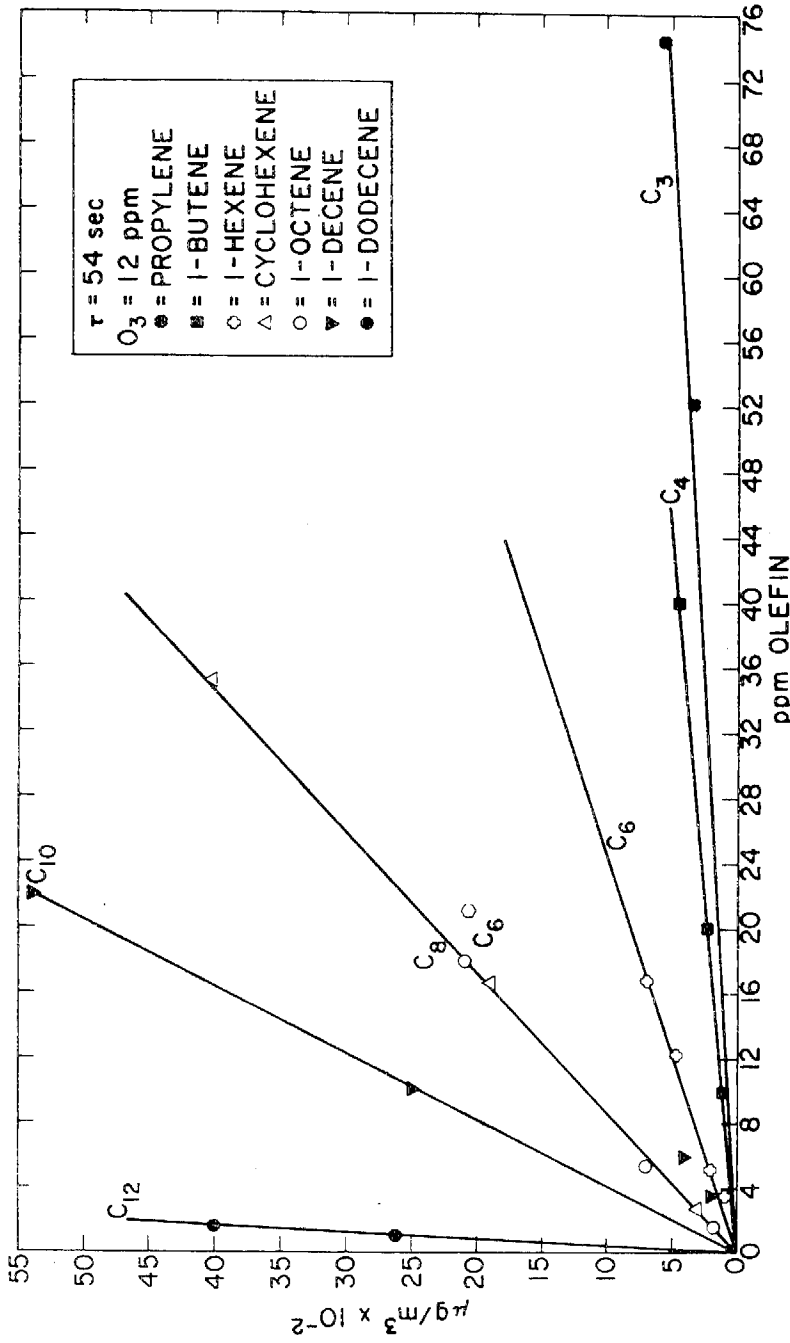


Figure 6-3. Mass Concentration of Aerosol Formation from Olefin-Ozone Reaction as a Function of Olefin Concentration

SC524.25FR

Thus this mechanism cannot in itself explain the limited observations of aerosol formation, though it appears to offer the most plausible mechanism available at this time. Other evidence such as the experiments of Burton et al⁽⁵⁶⁾ have demonstrated that aerosol formation in such mixtures using 10 ppm O_3 and 10 ppm hexene in dry air is heavily influence by the addition of water vapor. Furthermore, traces of butyraldehyde strongly inhibit the formation of aerosols in this system. Thus, the ozone-olefin reaction is an important candidate for explaining organic aerosol formation, but cannot be completely accepted at this time. This work suggests that the ozone-olefin reactions or other reactions such as oxygen atom-olefin, must be important. These classes of reactions involving high molecular weight olefins are known to produce polymerized oxygenated species that will condense at ppb vapor concentrations. For carbon number greater than six, yields of polymerized material should exceed several percent of the vapor concentration. Such reactions are likely to be promoted on particle surfaces when the surface of large particles could act as a preconcentrator for the olefin or air intermediate species.

To improve the knowledge of organic aerosol formation, it is necessary to identify the aerosol precursors. Therefore, we recommend that steps be taken to initiate studies to identify and measure hydrocarbon vapors in urban air with molecular weights equivalent to carbon number six and higher.

SC524.25FR

VII. THE ROLE OF LIQUID WATER IN AEROSOL CHEMISTRY AND ATMOSPHERIC VISIBILITY

A. INTRODUCTION

Significant amounts of liquid water can exist in aerosol particles at relative humidities well below saturation. This water is either sorbed on the surface of the aerosol (a small effect) or is present as a solution with other compounds in the particle. The water in the aerosol is in vapor pressure equilibrium with the ambient air, and the amount of water absorbed is dependent on the chemical composition of the aerosol and the relative humidity.

Atmospheric scientists have been interested for sometime in the nature and behavior of hygroscopic aerosols because of the importance of these particles in the nucleation of rain droplets. For purposes of ACHEX, the effects of hygroscopic aerosols on visibility, aerosol composition, and secondary aerosol production are of primary concern. It is of considerable importance to develop an understanding of these effects in order to establish a rational for visibility control strategy in California.

It is well known that haze in the atmosphere causes degradation of the visibility under conditions of high humidity.⁽⁵⁷⁻⁵⁹⁾ At relative humidities above 60% to 70%, the opacity of haze often begins to increase markedly because of the ability of airborne particles to absorb significant amounts of water vapor. Experiments of Hanel⁽⁶⁰⁾ and Covert *et al.*⁽⁶¹⁾, have demonstrated that atmospheric aerosols are hygroscopic and indeed undergo a substantial increase in mass as the particles equilibrate to increased relative humidity. It was noted in 1969 that the light scattering coefficient of Los Angeles smog was at times markedly correlated with relative humidity⁽⁶²⁾. Recent work on the chemistry of aerosols, particularly in urban air, has suggested that water plays an important role in particle behavior even at relative humidities well below 70%. Goetz and co-workers⁽⁶³⁾ have reported that liquid particles which appear to have coatings of organic material have been collected in the Los Angeles area. These particles grow on the collection substrate when exposed to water vapor. Indirectly, it appears to be necessary to

SC524.25FR

postulate a liquid water content of at least 10% to account for the total mass composition of filter collected aerosol equilibrated with air of a relative humidity less than 50%.⁽¹⁶⁾ Attempts to measure water content of filter collected aerosols in California suggest a water fraction of $\sim 10\%$ or greater by mass⁽⁶⁴⁾ for samples collected in air of a humidity range between 40-60%. From volume size distribution measurements in Los Angeles^(5,65) it has been estimated that 30%-70% of the aerosol mass may be liquid water.

The purpose of the special experiments discussed here was to study the hygroscopic nature (i.e., the liquid water uptake as a function of relative humidity) of aerosol particles in order to better understand the role of liquid water in the physics and chemistry of atmospheric aerosols found in California. Specific goals were:

- 1) To test and compare two instrumental methods (humidograph and waterometer) for measuring aerosol liquid water content.
- 2) To measure the amount of liquid water in the aerosol present in the areas of study.
- 3) To determine the effect of aerosol water content on visibility at high relative humidity.
- 4) To relate the hygroscopic nature of the aerosol to its measured chemical composition.

The first three of these goals were met. The fourth goal has been met only to a preliminary extent due to incomplete data.

The following sections contain a description of the main theoretical considerations which bear on the hygroscopic nature of aerosols, a brief description of instrumental techniques, an example of the data, and the analysis and interpretation of the data. In addition to results obtained as a part of ACHEX, the results of similar experiments performed elsewhere in the U.S. and Europe since then are included for completeness and as they bear on the conclusions to be drawn from the California data.

SC524.25FR

B. REVIEW OF THEORY GOVERNING LIQUID WATER CONTENT OF AEROSOL PARTICLES

Water is a major and highly variable constituent of the atmosphere. Water vapor concentrations in the troposphere range from 40 parts per million by volume (ppm) to as high as 40,000 ppm. The relative humidity (RH) of an air parcel can vary by a factor of two or three on a time scale of hours due to temperature changes, mixing, and adiabatic processes.

The interactions which occur between water vapor and aerosol particles are quasi-equilibrium processes which depend on the physical and chemical properties of water and the aerosol. Water is a good solvent for many of the compounds found in atmospheric aerosols. Aerosol particles can have a variety of sizes, surface structures, and chemical compositions. The specific processes by which water interacts with the particles are outlined in the following paragraphs.

Even for insoluble compounds, water can be held on the surface of the particles by physical adsorption. Because of the polar nature of water and the possibility of irregularities, capillaries, etc. on the aerosol surface, the physically adsorbed water can be 5-10% of the aerosol mass at 90% relative humidity. (66,67)

If the aerosol is a water soluble liquid or solid, adsorption is no longer a surface limited phenomenon. Water vapor is adsorbed until the soluble aerosol fraction consists of a homogeneous solution, the surface of which is in vapor pressure equilibrium with the surrounding air. Compounds which respond in such a way are termed hygroscopic.

Deliquescence, a special case of hygroscopic behavior, is defined as the formation of a solution when a solid salt is exposed to water vapor at a partial pressure greater than that of the saturated solution of its highest hydrate. In the case of many soluble salt aerosols, water vapor is adsorbed only on the surface below a certain humidity. Above that humidity such salt aerosols suddenly adsorb considerable water and act as a hygroscopic solution droplet. The point at which the step change occurs is called the deliquescence point for a given salt. The deliquescence point ranges from 10-99% relative humidity for different salts and salt mixtures and is dependent primarily on chemical composition.

SC524.25FR

Particle size, i.e. radius of curvature, has a minimal effect on the deliquescence point for particles with a diameter D_p larger than $0.2 \mu\text{m}$. Table 7-1 gives a listing of bulk deliquescence points for a number of salts which are possible constituents of atmospheric aerosols. Small particles deliquesce at slightly lower relative humidities than those indicated.

The reverse effect, crystal formation when a salt solution is exposed to a vapor pressure lower than that of the saturated solution, is termed efflorescence. Due to supersaturation effects the relative humidity at which efflorescence occurs is generally lower than the deliquescence point and is imprecise. It depends upon temperature, relative humidity, chemical composition, and the presence of crystallization nuclei in a complex way. This leads to the phenomenon of hysteresis,⁽⁶⁸⁾ which is the difference in response of hygroscopic/deliquescent aerosols between increasing and decreasing relative humidities. The amount of water adsorbed in the case of hygroscopic/deliquescent aerosols can be 50% to 90% of the total aerosol mass at a relative humidity of 90%. This amount, and the deliquescence point, if present, depends on the chemical nature of the aerosol.

The chemical compounds commonly found in atmospheric aerosols can be divided into three categories based on their affinity for water vapor:

(Water Insoluble)

- 1) non-hygroscopic compounds, such as montmorillonite, silicon oxides, and high molecular weight hydrocarbons.

As the term implies, water does not readily condense on such aerosols even at relative humidities approaching 100%.

(Water Soluble)

- 2) hygroscopic compounds such as sulfuric acid, low molecular weight alcohols, aldehydes, and organic acids.

Such compounds absorb water vapor over a wide range of partial pressures and the mass fraction of water associated with such aerosols increases continuously with relative humidity.

SC524.25FR

TABLE 7-1
DELIQUESCENT COMPOUNDS

	Deliquescence Points, % RH
$MgCl_2$	33
KNO_2	45
$NaBr$	58
NH_4NO_3	62
$NaNO_2$	66
$NaNO_3$	74
$NaCl$	76.
NH_4Cl	77
$(NH_4)_2SO_4$	80
Na_2SO_4	86
$ZnSO_4$	88
$Pb(NO_3)_2$	88.4
$MgSO_4$	91

SC524.25FR

- 3) deliquescent compounds such as NaCl , $(\text{NH}_4)_2\text{SO}_4$, Na_2SO_4 , MgCl_2 . These are deliquescent compounds which absorb water to form a hygroscopic aerosol droplet only above their deliquescence point. Below the deliquescence point they behave as a crystalline non-hygroscopic aerosol.

In almost all atmospheric situations the aerosol particles will be mixed with respect to chemical composition and hygroscopic nature both internally (within individual particles) and externally (between particles). Thus any classification of atmospheric aerosols according to their hygroscopic nature is a subtle one of degrees at best.

The thermodynamics which govern the equilibrium size and growth rates of hygroscopic aerosols as a function of relative humidity has been discussed by Köhler in 1921 and since then by numerous authors, e.g., Keith and Arons⁽⁶⁹⁾, Mason⁽⁷⁰⁾, Orr, *et al.*⁽⁶⁸⁾, and Fletcher⁽⁷¹⁾. Although these authors have been interested mainly in cloud nucleation processes at near or above saturation humidities, the concepts apply equally well at lower relative humidities. Application of these concepts to atmospheric aerosols at relative humidities less than 95% is considered impossible by most due to the complex, mixed chemical and physical nature of the aerosol. For this reason the experimental approaches to the subject as reported here have been made.

Many inorganic salts interact with water vapor to form hydrates, in which the water is included in the crystal structure and is not liquid. No special efforts were made in this section to account for this interaction. The presence or uptake of water of hydration by ambient aerosols was not distinguished from that of liquid water.

Gas to particle conversion has been shown to proceed more rapidly at higher relative humidities under some smog conditions.⁽⁷²⁾ Such interactions are separate from those under consideration in this section of the report.

SC524.25FR

C. DISCUSSION OF EXPERIMENTAL RESULTS

1. LABORATORY RESULTS FROM THE HUMIDOGRAPH

The results of initial laboratory experiments on aerosol light scattering versus relative humidity for pure compounds as determined by the methods of this study have been reported and discussed by Covert, *et al.*⁽⁶¹⁾ and are included here in Figure 7-1. All laboratory test aerosols were generated using the bubbler technique from dilute aqueous solution.

Of particular importance are the sulfate aerosols, H_2SO_4 , NH_4HSO_4 , $(NH_4)_2SO_4$, which are suspected to be frequent and dominant species in some urbanized regions⁽⁷³⁾. The humidograms for both H_2SO_4 and $(NH_4)HSO_4$ aerosol, show a light scattering coefficient which increases monotonically with increasing RH. The humidogram for $(NH_4)_2SO_4$ aerosol exhibits a sudden, step increase in scattering ratio at ~80% RH due to deliquescent particle growth. The marked difference between these humidograms is the basis for a suggested method of analysis for H_2SO_4 and/or NH_4HSO_4 aerosol⁽⁷⁴⁾. The method depends on the *in situ* reaction of NH_3 added to the aerosol to convert it to $(NH_4)_2SO_4$ and observation of the accompanying change in the shape of the humidogram. The results of a laboratory test of the method are shown in Figure 7-2. Positive results using this technique on atmospheric aerosol in the St. Louis region have been reported by Charlson *et al.*⁽⁷³⁾, as illustrated in Figure 7-17.

The humidograms for $Ca(NO_3)_2$, NH_4NO_3 , $NaNO_3$ and KNO_3 are illustrated in Figure 7-3. Although all of these salts are deliquescent (with deliquescence points of 54, 62, 74, and 92 per cent, respectively) none of them exhibited any deliquescent character in the humidograms. The aerosols were produced from solution droplets which were dried to about 15% RH. To eliminate the possibility of hysteresis effects, some samples of the aerosols were subjected to humidities of 1% (over P_2O_5) and temperatures of about 80C. It was found that the humidograms were unchanged. Similar behavior can be expected in the case of nitrate containing atmospheric aerosols.

SC524.25FR

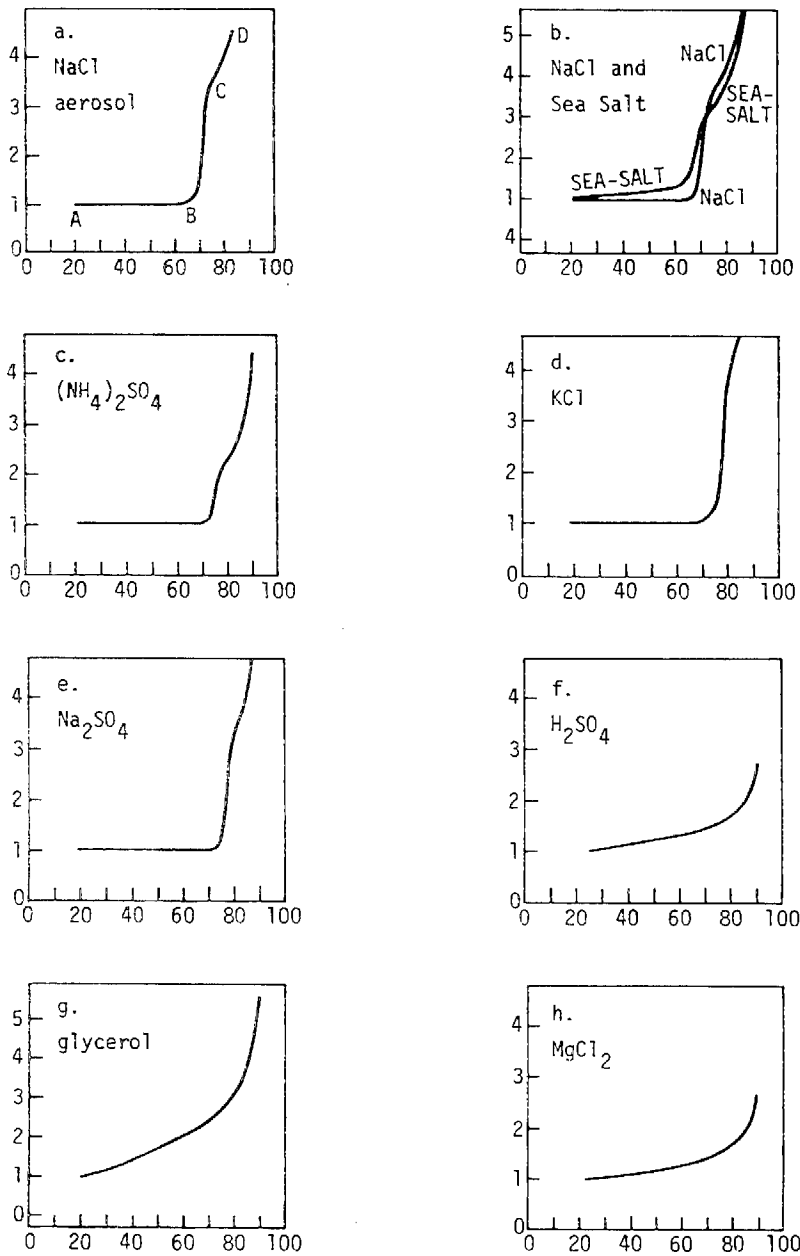


Figure 7-1. Laboratory Measurements of Light Scattering Ratio, b_{sp}/b_{sp} (RH=20%), vs. Relative Humidity-Smoothed Curves ($b_{sp} = b_{scat}$ minus the Rayleigh scattering)

SC524.25FR

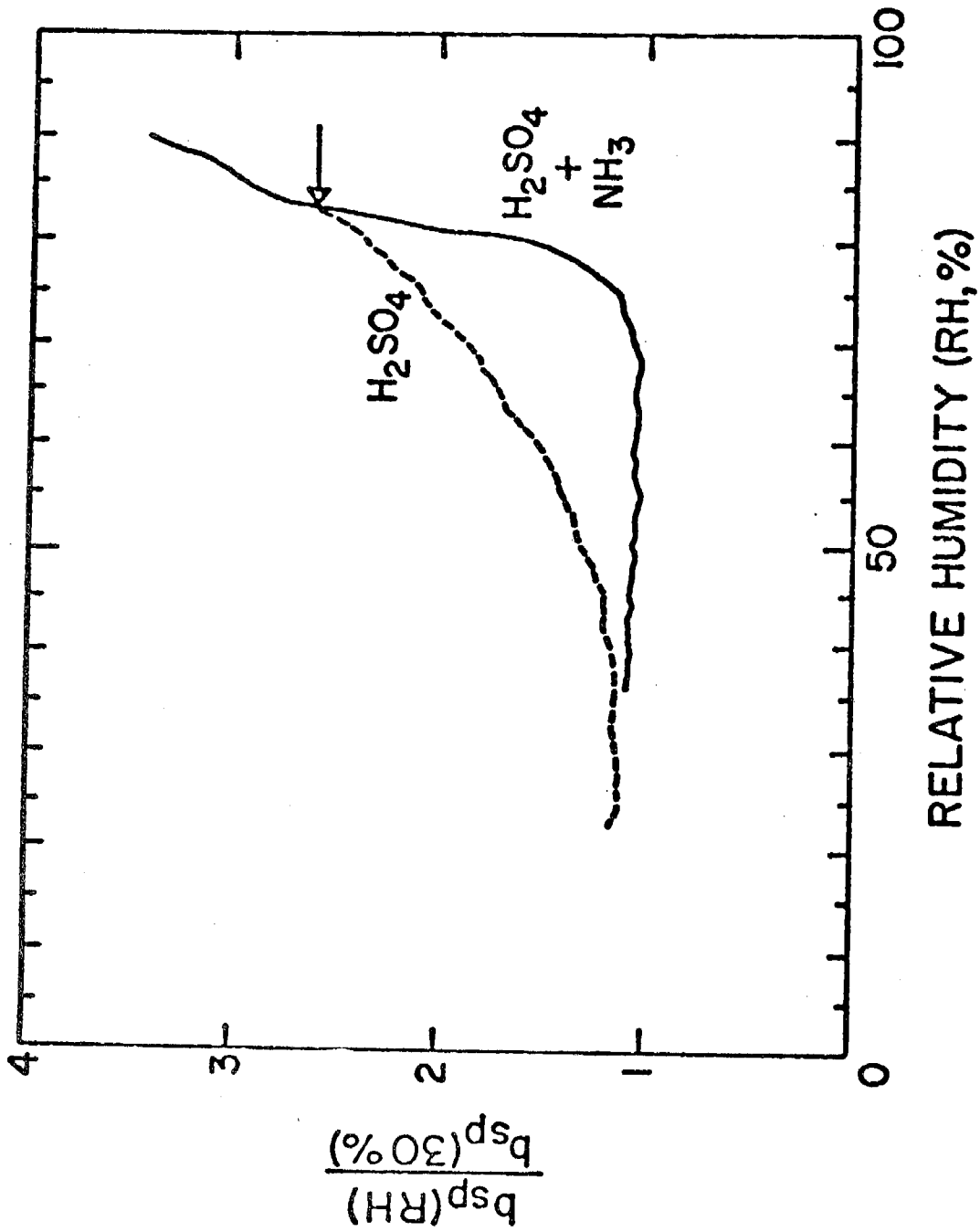


Figure 7-2. Humidogram of H_2SO_4 Aerosol and H_2SO_4 Aerosol Plus NH_3

SC524.25FR

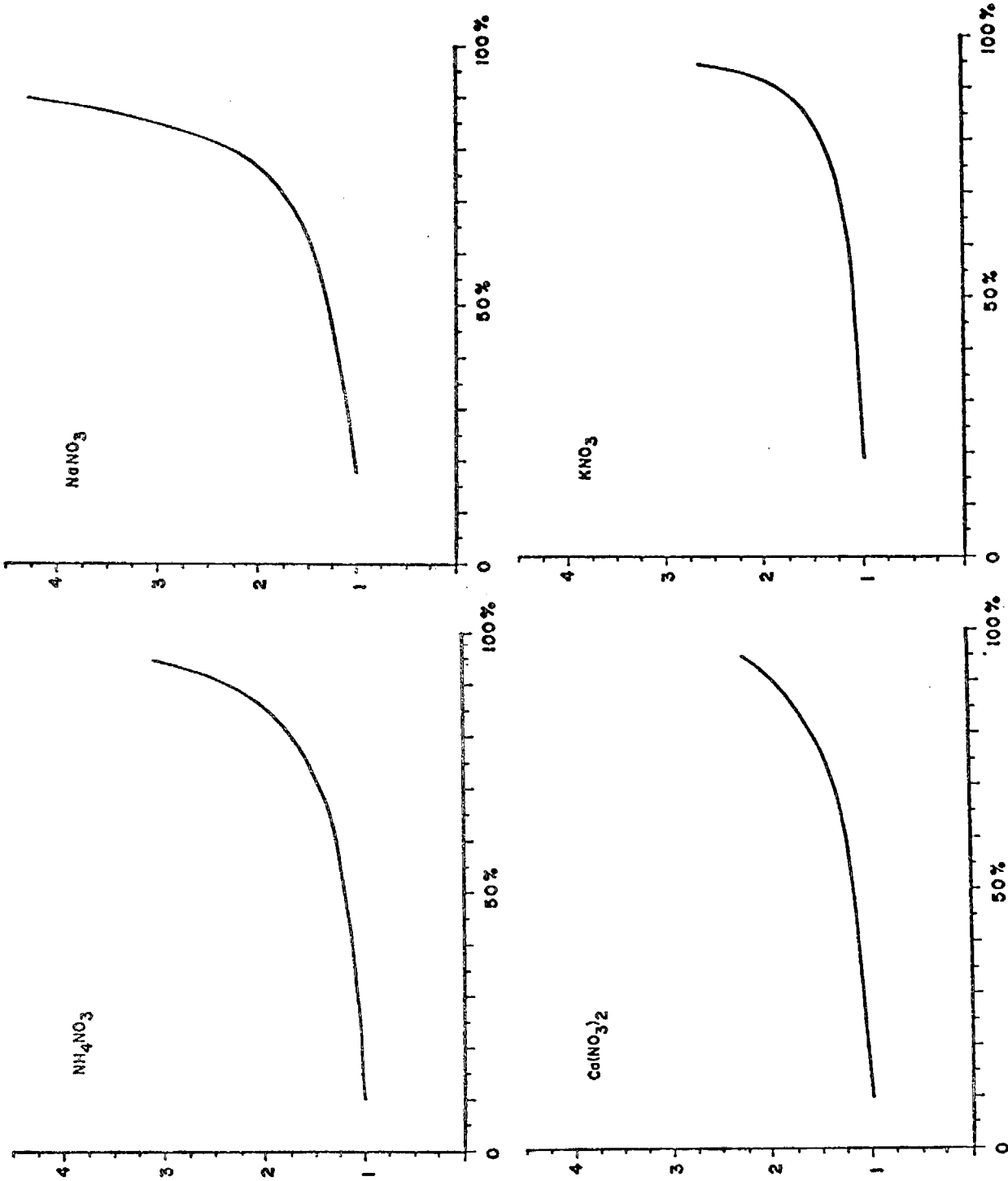


Figure 7-3. Humidograms of Nitrate Aerosols

SC524.25FR

Two other chemically pure aerosols which were investigated were Carbowax 600 R, and Aerosil R. Carbowax R is a commercial polyethylene glycol with a molecular weight of 500. Aerosil R is a manufactured quartz dust, SiO_2 , with a mean diameter of $0.03 \mu\text{m}$. These aerosols are both typical of hydrophobic aerosols. Their humidograms are shown in Figure 7-4. The amount of water absorbed by the Carbowax R aerosol up to 75% RH is negligible and increases slowly above 75%. Aerosil R adsorbs almost no water up to humidities of 90%. From 90% to 95% RH some water was adsorbed, presumably by physical processes in pores and capillaries or due to small amounts of soluble impurities.

An atmospheric aerosol will, in most cases, be of mixed chemical composition and in many cases the composition will be extremely complex. Thus to provide a basis for comparison and analysis of results from atmospheric aerosols, artificial aerosols of mixed chemical composition were produced in the laboratory and their response to relative humidity measured.

In consideration of aerosols of mixed chemical composition there are two possibilities which have been enumerated by Winkler⁽⁷⁵⁾: internal and external mixtures. One can conceive of an externally mixed aerosol in which the different chemical compounds present are in separate particles. An internal mixture, then, is one in which the composition of each aerosol particle is of mixed chemical nature and the same as all others. In an internally mixed aerosol one can also conceive of homogeneous and inhomogeneous particles.

An example of the results from laboratory experiments are shown in Figure 7-5. An ammonium sulfate, sodium chloride, potassium nitrate aerosol with a mass ratio of 0.5:0.25:0.25 was tested as both an external mixture and an internal mixture. The most obvious conclusion to be drawn in this case is that an internally mixed aerosol of deliquescent salts exhibits a less pronounced deliquescence step. Particularly, the presence of nitrates in small amounts has been observed to mask the deliquescent nature of other compounds in an internally mixed aerosol. This is not surprising in view of the hygroscopic behavior of pure nitrate compounds as discussed earlier in this section.

SC524.25FR

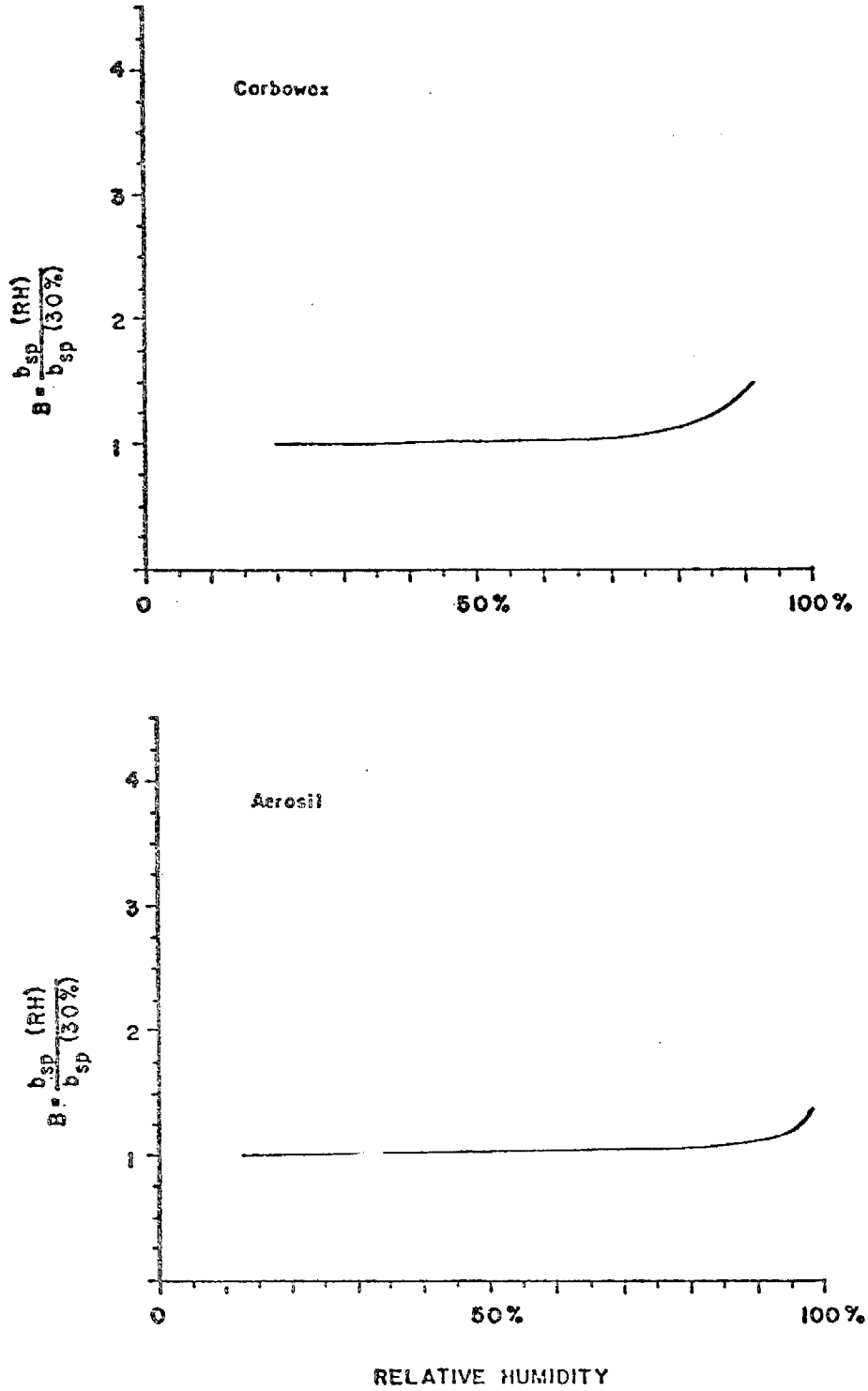


Figure 7-4. Humidograms of Aerosil R and Carbowax R

SC524.25FR

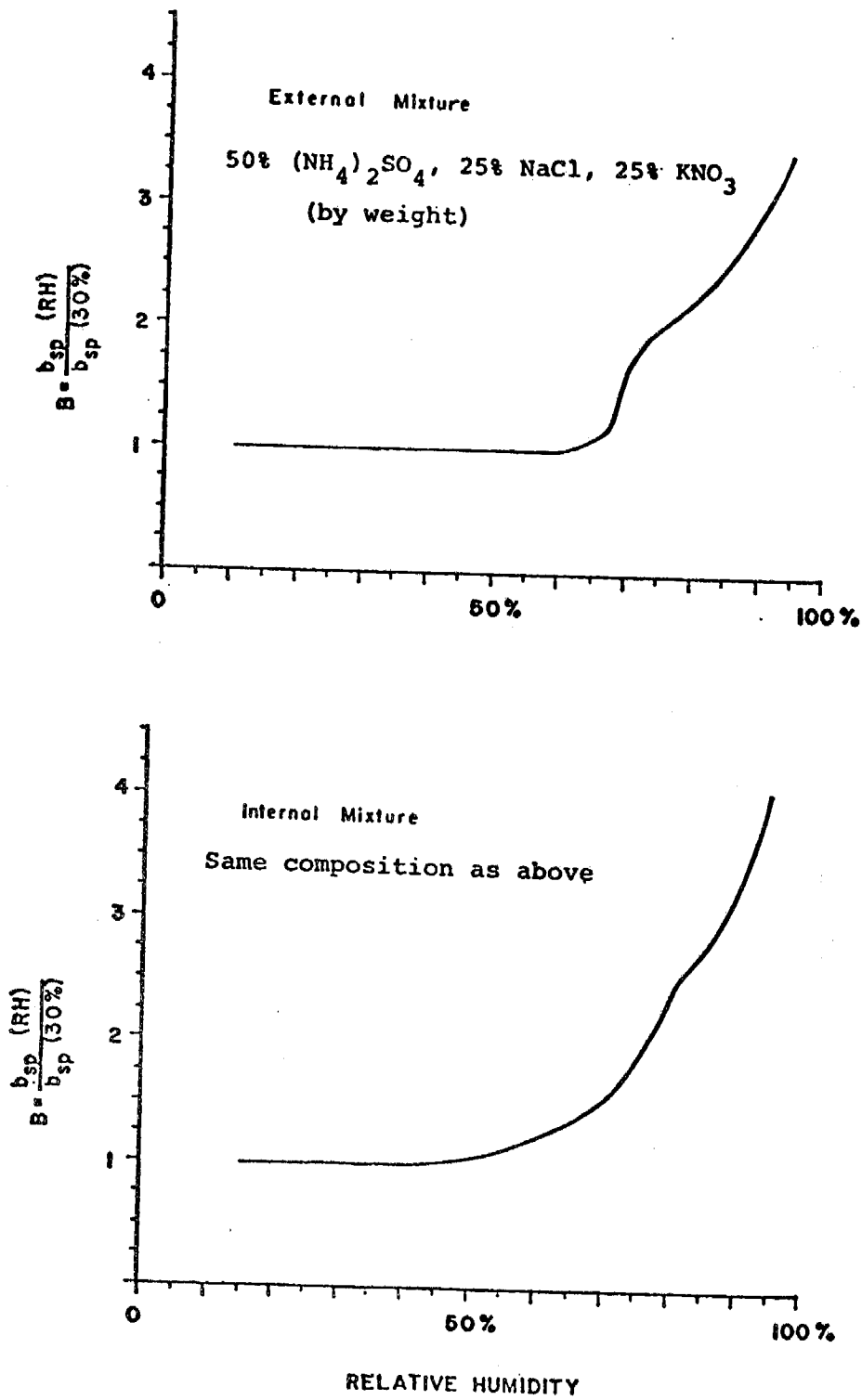


Figure 7-5. Humidograms of Internal and External Mixtures

SC524.25FR

The inference of chemical information from humidogram measurements relies on the deliquescent properties of inorganic salts (Table 7-1). The observation of a deliquescence point, or inflections, in the humidogram indicates the presence of a deliquescent salt. The relative humidity at which deliquescence is observed identifies the compound more specifically. The sharpness of the deliquescence step and its magnitude indicate the mass fraction of this compound in the aerosol. Non-deliquescent compounds such as H_2SO_4 and NH_4HSO_4 can be determined by reacting them with a known compound (NH_3) to form a deliquescent salt upon which the humidogram measurement is then made. It is estimated that in case of an internal mixture it is necessary that a given deliquescent compound be present as at least a 30% mole fraction to allow detection. Requirements are less stringent in the case of an externally mixed aerosol. For compounds which are non-deliquescent but hygroscopic there will be no inflection points and one can only distinguish between their relative hygroscopicity. This distinction becomes rather arbitrary, but one can clearly distinguish between hygroscopic and non-hygroscopic aerosols and some degrees of intermediate behavior.

2. HUMIDOGRAPH FIELD RESULTS

a. Description of Sites

Measurements of atmospheric light scattering coefficient versus relative humidity (humidograms) were made in a wide variety of urban and background sites (locations subject to minor or infrequent anthropogenic influence) on the west coast of the United States. Three continental sites, Denver, St. Louis, and Mainz, Western Germany were also visited.

The majority of the atmospheric data presented here was gathered in California in cooperation with the Aerosol Characterization Experiment (ACHEX) sponsored by the State of California Air Resources Board (ARB). Sites in each of the the three major populated basins (San Francisco Bay area, San Joaquin Valley and the South Coastal Basin) as well as more remote locations representative of region background quality conditions were visited.

A listing of the sites, their geographical location and the general nature of the environment and expected aerosol are given in Table 7-2.

SC524.25FR

 TABLE 7-2
FIELD SITE LOCATIONS AND DESCRIPTIONS

Date	Site	Geographical Location	Environment
Jan. 1971	University of Washington, Seattle, Washington	Puget Sound Basin	Urban-residential
Sept 1971	Altadena, California	South Coastal Basin, California	Urban-residential and light industry. Los Angeles photo- chemical smog aerosol.
Oct. 1971 Nov. 1973	Denver, Colorado	High Central Plains	Urban-industrial. Diesel exhaust from railroad switching yards.
July 1972	Port Townsend State Park, Washington	Puget Sound Basin	Marine-vegetation aerosol. Subject to plume from Kraft paper pulp mill, Na ₂ SO ₄ aerosol.
July 1972	Berkeley, California	San Francisco Bay Area	Urban residential
Aug. 1972	Richmond, California	San Francisco Bay Area	Urban industrial. Near petro- chemical complex.
Aug. 1972	Pt. Reyes Lighthouse, Pt. Reyes National Seashore, California	North Coastal California	Background--Marine aerosol.
Aug. 1972	Kehoe Beach, California	North Coastal California	Surfzone--Marine aerosol.
Aug. 1972	Fresno, California	San Joaquin Valley	Urban and agricultural. Photo- chemical smog aerosol.
Sept 1972	Hunter Liggett Military Res., California	Coastal Mountains, Southern California	Background, semi-arid vegetative aerosol.
Sept 1972	Montana de Oro State Beach, California	South Coastal California	Marine-urban. Fossil fuel power plant 10 km N.
Sept 1972	El Capitan State Beach, California	South Coastal California	Marine-urban. Photochemical smog aerosol.
Sept 1972	California Institute of Technology, Pasadena, California	South Coastal Basin, California	Los Angeles photochemical smog aerosol.

SC524.25FR

 TABLE 7-2
 FIELD SITE LOCATIONS AND DESCRIPTIONS (Continued)

<u>Date</u>	<u>Site</u>	<u>Geographical Location</u>	<u>Environment</u>
Oct. 1972	Pomona, California	South Coastal Basin, California	Los Angeles photochemical smog aerosol.
Jan. 1973	Mainz, Western Germany	Rhein-Main Valley	Central European anthropogenic aerosol.
Aug. 1973	St. Louis, Missouri	Mississippi Valley	Urban-industrial aerosol.
Sept 1973	Tyson, Missouri	33 km WSW St. Louis Ozark foothills	Midwestern regional background aerosol.
Nov. 1973	Denver, Colorado	20 km NE, high Central Plains	Urban-industrial aerosol.

SC524.25FR

b. Data Collection

During the studies in California and St. Louis humidograms were made automatically at time intervals of 15 or 30 minutes with additional manually initiated measurements at intermediate times. At other sites measurements were initiated manually at frequent intervals to correspond with measurement of other atmospheric parameters. Humidograms were recorded on X-Y graphs and/or on magnetic tape for future computer processing.

Measurement of only one aerosol parameter (e.g., humidograms) yields data of limited value to the study of atmospheric chemistry. For this reason our experiments were coordinated with those of other investigators when possible. Parallel measurements of aerosol mass, size distribution and chemical composition, among others, were made at most of the sites visited. When available this data is presented and used in evaluation of the humidograms.

Continuous measurements of the absolute scattering coefficient at four wavelengths in the visible range were also made. These were used as a supplementary indication of the size distribution in the optical sub-range (0.1 μm to 1.0 μm).

c. Computer Processing and Visual Display for Analysis

In order to analyze the mass of data which is produced in an experiment where humidograms are taken on a regular basis (one to five times an hour for a period of weeks) computer processing is necessary. One humidogram consists of about one hundred data pairs of b_{sp} and RH.

Original data as well as being recorded in analog form on an X-Y graph are also recorded on magnetic tape in digital form. Subsequently, these data are put into an array which is normalized so that b_{sp} is unity at a given relative humidity, usually 30%, and averaged over one per cent humidity intervals. The humidograms are then printed on paper or displayed on a cathode ray tube for editing and preliminary analysis. A 16 mm motion picture film of the CRT display is then made for time sequence analysis as a function of time of day, weather conditions, location, etc. This provides an overview of the data from which further computer processing of significant data can proceed. Time averages of humidograms are made as needed to correspond with site location, parallel chemical information, weather conditions or other available aerosol parameters

SC524.25FR

and atmospheric data. An example of the raw data and a 14-hour average of humidogram data corresponding to a specific weather condition are shown in Figures 7-6a and 7-6b.

The variation in the form of the humidogram with time and site location is due primarily to the changing chemical nature of the aerosol. The film or CRT display thus provides a three-dimensional presentation (in X, Y and t) of the variables B, RH and chemical composition.

3. DISCUSSION OF HUMIDOGRAPH DATA

A wide range of spacial and temporal variability is observed in the data, (see Figures 7-6, 7-7, and 7-18). The aerosol response to relative humidity ranges from hygroscopic to nearly hygrophobic to strongly deliquescent. These examples represent the extremes of observed variability, however. With two exceptions, the data collected thus far show that the hygroscopic nature of aerosols is generally much more regular. Figure 7-7d illustrates the range of variability for the humidograms averaged at each site. The light scattering ratio increased by a factor of 1.5 to 1.7 at a relative humidity of 80%. This would imply that the mass fraction of condensed water ranges between roughly 0.3 and 0.4.

The data collected at Pt. Reyes Lighthouse, California, and Tyson Hollow, Missouri deviate notably from this pattern as shown by the vertically hatched area in Figure 7-7d. The aerosol response to relative humidity was strongly deliquescent approximately forty per cent of the time that observations were made. The light scattering ratio increased by a factor of two at 80% RH indicating a water fraction of about 0.5.

Measurements of the aerosol size distribution which were made concurrently with humidogram measurements at most sampling sites in California and in Denver and St. Louis showed the size distribution in the optical sub-range to be relatively constant. Thus, the hypothesis that variation in the humidograms is due to chemical differences is supported.

SC524.25FR

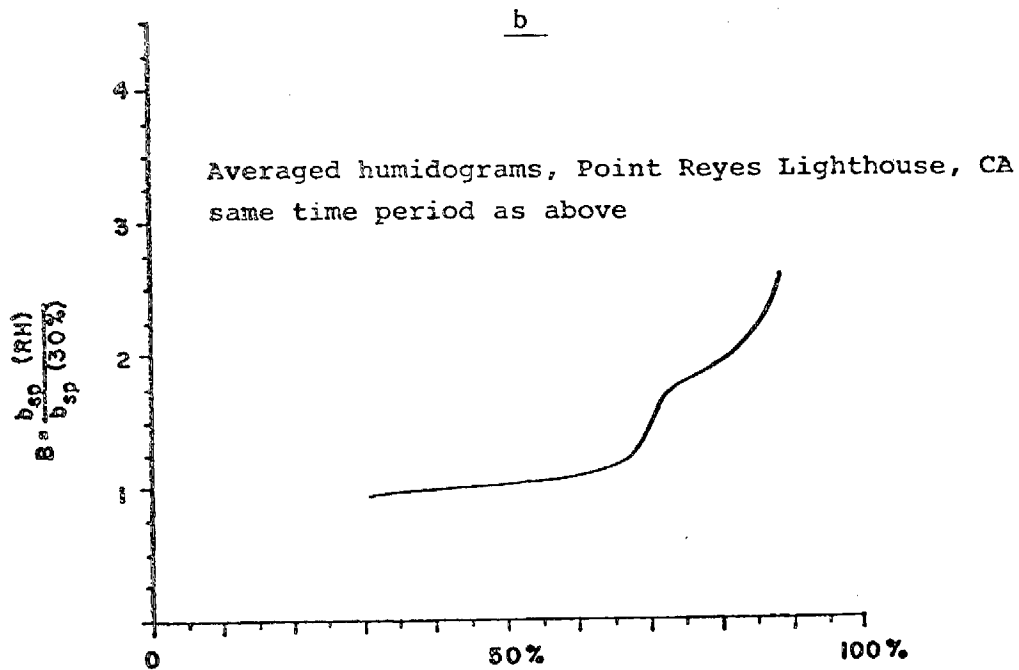
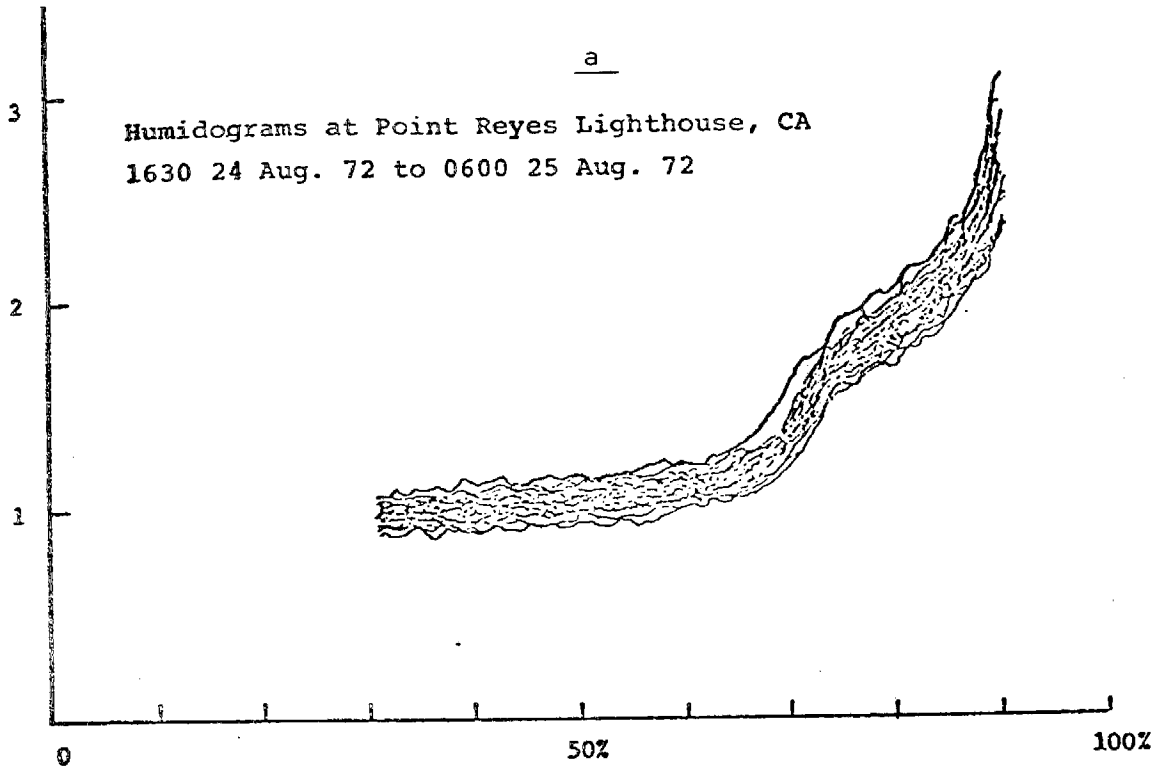
The degree of variability in the humidograms which was observed at times is not surprising in view of the diverse aerosol composition which is to be expected at the different sampling locations and under the changing weather conditions which were encountered. The fact that the humidograms were regular in nature much of the time does not, however, imply that the chemical composition was the same at these times. Many aerosols will have similar humidity response curves due to the effects of internal mixing of both soluble and insoluble material. The observation of a strong deliquescent character as at Pt. Reyes and Tyson Hollow indicates an aerosol of nearly pure, singular chemical composition and/or external mixing.

The more specific results observed at each site are discussed in the next section.

4. SPECIFIC DISCUSSION AND COMPARISON WITH CHEMICAL AND METEOROLOGICAL DATA Richmond, California

The humidograms showed the widest variability here of all the sites visited, as illustrated in Figure 7-8. Figure 7-8a is the average of all humidograms recorded at Richmond. Roughly one-third of the time a deliquescent aerosol was observed as depicted in Figure 7-8c. The deliquescent substance is presumed to be sea salt from the ocean or San Francisco Bay from the observed deliquescence point at about 75% RH which corresponds to that of NaCl, the major chemical constituent. For one period of several hours aerosol response was like that of Figure 7-8d highly hygroscopic with a slight deliquescent character. At other times the response was less hygroscopic, Figure 7-8b. Chemical analysis for these specific times is unfortunately not available; it would be of great interest to know something of the chemistry which caused these different aerosol responses. At the time it was suspected that sulfuric acid may have been causing the monotonic hygroscopic response often observed. Gaseous ammonia was added per the procedure described in Volume II in an attempt to qualitatively detect the presence of H_2SO_4 . The tests were negative. Due to the limited extent of these tests and to the effects of internal mixing, this is not conclusive evidence that H_2SO_4 was not in part responsible for the highly hygroscopic humidograms which were observed.

SC524.25FR



RELATIVE HUMIDITY

Figure 7-6. Humidograms at Point Reyes Lighthouse, CA
1630 24 Aug. 72 to 0600 25 Aug. 72

SC524.25FR

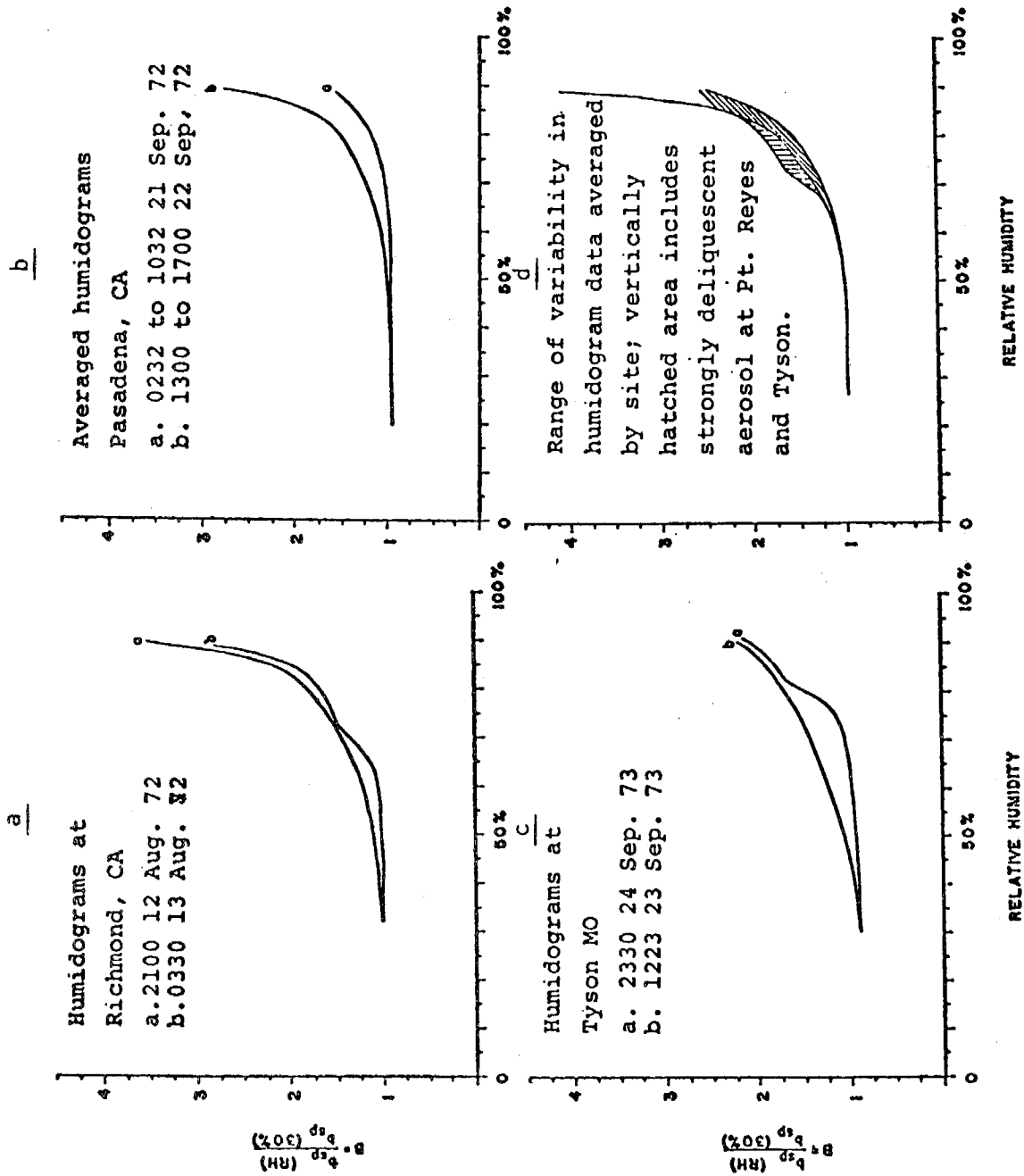


Figure 7-7. Comparison of Humidograms at Richmond, Ca; Pasadena, Ca; Tyson, MO

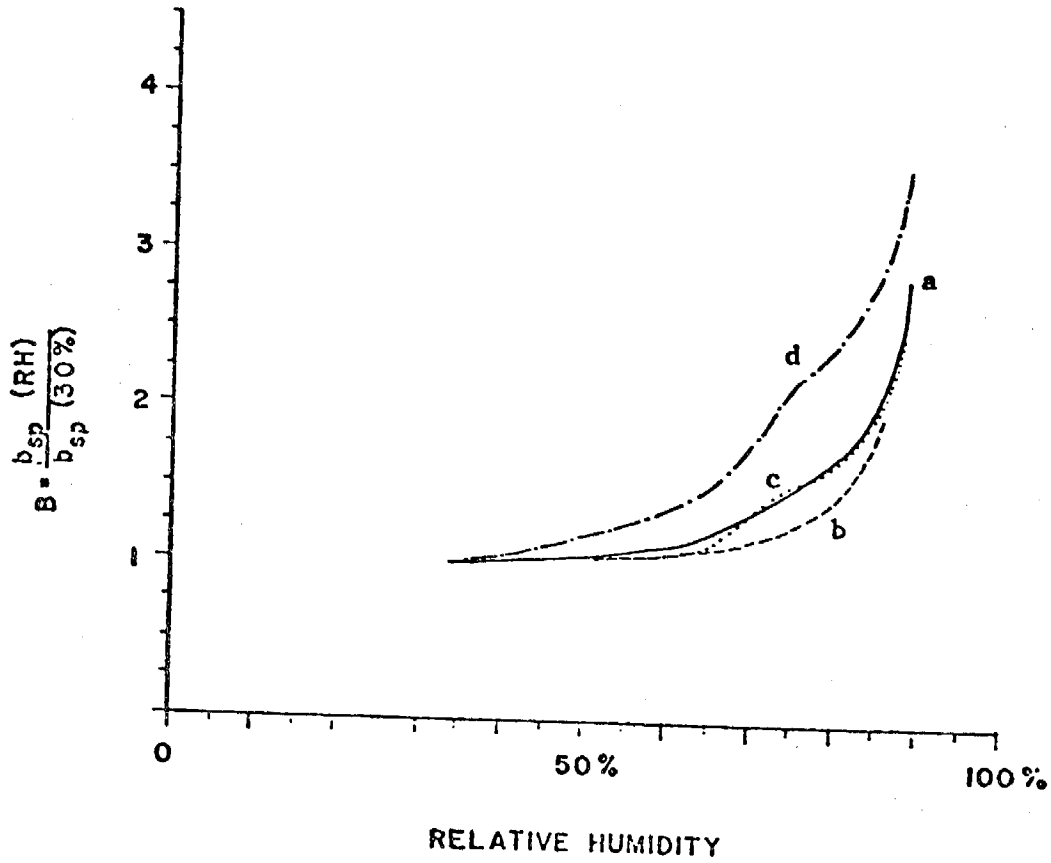
SC524.25FR

Point Reyes Lighthouse, California

Pt. Reyes Lighthouse is located on a peninsula which extends some 10 km. westward of the mainland 50 km. northwest of San Francisco. The sampling site was on a cliff 150 m. above sea level and well exposed to onshore winds. The data collected here are presumably representative of background marine coastal conditions along the Central Pacific Coast of the United States. Data were collected over a ten-day period 15-25 August, 1972.

In spite of the site's proximity to the Pacific Ocean the aerosol at Pt. Reyes was not always dominated by sea salt as the humidograms in Figure 7-9 show. Response such as curve 7-9a was observed roughly fifty per cent of the sampling time during the period, when b_{sp} was low, i.e., about equal to Rayleigh scattering, $b_{Rg} = 0.12 \times 10^{-4}$ ($\lambda = 550\text{nm}$). Synoptically, this was a period of 2 to 5 m/s onshore winds from the west to northwest, generally with an onshore component. This aerosol is presumably typical of that encountered above the surface layer over the Pacific. The passage of ships off shore could have had some influence on these measurements, especially considering the low aerosol concentrations.

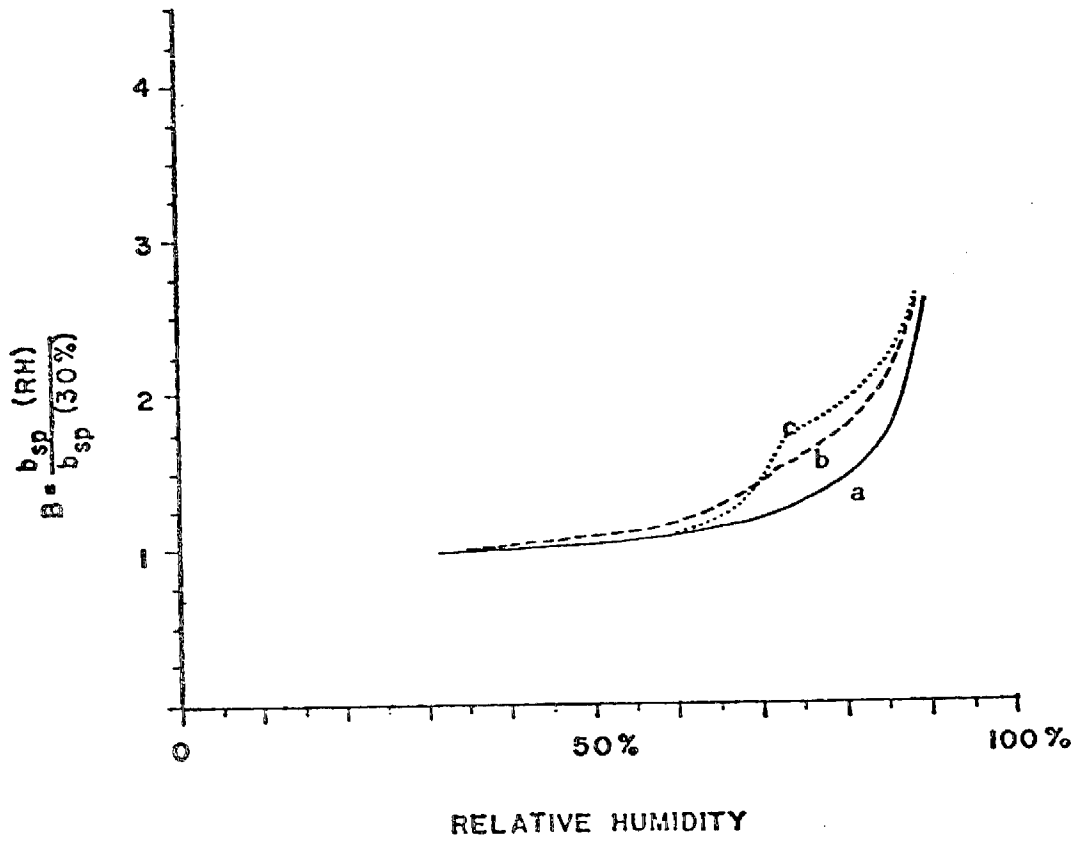
During the second week of sampling at Pt. Reyes - a period of higher winds - an aerosol response such as in Figure 7-9b and 7-9c was measured. Curve 7-9c shows the pronounced influence of sea salt which was observed with varying strength about forty per cent of the time. Response such as curve 7-9a was noted about ten per cent of the time, also during periods of strong winds. The winds during this period were onshore from the northwest 10-15 m/s with higher gusts. Surface trajectories were alongshore, however, and 850 mb winds had an off-shore component. Thus the presence of continental and anthropogenic aerosol cannot be discounted. Observation of the humidograms with time shows an aerosol response that varies between curves 7-9b and 7-9c over periods of a few hours. This is presumably due to variation in sea salt aerosol production rate and boundary layer depth, both of which are a function of wind speed. Local wind direction was rather consistently onshore from the northwest during this period.



- a. Site average 10 to 13 Aug. 72
- b. 0800 12 Aug. 72
- c. 0330 13 Aug. 72
- d. 1830 12 Aug. 72

Figure 7-8. Humidogram at Richmond, California

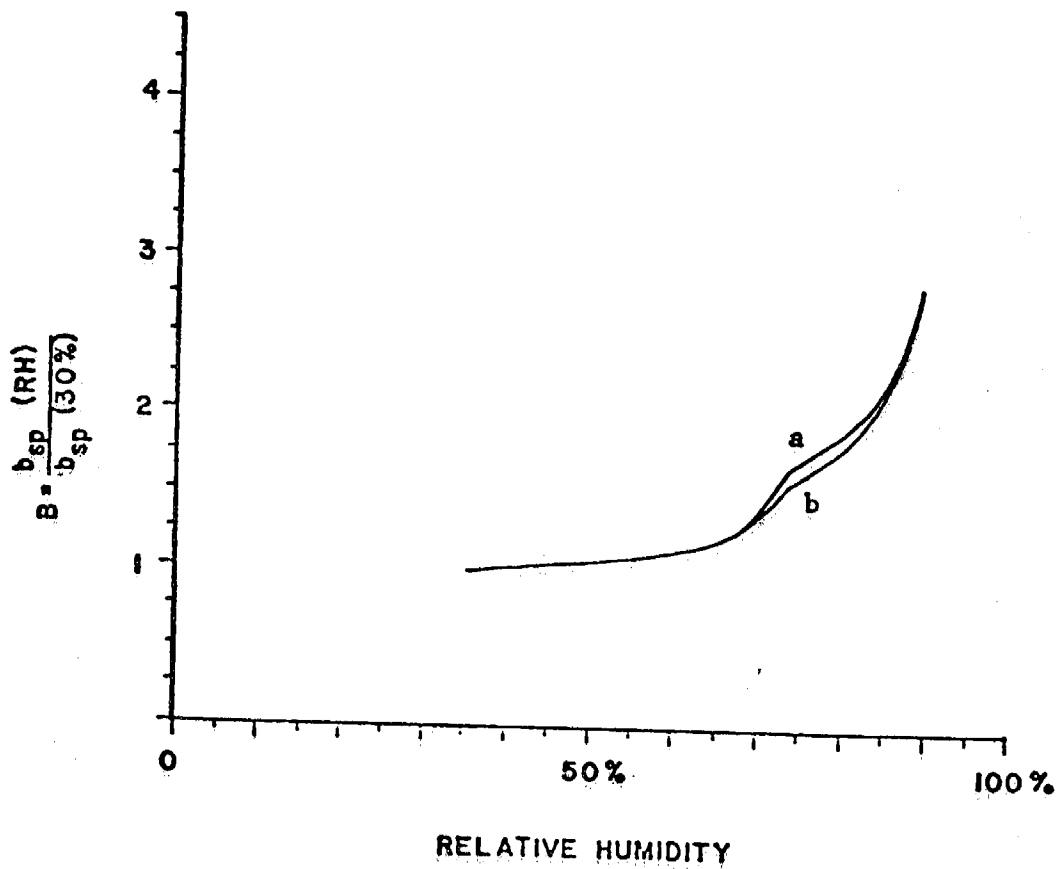
SC524.25FR



- a. 1045 to 1100 17 Aug. 72
- b. 1132 to 1532 23 Aug. 72
- c. 1400 24 Aug. to 0600 25 Aug. 72

Figure 7-9. Averaged Humidograms at Pt. Reyes, California

SC524.25FR



- a. Sample #76, 1030 17 Aug. to 1530 18 Aug. 72
- b. Sample #77, 1715 22 Aug. to 1530 23 Aug. 72

Figure 7-10. Humidograms at Pt. Reyes, California Taken During Periods for Which Chemical Analyses Were Made

SC524.25FR

The magnitude of the deliquescence increase in light scattering ratio is reduced considerably from that which would be expected on the basis of laboratory results with sea salt aerosol (Figure 7-1b). The cause for this could be chemical, i.e., the influence of other compounds (soluble or insoluble) or optical, due to an abnormal size distribution. Other optical measurements⁽⁷⁶⁾ made at the same time did in fact indicate that the size distribution was fairly monodisperse, $\sigma_g \approx 1.5$ with a maximum at $r_g \approx 0.5 \mu\text{m}$. Using these size distribution parameters and the humidograms illustrated in Figure 7-10 the fraction of sea salt in the aerosol was calculated assuming that the non-sea salt fraction was insoluble. The results are given in Table 7-3 and are compared with the chemical analysis of filter samples which were taken simultaneously. Chlorine concentrations determined by x-ray fluorescence spectroscopy were converted to sea salt concentrations according to the formula of Winkler⁽⁷⁵⁾. The results agree quite well considering that the errors involved in the optical calculations are of the order of +100% to -50%⁽⁷⁷⁾.

Pasadena, California

The sampling site was located in an urban residential district just south of the California Institute of Technology campus in Pasadena. The area is subject to the photochemical smog typical of the South Coastal and Los Angeles basins. The average of the humidograms taken in Pasadena is shown in Figure 7-11. Extreme deviations from this average are shown in Figure 7-7.

Of specific interest at this site was a three-day period 0600 20 September to 0700 23 September 1972 during which intensive sampling for chemical analysis was done. The results of the chemical analysis for the four sampling intervals are summarized in Figure 7-13 and Table 7-4. The averaged humidograms for specific meteorological conditions and sampling intervals are shown in Figure 7-12. The weather situation during these three days began with a mild Santa Ana prevailing over the entire South Coast Basin. This was interrupted during mid-day (1000-1900) on the 20th and again about 1300 on the 21st by weak onshore flow from the west to southwest. By the morning of the 22nd the continental air had been displaced by a marine layer 100-150 meters in depth. This layer spread inland and persisted until about 1200 PST after

SC524.25FR

TABLE 7-3

OPTICALLY AND CHEMICALLY DETERMINED SEA SALT CONCENTRATIONS

<u>Date</u>	<u>Sample #</u>	<u>Chemically Analyzed Sea Salt Concentration, $\mu\text{g}/\text{m}^3$</u>	<u>Optically Derived Sea Salt Concentration $\mu\text{g}/\text{m}^3$</u>
17-18 Aug.	76	9.5	5.0
22-23 Aug.	77	4.4	4.1

SC524.25FR

which mixing heights increased to 600 meters or more. Light smog conditions existed during the day on the 20th and 21st. A moderate smog condition developed or advected into the Pasadena area by 1200 PST on the 22nd after which rapid dispersion with the break of the inversion occurred.

The humidograms in Figure 7-12 reflect the weather conditions in an understandable way. The aerosol response to increasing relative humidity was markedly hygrophobic during the period of strongest unmodified Santa Ana conditions. This is presumably due to the presence of a large insoluble, mineral fraction in the aerosol, although no determinations of silicon or aluminum are available to support this. At other times, during the day on the 20th and to a greater degree on the 21st and 22nd, the aerosol response was more typically hygroscopic. The humidograms during the light and moderate smog conditions were monotonic with no indication of specific chemical compounds (deliquescence points) or strongly hygroscopic nature at low relative humidity. In this respect the conclusions which can be drawn regarding the effects of chemical composition are limited and possibly even contradict some of the previous conclusions about the chemistry controlling the form of humidograms. The chemical data in Table 7-4 and Figure 7-13 show that on the day of the Santa Ana condition, 20 September, as well as during the afternoon of the 22nd to the morning of the 23rd, water soluble inorganics comprised a major mass fraction of the aerosol. Ammonium sulfate dominated this class on the 22nd-23rd. Nitrate and sulfate were present on the 20th in about equal proportions. There was no indication of $(\text{NH}_4)_2\text{SO}_4$ deliquescence on the 22nd-23rd however and, more surprisingly, a very hygrophobic response on the 20th considering the amount of soluble material present. It is possible that the presence of the other water soluble components in an internal mixture on the 22nd-23rd was sufficient to suppress or cover the $(\text{NH}_4)_2\text{SO}_4$ deliquescence. Notable on this occasion was the increase in light scattering ratio at low RH, possibly attributable to the $(\text{NH}_4)_2\text{SO}_4$ plus some minor amounts of other soluble material. The same could be true in the case of sample period #87 where a ten per cent organic soluble fraction was determined along with the nearly forty per cent $(\text{NH}_4)_2\text{SO}_4$ fraction. The strongly hygroscopic aerosol

SC524.25FR

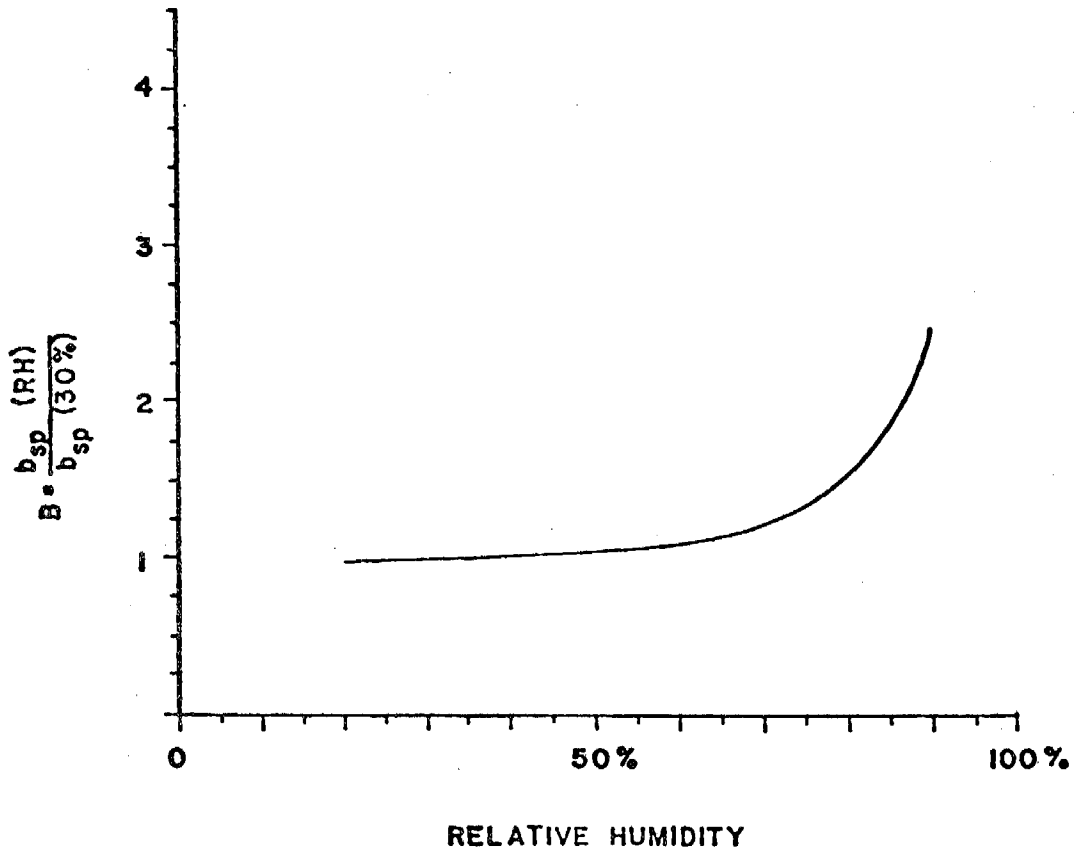


Figure 7-11. Averaged Humidogram, Pasadena, California
20 Sep. to 02 Oct. 72

SC524.25FR

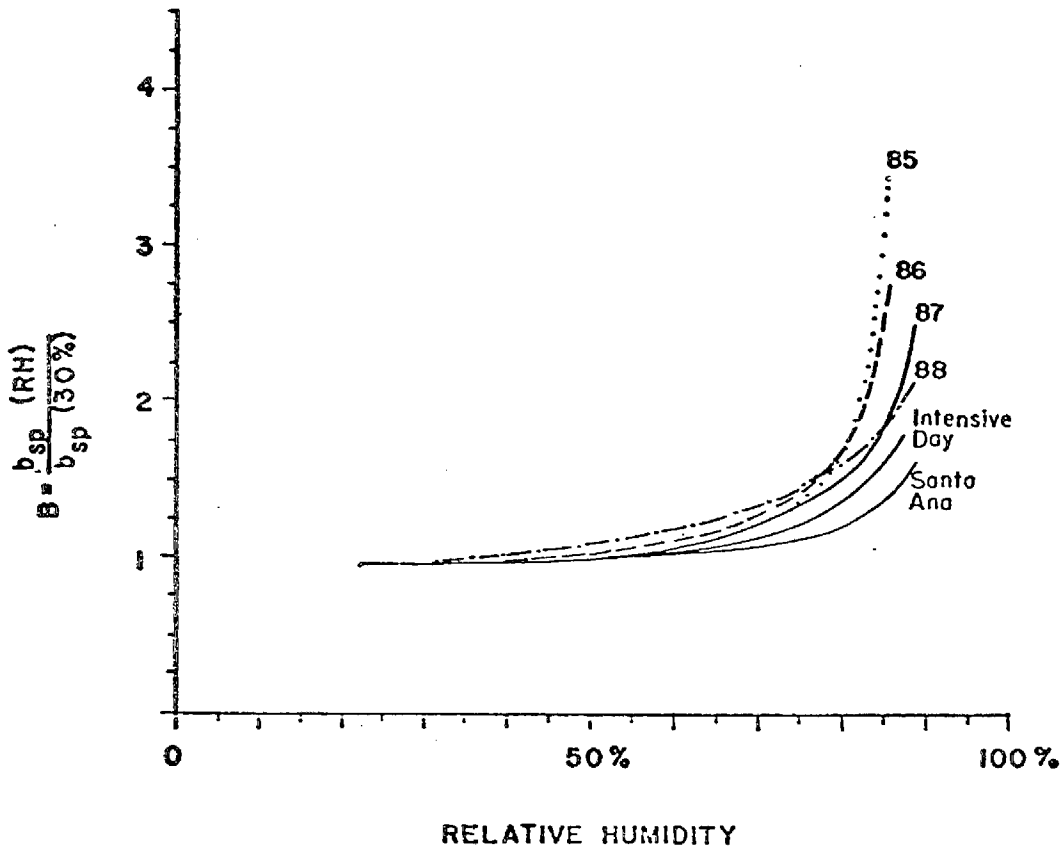


Figure 7-12. Averaged Humidograms at Pasadena, California
Corresponding to Chemical Analyses, See Table 7-4

SC524.25FR

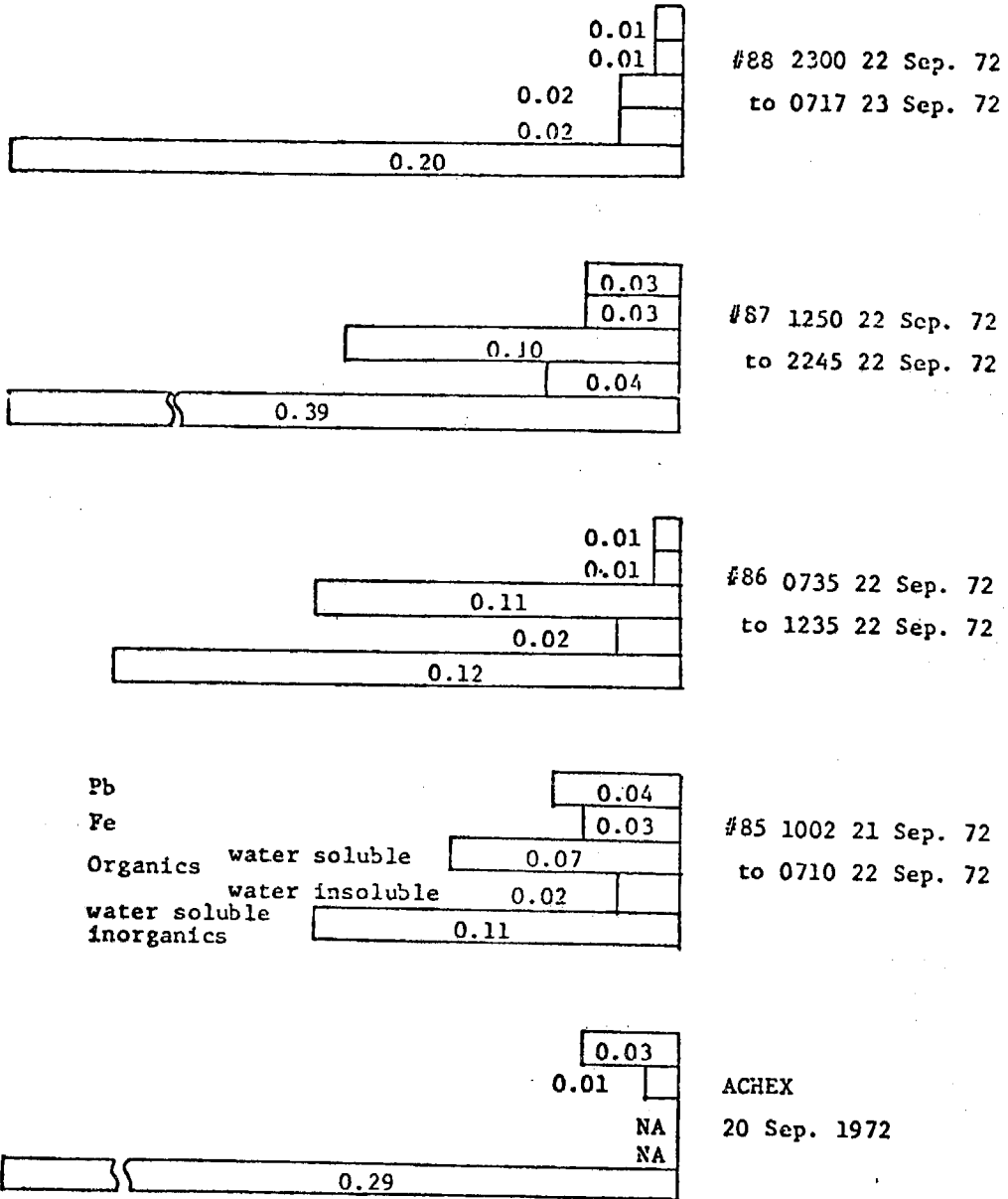


Figure 7-13. Relative Concentrations (Fraction by Weight of Total) of Some Chemical Components of South Coastal Basin Aerosol. California Institute of Technology, Pasadena, California, 20-23 Sep. 1972

TABLE 7-4

RESULTS OF CHEMICAL ANALYSES, PASADENA, CALIFORNIA, 20-23 SEPTEMBER 1972

Sampling Times	Sample #	Aerosol Total		Conc. $\mu\text{g}/\text{m}^3$	Water Soluble Inorganics (c)		Water Soluble Organics (d)		Fe	Pb	Fraction of Total Accounted for
		(a)	(b)		μg	μg	Organics	Insoluble Organics			
20 Sept. 1972	ACHEX (1973)	67	--	--	--	16.0	--	--	0.7	2.0	
						.29	--	--	.01	.03	.33
1002, 21 Sept 72	85	53	37	50	6.3	6.0	4.0	0.8	1.4	2.2	
0710, 22 Sept 72 (Schuetzle, 1973)						.11	.07	.02	.03	.04	.27
0735, 22 Sept 72	86	167	205	157	10.4	28.0	18.5	3.4	2.3	1.4	
1235 22 Sept 72 (Schuetzle, 1973)						.17	.11	.02	.01	.01	.32
1250, 22 Sept 72	87	69	74	59	9.7	27.0	7.2	3.1	2.0	2.1	
2245, 22 Sept 72 (Schuetzle, 1973)						.39	.10	.04	.03	.03	.59
2300, 22 Sept 72	88	73	113	54	19.	15.0	1.2	1.6	1.0	1.0	
0717, 23 Sept 72 (Schuetzle, 1973)						.20	.02	.02	.01	.01	.26

(a) Filterable mass

(b) Calculated from b_{sp} (c) Including SO_4 as $(\text{NH}_4)_2\text{SO}_4$, Na as NaCl, NH_4 as NH_4Cl , NO_3 as NH_4NO_3 .

(d) Including organic acids and diacids, alcohols, aldehydes, and nitrates (Schuetzle, 1973).



SC524.25FR

response at 80% relative humidity may be due to the roughly equal amounts of soluble organic and inorganic compounds analyzed in samples #85 and #86.

Fresno, California

The humidograms observed in Fresno were uniformly hygroscopic during the two-week sampling period. A typical humidogram is illustrated in Figure 7-14; deviations from this response were small. Chemical and size distribution data obtained at Fresno indicated the sub-micron aerosol to be typical of moderate photochemical smog. The meteorological situation was relatively constant during the sampling period; no dramatic changes in air mass occurred. The one meteorological occasion, a band of strong cumulus and shower activity, which could have dispersed local anthropogenic aerosol and suppressed agricultural aerosol sources, happened during a period of equipment outage. Meteorological conditions stabilized rapidly and no change in the nature of the aerosol was observed once the equipment was repaired.

Hunter Liggett Military Reservation

The Hunter Liggett site was located in the coastal mountains of Southern California 20 km from the Pacific Ocean at an elevation of 400m. Although close to the ocean, the site is separated from it by a ridge of mountains 600 to 1000m in elevation. This coupled with the low marine inversion and absence of urban centers provided a site with predominantly background, continental air quality. The illustrated data in Figure 7-15 are averages of 24 measurements made over separate 12-hour periods. One humidogram reveals a hint of deliquescent character, perhaps due to an intrusion of marine air. From trajectory analyses it is unclear that such an intrusion was possible. Winds at the surface and aloft were onshore but weak, 2 m/s. The other humidogram in Figure 7-15 is more typical of that observed during four days of sampling. Winds were light, 2 m/s and variable from the south at surface and aloft. It shows the aerosol to be less hygroscopic than earlier when the possible presence of sea salt was indicated.

SC524.25FR

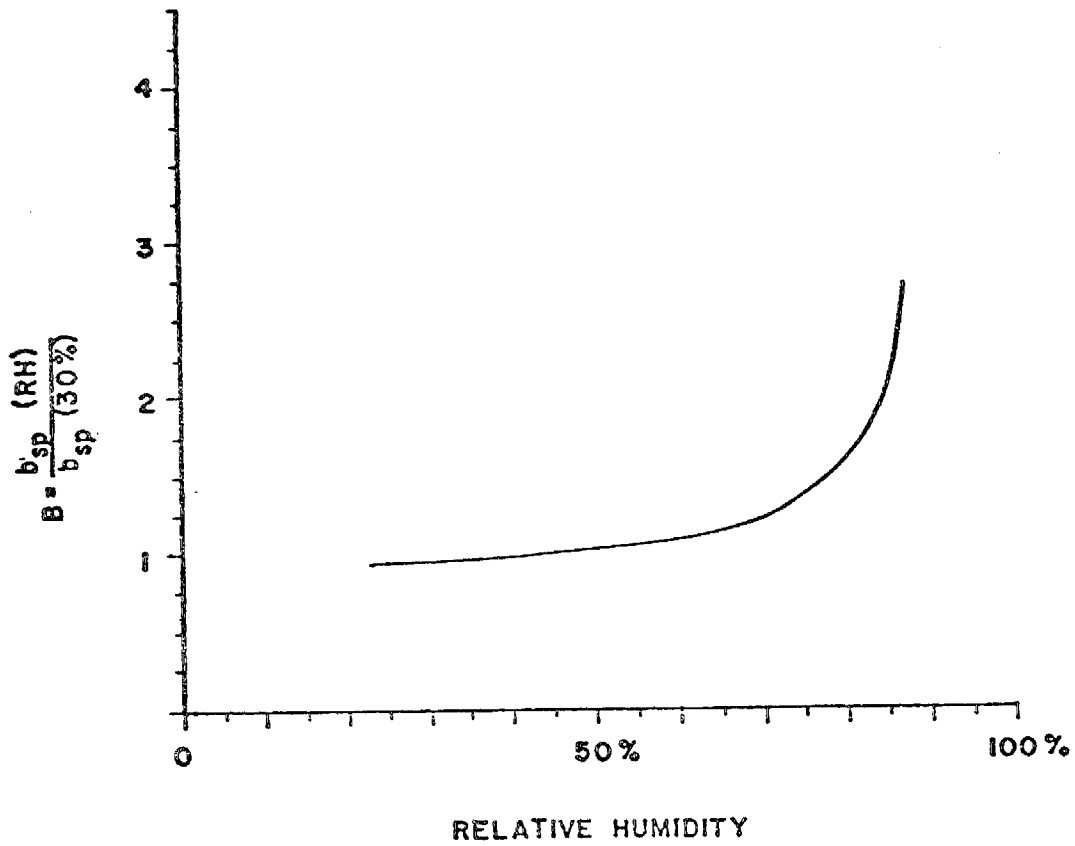


Figure 7-14. Averaged Humidogram, Fresno, California
29 Aug. 72 to 08 Sep. 72

SC524.25FR

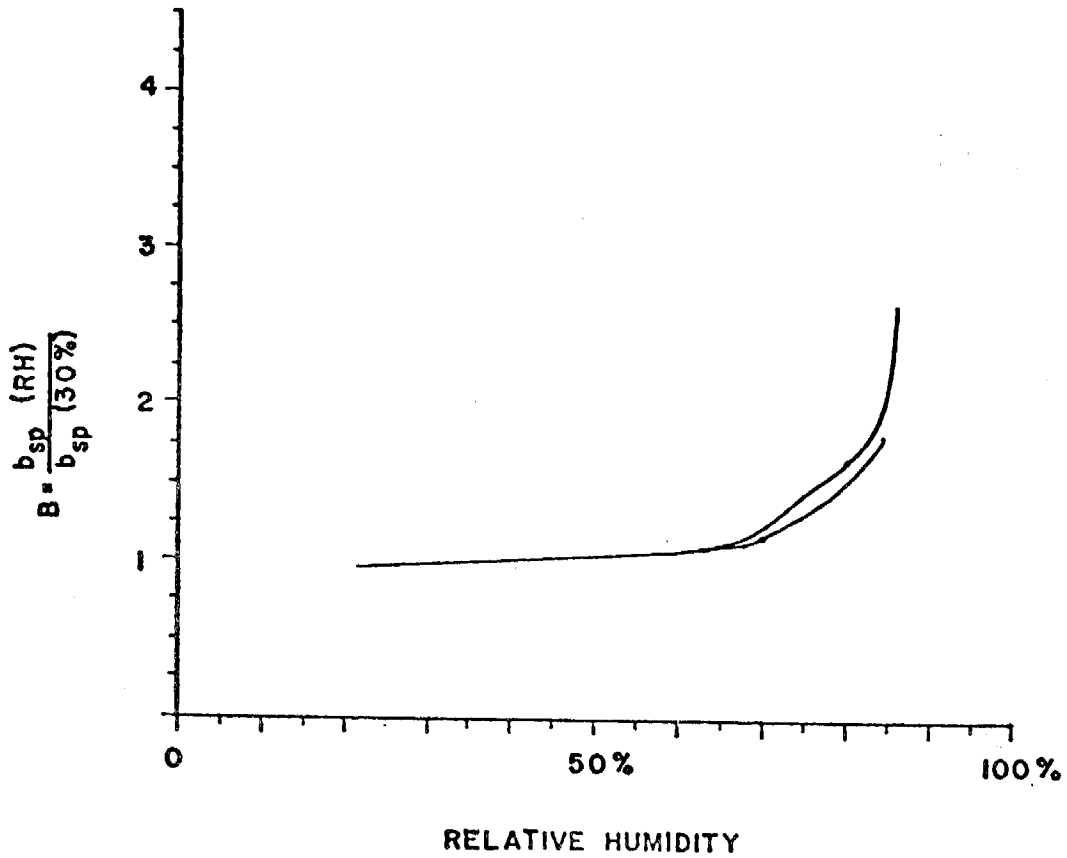


Figure 7-15. Averaged Humidogram, Hunter Liggett Military Reservation
13 Sep. 72 to 15 Sep. 72

SC524.25FR

South Coastal Beach Sites

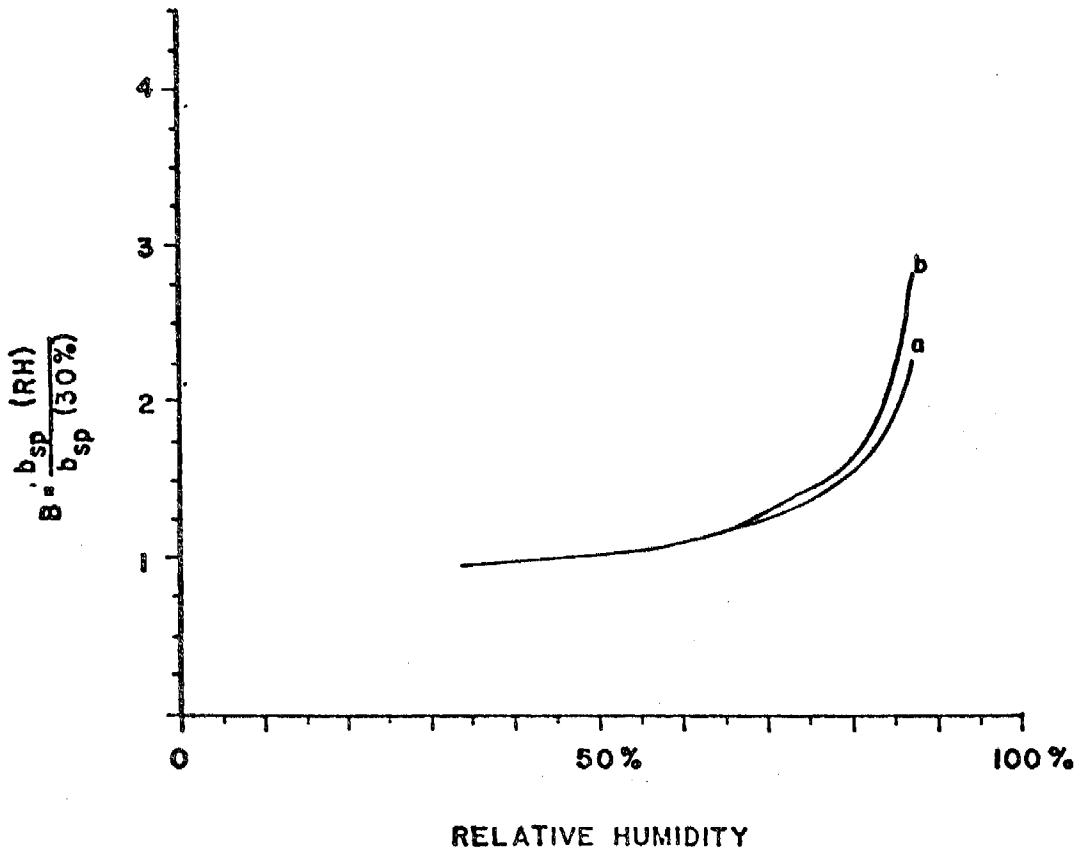
Two sites directly on the coast north of the Los Angeles area, Montana de Oro State Beach and El Capitan State Beach, were visited for further observation of marine aerosol. The meteorology at both sites was dominated by a diurnal land-sea breeze pattern which provided a well-mixed aerosol of marine and anthropogenic origin. From the El Capitan site layers and parcels of Los Angeles urban aerosol could be observed offshore. Indications of the presence of sea salt aerosol was masked in the humidograms as can be seen in Figure 7-16a and 7-16b. Chemical analysis showed the sea salt fraction to be roughly fifty per cent of the total aerosol mass at both of these sites. This fraction, if present in the sub-micron mass, should be easily detectable in the humidograms. The proximity of the site to the surf zone means that a large fraction of the sea salt particles were probably not in the sub-micron class and that the remaining sea salt fraction in the sub-micron class could have easily been masked by a mixed anthropogenic aerosol.

St. Louis, Missouri and Environs

Two of the field sites were in the urban St. Louis area and subject to urban-industrial aerosol sources. The third site was located 35 km west of the city on a hill, ca. 200m elevation. The results have been reported in detail by Charlson, *et al.* ⁽⁷³⁾ and are summarized here. Figure 7-17D illustrates a humidogram typical of those observed roughly two-thirds of the time at the urban sites. The dotted curve indicates the response with the addition of ammonia to the sample aerosol as described in Volume II. About one-fourth of the humidograms indicated the presence of a deliquescent compound (most likely ammonium sulfate on the basis of the observed deliquescence at about 80% RH) in varying amounts, estimated to be thirty to fifty mole per cent of the aerosol mass. This observation has been supported by an x-ray fluorescence analysis for elemental sulfur in the sub-micron size range.

At the Tyson site the ambient aerosol was dominated by the presence of H_2SO_4 or one of its reaction products with NH_3 , i.e., NH_4HSO_4 , $(NH_4)_3H(SO_4)_2$ or $(NH_4)_2SO_4$. Figures 7-17A, 7-17B, and 7-17C illustrate typical examples of the types of humidograms observed. Figure 7-17C, from the sharpness and

SC524.25FR



- a. Montana de Oro State Beach, California
16 Sep. 72
- b. El Capitan State Beach, California
18 Sep. 72

Figure 7-16. Averaged Humidograms at Montana de Oro State Beach, California and El Capitan State Beach, California

SC524.25FR

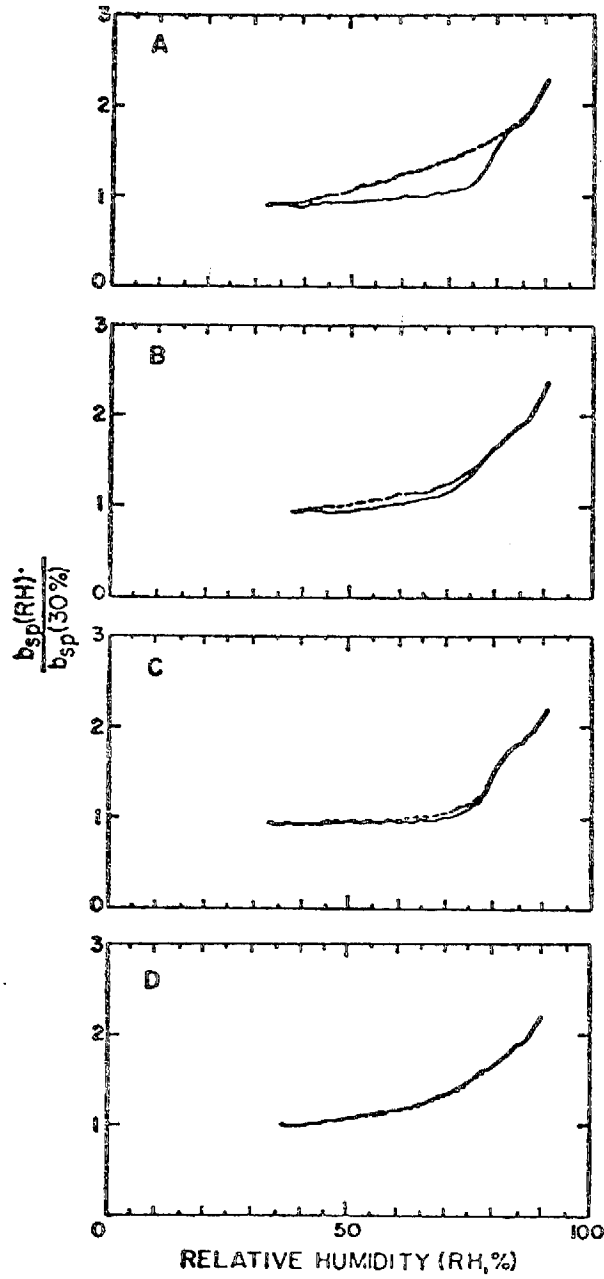


Figure 7-17. Humidograms for St. Louis Area, 21 to 28 Sep. 73 (Sheet 1 of 2)

SC524.25FR

- A. Hygroscopic aerosol; addition of NH_3 caused aerosol to become strongly deliquescent at 80% RH; 1208 to 1219 23 Sep. 73, Tyson, Missouri.
- B. Moderately deliquescent aerosol; deliquescence at 80% RH enhanced by addition of NH_3 ; 2030 to 2047 21 Sep. 73, Tyson, Missouri.
- C. Strongly deliquescent aerosol; little or no change upon addition of NH_3 ; 2245 to 2303 24 Sep. 73, Tyson, Missouri.
- D. Hygroscopic aerosol; unaffected by addition of NH_3 ; St. Louis University, St. Louis, Missouri

Figure 7-17. Humidograms for St. Louis Area, 21 to 28 Sep. 73 (Sheet 2 of 2)

magnitude of the deliquescence step indicates the presence of fairly pure $(\text{NH}_4)_2\text{SO}_4$ aerosol, with no significant change upon artificial addition of NH_3 . Figure 7-17A indicates the presence of H_2SO_4 aerosol (dotted humidogram) which upon addition of NH_3 yielded a $(\text{NH}_4)_2\text{SO}_4$ type humidity response similar to that in Figure 7-17C. Figure 7-17B shows an intermediate type response which is believed to be due to an intermediate reaction product, perhaps of more mixed composition, but which still reacts with NH_3 to yield an evident though weaker $(\text{NH}_4)_2\text{SO}_4$ deliquescence step. These three responses, as in Figure 7-17A, 7-17B, and 7-17C were noted roughly 25%, 25% and 50% of the time respectively, independent of gross meteorological conditions. It is suspected that this sulfate aerosol, in its various combined states is of regional background nature.

SC524.25FR

Denver, Colorado

This site was visited as part of an E.P.A. aerosol characterization study of the Denver metropolitan smog. The site was outside the city to the northeast, away from urban sources. The aerosol here was unique in its general non-hygroscopic character. Of particular interest was the presence at times of an extremely hygrophobic aerosol response as illustrated in Figure 7-18. This type of response was not infrequent (ca. 20% of the time) and was associated with post inversion conditions with good mixing and winds from rural or sub-urban areas.

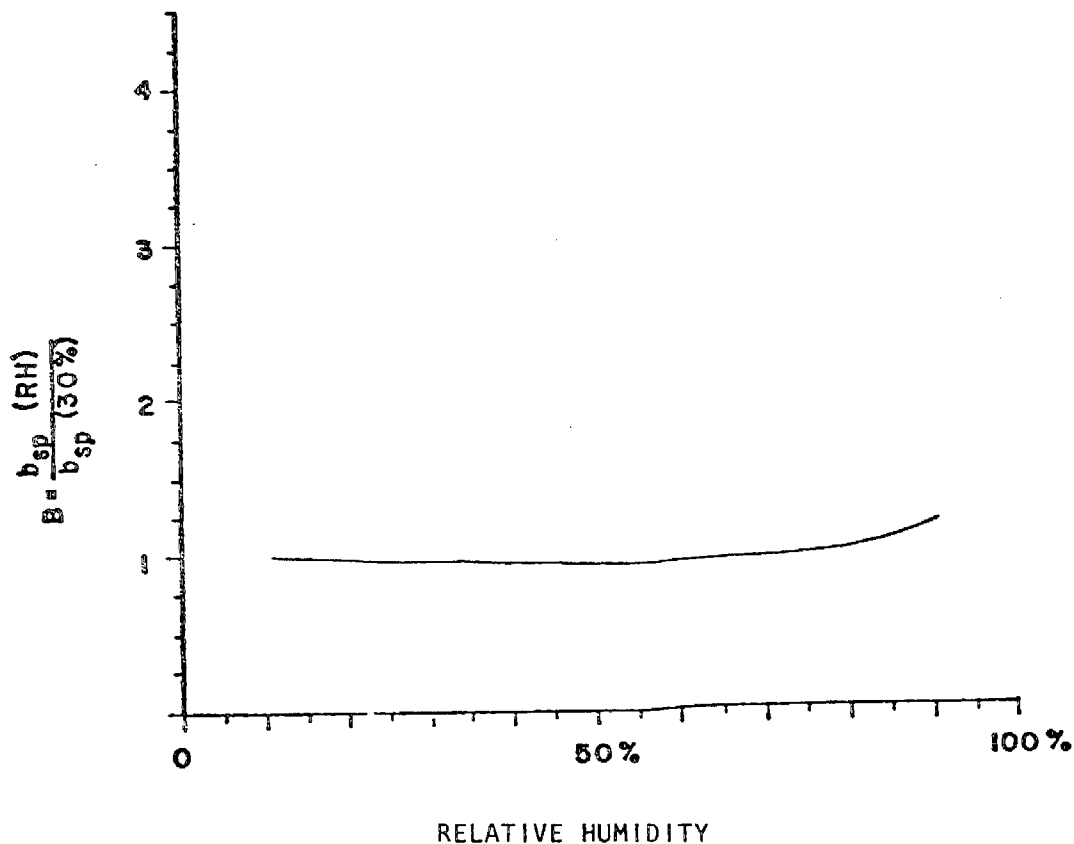


Figure 7-18. Humidogram of Hygrophobic Aerosol, Denver, Colorado 21 Nov. 73

SC524.25FR

5. WATEROMETER RESULTS

a. Field Observations.

To test the feasibility of measuring liquid water content in aerosols, a prototype microwave waterometer was used in the field in late summer and fall of 1972. The instrument was operated at the California Institute of Technology, Pasadena, California, and on the ACHEX mobile laboratory. With the waterometer, the mobile laboratory was located (a) next to the Harbor Freeway in downtown Los Angeles, (b) at the Los Angeles County Fairgrounds in Pomona, California, (c) Goldstone Tracking Station, California, and (d) Pt. Arguello, California (Marine). The first sites were urban locations ranging from a "source enriched" site for auto exhaust to "receptor" sites chosen to provide samples of air pollution away from the neighborhood of major sources. The goldstone site was chosen to be representative of a remote desert location more than 100 km from any community. The Pt. Arguello location was next to the Pacific Ocean approximately 20 meters above sea level and represents marine air for sampling.

In both the Pasadena station and the mobile laboratory, meteorological instrumentation, trace gas monitors and integrating nephelometers were in operation at the same time the waterometer was used. Because of the geometrical design and nature of the aerosol sampling system at Pasadena and in the mobile laboratory, aerosols larger than approximately 10 μm diameter could not be detected.

The air sampling was conducted under conditions ranging from no photochemical smog to moderate smog (maximum ozone concentration > 20 pphm) at the urban locations. On one occasion at Pasadena, drizzle and fog were observed. The weather at Goldstone was warm and dry, with observations taken just after passage of a weak storm front. Conditions at Pt. Arguello were characterized by moderate to brisk winds with scattered clouds.

Experiments were conducted over periods of 24 hours to investigate the diurnal behavior of water content and total mass concentration. The waterometer observations were compared with nephelometer readings and with the total mass concentration as measured with the β -attenuation monitor. Other

SC524.25FR

supporting data included the relative humidity or dew point, the winds, as well as a variety of aerosol data including nephelometer readings.

b. Results and Discussion

The aerosol sampling conducted during the 1972 season indicated that significant amounts of water were present in atmospheric aerosols even at relative humidities well below 100%. The hygroscopic nature of airborne particles was well illustrated in the urban air of Los Angeles and near the ocean at Pt. Arguello. In contrast, the desert aerosol at Goldstone was found to contain essentially no detectable water.

Some typical results from this initial study are shown in Figures 7-19, 7-20, 7-21, and 7-22 illustrating diurnal changes in urban air. Included with these data are results from the total mass monitor. In Figure 7-19 are the diurnal changes measured in Pasadena for conditions of moderate photochemical smog, where the oxidant level exceeded 25 pphm by midday. In this case the total mass concentration of airborne particles was maximum near midday; this maximum was accompanied by a maximum in the apparent water content of the particles. The change in fractional water content of the aerosols follows the change in relative humidity, whose values are noted in the figure.

The data in Figure 7-21 are for another sampling day in Pasadena. Here there was essentially no photochemical smog. The weather was overcast with drizzle and fog through the morning, but with clearing in the afternoon. The data from the β gauge are only semi-quantitative because of large errors in mass measurement induced in this instrument at relative humidity $> 70\%$ ⁽⁷⁸⁾. However, qualitatively, the changes in liquid water content follow well the changes detected in total aerosol mass, as found for the data in Figure 7-19. During the morning when fog and drizzle were observed, the liquid water content of material collected was a very large fraction of the total aerosol mass. In some cases the mass fraction of water exceeded 50%.

SC524.25ER

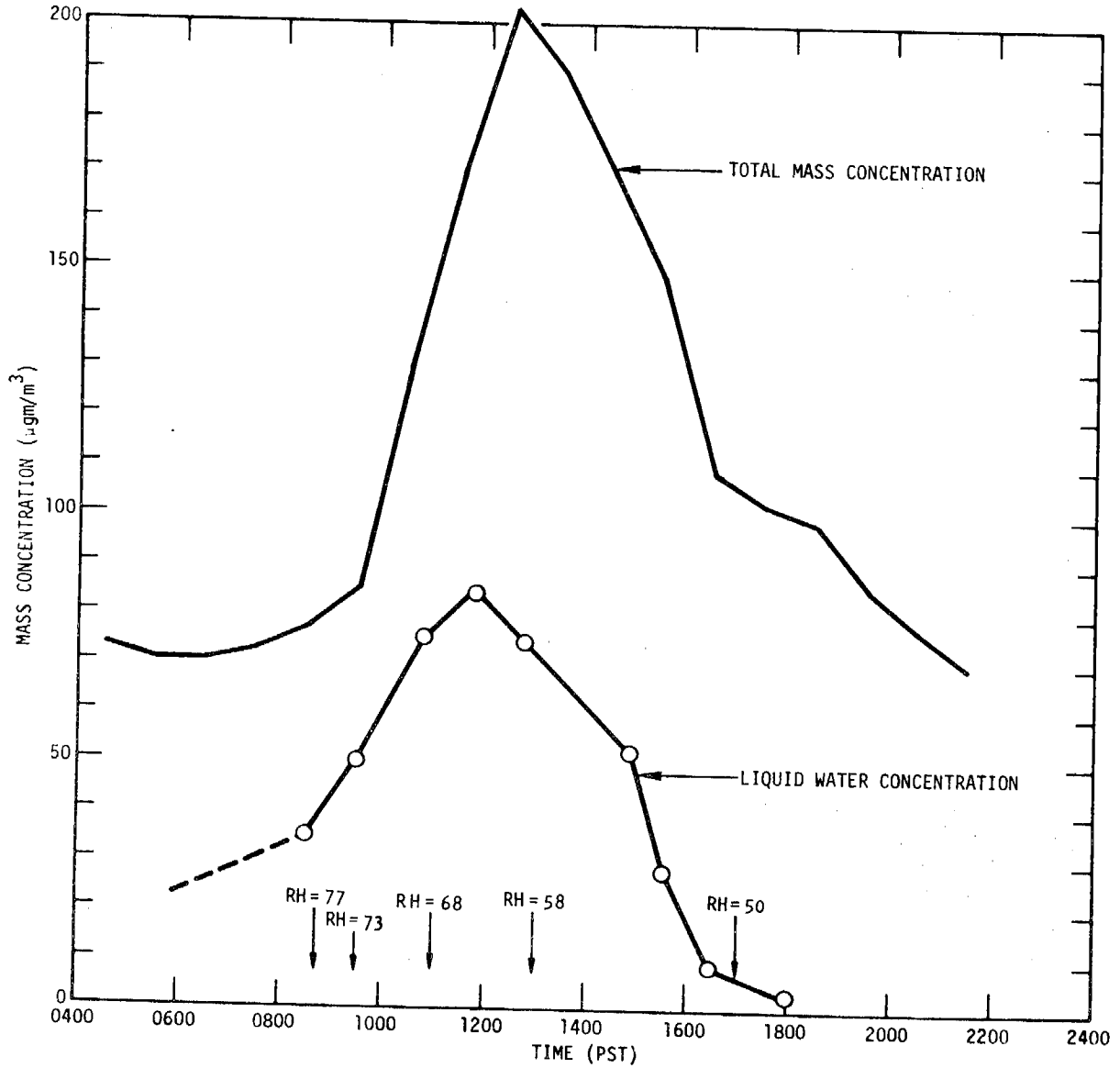


Figure 7-19. Liquid Water Concentration in Atmospheric Aerosols at Pasadena, September 15, 1972

SC524.25FR

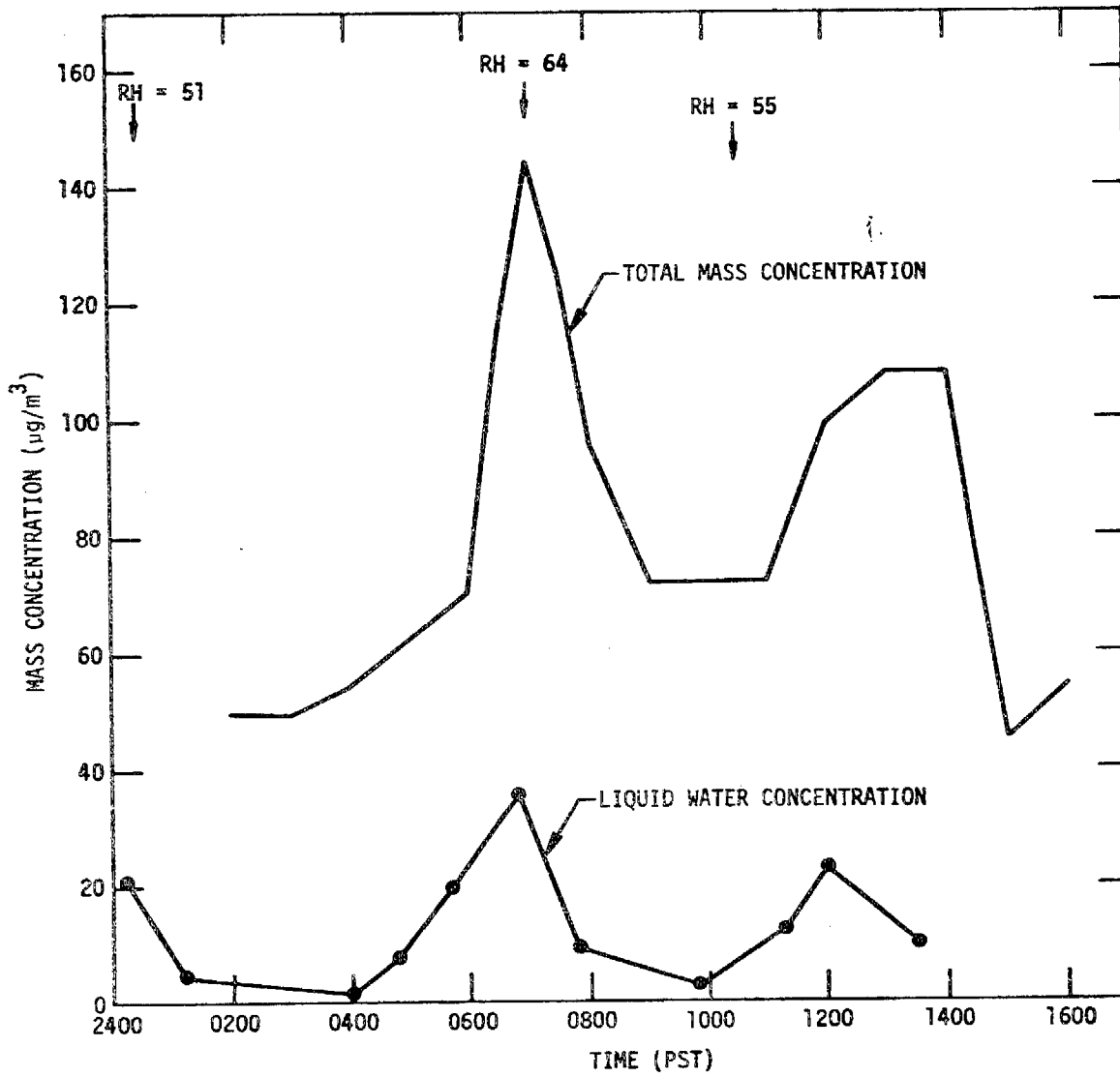


Figure 7-20. Liquid Water Concentration in Atmospheric Aerosols at Pasadena, September 20, 1972

SC524.25FR

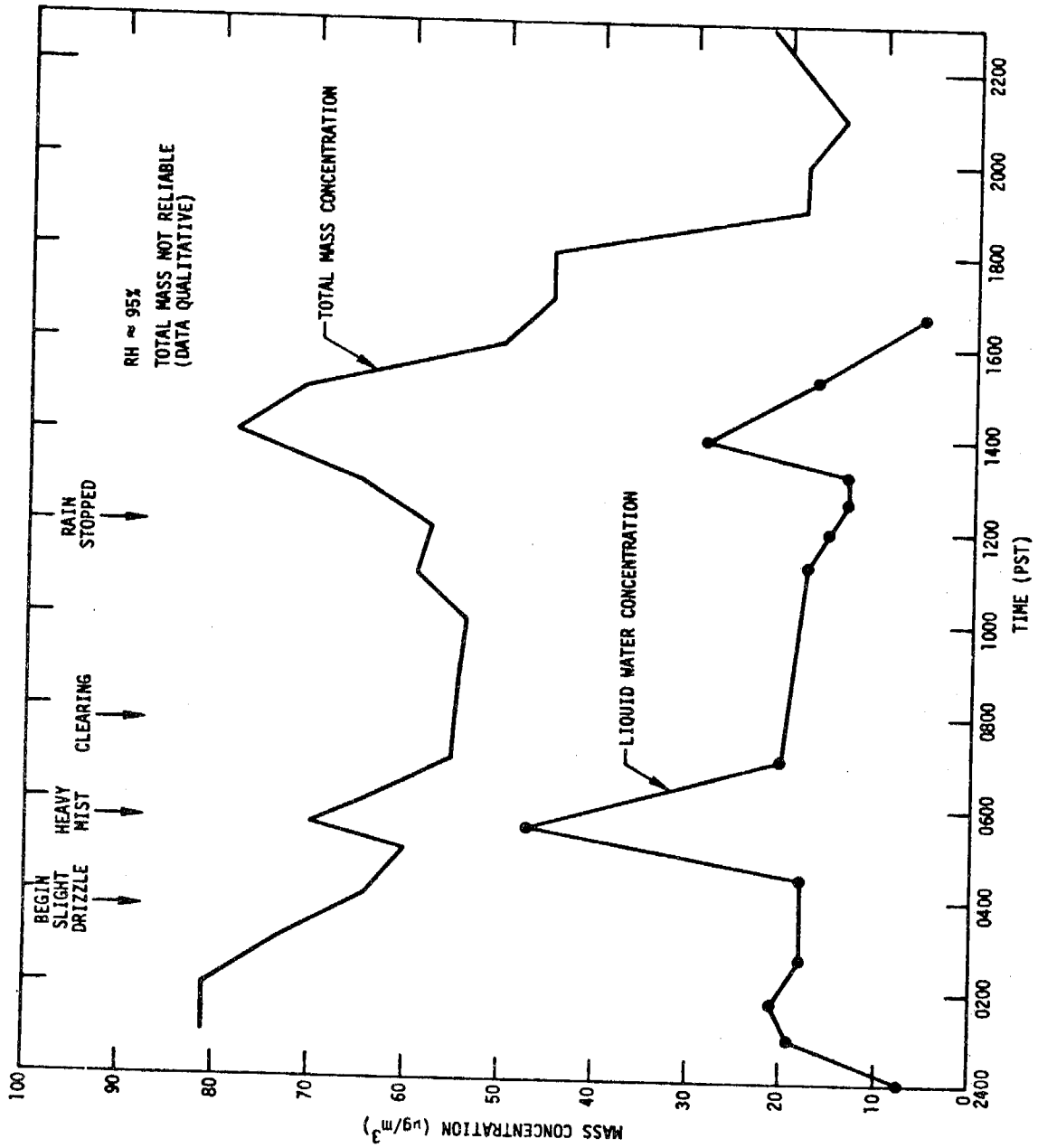


Figure 7-21. Liquid Water Concentration in Atmospheric Aerosols at Pasadena, September 9, 1972

SC524.25FR

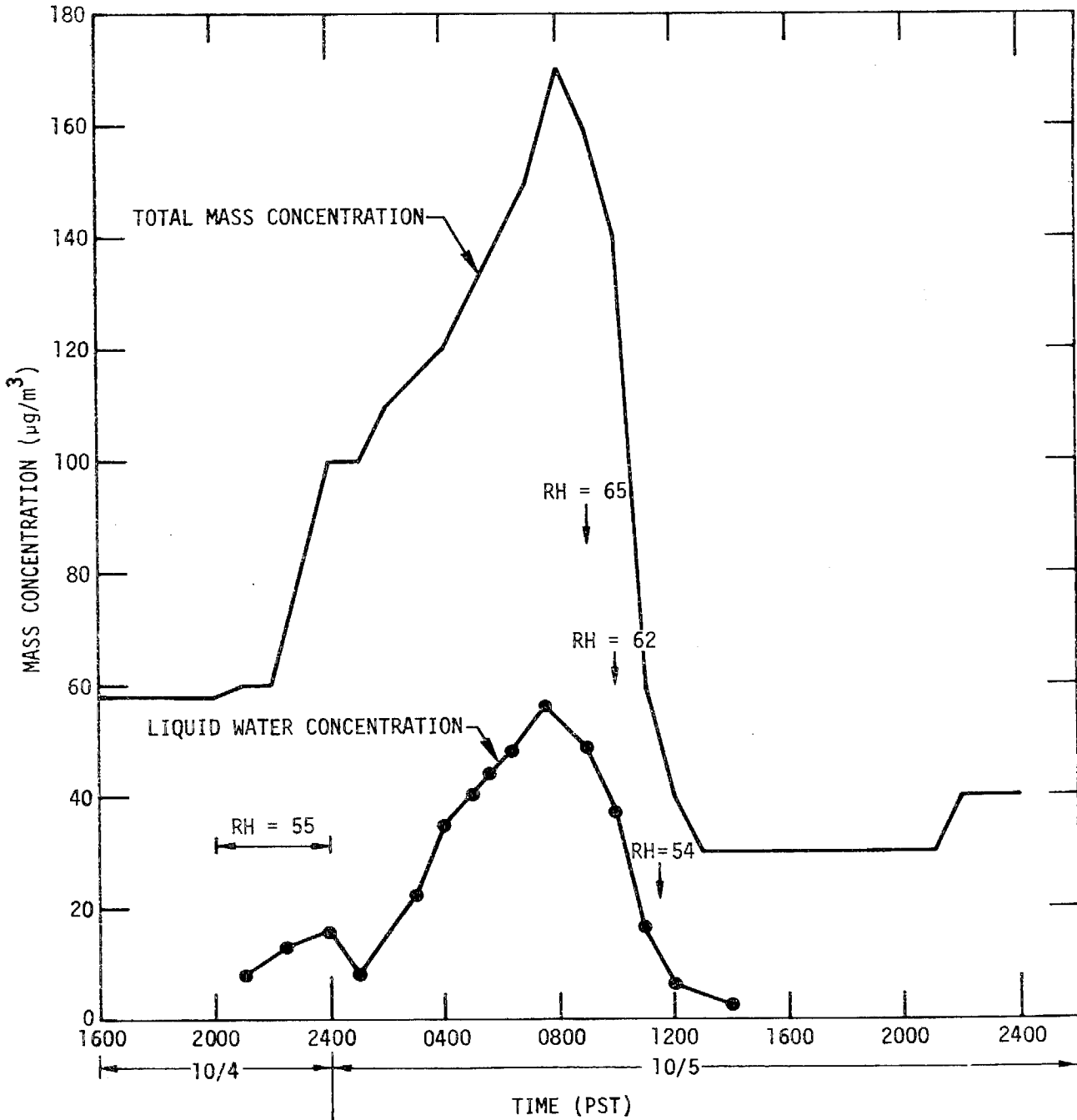


Figure 7-22. Liquid Water Concentration in Atmospheric Aerosols at Pomona, October 4-5, 1972

SC524.25FR

Another case of measurements of liquid water content in urban air, taken at the Los Angeles County Fairgrounds in Pomona, is shown in Figure 7-22. This was a condition of light smog where maximum oxidant levels remained below 10 pphm. Again the pattern of change in liquid water content following total mass concentration is observed. However, the maxima in these parameters is observed in the morning hours in contrast to the Pasadena case in Figure 7-19. Again, there appears to be a correspondence between changes in relative humidity and water content during the day.

Figure 7-20 shows the diurnal pattern in liquid water content for the data obtained at Pasadena on another occasion. Two peaks were observed in the total mass concentration with corresponding increases in liquid water content. The decrease in mass concentration at 10 AM corresponded to a change in wind direction, and the second peak corresponded to a decrease of wind speed to almost zero.

The observation of liquid water content of urban aerosols in the Los Angeles area suggested a fraction of total mass ranging from 10-40% under conditions of relative humidity from 40-70%. With humidity over 70%, the fraction of liquid water can exceed this range significantly.

Measurements of the water in aerosols at the remote desert site are shown in Figure 7-23. At this location the mass concentration of particles was extremely low and the visibility was virtually unlimited during most of our visit. Within the limits of detection of the waterometer, essentially no water was present. This conclusion was confirmed by measurement of the water in filter collected aerosols by a gas chromatographic technique⁽⁶⁴⁾.

The observations of liquid water in airborne particles samples at Pt. Arguello was found to be highly variable. There were marked changes in water content depending on the wind direction and speed, which were related to nearby spray formation in the surf zone. In any case, the fresh sea salt aerosol being produced at the shoreline appeared to have a water content above 50% water by mass.

In Figure 7-24, our measured values of liquid water content with relative humidity are plotted and compared with the results of the humidograph. Our

SC524.25FR

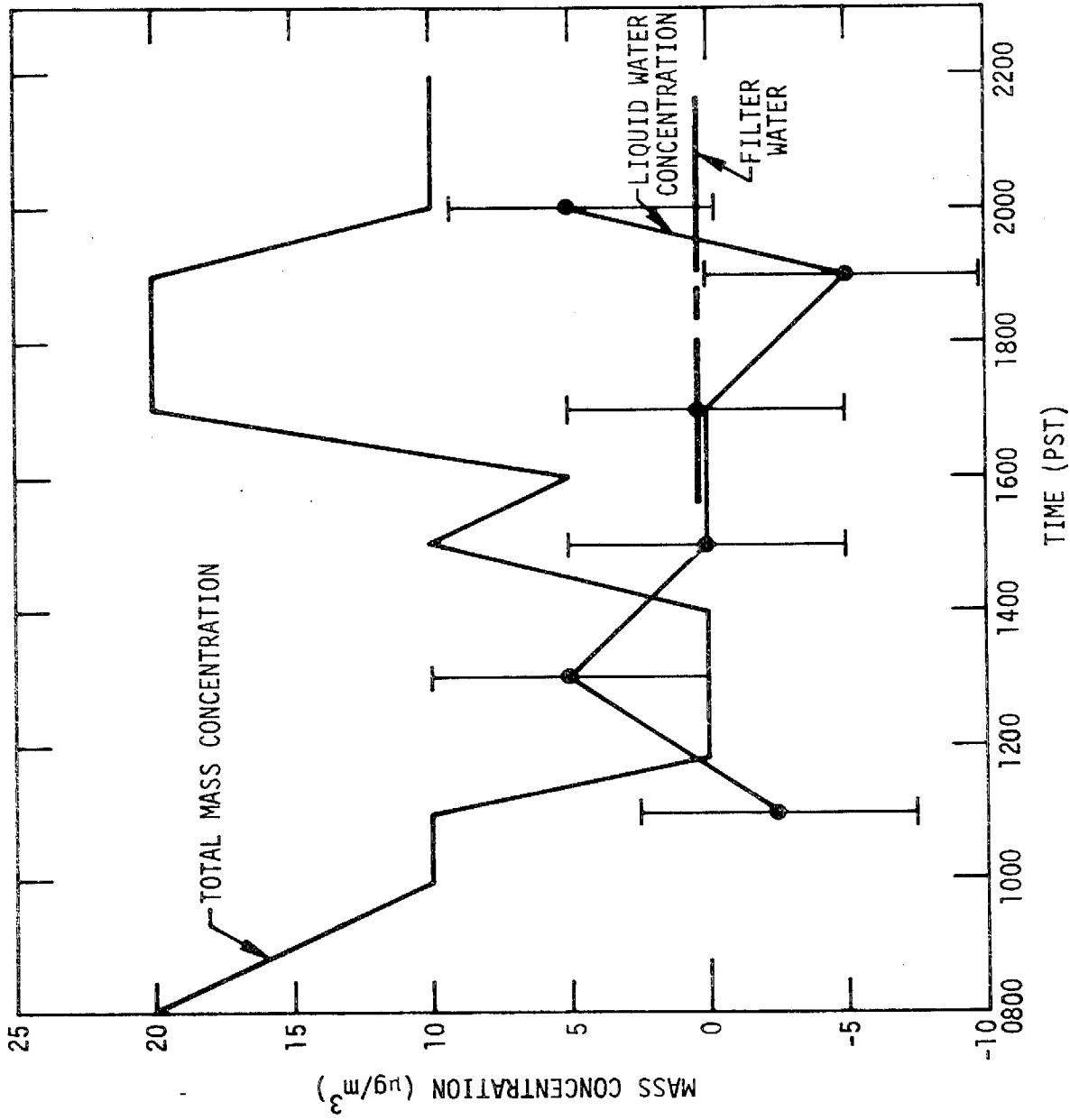


Figure 7-23. Liquid Water Concentration in Atmospheric Aerosols at Goldstone Tracking Station November 1972

SC524.25FR

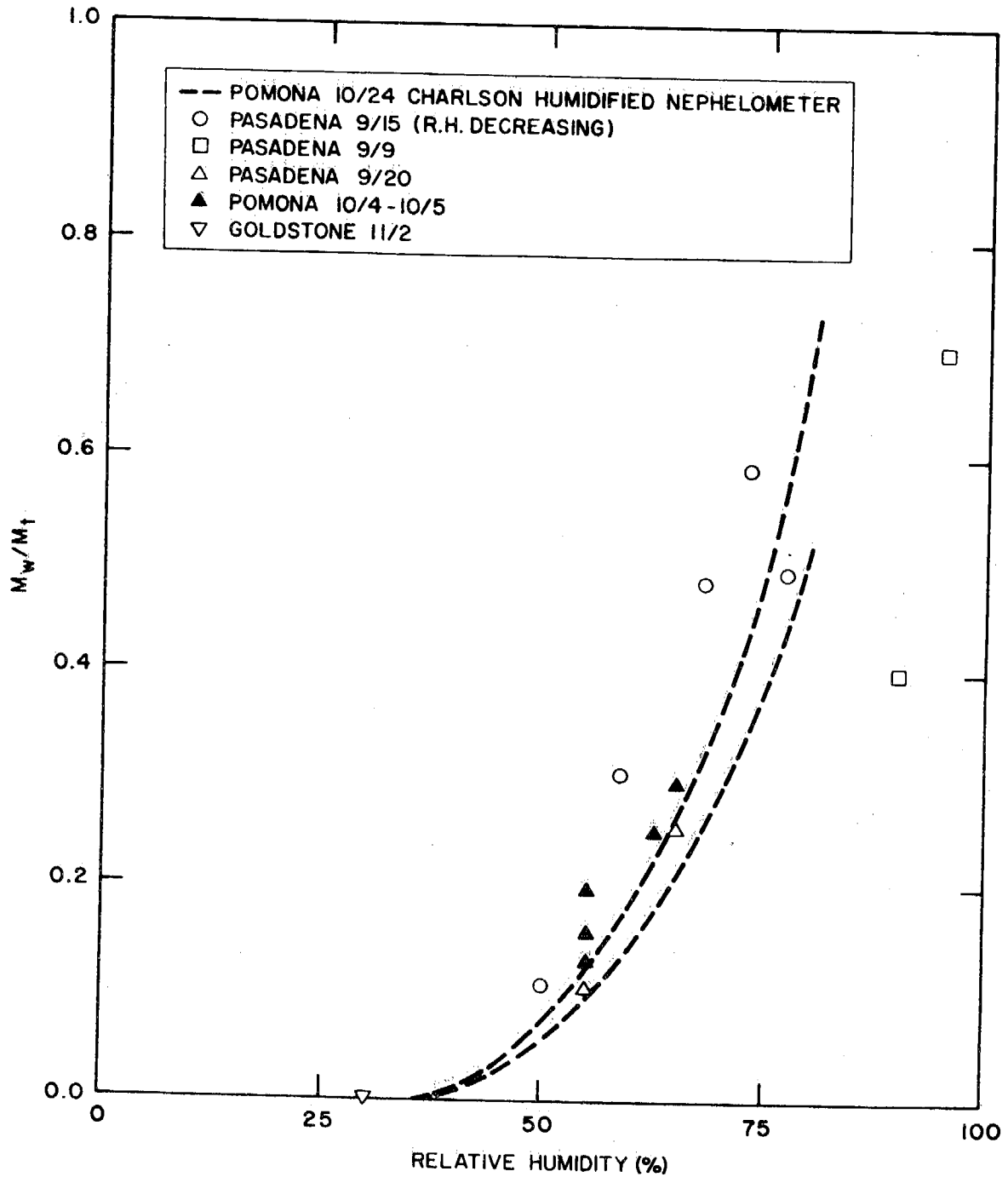


Figure 7-24. Weight Fraction of Liquid Water as a Function of Relative Humidity for the Los Angeles Basin Area. The Data Points are Results From the Present Investigation; and the Dotted Curves are the Results Obtained by the University of Washington Humidograph.

SC524.25FR

data agree fairly well with the humidified nephelometer data. Our data taken at high relative humidity are not considered reliable due to the previously mentioned difficulty in determining the total aerosol mass as well as the probability of increased water loss in the sampling procedure at high humidity, as related to the pressure drop across the filter.

Observations during ACHEX-I in the Los Angeles area indicated that the $\text{SO}_4^{=}$ and NO_3^- found in the aerosol from 24 hour filter samples could be accounted for stoichiometrically as ammonium salt. Using the measurements of liquid water content, it was found that the salt solutions in the aerosol would be highly concentrated, exceeding 1 molar in many cases. The high concentration of equivalent salt solution would influence the dielectric constant, especially the dielectric loss ϵ'' . However, the uncertainty introduced in the deduced liquid water content is comparatively small. The uncertainty, due to all causes, in the measurements reported here is estimated to be $\pm 30\%$.

The systematic and marked changes in liquid water content with total mass concentration in the aerosols observed in 1972 indicate the importance of water in behavior of the suspended particles. Of particular interest are the diurnal changes found in urban air in the Los Angeles area. At this point it is not certain whether or not the changes in water content result from (a) the advection of more heavily polluted air containing a roughly fixed ratio of water to total mass or (b) the chemical changes taking place in the aerosol. Other measurements of the chemical composition of aerosols observed at the same time show strong systematic changes in sulfate, nitrate, and organic fraction in the urban aerosol that accompany changes in total mass. The observations of changes in "free" water may be related to the equilibration of the aerosol to moist air as hygroscopic salts such as the nitrates or sulfates are formed by atmospheric chemical transformations. If pure ammonium sulfate is being produced, the substantial absorption of water at relative humidity below 80% cannot be explained. However, if mixtures of ammonium sulfate and nitrate are present, their hygroscopicity may be greater, reflecting a more efficient absorption of water at relative humidity below 70%.

SC524.25FR

A third possibility is that liquid water may actually be produced in chemical reactions on the aerosol particles. There are no known inorganic reactions related to atmospheric reaction that can be invoked to rationalize this. However, there are organic reactions of the decomposition of unstable intermediates from ozone-olefin reactions that could generate liquid water in the airborne particles. This may be of particular interest with the very high organic content found in the Los Angeles aerosol.

There has been indirect evidence available for many years that liquid water incorporated in aerosol particles is a major factor in visibility reduction, particularly at relative humidity above 70%. Visibility is generally accepted as being related to the extinction coefficient for visible light, measure by an integrating nephelometer (b_{scat}). Our observations of b_{scat} and liquid water content have been plotted and correlated in Figure 7-25.

Within the experimental error of the 1972 measurements ($\pm 30\%$ fractional error) there is a linear relation between b_{scat} and liquid water content. The correlation holds to the Rayleigh light scattering limit, exemplified by the observations at the desert site in Goldstone. This strong relationship over the range of relative humidity of $\sim 40\%$ to 70% indicates the significance of liquid water content to the optical properties of atmospheric aerosols.

The correlation between b_{scat} and liquid water content, as measured by the microwave instrument also was checked for data obtained during the 1973 testing period. The scatter diagram is shown in Figure 7-26. The scatter in the 1973 results is somewhat larger than found in 1972, particularly at high values of b_{scat} . For values below 4 to $5 \times 10^{-4} \text{ m}^{-1}$, the correlation based on the 1972 data holds satisfactorily, noting that the fractional error band of the data is larger in 1973 than in 1972. In cases of heavy haze, when $b_{\text{scat}} \gtrsim 5 \times 10^{-4} \text{ m}^{-1}$ other influences evidently contribute as much or more than liquid water content to aerosol light scattering.

It is interesting that the correlation shown in Figure 7-25 is analogous to the correlation of b_{scat} and total mass concentration. Using the slope of the line in this figure and comparing it with the slope of the b_{scat} vs. total mass concentration correlation⁽⁷⁷⁾, one finds qualitatively that the water

SC524.25FR

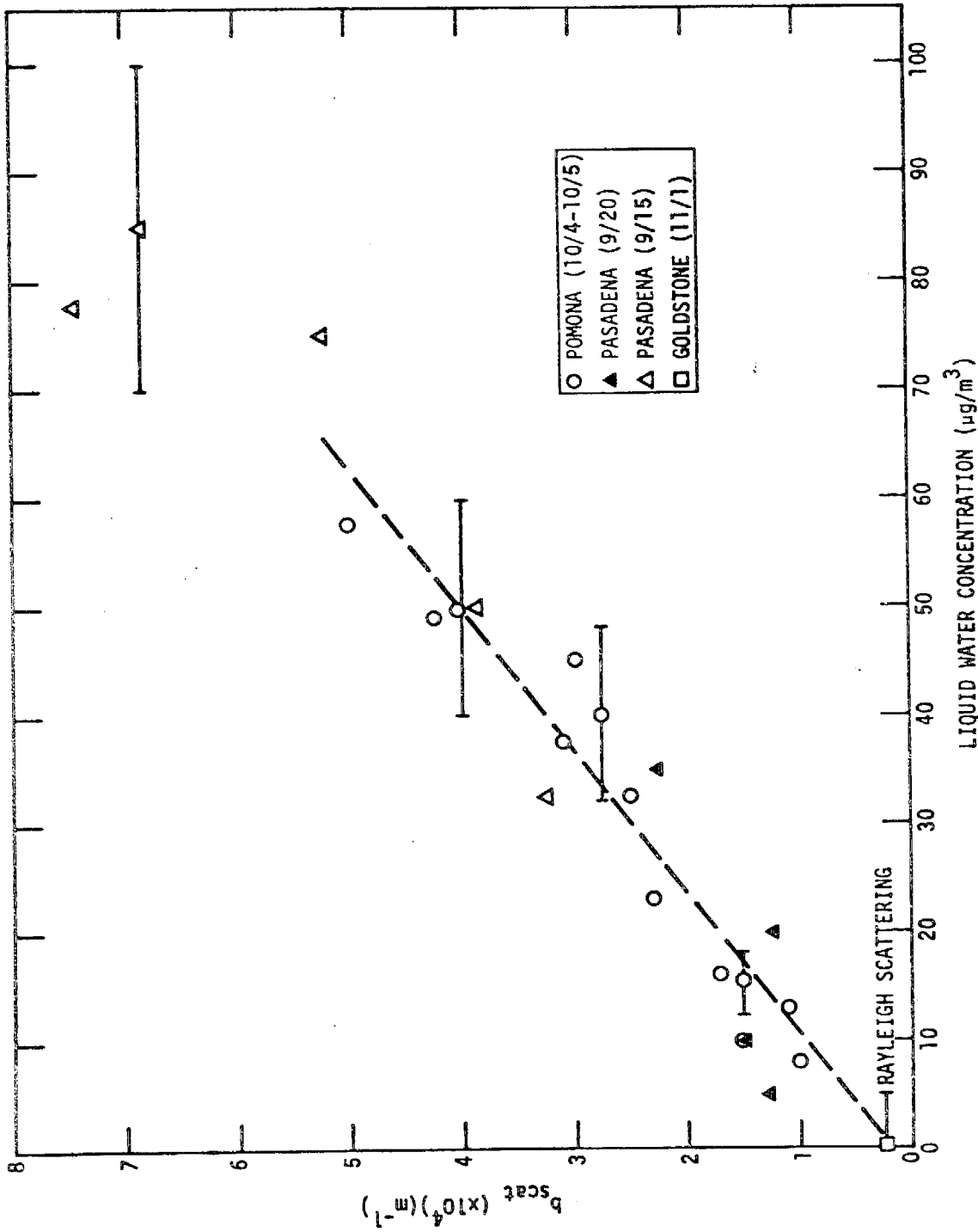


Figure 7-25. Comparison of Light Scattering Coefficient with the Liquid Water Concentration in Atmospheric Aerosols

SC524.25FR

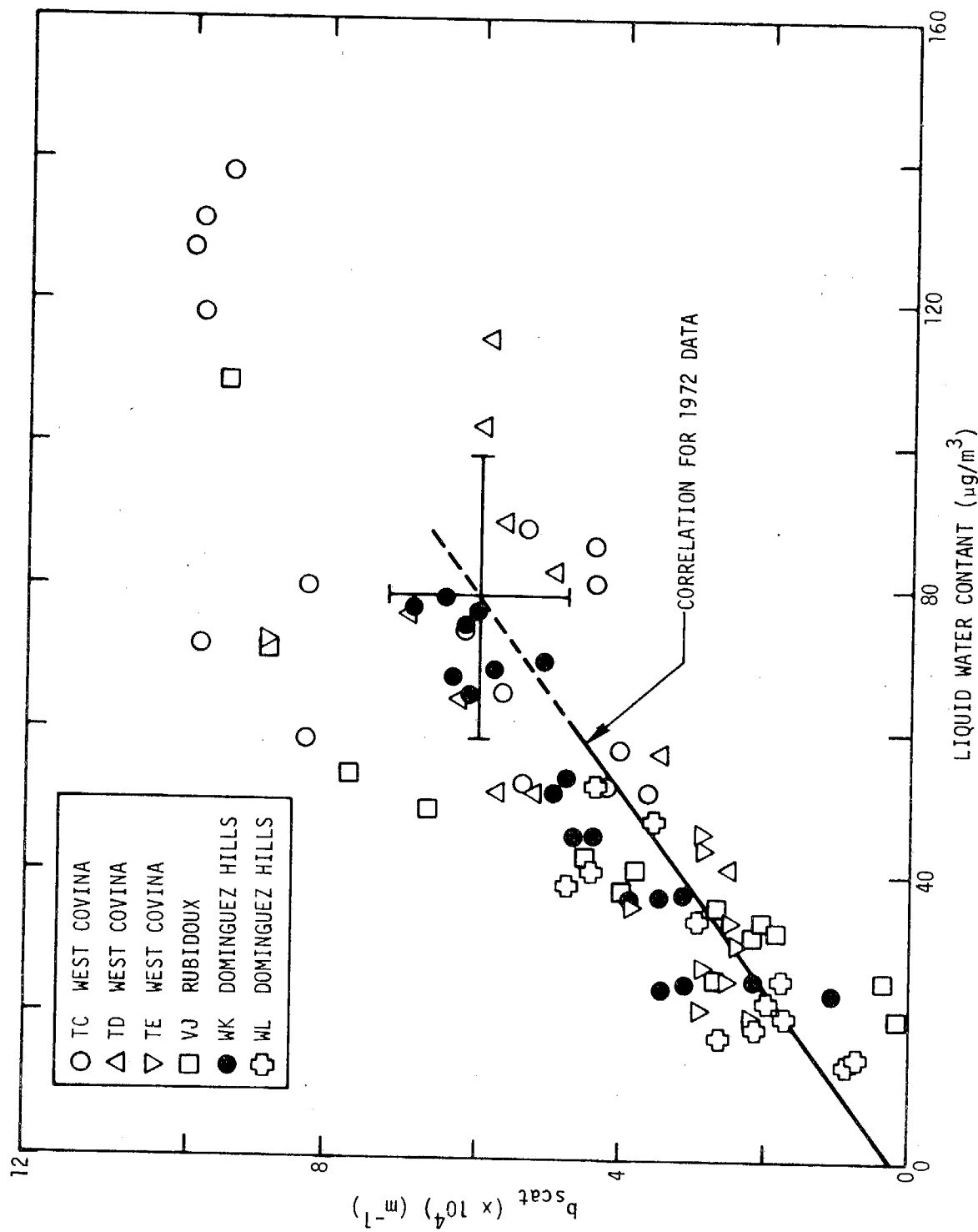


Figure 7-26. Correlation of b^{scat} vs. Liquid Water Content for 1972 and 1973

SC524.25FR

content in the Los Angeles aerosols is roughly 30% by mass over the 40% - 70% RH range. This fraction appears to be consistent with estimates from humidified nephelometry observations using the method of Covert et al. (61)

The correspondence between the microwave waterometer and humidograph results is consistent with the hypothesis that hygroscopic compounds (NO_4^- , SO_4^- , organics) are primarily in the sub-micron size range. The humidograph measures the hygroscopic nature of particles mainly $< 1 \mu\text{m}$ whereas the waterometer is sensitive to particles of all sizes.

The correlation obtained in Figure 7-25 may be specific to the aerosol conditions which were encountered in 1972 during the few days of sampling in the South Coast Basin but provide interesting information for speculation on the chemical and physical nature of the aerosol particles. b_{sp} is a function of a number of parameters, non-water mass concentration being the most important at low relative humidities ($< 60\%$). At higher humidities ($> 60\%$) relative humidity and chemical composition become increasingly important as they determine the amount of equilibrium water sorbed on aerosol particles. For hygroscopic aerosols the amount of liquid water present is a function of relative humidity in the range 40% to 70% RH. The data illustrated in Figure 7-26 seems to indicate a rather constant liquid water fraction (30%) in spite of the variation in RH between the observed data points. It was also noted in analysis of the data in figures 7-19 to 7-22 that liquid water content was not always well correlated to relative humidity. Such a stabilized liquid water fraction is consistent with other measurements and hypotheses on the chemical and physical composition of South Coastal Basin aerosol. It is indicative of a sub-micrometer aerosol of highly complex and internally mixed chemical composition as was concluded from the humidograph results of section 7-4. Any strong differentiation of chemical composition between data points, would have the effect of reducing the correlation coefficient. The presence of super-micrometer hygroscopic aerosol particles would have the same effect since the b_{sp} measurement is relatively insensitive to particles $> 1 \mu\text{m}$. The presence of certain organics in a surface film could inhibit condensation and evaporation of water. Nitrates have been observed to exist as

SC524.25FR

supersaturated solution aerosol droplets and are present in South Coastal Basin aerosol. These two effects could cause a stabilization of the liquid water in the aerosol - the hysteresis effect which has been often discussed but never directly observed.

6. A COMPARISON OF HUMIDOGRAPH RESULTS WITH THOSE OF OTHER TECHNIQUES

a. Comparison with Microbalance Weighing Results

The opportunity to directly compare light scattering increase and mass increase measurements arose through a cooperative experiment with the Institute of Meteorology at Johannes Guttenberg University and the Max Plank Institute for Chemistry both in Mainz, Western Germany. Winkler and Junge⁽⁷⁹⁾ have developed a method for collecting aerosol samples and subsequently measuring their mass as a function of relative humidity. Such samples were collected during the period of operation of the humidograph on a number of days in January and February 1973. A comparison of the results from 18 January 1973 is illustrated in Figure 7-27. The aerosol sample was collected over a one-hour period during which five humidograms were made. The averaged humidogram is shown. The light scattering ratio is consistently higher than the measured mass ratio. At low RH (50% to 60%) the inferred mass fraction of water differs from the measured water fraction by a factor or two to three. At higher relative humidities the differences decrease to the order of thirty per cent. The large discrepancies at low relative humidities are most likely due to the sensitivity of B to the normalization value, when B is near 1. Rapid fluctuation of the aerosol concentration during a humidogram run made an accurate determination of the normalization value difficult. The differences at higher humidities can be ascribed to the same cause. Renormalization of the data by b_{sp} averaged over a range of RH ($15\% < RH < 30\%$) in an attempt to more effectively average out the effect of fluctuations reduces the differences to around twenty per cent over the entire range of relative humidity. This is within the experimental error and errors involved in relating the two parameters.

SC524.25FR

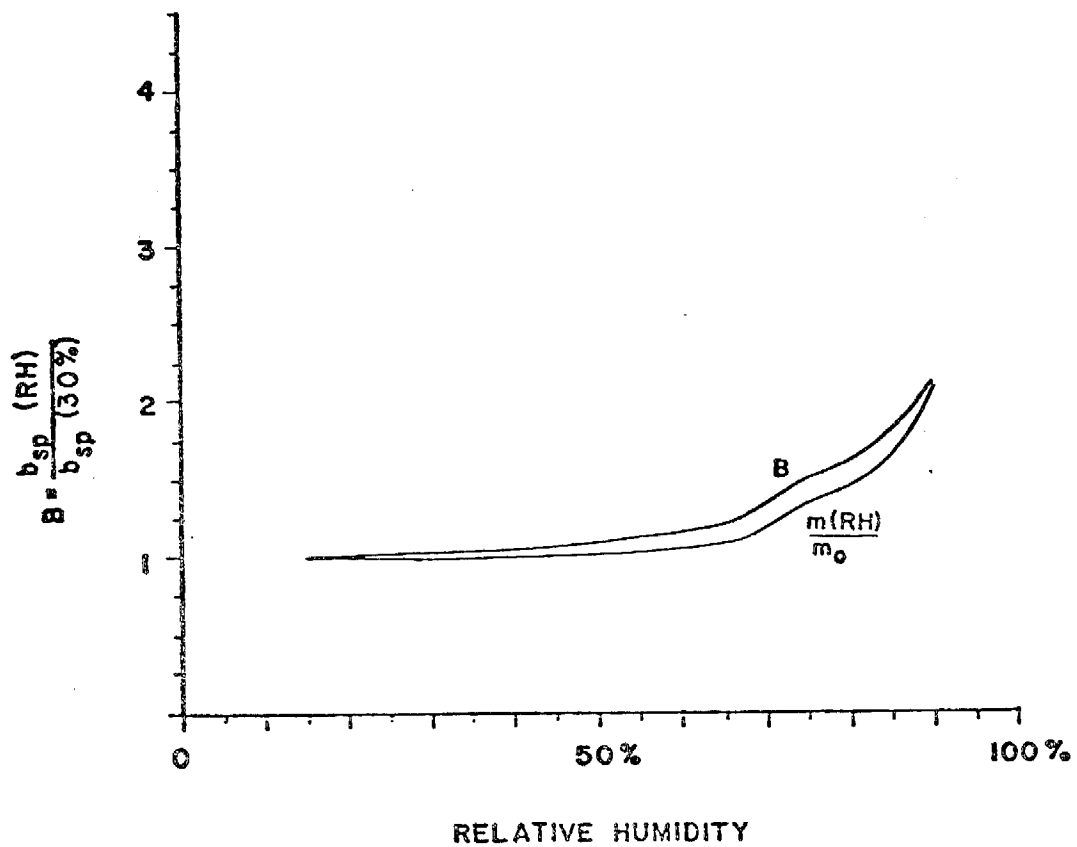


Figure 7-27. Comparison of Microbalance and Humidograph Results

SC524.25FR

An indication of the presence of deliquescent compounds is evident in both curves. The deliquescence step, though masked by the effects of mixed chemical composition, occurred at about 75%. The meteorological situation was not such that a large maritime aerosol component would have been expected. The aerosol response to relative humidity, too, would indicate a barely detectable fraction (ca. thirty mole per cent) of sea salt in the aerosol. Such highly masked deliquescence could also in part be due to the presence of ammonium sulfate in the mixture.

Further conclusions await the analysis of other data.

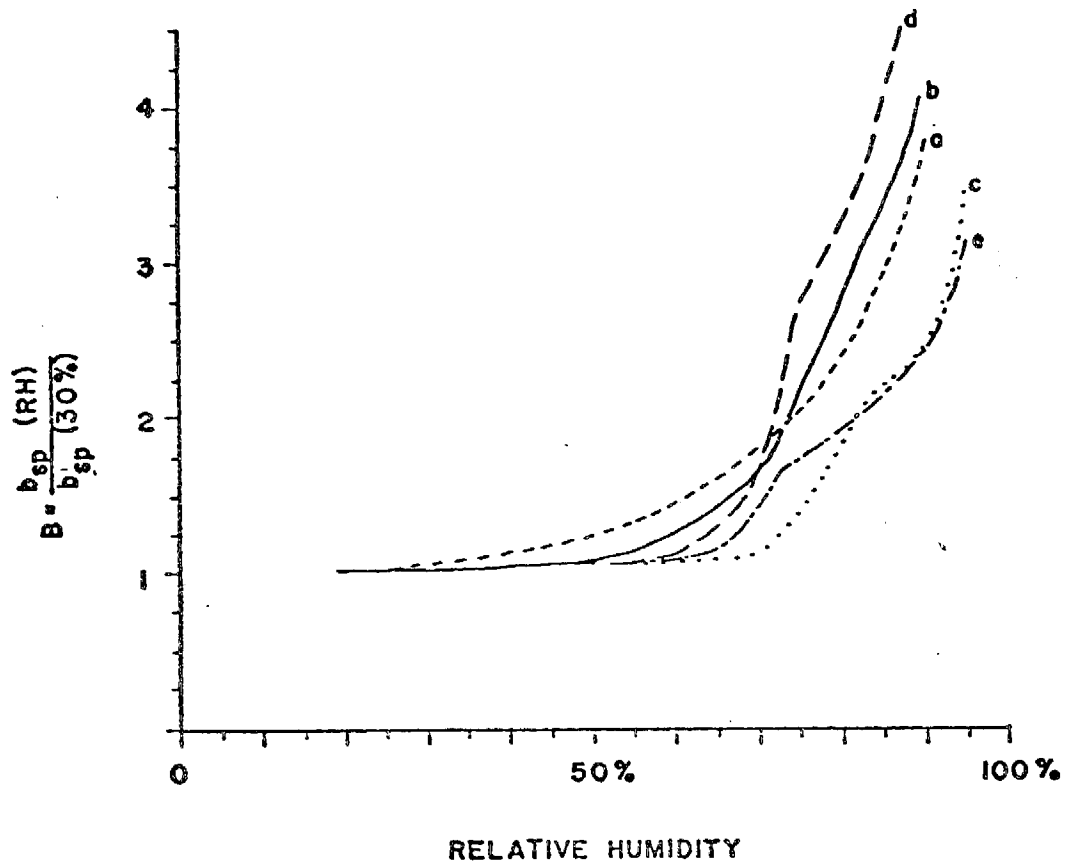
b. Comparison with Calculations by Hänel

Hänel's calculations of light scattering as a function of relative humidity ratio based on the necessary aerosol properties measured as a function of RH are described in Reference ⁽⁸⁰⁾ and illustrated in Figure 7-28. By comparison with the measured light scattering ratio, B , of this report (cf. Figures 7-6 through 7-18) it can be seen that his results were generally much higher for cases of comparable aerosol type. Hänel's calculated results lie generally at or above the extremes of the measured values of B for any given aerosol type. Only Hänel's calculated data for "Atlantic sea salt aerosol with Sahara dust" compare favorably with the measured results for sea salt aerosol at Pt. Reyes, Figure 7-6. While these comparisons are not conclusive due to the fact that measurements were not made on the same aerosol sample, the discrepancies are surprisingly large, especially comparing the results obtained for Mainz urban aerosol (cf. Figures 7-28a, b and 7-27).

D. SUMMARY OF ATMOSPHERIC OBSERVATIONS

A few statements are needed to summarize the results discussed above. Urban aerosols of anthropogenic origin are observed to be more hygroscopic than continental aerosols. The details of this hygroscopic nature are apparently controlled by the chemistry of the urban aerosol. In urban areas with a history of photochemical smog and relatively low SO_2 emissions (i.e. Los Angeles and Fresno) the hygroscopic nature seems to be controlled by a complex mixture of chemical compounds, none of which predominate due to the effects of internal mixing. The aerosol response to RH in an area surrounded

SC524.25FR



- a. urban aerosol, Mainz, summer 1966
- b. maritime aerosol, Atlantic, Apr. 1969
- c. maritime aerosol with Sahara Dust, Atlantic, Apr. 1969
- d. urban aerosol, Mainz, Jan. 1970
- e. continental aerosol, Hohenpeissenberg, 1970

Figure 7-28. Humidograms from Hanel's Calculated Values of light Scattering Ratio as a Function of Relative Humidity⁽⁸⁰⁾

SC524.25FR

by large regional sources of SO_2 , eg. St. Louis, seems to be dominated by sulfate aerosol. This aerosol is often deliquescent - most likely predominately ammonium sulfate. At other times the aerosol - sulfuric acid or ammonium bisulfate - can be reacted with ammonia to yield an ammonium sulfate-like deliquescent response.

Continental background aerosol, as exemplified by the data from Denver and Pasadena (under Santa Ana conditions), is non-hygroscopic in nature as might be expected for aerosols of high mineral composition.

Background marine aerosol is the most hygroscopic in nature of all the observed aerosol types. Its hygroscopic behavior is not dominated by the presence of sea salt except during conditions of high winds, and presumably in the surf zone. The hygroscopic nature of marine aerosol is rapidly modified by urban contributions.

SC524.25FR

Run 55, 0700-0859, 9-20-72

During this period when the wind was blowing toward the freeway it can be seen that the nuclei count had decreased to $0.25 \times 10^6 \text{ cm}^{-3}$ and the volume below $0.1 \mu\text{m}$, V2, to $9.41 \mu\text{m}^3/\text{cm}^3$. It is significant, however, that the carbon monoxide had only decreased to 13.3 ppm, indicating that while the nuclei count and the number of particles below $0.1 \mu\text{m}$ decrease very rapidly due to coagulation, the CO does not disappear as quickly and only diminishes by dilution. It was now being blown back from the direction opposite the freeway.

Characterization of the Freeway Aerosol Size Distribution

When Run 54, measured when the wind was blowing from the freeway during rush hour, is compared with Run 55, when the wind was blowing from the opposite direction, it is seen that the surface distributions shown in Figure 8-1 are nearly identical in shape and concentration for sizes larger than $0.15 \mu\text{m}$. For the smaller particles there is a large difference. The difference distribution, Run 54 minus Run 55, shown in Figure 8-1 for sizes less than $0.15 \mu\text{m}$, may therefore be presumed to be the direct contribution of the freeway rush hour traffic to the ambient aerosol.

Important parameters of the difference size distribution are given in Table 8-1. From Table 8-1 and Figure 8-1 a number of significant observations may be made.

- 1) The aerosol emitted by automobiles during freeway travel is predominantly smaller than $0.15 \mu\text{m}$ and hence below the visible range. The volume size distribution is narrow and approximately log normal in shape.
- 2) The surface area of $2870 \mu\text{m}^2/\text{cm}^3$ and volume of $17.1 \mu\text{m}^3/\text{cm}^3$ are relatively large for this small size.
- 3) This aerosol accounts for 99.4% of the aerosol number concentration during the rush hour. Because of its high number concentration, the aerosol coagulates rapidly, by both monodisperse and heterodisperse coagulation.

This may be shown for Run 54 by calculating the coagulation coefficient and comparing it with literature values.

SC524.25FR

TABLE 8-1

CHARACTERISTICS OF THE FREEWAY AEROSOL SIZE DISTRIBUTION
COMPUTED FROM THE DIFFERENCE BETWEEN RUNS 54 AND 55

Surface area	2870 $\mu\text{m}^2/\text{cm}^3$
Volume	17.1 $\mu\text{m}^3/\text{cm}^3$
Number concentration	$2.31 \times 10^6/\text{cm}^3$
Arithmetic surface mean diameter	.0358 μm
Arithmetic volume mean diameter	.0488 μm
Volume geometric standard deviation	1.9

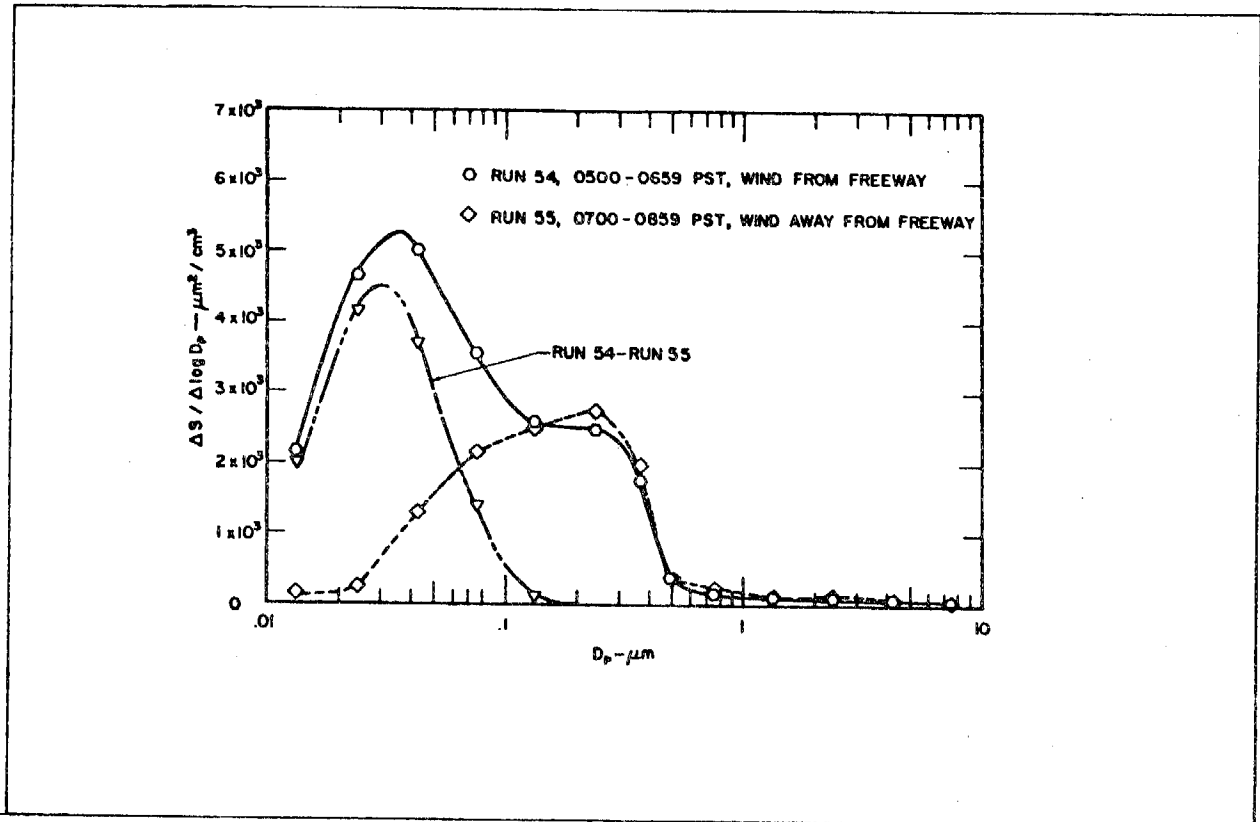


Figure 8.1 Plot of the Surface Size Distributions, $\Delta S/\Delta \log D_p$ for Run 54 When the Wind was From the Freeway, Run 55 When the Wind was Toward the Freeway, and the Difference Distribution, Run 54 Minus Run 55 for D_p Less Than .15 μm .

SC524.25FR

For a wind speed of 2.97 Km/hr. and a wind direction of 309° , it is estimated that the aerosol traveled approximately 70m from source to laboratory in 85 seconds. If it is assumed that the aerosol has traveled far enough so that the aerosol has decayed in concentration and so that the initial concentration is no longer important, then the monodisperse coagulation coefficient, K_m , is given by:

$$K_m = \frac{1}{N t} \quad (8-1)$$

For Run 54, N is equal to $2.56 \times 10^6 / \text{cm}^3$, and therefore $K_m = 4.6 \times 10^{-9} \text{ cm}^3 \text{ sec}^{-1}$. For a monodisperse aerosol of $0.02 \mu\text{m}$ diameter, Fuchs¹² gives $K_m = 1.2 \times 10^{-9} \text{ cm}^3 \text{ sec}^{-1}$. Since the aerosol is not truly monodisperse and the polydisperse coagulation coefficient is higher, the calculated value of $4.6 \times 10^{-9} \text{ cm}^3 \text{ sec}^{-1}$ is in satisfactory agreement with the theoretical values.

The percentage increase in selected aerosol, gas, and particle chemistry parameters when the wind came from the direction of the freeway (Run 54 - Run 55) $\times 100/\text{Run 55}$, is shown in Table 8-2. The parameters have been arranged into four groups according to the percentage change.

Group IV consists of those parameters which show a small negative change of -27%. This indicates that they are not emitted in significant quantity by the automobile on the freeway and that their concentration is dominated by the general behavior of the city atmosphere. This group includes b_{scat} , which indicates that direct emissions from automobiles have negligible direct effect on visibility. It also includes SO_2 and the oxidized sulfur on the after-filter. This indicates that SO_2 and oxidized sulfur are dominated by the concentration in the general urban atmosphere or by sources other than the automobiles on the freeway.

Comparisons of the Freeway Aerosol with Laboratory Aerosol Measurements

As a result of some collaborative research studies with the Battelle-Columbus Laboratory under EPA sponsorship, it was possible to make some comparisons of the freeway aerosol size distributions and concentration with the size distribution and concentrations of aerosols measured in a dilution tunnel and in a smog chamber at Battelle. These studies, performed at the

SC524.25FR

TABLE 8-2

 PERCENTAGE DIFFERENCE OF SELECTED AEROSOL, PARTICLE CHEMISTRY,
AND GAS CHEMISTRY WITH THE WIND FROM THE FREEWAY

Group	Parameter	Percent increase when wind was from the freeway	
		$\frac{\text{Run 54} - \text{Run 55}}{\text{Run 55}} \times 100$	
I	Number conc. (CNC)	924	
II	Surface 0.01 to 0.1 μm	280	
	Volume 0.01 to 0.1 μm	173	
	NO	147	
	Pb (AF)	148	
	S ⁻ (AF)	114	
	Br (AF)	258	Avg = +187
III	Total hydrocarbon	24	
	CH ₄	26	
	CO	28	
	C ₂ H ₂	25	
	C ₂ H ₄	25	
	Mass (AF)	5.9	Avg = 22
IV	O ₃	-59	
	Total Mass	-9.5	
	S ⁺ (AF)	-25	
	Surface 0.1 to 1 μm	-7	
	Surface 1 to 10 μm	-31	
	Surface >10 μm	-16	
	Volume 0.1 to 1 μm	-15	
	Volume 1 to 10 μm	-29	
	Volume 10 μm	-17	
	NO ₂	-57	
	SO ₂	-29	
b _{scat}	-30	Avg = -27	

AF = afterfilter

SC524.25FR

suggestion of William E. Wilson of EPA and under the direction of David Miller and Art Levy of Battelle, were primarily intended to measure the photochemical aerosols produced by the irradiation of auto exhaust mixtures. The University of Minnesota provided aerosol measuring instrumentation and direction for the aerosol measurement part of the study. The bulk of these data will be described in a separate paper. Only a few data especially relevant to the freeway results are included here.

The essential features of the Battelle dilution tunnel and smog chamber are shown in Figure 8-2. The automobile was a 1971 Ford with about 10,000 miles accumulated, and was operated on a chassis dynamometer. For the samples taken directly from the tunnel, the auto was operated over the 23-minute EPA driving cycle. At the end of the cycle, size distribution measurements in the smog chamber were begun and continued for several hours. Only the initial size distributions in the chamber are discussed here together with those measured in the dilution tunnel. The Minnesota Aerosol Analyzing System (MAAS) consisted of a new Electrical Aerosol Analyzer (EAA)⁽⁸²⁾, a Royco 220 Optical Particle Counter, and an Environment/One Condensation Nuclei Counter (CNC).

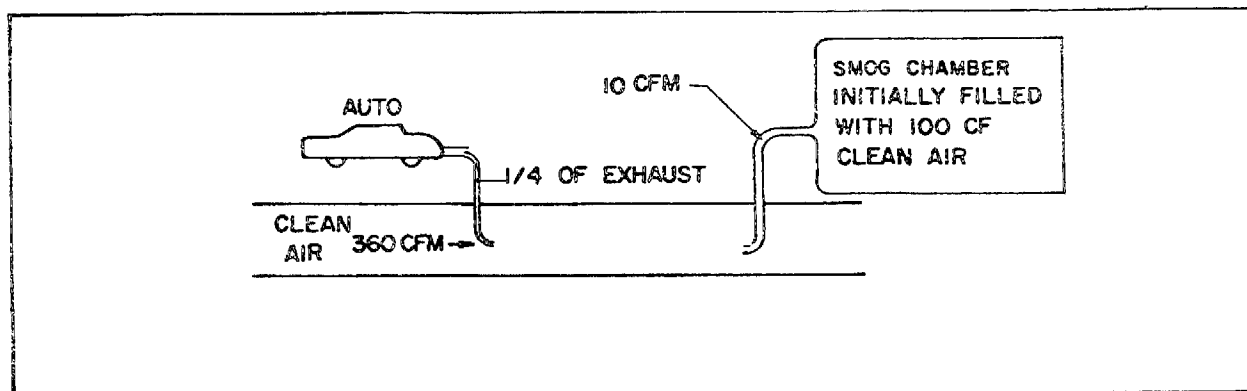


Figure 8-2. Schematic of the Battelle-Columbus Auto Dilution Tunnel and Smog Chamber. A Splitter was used on the Tailpipe of the Automobile so that Approximately 1/4 of the Exhaust was Directed into the Dilution Tunnel. Effective Dilution Ratio in the Tunnel was Approximately 40 for the Driving Cycle and 56, 17, and 10 for Idle, 35 mph and 50 mph Respectively.

SC524.25FR

Figure 8-3 compares the surface distribution of aerosols measured from the dilution tunnel with the freeway contribution aerosol. It will be noted that the shape, spread, and mode size of the distributions are very similar, which suggests that the rate and magnitude of the dilution in the tunnel approximate that occurring on the freeway. The aerosol from the smog chamber has a mode size of about 0.12 μm compared with the 0.03 μm mode size for the fresh freeway aerosol.

The aerosol measurements indicate that in the smog chamber the CNC number is more than two orders of magnitude less than when the aerosol is sampled directly from the tunnel. It is also interesting to note that if equation (8-1) and the computed coagulation coefficient are used to calculate the initial concentration on the freeway corresponding to a time of 1 second, the concentration is 4×10^8 , a value on the same order of magnitude as that measured in the dilution tunnel.

It was found that the volume concentration, VT, is similar for the tunnel and smog chamber samples for leaded fuel. The aerosol volume concentration is about one order of magnitude less for unleaded fuel.

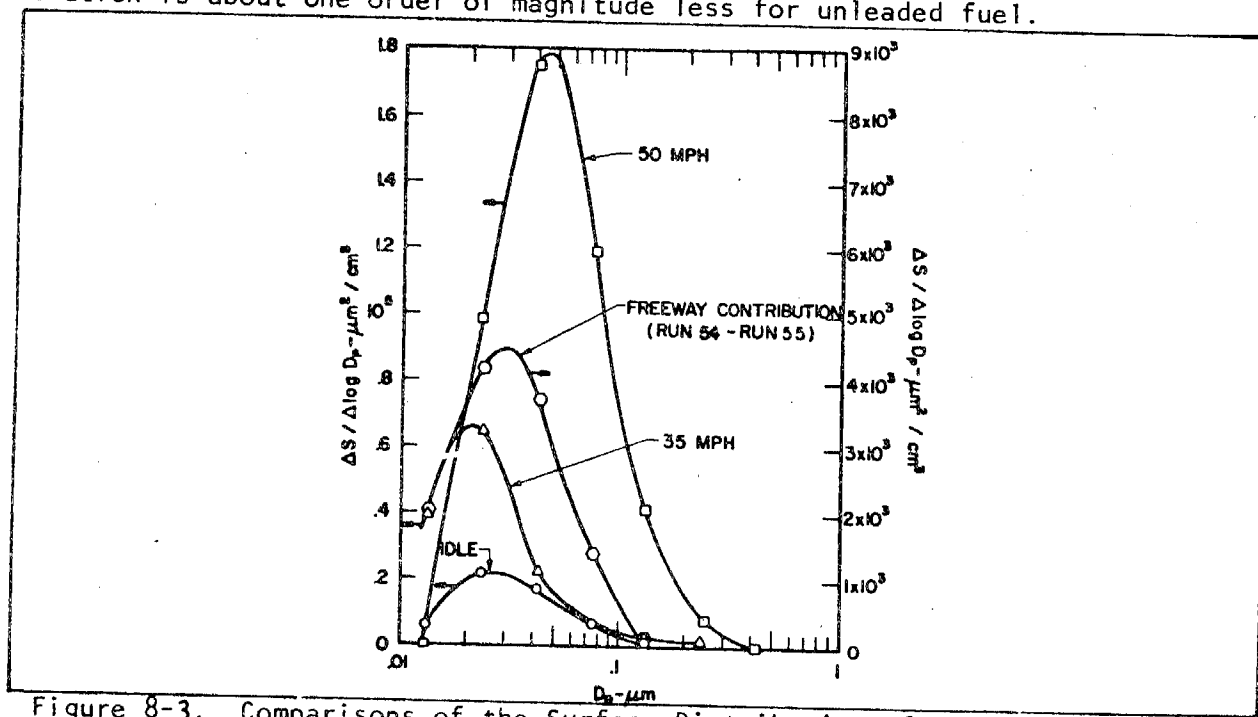


Figure 8-3. Comparisons of the Surface Distributions for the Freeway Difference Size Distribution, Run 54 Minus Run 55, from the Harbor Freeway with Aerosol Size Distributions Measured in the Battelle Dilution Tunnel at Idle, 35 mph, and 50 mph.

SC524.25FR

It is of considerable interest to compare the aerosol concentration measured in the laboratory with the concentrations measured near the freeway. Of the several ways of making such a comparison, only two will be presented here. Such comparisons require making so many assumptions that the results should be taken more as indicative of an approach than as numerical evidence that the laboratory data agree with the field data.

Aerosol volumes, total hydrocarbons, nitrogen oxide, and carbon monoxide were measured in both places. If the characteristics of the emissions from the freeway and the laboratory auto are the same, then the ratios of the concentrations of the various pollutants should be approximately the same. A comparison of the ratio of the freeway parameters to the Battelle parameters for 35 mph were made using leaded fuel, a complete driving cycle, and sampling from the tunnel. In computing the ratios, the data were normalized with the total aerosol volume. Except for NO, which at 10.55 is almost an order of magnitude high, it is seen that the ratios of HCTOT = 3.03 and CO = .95 are as close to one as could be expected. While it is straightforward to make comparisons based on relative concentrations of gaseous and particulate emissions, to make comparisons of absolute concentrations it is necessary to assume a model for the mixing of the pollutants emitted by the moving automobiles on the freeway and to have traffic counts available.

A mixing model assumes that the emissions from the freeway are mixed uniformly into a layer of thickness Z downwind of the freeway. If it is further assumed that the mixing is two-dimensional, and that there are n autos emitting w gms/mile of an aerosol of density ρ_p , then it can be shown that the emission per auto in gm/mile is:

$$w = \frac{1.6 \times 10^5 \rho_p v Z V}{n}$$

Using the difference between Runs 54 and 55,

$$w = 1.6 \times 10^5 Z v \left(\frac{\rho_{P54} V_{54}}{n_{54}} - \frac{\rho_{P55} V_{55}}{n_{55}} \right)$$

SC524.25FR

$$\begin{aligned} \text{where } \rho_{p_{54}} &= 1.16 \text{ gm/cm}^3 & V_{54} &= 40.1 \times 10^{-12} \text{ cm}^3/\text{cm}^3 & **n_{54} &= 2.15 \text{ sec}^{-1} \\ \rho_{p_{55}} &= 1.19 \text{ gm/cm}^3 & V_{55} &= 23.0 \times 10^{-12} \text{ cm}^3/\text{cm}^3 & n_{55} &= 3.93 \text{ sec}^{-1} \end{aligned}$$

$$v = .825 \text{ m/sec.}$$

If $Z = 30\text{m}$, then $w = 0.581 \text{ gm/mi}$.

A comparable value for w may be calculated from the Battelle data using the following equation:

$$w_B = 360 \times 4 \times \rho_p \times VT_m/\text{mph} \times \text{conversion factors}$$

$$w_B = 3.91 \times 10^9 \frac{VT_m}{\text{mph}} \quad (8-2)$$

where VT_m is the volume aerosol concentration (cm^3/cm^3) measured by the MAAS and $VT_m = VT$. Using equation (8-2) and assuming $\rho_p = 1.6 \text{ gm/cm}^3$ *, it is found that $w_B = .344 \text{ gm/mi}$ at 50 mph and $.046 \text{ gm/mi}$ at 35 mph. Considering the assumptions made in the calculations and the fact that the Battelle data were obtained with a carefully tuned late-model auto, the agreement between Battelle emissions and those calculated from the freeway data is better than it probably should be. Thus it appears that the most likely value for the emissions of fine particles from automobiles moving on a freeway is in the range from 0.1 to 0.5 gm/mi.

Conclusions

From measurements of the size distribution, concentration, and chemistry of aerosols sampled during the 24-hour intensive period from 2100 on September 19 to 2100 on September 20, 1972, alongside the Harbor Freeway in Los Angeles, it is possible to draw a number of conclusions regarding the nature of freeway aerosols.

* A density of 1.6 gm/cm^3 was assumed because the humidity in the chamber was less than at the freeway.

** The traffic count data were furnished by the California Department of Highways.

SC524.25FR

- 1) The fresh freeway aerosol sampled at a distance of 30m from the freeway is mostly below $0.15 \mu\text{m}$ in diameter. The direct freeway contribution was $17.1 \mu\text{m}^3/\text{cm}^3$ during the morning rush hour. The nuclei count was between two and three million particles/cc, and the surface area for the fresh aerosol was approximately $3000 \mu\text{m}^2/\text{cm}^3$.
- 2) Comparison of the size distributions measured alongside the freeway with size distributions measured in the dilution tunnel at Battelle-Columbus suggest that the rate of dilution and extent of dilution behind a moving automobile on a freeway are comparable if the dilution is rapid enough.

B. CHEMICAL TRACER METHOD

The approach of investigating the sources of aerosols using exclusively the source dominated physical properties of particle clouds can provide only limited information on sources and ambient air pollution. This technique can be enhanced significantly by adding the information contained in the chemical composition of the collected aerosol particles. This approach has been illustrated in a series of papers with an application to the results of measurements of the Pasadena Aerosol Study in 1969^(16,83,84). Basically, the method consists of (1) estimating certain primary source contributions to the pollution at a point using chemical elements as tracers, (2) supplementing these estimates using emission inventory data for those sources for which characteristic tracers are not available and (3) calculating the contributions of gas-to-particle conversion from the measured values of sulfate, nitrate, organic and ammonium ion. In this way data of different types are reduced to a common basis - source contributions to the mass of particulate at a given sampling point.

The products of gas-to-particle transformation processes are then distributed with respect to size by calculations made according to certain growth laws, based on theory and/or experiment. The calculated distribution of chemical elements with respect to size can then be checked against the experimentally measured distributions. Finally, the calculated light scattering can be compared with the experimentally measured value. In this way, the contributions of different sources to the deterioration of visibility can be estimated.

SC524.25FR

The method has been summarized by Friedlander⁽⁸³⁾ in a set of fundamental equations relating the output of standard measurement systems to the input from sources. An integrated measurement system suitable for the determination of the aerosol properties used in the calculations includes (1) a total filter to collect material for total mass and chemical analysis and/or a fractionating device such as the cascade impactor to collect material according to size for chemical analysis, (2) analytical methods for determining the concentrations of certain trace elements, (3) particle size analyzers to provide a detailed breakdown on particle size distribution and (4) an instrument which measures light scattering by the aerosol.

Such information was obtained in the ACHEX. In this section, some of the data obtained in the ACHEX are analyzed by the methods described above⁽⁸⁵⁾.

The method, once perfected, will have a variety of applications: Contributions of natural background and of primary and secondary contributions to the total particulate can be estimated, and these are important for air pollution control strategies. If air flow patterns and the source area distributions are known, complete particulate pollution models for urban and industrial basins can be developed as suggested by White, Husar and Friedlander,⁽¹⁰⁰⁾

Chemical element balances were carried out for the data collected at Pasadena and Riverside, on September 20, 1972; San Jose on October 20; Fresno on September 1; and Pomona on October 24. For all of these sites twenty-four hour averages for the chemical data were used in the calculations. In addition, the data for two two-hour periods were analyzed, one set from Pasadena, on September 20, 1200-1400, and the other from Pomona, on October 24, 1200-1400. The Pasadena time period corresponded to a low total mass of aerosol and high visibility, while for Pomona the total mass was high and the visibility low.

SC524.25FR

Source-mass contributions have been estimated by Heisler and Friedlander⁽⁸⁴⁾ for eight time periods using data collected in 1973. The time periods and locations used were: West Covina, 1200-1400 PST, 7/24/73 and 2110 PST, 7/23/73 to 2110 PST, 7/24/73; Pomona, 1200-1400 PST, 8/17/73 and 2100 PST, 8/16/73 to 2100 PST, 8/17/73; Rubidoux, 1200-1400, 9/6/73 and 2300 PST, 9/5/73 to 2300 PST, 9/6/73; and Dominguez Hills, 1000-1200 PST, 10/5/73 and 2100 PST, 10/4/73 to 2105 PST, 10/5/73.

The calculation method varied little from that used by Gartrell and Friedlander⁽⁸⁵⁾ and only the differences are described.

1. CHEMICAL ELEMENT BALANCE

The concentration x_i of an element i found in the aerosol at a receptor site is given by the following relation:

$$x_i = \sum_j z_{ij} \alpha_{ij} m_j \quad (8-3)$$

where m_j is the mass of material from source j per unit mass of receptor material or unit volume of air, z_{ij} is the fraction of element i found in the source j , and α_{ij} is the coefficient of fractionation between source and atmosphere. By measuring elemental concentrations in the particulate, x_i , the value of m_j can be determined if z_{ij} and α_{ij} are known. There are, however, several difficulties with this method. The α_{ij} are difficult to determine, and may be functions of local meteorology. In addition, if the aerosol chemical composition is a function of particle size, sedimentation and other deposition processes modify α_{ij} . Thus it is necessary to choose elements for which there is reason to believe that α_{ij} is near unity. A further consideration in choosing an element to be used in the determination of m_j is that all the important sources of that element must be known along with the corresponding concentrations. For example, one source of zinc is tire dust, but there are other significant sources as well.

As in the references cited above, sodium, aluminum, calcium, lead, potassium, vanadium and magnesium were used as the tracer elements in calculating contributions by the primary sources. For these elements automobile exhaust, soil dust, sea salt, cement dust, and fly ash from fuel combustion,

SC524.25FR

as explained in detail by Miller *et al.*⁽¹⁶⁾, are believed to be the dominant sources. The coefficients z_{ij} were those given by Miller, Friedlander, and Hidy⁽¹⁶⁾ and Friedlander⁽⁸³⁾. Since there are seven elements and five sources, the calculation was carried out by minimizing the mean square error between measured and calculated values, weighted by the experimental error.

Magnesium was measured using neutron activation analysis, and in some cases the concentration of this element was below the limits of detection of the method. In those cases, the concentration and the associated error of the measurement were taken to be one-half the value of the lower limit of detection for magnesium. This had little effect on the results since the calculations were insensitive to magnesium concentrations.

The concentrations used for the two-hour periods were determined with a Lundgren impactor and after-filters. Potassium was not used in this set of calculations. Since wall losses in the impactor may be a significant problem, particularly for the larger particles, the element contributions as well as the source strengths for these periods should be considered a minimum.

The values for the twenty-hour periods are from Hi-vol filters, unless otherwise noted. Sodium, calcium, aluminum, vanadium and magnesium were measured using neutron activation analysis; lead and potassium were measured by x-ray fluorescence. In some cases, which are noted, sodium was measured using wet chemistry, and calcium was measured by x-ray fluorescence. Errors associated with the measurements are analytical errors.

The data used in the calculations were taken from the aerosol chemistry portion of the data bank. The numerical values and the associated (estimated) errors are tabulated in Volume II of this report.

a. Chemical Composition of the Freeway Aerosol

The impactor and filter samples that were collected near the Harbor Freeway in Los Angeles on September 20, 1972 were used to obtain an improved freeway primary aerosol chemical composition to be used in the analysis of the 1973 data. The resulting elemental breakdown is for all freeway sources: automobile exhaust, diesel exhaust and tire dust.

SC524.25FR

The wind was blowing directly from the freeway during two two-hour periods in which samples were collected. These periods were 0500-0700 PST and 1700-1900 PST. Elemental analyses from the Lundgren impactor after-filters and total carbon analyses from silver membrane total filters were used. The after-filters collected particles with diameters less than $0.6 \mu\text{m}$ and were chosen for the calculations for two reasons: First, large particles fall out near the freeway; although particles larger than $0.6 \mu\text{m}$ will remain airborne, no data on mass concentrations were available for the impactor stages. Second, during both time periods 85 percent of the lead in particles smaller than $1.5 \mu\text{m}$ (sum of after filter and last impactor stage) was on the after-filter, indicating that most of the freeway aerosol mass is below $0.6 \mu\text{m}$. Data on carbon concentration were not available for the after-filters. It was assumed that the carbon on the silver membrane total filters was associated with particles smaller than $0.6 \mu\text{m}$ and was solely from the freeway. The resulting carbon concentration is therefore an upper limit. The results of the chemical analyses are shown in Table 8-3.

The concentrations of sodium, aluminum, calcium, and vanadium were used to estimate the contributions of sea salt, soil dust, cement dust, and fuel oil flyash to the material on the after filters. The oxidized sulfur concentrations (S+) were scaled up to give sulfate concentrations. These estimates are shown in Table 8-4 and are less than 7 percent of the total mass, the sulfate dominating. The concentrations of lead, bromine, chlorine, zinc, carbon, and reduced sulfur (S-) in the remaining masses were then calculated and the results are shown in Table 8-5. Since some of the chloride in the samples was contributed by sea salt, the freeway chloride was calculated by an electrical charge balance on lead, bromine, and chlorine, the lead expected to be present as lead halides (Hirschler, et al.,⁽⁸⁶⁾). These species along with some hydrogen and oxygen associated with the carbon are expected to comprise the freeway aerosol.⁽¹⁶⁾ It is seen in Table 8-5 that when the carbon compounds are assumed to be 15 percent hydrogen and oxygen the sum is only 78.5 ± 7.8 percent of the mass. This indicates that sources other than those accounted for, probably industrial, for which no tracers are available, contributed to the samples. The concentrations were therefore normalized to 100

SC524.25FR

TABLE 8-3

 CHEMICAL ELEMENT CONCENTRATIONS FROM HARBOR FREEWAY
9/20/72

Species	After Filter Concentration ($\mu\text{gm}/\text{m}^3$)			
	0500-0700 PST		1700-1900 PST	
Al (N)	0.0334	\pm .0099	0.0473	\pm .0092
Br (N)	6.32	\pm .14	4.40	\pm .10
Ca (x)	0.097	\pm .024	0.054	\pm .022
Cl (N)	3.19 (1.75)	\pm .10 (.27)	1.57 (1.10)	\pm .07 (.13) (c)
Fe (x)	0.112	\pm .005	0.126	\pm .005
Na (N)	0.136	\pm .032	0.158	\pm .030
Pb (x)	13.3	\pm .5	8.91	\pm .36
V (N)	0.00712	\pm .00039	0.00454	\pm .00027
Zn (x)	0.094	\pm .004	0.053	\pm .002
S+ (E)	1.20	\pm .3	0.5	\pm .5 (b)
S- (E)	1.50	\pm .3	0.5	\pm .5 (b)
Mass	68.6	\pm 7.6	50.3	\pm 5.5
C (a)	U		14.9	\pm 2.2

- (a) As carbon. From silver membrane total filter.
 (b) Not detected. Value is one-half of detection limit.
 (c) From charge balance with Pb and Br used in concentration calculations.
 (N) Neutron activation analysis.
 (x) X-ray fluorescence analysis.
 (E) ESCA analysis.
 U = Unknown

SC524.25FR

percent, and the results are shown in Table 8-5.

Also shown in Table 8-5 is the freeway chemical composition used by Friedlander⁽⁸³⁾ and Gartrell and Friedlander⁽⁸⁵⁾. The estimates for the lead concentration are essentially the same while the new carbon estimate is lower. The lower carbon-to-lead ratio leads to the calculation of lower primary freeway carbon in carbon balances. The total primary freeway mass contributions from chemical element balances will be the same with the new composition as with the old.

For the purpose of detailed source breakdowns it was necessary to estimate the individual contributions of automobile exhaust, diesel exhaust and tire dust. Following Gartrell and Friedlander⁽⁸⁵⁾, emission inventories were used to estimate their relative contributions.

2. SECONDARY CONSTITUENTS

The 1972 ACHEX data were treated without considering indirect means of accounting for the composition of sulfate or nitrate salts. Based on further knowledge, Heisler and Friedlander have modified the 1972 approach to include assumptions about the ammonium ion contribution and water. In particular, an attempt was made to assign these constituents to specific chemical compounds on a stoichiometric basis. Replacement of chloride by sulfate in sea salt was included as in Miller, Friedlander and Hidy⁽¹⁶⁾. The compounds used were NaHSO_4 , NH_4NO_3 , NH_4HSO_4 and $(\text{NH}_4)_2\text{SO}_4$. Since measurements of aerosol water content were not available, water was estimated by assuming the NaHSO_4 and NH_4NO_3 were present as saturated solutions. The solubilities used were 28.6 gm/100 gm H_2O at 25°C and 241.8 gm/100 gm H_2O at 30°C respectively⁽⁸⁷⁾.

3. EMISSION INVENTORY SCALE-UP

Emission inventory data were used to estimate contributions of industrial aircraft and agricultural sources for which characteristic tracers were not available. The total mass inputs of primary particulate pollutants from various sources into the air basins of California have been estimated⁽⁸⁸⁾. The inputs, relative to the automobile exhaust, are listed in Table 8-6 for various sources and locations. If the air basins into which these particulates are emitted are well mixed, the contributions to the aerosol can be

SC524.25FR

TABLE 8-6
PRIMARY PARTICULATE INPUTS RELATIVE TO AUTOMOBILE⁽⁸⁸⁾

	<u>Los Angeles County</u>	<u>S.F. Air Basin</u>	<u>Riverside County</u>	<u>Fresno County</u>
Automobile	1.0	1.0	1.0	1.0
Diesel	.27	.26	.24	.26
Industrial (less fuel comb)	.92	2.8	4.3	8.7
Aircraft	.25	.59	1.9 ^(a)	.41
Agriculture	---	.51	.95	8.9
Automobile ^(a) (tons/day)	44.5	28.1	2.1	2.7
Total ^(b) (tons/day)	129	174	18.8	54.1

(a) Errors in these estimates are unknown.

(b) Includes fuel combustion.

SC524.25FR

approximated by scaling to the automobile exhaust contribution found in the chemical element balance. This assumption cannot be applied, however, to a site where there is a large local source of particulate pollution. For example, at the Harbor Freeway, high ambient concentrations of lead were measured; other sources cannot be scaled to the automobile contribution to the aerosol because of the proximity of the freeway to the sampling site. The errors associated with these mass input estimates are not known; since these inputs are annual averages and do not reflect short term fluctuations, the errors could reasonably be assumed to be as large as $\pm 100\%$. For most of the cases considered, the contributions of the sources estimated in this way are not large and the effect of error on the overall balance is not great.

4. RESULTS OF SOURCE BREAKDOWN CALCULATIONS

Tables 8-7 and 8-8 show the results of the source breakdown calculations for various locations based on twenty-four hour and two-hour sampling periods, respectively. The sea salt, soil dust, auto exhaust, cement dust and flyash contributions were based on the chemical element balance while diesel exhaust tire dust, agricultural and industrial, and aircraft aerosol were scaled to the automobile through an emission inventory. Secondary conversion products, sulfate, nitrate, ammonia and water were measured directly while the organics were corrected for primary contributions by the carbon balance. The measurements for water are from water-filters or the waterometer experiments at the sites.

The results for Pasadena, Pomona and Riverside show quite acceptable agreement between the sum of the calculated source contributions and the measured total mass. As in previous studies in this series, the products of the conversion of organic vapors, nitrogen oxides and sulfur dioxide represent a significant fraction of the total aerosol. The data for Pomona show much higher concentrations of sulfate, nitrate and ammonia than for Pasadena although organic concentrations are about the same. In both cases, there is about enough ammonium ion on a molar basis to account for nitrate and sulfate as NH_4NO_3 and $(\text{NH}_4)_2\text{SO}_4$.